International School for Andavced Studies
Neurobiology Sector

The role of prolyl-isomerase PIN1 in GABAergic and glutamatergic synaptic transmission

Thesis submitted for the degree of

"Doctor Philosophiae"

November 2015

Candidate:

Roberta Antonelli

Supervisors:

Prof. Enrico Cherubini

Dr. Paola Zacchi

Prof. Anna Menini

Declaration

The original work presented in this thesis was carried out at the International School for Advances Studies SISSA, Trieste, between November 2011 and November 2015 under the supervision of Prof Enrico Cherubini and Dr Paola Zacchi. I performed and analyzed all the experiments at exeption of electrophysiological recording and analysis achieved by Rocco Pizzarelli, Roberto DeFilippo, Andrea Pedroni and Stefka Stancheva

ABSTRACT

The correct functioning of the central nervous system relies on the rapid and efficient communication between neurons. This occurs at highly specialized functional points of contact called synapses. Synapses are extremely plastic in structure and function, strongly influenced by their own histories of impulse traffic and by signals from nearby cells. Synaptic contacts are fundamental to the development, homeostasis and remodeling of neural circuits. All these events are achieved through different mechanisms operating at both pre- and postsynaptic sites. At the level of the post synaptic density (PSD) compartment, scaffolding molecules and trans-membrane proteins are known to orchestrate proper synapses formation, maturation and rearrangement required to sustain plasticity processes.

Protein phosphorylation represents one of the most important mechanisms engaged in affecting the molecular composition of the post-synaptic device. Most studies have focused on the impact of phosphorylation on the gating properties, surface mobility and trafficking of neurotransmitter receptors while much less is known about the effect of post-translational modifications on scaffolding and cell adhesion molecules functionally linked to neurotransmitter receptors.

At GABAergic synapses specific phosphorylation events of the scaffolding molecule gephyrin were shown to alter its multimerization properties, thus producing parallel changes in the number of receptors trapped by the scaffold leading to alterations of synaptic strength. Most of these phosphorylation events occur at serine or threonine residues preceding a proline, underlying a potential role of proline-directed phosphorylation as modulator of synaptic strength. The key player of such signalling cascade is represented by a small enzyme called peptidyl-prolyl isomerase Pin1 (protein interacting with NIMA 1). Pin1, upon recruitment by its substrates in a phosphorylation-dependent manner, catalyzes the *cis/tran* isomerization of phospho-Ser/Thr-Pro motifs leading to changes in target protein conformation and biological activity. Pin1 is highly expressed in neurons suggesting that it can exert a crucial role in synaptic transmission and plasticity processes at both inhibitory and excitatory synapses.

In the first part of my PhD thesis I focused on the impact of Pin1-dependent signalling on GABAergic transmission. I found that the cell adhesion molecule of the neuroligin family enriched at GABAergic synapses, Neuroligin 2 (NL2), undergoes post-phosphorylation prolyl-

isomerization modulation of its activity. Using biochemical approaches I found that the unique Pin1 consensus motif present within the cytoplasmic tail of NL2, serine 714-proline, is indeed phosphorylated *in vivo*. Proline-directed phosphorylation at serine 714 of NL2 strongly impacts on NL2 ability to complex with gephyrin. In particular, at this site, post-phosphorylation prolyl-isomerization negatively regulates the ability of NL2 to interact with gephyrin. In line with biochemical results, immunocytochemical analysis reveal that, in the absence of Pin1 expression, NL2/gephyrin complexes are enriched at GABAergic post-synaptic sites and this enrichment is accompanied by an enhanced synaptic recruitment of $GABA_A$ receptors ($GABA_AR$). This effect was associated with a concomitant increase in the amplitude, but not in frequency, of spontaneous inhibitory post-synaptic currents (IPSCs). These findings unveil the existence of a new signalling pathway operating at inhibitory GABAergic synapses able to alter the efficacy of GABAergic transmission by modulating NL2/gephyrin interaction.

Given the high abundance of Pin1 at excitatory synaptic contacts, in the second part of my PhD thesis I focused on the impact of Pin1-dependent signalling on excitatory glutamatergic transmission. In particular, I started to investigate whether the scaffolding molecule PSD-95, a member of the Disc-Large (DGL)-Membrane-associated guanylate kinase, could be a target of Pin1-dependent signalling cascade. I observed that Pin1, known to reside in post-synaptic structures, is recruited by PSD-95 at specific Serine-Threonine/Proline consensus motifs localized in the linker region connecting PDZ2 to PDZ3 domains. These sites are represented by Treonine287-Proline, Serine290-Proline and Serine295-Proline, and deletion of all of them almost completely abolished Pin1 interaction with PSD-95. Pin1 exerts a negative control on PSD-95 ability to complex with N-Methyl-D-Aspartate receptors (NMDARs). Indeed an enhanced PSD-95/NMDAR complex formation was detected in brain extracts derived from Pin1-/- mice. In electrophysiological experiments, larger NMDA-mediated synaptic currents were detected in CA1 principal cells in hippocampal slices obtained from Pin1-/- mice as compared to controls, an effect that was associated with an enhancement in spine density and size.These data indicate that Pin1 controls the synaptic content of NMDARs via PSD-95 prolyl-isomerization and the expression of dendritic spines, both required for the maintenance of long-term potentiation.

Overall, this study highlights the crucial role of Pin1-dependent signalling in the functional organization of both inhibitory and excitatory synapses.

ABBREVIATIONS

AChE	Acetylcholinesterase
AD	Alzheimer disease
AMPA	α-amino-3-idrossi-5-metil-4isoxazolone propinato
AMPAR	AMPAreceptor
AP2	Adaptor protein 2
APP	Amyloid precursor protein
CaMKII	Ca^{2+}/calmodulin-dependent protein kinase
CAML	Calcium-modulating cyclophilin ligand
CB	Collybistin
CDK	Cyclin-dependent kinase
c-JNK	c-Jun N-terminal kinase
CK2	casein kinase II
CNS	Central Nervous System
D-AP5	D-2-amino-5-phosphonopentanoic acid
DLG1	Drosophila disc large tumor suppressor
DNQX	6,7-dinitroquinoxaline-2,3-dione
EGFP	Enhanced Green Fluorescent Protein
EPSC	Excitatory Post Synaptic Current
ERK 1	Extracellular signal-regulated kinases
GABA	Gamma-Aminobutyric Acid
$GABA_AR$	GABA receptor
GBD	Gephyrin binding domain

GK	Guanylate kinase
GlyR	Glycine receptor
GRIP1	Glutamate receptor interacting protein 1
GSK-3β	Glycogen synthase kinase 3 beta
HAP1	Huntingtin-associated protein 1
HEK293T	Human Embryonic Kidney 293 cells, transformed by T antigen
iGluR	ionotropic Glutamate Receptors
IPSC	Inhibitory Post Synaptic Current
LRRTM	Leucine-Rich Repeat Transmembrane
LTD	Long-Term-Depression
LTP	Long-Term- Potentiation
MAGUks	Membrane-associated guanylate kinase
mGluRs	metabotropic Glutamate Receptors
nAChRs	nicotinic acetylcholine receptors
NLs	Neuroligins
NMDA	N-Methyl-D-Aspartate
NMDA-R	NMDA receptor
Nrxs	Neurexins
PDZ	PSD95-Dlg1-zo1
PH	Pleckstrin homology
Pin1	Protein interacting with NIMA
PKA	Protein kinase A
PKB or AKT	Protein kinase B
PKC	Protein kinase C

PP1	Protein phosphatase 1
PPIases	Peptidyl-prolyl cis-trans isomerases
PSD	Post Synaptic Density
PSD-95	Postsynaptic density protein 95
SAP-97	Synapse-associated protein 97
SH3	Src-homology 3
TM	Transmembrane
TPMPA	1,2,5,6-tetrahydropyridin-4-yl)methylphosphinic acid
VGAT	Vesicular GABA Transporter
VGLUT	Vesicular Glutamate Transporter
Zo-1	Zonula occludens-1 protein

INDEX

“A scientist in his laboratory is not a mere technician: he is also a child confronting natural phenomena that impress him as though they were fairy tales. ”
-Marie Curie-

1.INTRODUCTION

1.1 The synapse

1.1.1 Structural organization of synapses

The correct functioning of the central and peripheral nervous systems relies on the efficient communication between highly specialized cell types called neurons. These highly polarized cells are designed to efficiently transmit the nervous impulse at specific functional points of membrane apposition called synapses, a term introduced by Charles Sherrington in 1897 (Foster, 1897). Synapses are intercellular junctions built between neurons or between neurons and other excitable cells where signals are propagated from one cell to another with high spatial precision and speed. Synapses can be divided into electrical or chemical depending on whether transmission occurs through the direct or indirect propagation of electrical and chemical signals (neurotransmitters), respectively.

Chemical synapses are composed of three compartments: the presynaptic terminal, the synaptic cleft and the postsynaptic reception apparatus. Presynaptic terminals are characterized by the presence of a high concentration of synaptic vesicles filled with neurotransmitter substances, e.g small peptides or amino acids or their derivatives that are released into the synaptic cleft in an activity-dependent manner (Kandel et al., 2000). Once released, neurotransmitter molecules bind and activate neurotransmitter receptors embedded in the post-synaptic density (PSD), an electron-dense protein matrix containing also scaffold proteins, signaling enzymes and cell adhesion molecules (Harris and Weinberg, 2012; Sheng and Hoogenraad, 2007).

Neurotransmitters are classified as excitatory, inhibitory or modulatory depending on their action on selected receptor types. In the brain, L-glutamate is considered to be the most abundant excitatory neurotransmitter, whereas γ-aminobutyric acid (GABA) is the main inhibitory neurotransmitter.

Morphological studies of CNS synapses led Edward George Gray to classify them into two major groups, type I and type II (Grey, 1959) or asymmetric and symmetric, respectively (Colonnier, 1968). Type I synapses, which involve dendritic spines and shafts, are formed by axon terminals that contain round vesicles (Akert et al., 1972). These synapses have a synaptic cleft of about 20 nm and a prominent PSD on the cytoplasmic face of the

postsynaptic membrane. Type II synapses involve neuronal perikarya and dendritic shafts. In respect to type I, type II synapses have a narrower synaptic cleft (about 12 nm), and a less prominent density beneath the postsynaptic membrane. In addition, the vesicles in the presynaptic terminals are smaller. It is widely accepted that terminals with larger vesicles (belonging to asymmetric synapses) are excitatory while those with smaller vesicles (belonging to symmetric synapses) are inhibitory (Van Spronsen and Hoogenraad, 2010) (Fig.1).

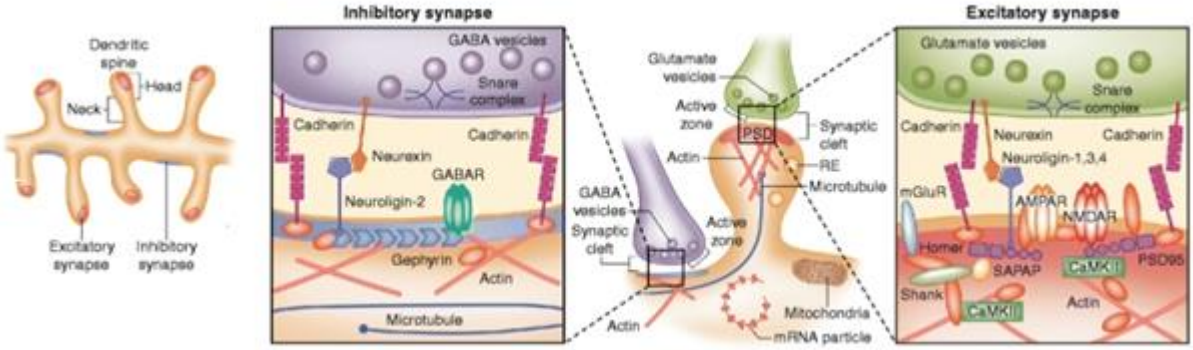

Figure 1. Molecular architecture of excitatory (type I) and inhibitory (type II) synapses: Excitatory synapses are targeted on mature mushroom-shaped spines and contain a prominent postsynaptic density (PSD), while inhibitory synapses are present along the dendritic shaft and lack postsynaptic thickening (Modified from Van Spronsen and Hoogenraad, 2010).

1.1.2 Synaptic transmission

Excitatory and inhibitory inputs contribute to set the resting membrane potential of the cell, which in turn determines whether the neuron will reach the threshold for producing an action potential. Excitatory inputs depolarize the neuron, bringing it closer to the threshold for firing an action potential, whereas inhibitory inputs hyperpolarize the neuron, bringing the membrane potential away from the action potential threshold. Once the action potential is initiated, it propagates along the axon and triggers exocytosis of synaptic vesicles and the release of neurotransmitters from the axon terminal. The properties of the postsynaptic receptors binding the neurotransmitter determine whether the resulting synaptic potential is excitatory or inhibitory.

The unidirectional signal propagation inferred by Cajal and his contemporaries has been challenged by recent findings revealing that information can be retrogradely transmitted from the postsynaptic neuron to the presynaptic one *via* small molecules, neuromodulators

(Nusbaum et al., 2001; Kandel et al., 2000) and cell adhesion molecules. In particular a growing number of synaptic cell adhesion molecules have been identified, being the neurexins/neuroligins family the most extensively characterized (Scheiffele et al., 2003).

1.1.3 Synapse as dynamic device

For long time, synapses were viewed as simple devices able to transfer information between neurons or neurons and other excitable cells. It was thought that these connections, once established during development, were relatively fixed in their strength, just as hard-wired elements built for fast electrochemical transmission. One exciting development in neurobiology is the realization that synapses are instead extremely dynamic: they are able to change their strength as a result of either their own activity or the activity of the network. These changes can be achieved through different mechanisms operating at both presynaptic and postsynaptic levels. For instance, at presynaptic level, their efficacy can be influenced by changes in the probability of transmitter release and/or changes in the number of release sites (Turrigiano and Nelson, 2004). At postsynaptic level, ionotropic neurotransmitter receptors can undergo alterations in their biophysical properties, such as conductance or open probability, as well as in their abundance (Banke et al., 2000; Derkach et al., 1999; Scannevin and Huganir, 2000). In this context reversible phosphorylation of synaptic proteins represents one of the major mechanisms promoting the rapid and reversible remodeling at both synaptic compartments. In keeping with this notion, the majority of synaptic proteins are indeed phosphoproteins.

This thesis work focuses on the molecular mechanisms operating at the postsynaptic site. In particular, we aimed at investigating the functional role of proline-directed phosphorylation signaling cascade in remodeling the post-synaptic devise by acting on pivotal constituents such as protein scaffolds and cell adhesion molecules.

1.2 Proline-directed phosphorylation signaling cascade

1.2.1 General features of the signaling cascade

The phosphorylation of proteins on serine or threonine residues that immediately precede a proline (phosphoserine/phosphothreonine–proline) represents a signaling cascade which plays well-recognized roles in regulating cellular processes such as cell proliferation and differentiation (Blume-Jensen and Hunter 2001; Lu et al., 2002a). The main feature of such

signaling is to promote conformational changes on the target substrate that are not simply due to the phosphorylation event *per se*. Phosphorylation in fact generates recruitment sites for a unique rotamase, the peptidyl-prolyl isomerise Pin1, which catalyzes the isomerisation of the peptide bond preceding proline thus switching the target substrate between different conformations that are functionally diverse (Ranganathan et al., 1997; Shen et al., 1998) (Fig. 2). The existence of such a mechanism relies on the unique stereochemistry of proline residues that, within native polypeptides, can adopt both *cis* and *trans* conformations. Even though the amino acid sequence surrounding proline residues can influence the amount of *cis* and *trans* isomers present into a given polypeptide, it has been estimated that the *cis* conformation occurs with a frequency of about 5-10% in protein structure (Schonbrunner and Schmid, 1992). *Cis*-to-*trans* and *trans*-to-*cis* isomerizations occur spontaneously but at very low rate, which becomes even slower upon serine or threonine phosphorylation (Yaffe et al., 1997). These conversions are therefore accelerated by several order of magnitude by ubiquitous enzymes named peptidyl-prolyl *cis-trans* isomerases (PPIases) or rotamase (Fischer and Aumuller, 2003).

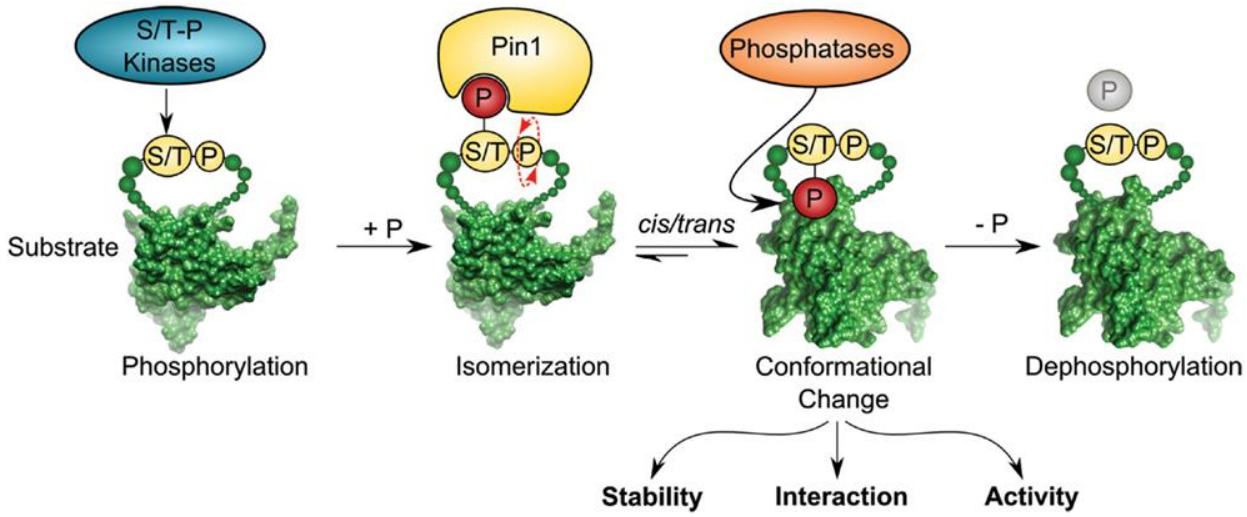

Figure 2. Pin1 isomerase induces *cis/trans* conformational change of substrates containing pSer/Thr–Pro motifs: Ser/Thr–Pro-directed kinases phosphorylate diverse substrates to create a putative binding site for the foldase Pin1. In a subsequent step Pin1 can catalyze *cis/trans* isomerization of the protein target (From Polonio-Vallon et al., 2014).

PPIases comprise four families that are unrelated in their primary sequences and in their three-dimensional structures even though they catalyze the same reaction: cyclophilins (Cyps), FK506-binding proteins (FK506s), parvulins and the recently identified PP2Aactivator PTPA (Jordens et al., 2006). Pin1 and its homologs belong to the parvulin subfamily of PPIase

and are the only known enzymes able to isomerize phosphorylated ser/thr-pro sites resistant to the catalytic action of conventional prolyl-isomerases (Yaffe et al., 1997). This unique feature renders the action of Pin1 extremely relevant in modulating signalling events, taking into account that Pro-directed kinases and phosphatases are conformation-specific and act only on the *trans* conformation (Weiwad et al., 2000; Zhou et al., 1999).

1.2.2 The effector molecule of the signalling cascade: the prolyl-isomerase Pin1

Pin1 is a relatively small enzyme (18 kDa), which is arranged in two identifiable domains connected by a flexible linker: an N-terminal WW domain (named after two invariant Trp residues) (Lu et al., 1999) and a catalytic C-terminal (rotamase) domain that is distinct from other conventional PPIase (Ranganathan et al., 1997).

Both domains recognize phosphorylated serine or threonine-proline motifs (Shen et al., 1998; Lu et al., 1999). Since the WW domain possesses a ten-fold higher binding affinity for phosphorylated peptides than the PPIase domain *in vitro*, it is thought to be involved in substrate recognition (Lu et al., 1999; Smet et al., 2005). Nevertheless, the catalytic PPIase domain also exhibits structural elements critical for phosphate-directed binding (Yaffe et al., 1997). For instance, Lys-63 together with Arg-68 and Arg-69 were shown to build a positively charged phosphate-binding loop to coordinate the phosphorylated serine or threonine (Ranganathan et al., 1997, Behrsin et al., 2007).

It is still poorly understood how these two domains coordinate their activities on full-length substrates; it is also unclear whether all target phospho-proteins interact with the two domains of Pin1 in the same manner. At least several models have been proposed to explain how both domains of Pin1 coordinate binding and isomerization reactions: the sequential, multimeric, and catalysis-first models (Fig. 3). The sequential model relies on the apparent difference in affinity of the two domains for the target sequence. It proposes that the WW domain must either bind and then release, allowing the PPIase domain to catalyze the isomerization of the binding site; or remain bound, allowing the PPIase domain to act on one or more other sites in the same molecule (Zhou et al., 1999; Lu et al., 2002a). The WW-domain-directed sequential model is consistent with the large number of multiple phosphorylated Pin1 substrates. The multimeric model proposes that the WW domain anchors Pin1 in multimeric complexes that include the upstream kinase creating the Pin1 binding site (Jacobs et al., 2003). Thus, the substrate is phosphorylated and isomerized by two members of the same complex, with the PPIase domain already in high local

concentration when its binding site is created. Finally, the catalysis-first model proposes that the PPIase domain is required to create WW domain binding sites (Wintjens et al., 2001). In all available structures of the WW domain bound to substrate peptides, the binding site is in the *trans* conformation (Verdecia et al., 2000; Wintjens et al., 2001; Zhang et al., 2007). If the WW domain exhibits isomer-specific binding, this would give Pin1-catalyzed isomerization a *cis*-to-*trans* direction. The PPIase domain would isomerize the substrate and form a WW-domain binding site. This would allow the WW-domain to sequester the pool of trans-substrate so that the PPIase domain could not catalyze the reverse isomerisation reaction (Fig. 3).

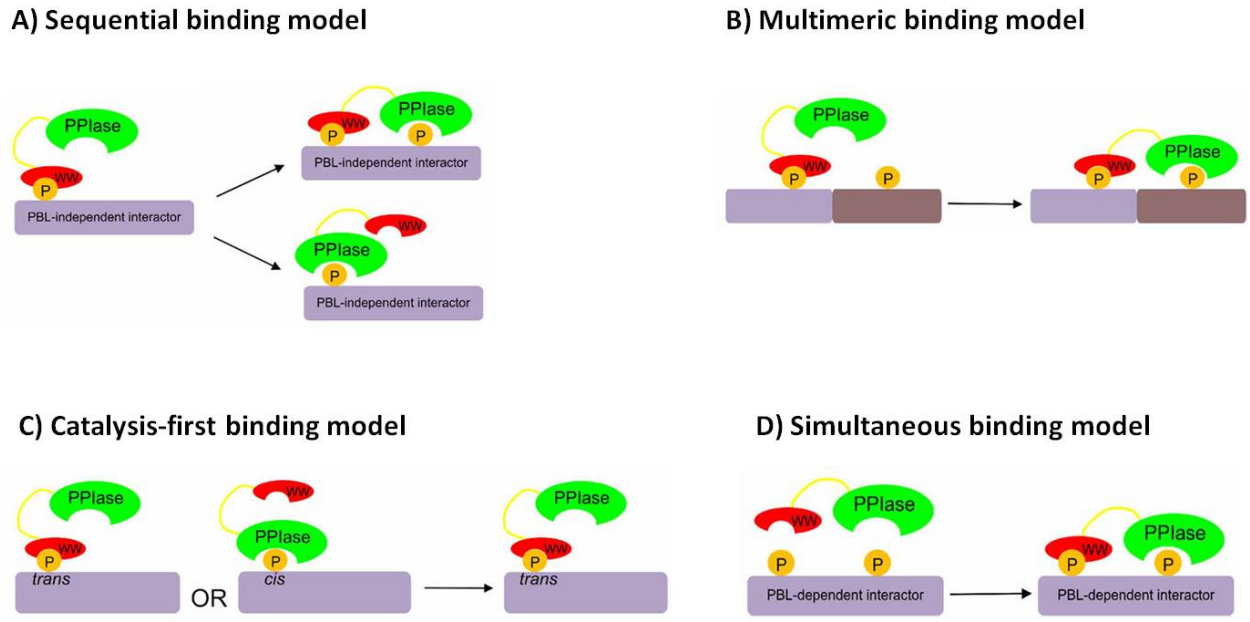

Figure 3. Models proposed to explain how both domains of Pin1 coordinate binding and isomerization reactions (A) The sequential binding model proposes that the WW domain binds first, bringing the PPIase domain proximal to its targets (Zhou et al., 1999; Lu et al., 2002). **(B)** The multimeric binding model proposes that the WW domain anchors Pin1 in multimeric complexes, allowing the PPIase domain to target other substrates in the complex (Jacobs et al., 2003). **(C)** The catalysis-first binding model proposes that the PPIase domain catalyzes the *cis* to *trans* isomerization of the targets to allow *trans*-isomer-specific WW domain binding (Wintjens et al. ,2001). **(D)** The simultaneous binding model proposes that the WW and PPIase domains bind simultaneously with low-affinity to multiply phosphorylated targets (From Innes et al., 2013).

Although the exact catalytic mechanism is still debated, Pin1 recruitment by its phosphorylated substrates produces marked kink in the backbone of the peptide chain. As a consequence, the substrate conformation is switched to a functionally different state, which represents the molecular basis for this type of signaling.

1.2.3 Pin1 functions in actively dividing cells

Pin1 was initially discovered by its ability to interact with the fungal mitotic kinase NIMA (Never In Mitosis A), pointing to an exclusive role for Pin1 in mitosis (Lu et al., 1996). Several studies have then extended the involvement of Pin1 in regulating cell cycle progression, DNA replication checkpoint and proliferation. Pin1 regulates progression of the cell cycle by interacting with a large number of mitotic phosphoproteins including cyclin D1, Cdc2 and Cdc25 D as well as transcription factors such as p53 (Zacchi et al., 2002; Zheng et al., 2002), c-Jun N-terminal kinase (c-JNK) (Wulf et al., 2001; Pulikkan et al., 2010), β-catenin (Ryo et al., 2001; Nakamura et al., 2012). Pin1 also regulates structure and function of RNA polymerase II during transcription (Xu at al., 2003). The identification of a growing number of Pin1 substrates has clearly unveiled that this enzyme exerts control over a plethora of cellular processes including transcription and RNA processing (Ryo et al., 2003; Xu and Manley 2007; Lu and Hunter 2014), DNA damage responses (Yeh and Means 2007; Polonio-Vallon et al., 2014), germ cell development (Atchison et al., 2003), and self-renewal of embryonic stem cells (Moretto Zita et al., 2010)**.**

1.2.4 Pin1 functions in neuronal context

While the different roles of Pin1 in dividing cells have long been established and characterized, its function in post-mitotic neurons in general, and at synapses in particular, is still poorly characterized. Pin1 levels, extremely high in neurons, increase upon neuronal differentiation (Lu et al., 1999; Liou et al., 2003; Hamdane et al., 2006), suggesting that this enzyme plays important roles in the nervous system distinct from cell cycle regulation and proliferation. It is interesting to note that mice lacking Pin1 expression develop a premature-age-dependent neurodegeneration similar to Alzheimer disease (AD) in humans that is characterized by neurofibrillary tangles composed mainly of abnormally phosphorylated microtubule-associated protein Tau and by an increase in the pathogenic processing of APP (Liou et al., 2003; Pastorino et al., 2006). Tau is phosphorylated at more than 30 sites and many proline-directed sites are hyperphosphorylated in AD brains (Wang et al., 1995; Sontag et al., 1996). Recent studies suggest that the lack of de-phosphorylation rather than increased phosphorylation contributes to the hyperphosphorylated state of Tau. In this context, Pin1 has emerged to play a protective role against the development of tangles since only upon Pin1-driven *cis-trans* isomerisation of Tau phospho(Ser/Thr)-Pro motifs the

phosphatase PP2A will efficiently dephosphorylate the substrate in *trans* conformation, thereby restoring the ability of Tau to bind microtubules and to promote their proper assembly *in vitro*. In agreement with this notion, in AD neurons, Pin1 is significantly down-regulated or inactivated by oxidative modifications (Sultana et al., 2006), promoter polymorphisms (Segat et al., 2007) and sequestration into pathological neurofibrillary tangles (Lu et al., 1999; Thorpe et al., 2001). Pin1 is also an essential regulator of another key player of AD neurodegeneration, the amyloid-β protein precursor. APP is a transmembrane glycoprotein whose normal function is still poorly understood (Guo et al., 2012) but whose cleavage products can generate amyloidogenic peptides that aggregate into plaques. Phosphorylation of APP at Threonine 668 has been shown to shift the processing of APP from the toxic amyloidogenic to the protective non-amyloidogenic due to Pin1 dependent *cis* to *trans* conformational change on APP (Lee et al., 2003). In addition Pin1 can indirectly regulate both APP processing and Tau accumulation by inhibiting the kinase activity of GSK3β, one of the kinases responsible for the phosphorylation of both Thr-668 in APP and Thr-231 in Tau (Ma et al., 2012).

A deregulation of proline-directed phosphorylation has been found also in other neurodegenerative disorders, like Parkinson and Huntington diseases. Pin1 has been shown to be present in Lewy bodies of Parkinson's patients and is known to facilitate the formation of α-synuclein inclusions in a cellular model of α-synuclein aggregation (Ryo et al., 2006). In Huntington's disease mutated forms of Huntingtin increase phosphorylation of the tumor suppressor p53 on a specific Pin1 consensus site Ser-46. Pin1-driven conformational changes on p53 shifts p53 response from cell-cycle arrest to apoptosis, leading to neuronal death (Grison et al., 2011).

1.2.5 Pin1 functions at synapses

There is a large body of evidence that phosphorylation of several components of the PSD affects its structural organization and dynamics. Mass spectrometry analysis performed by Jaffe and colleagues (2004) to identify phosphorylation sites on excitatory PSD proteins unveiled that phosphorylated Serine residues in several of the identified phosphorylation sites were followed by Prolines, suggesting a prominent involvement of proline directed kinases in the regulation of PSD components (Jaffe et al., 2004). Even though for certain phosphorylation sites the signaling cascade involved has been identified and the functional

consequences on the target protein characterized, the possible contribution of prolyl-isomerization has been completely neglected.

Only in 2010, Westmark and colleagues demonstrated for the first time that the prolyl-isomerase Pin1 is present and constitutively active in dendritic shafts and spines where it exerts a negative control on dendritic mRNA translation, therefore interfering with new protein synthesis required to sustain the late phase of LTP (Westmark et al., 2010). Pin1 is also present at inhibitory glycinergic synapses, where it is recruited by gephyrin, the main scaffolding molecule of the inhibitory system to enhance its ability to interact with GlyR (Zita et al., 2007).

1.3 Inhibitory GABAergic synapses

1.3.1 Postsynaptic organization of inhibitory GABAergic synapses

Inhibitory GABAergic synapses are mainly formed on the shaft of dendrites or around the cell body. At electron microscopy level, they show only a slight electron-dense thickening associated with the post-synaptic membrane and hence they are referred as symmetric (type II) synapses (Fig. 4).

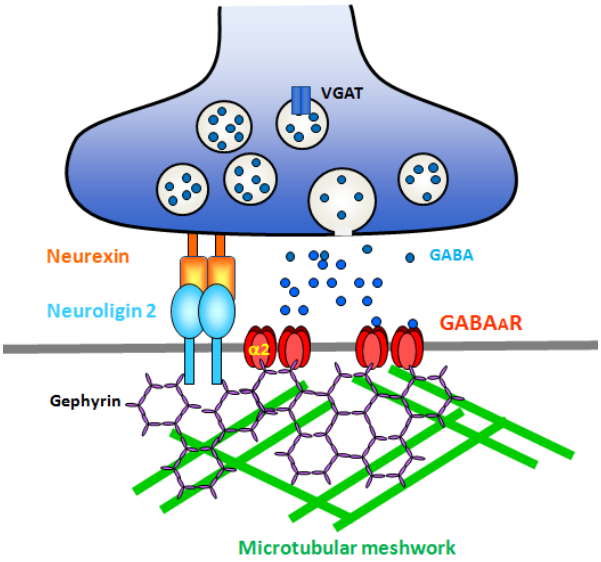

Figure 4. Organization of inhibitory GABAergic synapses.

The cardinal components of the postsynaptic specialization are represented by the ionotropic neurotransmitter receptors for GABA, or $GABA_A$ receptors ($GABA_ARs$) (Gray 1959; Peters and Palay, 1996). These receptor channels are correctly targeted, clustered and stabilized at postsynaptic membrane by virtue of their interaction with a large number of other proteins. Among them, gephyrin originally identified as a membrane-associated protein (Pfeiffer et al.,

1982) has emerged to play a crucial role in the functional organization of inhibitory synapses. Through its self-oligomerizing properties, gephyrin forms sub-membranous cytoplasmic lattices able to trap a high number of inhibitory neurotransmitter receptors and link them to the underlying cytoskeleton (Fritschy et al., 2008).

Another class of molecules, possibly involved in differentiation and maturation of GABAergic synapses is represented by the cell adhesion molecules of the neuroligins family (Varoqueaux et al., 2004; Huang and Scheiffele 2008). These transmembrane proteins, by interacting with presynaptically localized neurexins, mediate transynaptic recognition between pre- and post-synaptic compartments and coordinate signaling processes essential for the establishment, specification and plasticity of synapses (Chih et al., 2005; Graf et al., 2004).

1.3.2 $GABA_A$ receptors

1.3.2.1 GABAA receptor structure

$GABA_A$Rs are members of the superfamily of Cys-loop ligand-gated ion channels that include nicotinic acetylcholine receptors (nAChRs), glycine receptors (GlyR), and ionotropic 5-hydroxytryptamine (5-HT3) receptors (Unwin, 1989). nAChRs and 5-HT3 receptors are cation-selective channels while $GABA_A$Rs and GlyRs are anionic-selective channels. All the subunit members of this family show 30 % sequence homology but have a greater similarity at the level of their secondary and tertiary structure (Connolly et al., 2004).

These receptors are organized as pentameric membrane-spanning proteins surrounding a central pore forming the ion channel. Mature subunits share a common topological organization, which consists of a large extracellular N-terminal domain containing the Cys loop, followed by four hydrophobic transmembrane sequences (M1-M4). The N-terminus contains the binding site for the ligand and various drugs commonly used to cure several types of neuropsychiatric disorders including anxiety and epilepsy. M2 forms an amphipathic helix crucial for receptor channel gating and selectivity. Between M3 and M4 there is a large intracellular loop involved in protein-protein interaction.

Several proteins interacting with this cytosolic loop, implicated in regulation of receptor trafficking and anchoring at the postsynaptic membrane, have been identified. (Whiting, et al 1999; Vithlani et al., 2011) (Fig. 5) The short C-terminus of the receptor subunit is located extracellularly as the N-terminus.

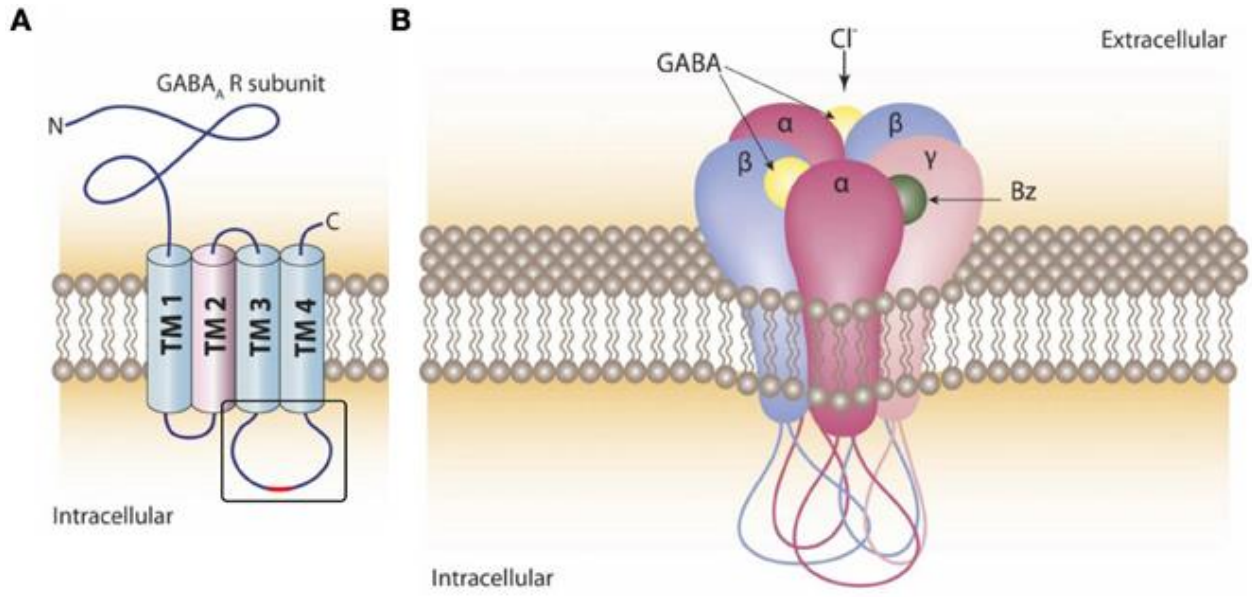

Figure 5. Domain-structure of GABA$_A$R- and its pentameric assembly: (A) Schematic representation of the transmembrane topology of subunits from GABA$_A$R. The intracellular loop between TM3 and 4 presents the main sites of interaction with intracellular scaffold and signaling proteins. **(B)** Pentameric assembly of subunits within the GABA$_A$R. The intracellular loops of all five subunits promote interactions with other proteins (from Tretter et al., 2012).

In mammals, GABA$_A$ receptors are highly heterogeneous. Twenty different subunits encoded by different genes, have been cloned to date. They have a molecular mass ranging between 48kDa (γ2) and 64kDa (α4), and can be subdivided into seven structurally related subfamilies (α1–6, β1–4, γ1–3, ε, δ, θ, π and ρ1–3) with a high degree of homology (Sieghart and Sperk, 2002). In addition, alternative splicing and RNA editing further increases their diversity (Wisden, et al., 1992). The most common native receptor stoichiometry is two α, two β and one γ/δ/ε subunits (Whiting et al., 2003).

1.3.2.2 GABA$_A$ receptors dynamic modulation

GABA$_A$Rs are not fixed entities on the neuronal membrane but they continuously cycle between the plasma membrane and intracellular compartments as well as between synaptic and extra-synaptic pools *via* lateral diffusion. In particular, the relative rate of receptor delivery (exocytosis), removal (endocytosis) and endocytic sorting (recycling) determines the steady-state levels of receptors on the neuronal surface available for a rapid exchange between extra-synaptic and synaptic compartments, thus contributing to the regulation of receptor number at synapses under basal conditions and during synaptic plasticity (Arancibia-Cárcamo and Kittler 2009; Kneussel and Loebrich, 2007; Triller and Choquet, 2005) (Fig 6.)

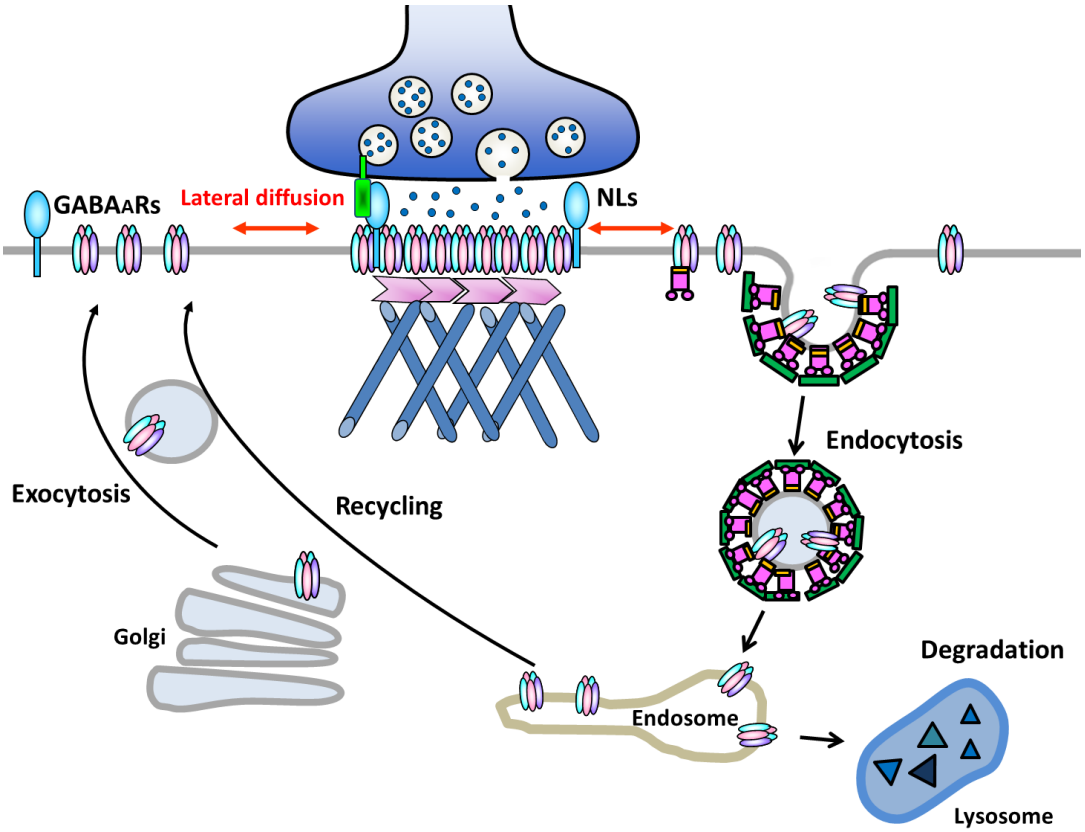

Figure 6. Trafficking of $GABA_ARs$: Lateral diffusion within the plasma membrane allows a continuous exchange between diffuse receptor populations and synaptic receptor clusters. The synaptic localization of α2-containing $GABA_ARs$ is maintained by gephyrin, which binds to microtubules and actin interactors**.** Clathrin-dependent endocytosis is the major internalization mechanism for neuronal $GABA_ARs$. The intracellular loops of β and γ subunits interact with the clathrin adaptor protein 2 (AP2) complex. Once endocytosed in clathrin-coated vesicles, the vesicles are uncoated and fuse with early or sorting endosomes. At this step they can be recycled to the plasma membrane or degraded in lysosomes.

Trafficking events are modulated by phosphoprylation/dephosphorylation at specific sites of receptor large intracellular domains. Calcium calmodulin kinase II (CaMKII)-mediated phosphorylation of Ser- 383 of the $GABA_AR$ β3 subunit was shown to promote the exocytosis and postsynaptic accumulation/immobilization of $GABA_ARs$ at synapses (Petrini et al., 2014). Along the same line, the serine/threonine kinase Akt, by phosphorylating Serine 410 of the β2 subunit, increases the number of surface $GABA_ARs$, an effect associated with an increase in inhibitory synaptic transmission in the hippocampus *in vitro* and *in vivo* (Wang et al., 2003). Phosphorylation events catalyzed by PKA, PKC, Akt and Src within the binding motifs for the endocytic adaptor protein AP2 on $GABA_ARs$ β (Ser- 408 on β1, Ser-410 in β2 in and Ser-408/409 in β3) and γ2 subunits was shown to preclude $GABA_ARs$ removal *via* clathrin-mediated endocytosis with consequent increase of their surface expression (Kittler et al., 2000; Kittler et al., 2008; Herring et al., 2003, Jacob et al., 2009; Smith et al., 2012) (Fig. 7).

Decrease of $GABA_AR$s can be achieved upon dephosphorylation of these sites by the activity of protein phosphatase 1 (PP1), PP2A and calcineurin (Brandon et al., 2002; Wang et al., 2003; Kittler et al., 2008). Regarding the fate of $GABA_AR$s internalized and localized in the endosomal compartment, they can either be ubiquitinated for lysosomal degradation (Bedford et al., 2001) or they can be recycled back to the cell membrane. Regulatory proteins such as Huntingtin-associated protein 1 (HAP1) (Kittler et al., 2004) and the calcium-modulating cyclophilin ligand (CAML) (Yuan et al., 2008) can interact with the cytoplasmic domain of the β and γ subunits, thus facilitating vesicular transport.

Phosphorylation events can also modulate the affinity of receptor/gephyrin scaffold interaction. For instance a phosphomimetic mutation of Thr- 347, located in the intracellular loop of the α1 subunit of the $GABA_AR$, was shown to reduce the affinity of $GABA_AR$-gephyrin interaction and receptor trapping at synapses (Petrini et al., 2014).

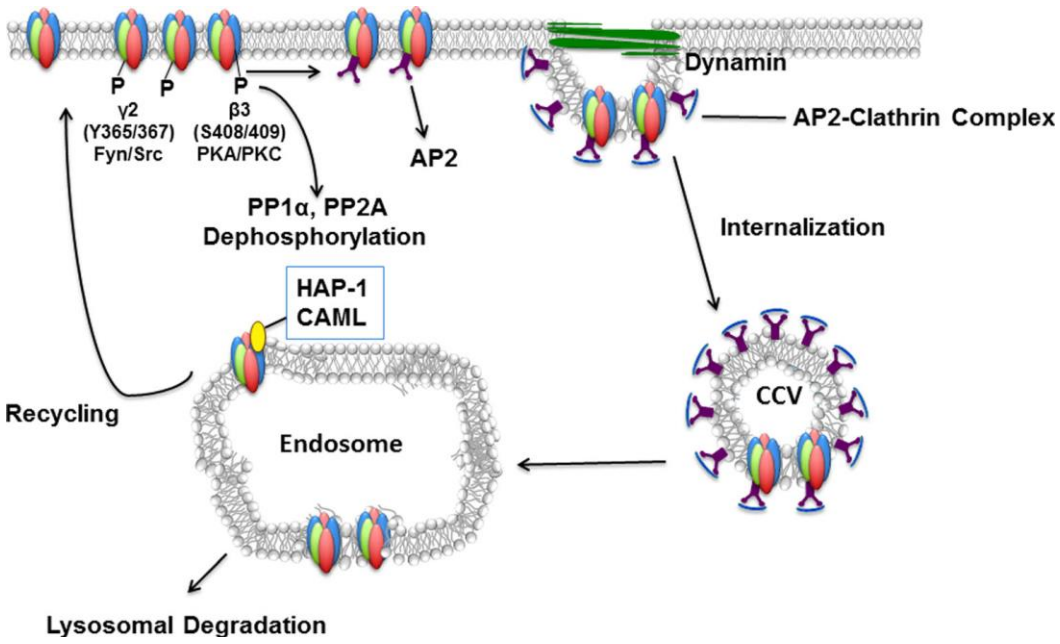

Figure 7. The cell surface stability of $GABA_AR$s is further regulated by phosphorylation: The intracellular loops of β3 and γ2 subunits interact with the clathrin adaptor protein 2 (AP2) complex. Phosphorylation events catalyzed by PKA, PKC, Akt and Src inhibit this interaction by blocking clathrin-dependent endocytosis and increasing cell surface receptor levels (Modified from Comenencia-Ortiz et al., 2014).

Likewise, a PKC-mediated phosphorylation of Serine 403, in the cytoplasmic domain of the GlyR beta subunit, was shown to increase receptor lateral mobility at synapses due to a reduction in the binding affinity between GlyR intracellular loop and gephyrin (Specht et al., 2011). Beside receptor phosphorylation, other types of post-translational modifications have been implicated in the control of surface expression of $GABA_AR$s. For instance, ubiquitination

of the β3 subunit of newly assembled receptors can redirect them from the ER into the cytosol to promote their subsequent degradation, thus depressing the efficacy of inhibitory transmission (Brandon et al., 2000; Comenencia-Ortiz et al., 2014; Petrini and Barberis, 2014). This mechanism is bi-directional, therefore if more receptors are required at synapses, their ubiquitination will be downregulated accordingly. Ubiquitination can also trigger receptors degradation *via* the lysosomal pathway when it modifies the intracellular loop of the γ2 subunit (Arancibia-Cárcamo and Kittler 2009). Another post-translational modification is palmitoylation, a reversible and covalent attachment of fatty acids, such as palmitic acid, to cysteine residues of the target substrate. The palmitoylation of the γ2 subunit of the $GABA_AR$ has been shown to favor the assembly and clustering of $GABA_ARs$ by promoting their translocation through the Golgi apparatus to the neuronal plasma membrane (Keller et al., 2004).

1.3.3.Gephyrin: the core scaffolding molecule of GABAergic synapses

1.3.3.1 Functional role of gephyrin

The core component of the inhibitory postsynaptic device is represented by a single 93 kDa molecule, called gephyrin. This molecule was originally identified based on its tight association with purified GlyRs preparations (Pfeiffer et al., 1982; Schmitt et al., 1987; Prior et al., 1992) and found to be localized at the postsynaptic site of glycinergic synapses (Triller et al., 1985). It was later shown to be enriched at both glycinergic and GABAergic synapses (Triller et al., 1987). Gephyrin binds with high affinity to the β subunit of GlyRs, and is essential for GlyR clustering in various neuronal tissues including spinal cord, hippocampus and retina (Feng et al., 1998; Fischer et al., 2000; Lévi et al., 2004; Meyer et al., 1995). Gephyrin was shown to act as a cargo adaptor for long distance microtubule-based transport of GlyRs to and from distal neurites (Maas et al., 2006; Maas et al., 2009), and to stabilize GlyRs at synaptic sites once they are inserted in the neuronal membrane (Ehrensperger et al., 2007; Meier et al., 2001). The function of gephyrin at GABAergic synapses is puzzling due to the heterogeneity of $GABA_AR$ channels and the subunit specific clustering of $GABA_ARs$ by gephyrin-independent mechanisms (Kneussel et al., 2001; Lévi et al., 2004). Nevertheless, gephyrin does play a major role in $GABA_AR$ clustering as revealed by the drastic impairment of synaptic $GABA_AR$ clustering upon gephyrin depletion (Essrich et al., 1998; Kneussel et al.,

1999 ; Marchionni et al., 2009; Yu et al., 2007). Jacobs and colleagues in 2005 have clearly demonstrated that, in the absence of gephyrin, $GABA_A$Rs are more mobile, suggesting that gephyrin contributes to confine $GABA_A$Rs at synaptic sites (Jacob et al., 2005).

In addition to its role as post-synapses organizer, gephyrin performs also a metabolic function: it is involved in the biosynthesis of the molybdenum cofactor (Moco), a highly conserved molecule, required for the activity of molybdenum enzymes, essential for the survival of all organisms from bacteria to eukaryotes (Stallmeyer et al., 1999). Targeted disruption of the gephyrin gene in mice leads to a lethal phenotype shortly after birth, and neonates display deficits in Moco biosynthesis, as well as impaired glycine and $GABA_A$R clustering (Feng et al., 1998; Kneussel et al., 1999). Interestringly, a mutation in the *GPHN* gene was found in patient with a novel and extremely rare form of Molybdenum Cofactor Deficiency (type C). Amplification of patient DNA revealed a deletion, encompassing exons 2 and 3 of *GPHN* gene which determines a frameshift after only 21 codons of the normal coding sequence, thus ablating gephyrin expression. The complete lack of gephyrin protein induces a fatal phenotype characterized by severe neurological damage (Reiss et al., 2001; Reiss et al., 2011)

1.3.3.2 Gephyrin structure

Gephyrin is a multifunctional protein extensively conserved across the entire living kingdom. The gene encoding for gephyrin (*GPHN*) has a complex intron–exon structure, and its primary transcript is subjected to alternative splicing leading to several splice variants that are mostly tissue-specific (Paarmann et al., 2006). The most frequently mentioned splice variant P1 of gephyrin, first described by Prior and colleagues (1992), is composed of a 20 kDa N-terminal G-domain (residues 1-181) and a 43 kDa C-terminal E-domain (residues 318-736) connected by a central linker region (18-21 kDa), also referred as C-domain or intervening region (Feng et al., 1998), which contains the binding sites for several gephyrin-interacting proteins (Fritschy et al., 2008). The G- and E-domains are homologous to the bacterial Moco-synthetizing enzymes MogA and MogE, respectively (Fig 8). X-ray crystallography and cross-linking of individual gephyrin domains (Schwarz et al., 2001; Sola et al., 2001; Sola et al., 2004; Schrader et al., 2004) suggest that gephyrin N-terminal G-domain and C-terminal E-domain can form trimers and dimers, respectively (Kneussel and Betz, 2000).

Figure 8. Gephyrin structure: splice variant P1 of gephyrin is composed of a N-terminal G-domain from residues 1 to 181, a linker domain C-domain from residues 182 to 317 and C-terminal E-domain from residues 318 to 736.

A model has been proposed where gephyrin builds a bidimensional hexagonal lattice underneath the synaptic membrane (Kneussel and Betz, 2000; Schwarz et al., 2001; Sola et al., 2001, 2004; Xiang et al., 2001), which exposes a high number of binding sites for inhibitory receptor anchoring/clustering (Sola et al., 2004; Kim et al., 2006; Fritschy et al., 2008) (Fig. 9).

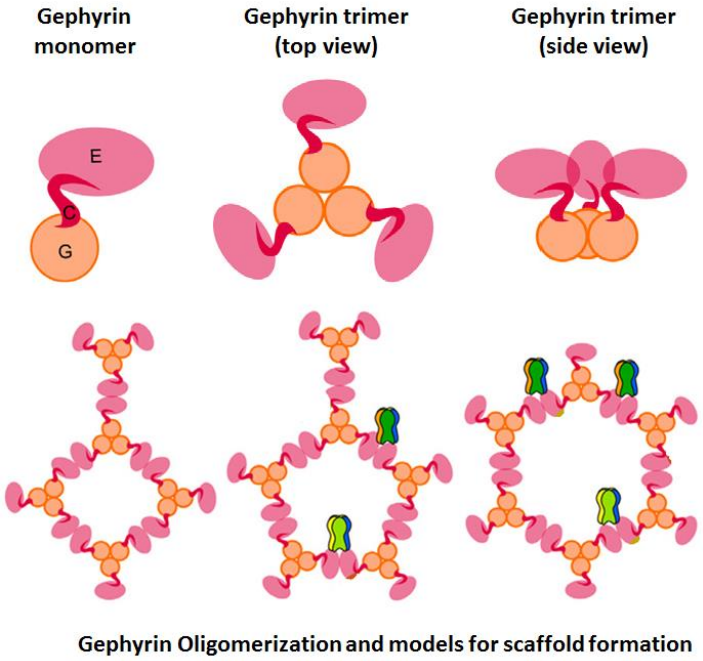

Figure 9. Gephyrin and $GABA_A$-R interaction: gephyrin monomers can builds a bidimensional hexagonal lattice underneath the synaptic membrane to interact with $GABA_A$ receptor (modified from Fritschy and Panzanelli 2014)

Consistent with this model, impairment of the oligomerization of G- and E-domains abolishes gephyrin clustering at synaptic sites (Saiyed et al., 2007; Lardi-Studler et al., 2007).Recently, an elegant study, based on quantitative three-dimensional nanoscopic imaging (Spetch et al., 2013), has confirmed that gephyrin clusters are indeed bi-dimensional planar structures, lying underneath the synaptic plasma membrane.

This study has also provided evidence that all gephyrin molecules in the cluster are potentially capable to interact with synaptic neurotransmitter receptors in a stoichiometry

ratio gephyrin-receptor of approximately 1:1. A consequence of this organization is that changes in gephyrin clustering could produce parallel changes in the number of receptors trapped by the scaffold, leading to alterations of synaptic strength.

1.3.3.3 Modulation of gephyrin scaffolding properties by phosphorylation

Post-synaptic gephyrin clusters contribute to ensure the accurate accumulation of neurotransmitter receptors in precise apposition to pre-synaptic release sites. They also must guarantee certain dynamism of the post-synaptic device to allow adjustment of receptors content necessary to sustain synaptic plasticity (Fritschy and Panzanelli 2014). Since gephyrin clusters are bidimensional planar structures lying underneath the synaptic plasma membrane, and all gephyrin molecules in the cluster are potentially capable to interact with neurotransmitter receptors, it has been proposed that changes in gephyrin clustering properties produce parallel modifications in the number of receptors trapped by the scaffold, leading to corresponding alteration of synaptic strength. Recent studies have identified specific signal transduction pathways that, by altering the scaffolding properties of gephyrin, indeed affect GABAergic transmission.

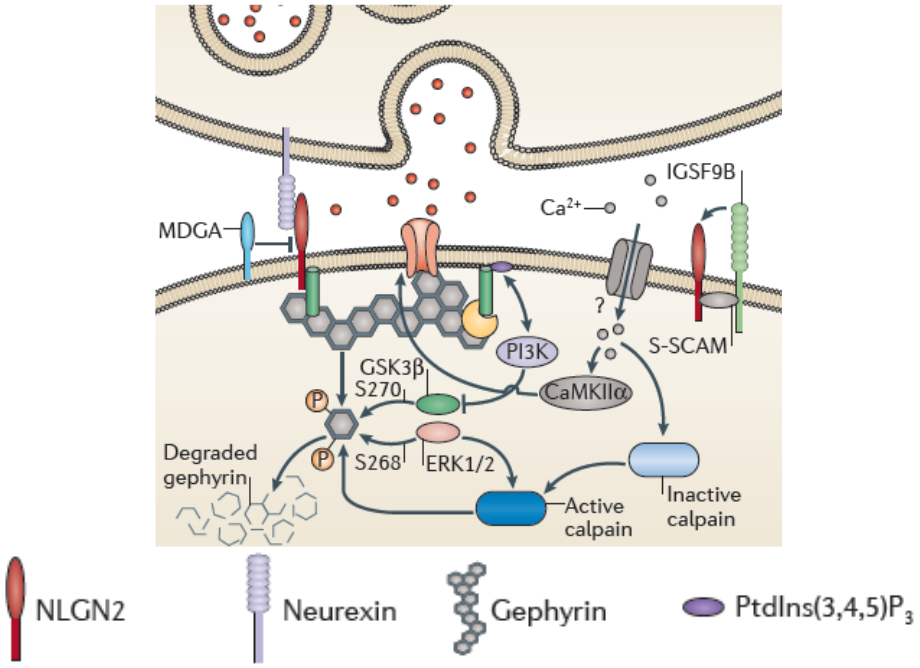

Figure 10 . Effects of gephyrin phosphorylation in GABAergic synaptic device

Work performed by Tyagarajan and colleagues (2011) demonstrated that the kinase belonging to the family of Glycogen Synthase Kinase 3 (GSK-3β) was able to phosphorylate gephyrin at serine 270 thus negatively regulating its cluster density. These authors were able

to show that gephyrin, once phosphorylated at this site, becomes substrate of the Ca^{2+}-dependent protease calpain-1, leading to its degradation (Tyagarajan et al., 2013). Soon after, ERK1, and to a lesser extent ERK2, were shown to be responsible for gephyrin phosphorylation at another Serine residue located in close proximity to the previously recognized target of GSK-3β activity, namely serine 268 (Ser268). ERK-mediated phosphorylation was shown to specifically affect the size of post-synaptic gephyrin clusters. Interestingly, ERK and GSK-3β–catalyzed phosphorylation at their corresponding positions were shown to be functionally interconnected, leading to a coordinated regulation of cluster size and density. All the observed changes in gephyrin clustering were associated with corresponding changes in amplitude and frequency of GABAergic transmission (Tyagarajan et al., 2011) (Fig. 10).

1.3.3.4 Modulation of gephyrin-neurotransmitter receptor interaction by phosphorylation

Although the findings described above have clearly highlighted the role played by phosphorylation in modulating gephyrin oligomerization, the possibility that phosphorylation impacts also on the attitude of gephyrin to interact with the $GABA_AR$ (or with other important components of the inhibitory synapse) has been neglected. The main reason for having ignored this aspect relies on the lack of a biochemical proof of a direct interaction between gephyrin and $GABA_ARs$. In fact it was neither possible to co-precipitate or co-purify gephyrin with $GABA_AR$ nor gephyrin was found in yeast-two-hybrid screens using several $GABA_AR$ intracellular loops as baits (Tretter et al., 2012). The unique evidence that phosphorylation on gephyrin can impact on the strength of receptor tethering at postsynapses concerns the glycinergic system and the involvement of proline-directed signaling cascade.

Gephyrin phosphorylation at three Serine residues located in its proline-rich domain, namely Serine 188, 194 and 200, were shown to promote the phosphorylation-dependent recruitment of Pin1. The functional consequence of Pin1-driven conformational changes on gephyrin was a selective enhancement of its binding affinity for the β subunit of the GlyR without affecting gephyrin oligomerization properties (Zita et al., 2007). Gephyrin possesses seven additional putative Pin1 consensus motifs outside the proline-rich region, mostly concentrated in its C-domain, and all of them have been found to be phosphorylated *in vivo* (Herweg and Schwarz 2012) (Fig. 11). This protein's region is positioned between the amino-

terminal G- and carboxyl-terminal E-domains, which are directly involved in gephyrin multimerization.

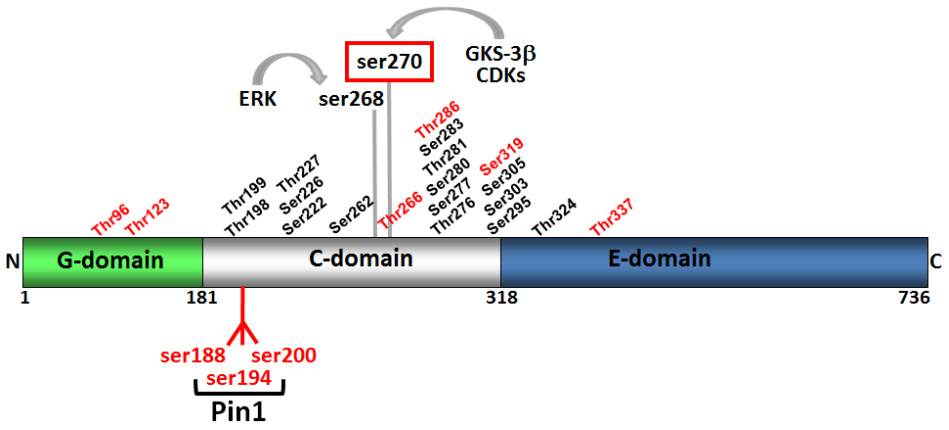

Figure 11. Schematic representation of gephyrin domains and the identified phosphorylation sites. Mass spectrometry has allowed identifying twenty-two serine and threonine residues within the C-domain and one (threonine 324), in the E-domain. In red are highlighted all putative Pin1 consensus motifs. Ser270 and Ser268 are recognized targets of GSK3β and ERK kinase activities, respectively.

It is interesting to note that the phosphorylation events catalysed by GSK3β and ERK1/2 and capable of modulating gephyrin clustering properties, are indeed consensus motifs for Pin1 recruitment. Even though the authors in their studies did not investigate the possible contribution of post-phosphorylation prolyl-isomerization in gephyrin clustering, these independent observations strongly suggest an active involvement of proline-directed signaling cascade in controlling GABAergic transmission.

1.3.3.5 Gephyrin binding partners

Several gephyrin-interacting proteins have been identified to date, linking gephyrin to the cytoskeleton, motor protein complexes, signal transduction mechanisms and phosphorylation-dependent processes (Arancibia-Cárcamo and Kittler, 2009; Fritschy et al., 2008) (Fig. 12). When ectopically expressed in human embryonic kidney cells (HEK 293), gephyrin forms large intracellular aggregates that trap glycine receptor β-subunits and other gephyrin-interacting partners (Kneussel et al., 1999; Zita et al., 2007). The reduction in size of these aggregates and their redistribution to submembrane regions was observed upon co-

expression of collybistin II, a brain-specific GDP/GTP exchange factor for the Rho-like GTPase Cdc42, identified as interacting partner of gephyrin by yeast two-hybrid screening (Kins et al., 2000). Like other dbl-like GEFs, collybistin harbors a dbl-homology (DH) and a pleckstrin-homology (PH) domain connected by a short linker sequence (Kins et al., 2000). Such DH/PH tandem represents a signature of this family of GEF. The DH-domain mediates the GDP/GTP-exchange activity of bdl-like oncoproteins, and the human homolog of collibystin hPEM-2 (Reid et al., 1999), while the PH region is thought to regulate the attachment of GEFs to membranes by binding to phosphoinositides (Hyvonen et al., 1995). In particular, the PH-domain of collybistin appears to interact specifically with membrane phosphatidylinositol-3-phosphate (PI3P); (Kalscheuer et al., 2009). Collybistin exists in three isoforms (CB I-III), differing in their C-termini and by the presence of an N-terminal *src* homology 3 (SH3) domain, which negatively regulates gephyrin targeting to the plasma membrane (Harvey et al., 2004; Papadopoulos et al., 2008).

SDS-PAGE and western blot analysis of whole brain lysates show that the vast majority of CB variants expressed in postnatal rodent brain contain an N-terminal SH3 domain, being the isoforms lacking it only barely detectable (Soykan et al., 2014). The SH3 domain is believed to maintain the protein in an inactive/close conformation through a mechanism based on intra-molecular interaction of the SH3 domain itself and the DH/PH tandem.

In this arrangement, the PH domain is masked and unavailable to interact with membrane phosphoinositides. Therefore only CB isoforms lacking the SH3 domain can promote a redistribution of gephyrin into small microclusters beneath the plasma membrane, while the corresponding variants provided of the SH3 domain are simply sequestered by the large gephyrin blobs (Papadopoulos and Soykan, 2011). Altogether, these finding suggest that, in specific neuronal subpopulations, SH3-containing CB isoforms must be locally activated by an SH3-interacting protein. Up to now, the cell adhesion molecule of the neuroligin family neuroligin2 (NL2) (Poulopoulos et al., 2009), the $\alpha 2$ subunit of $GABA_A$Rs (Saiepour et al., 2010) and the small GTP-binding protein TC-10 (Mayer et al., 2013) were identified as activator of collybistin.

Gephyrin provides a direct link with the cytoskeleton *via* its binding to polymerized tubulin (Kirsch et al., 1991). Further evidence for the role of gephyrin in microtubule-based transport was provided by its interaction with dynein and kinesin motor complexes (Fuhrmann et al., 2002; Maas et al., 2006; Maas et al., 2009). Gephyrin was shown to act as an adaptor protein

between GlyR carrying vesicles and microtubule motor complexes (namely the dynein light chain and kinesin family 5), mediating the transport of gephyrin-GlyR complexes to and from synapses (Maas et al., 2006; Maas et al., 2009). A similar role for gephyrin in the intracellular transport of $GABA_A$Rs has not been established yet. In addition to its association with the microtubules, gephyrin also interacts with several proteins of the actin cytoskeleton. Yeast two-hybrid screening revealed two gephyrin-interacting proteins that regulate actin polymerization, namely profilins 1 and 2 (Mammoto et al., 1998). Gephyrin was shown to form a complex with profilins and microfilament adaptors of the mammalian enabled (Mena)/vasodilator stimulated phosphoprotein (VASP) family, which are essential for submembranous actin filament generation and organization (Giesemann et al., 2003).

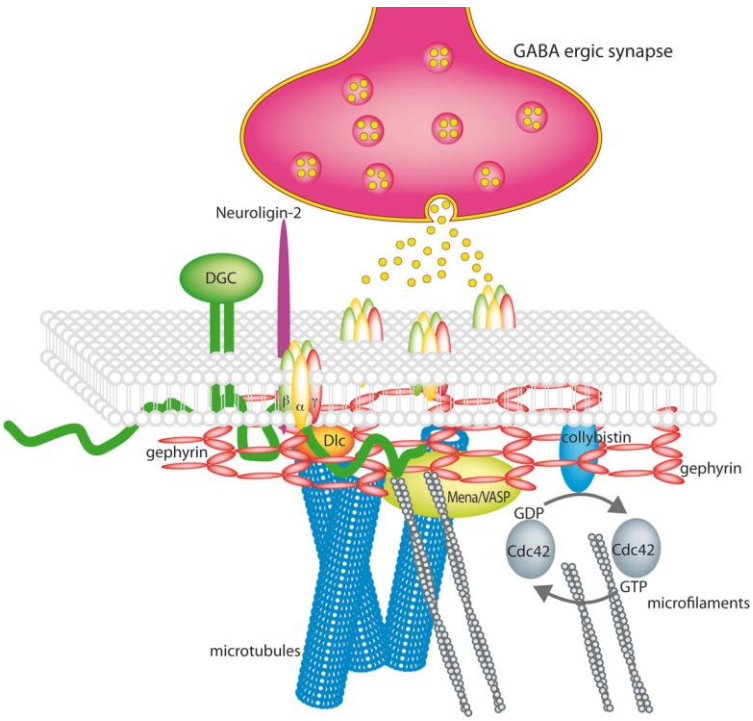

Figure 12. Gephyrin Interactors: Gephyrin is considered a major scaffolding protein at inhibitory synapses, it can interact with the glycine and $GABA_A$ receptors, collybistin and neuroligin 2, cytoskeleton elements, PIN 1, RAFT1 (Modified from Tretter and Moss 2008).

The functional role of gephyrin-microfilament interactions is still not clear, although disruption of the actin cytoskeleton resulted in a loss of small gephyrin clusters from immature neurons, suggesting an early role of the actin cytoskeleton in gephyrin scaffold formation (Bausen et al., 2006).

Other proteins identified as gephyrin-interacting partners include the rapamycin and FKBP12 target 1 (RAFT1), the peptidyl-prolyl isomerase NIMA interacting protein 1 Pin1 (Zita et al.,

2007, describe above), and the glutamate receptor interacting protein 1 (GRIP1) (Sabatini et al., 1999; Yu et al., 2008). RAFT1 mediates the *in vivo* effects of the immunosuppressant rapamycin and acts as an important regulator of messenger RNA translation (Sabatini et al., 1999). Through its interaction with RAFT1 and the concomitant signal transduction pathway, gephyrin might mediate translational control at synaptic sites. The precise role of GRIP1 in GABAergic transmission remains unclear, despite its direct interaction with gephyrin and GABARAP. GRIP1 was observed at GABAergic synapses in association with gephyrin and $GABA_A$ receptors (Li et al., 2005; Yu et al., 2008). Although GRIP1 knockout mice did not exhibit any changes in the number of $GABA_A$Rs on the cell surface (Hoogenraad et al., 2005), the regulated delivery of $GABA_A$Rs to synapses following long term depression induced by NMDA receptor activation was mediated by GRIP1 and its binding partner GABARAP (Marsden et al., 2007).

1.3.4 Cell adhesion molecules at GABAergic synapses

1.3.4.1 Cell adhesion molecules at GABAergic synapses, general evidences

As initially described, trans-synaptic cell adhesion complexes have come to the forefront as key players in the formation and maturation of synaptic connections.

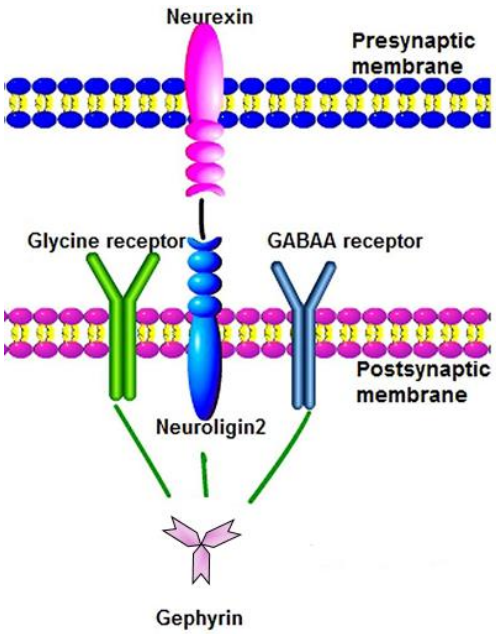

Figure 13. NLGNs bind to their pre-synaptic counterpart Nrxs: The extracellular domain of Neuroligin2 (NL2)can bind neurexins (NRXNs), to play an important role in synapse maturation and function. NL2 at PSD binds gephyrin and activate collybistin. NL2, gephyrin, and collybistin complexes are sufficient to inhibitory neurotransmitter receptors clustering (modified from Chen et al., 2014)

Neurexin–neuroligin is the first pair shown to be involved in these processes and the best characterized (Fig. 13) (Craig and Kang, 2007, Dalva et al., 2007, Dean and Dresbach, 2006 and Huang and Scheiffele 2008).

1.3.4.2 Neurexins structure

Neurexins (Nrx) were identified as presynaptic receptors for α-latrotoxin, a spider toxin that causes massive synaptic vesicle exocytosis (Ushkaryov et al., 1992, 1993, and 1994). Neurexins are presynaptic type-I membrane proteins with a large extracellular sequence and a short cytoplasmic tail. Vertebrates contain three Nrx genes, each of which encodes two neurexin isoforms with one promoter initiating transcription of a long mRNA encoding α-neurexin isoforms while a second promoter located within an intron initiates transcription of a shorter mRNA encoding β-nrx isoforms. The extracellular domain of α-neurexins contains three EGF-like domains, each of which is flanked by a pair of Laminin G/Neurexin/Sex Hormone Binding Globulin (LNS) domains. Instead of six LNS domains, only one is present in the β-neurexins, which lack all of the EGF repeats. The extracellular domains of both α- and β-nrxs are followed by a transmembrane domain and a cytoplasmic domain containing a C-terminal PDZ-interacting site, which orchestrate the recruitment of the presynaptic release machinery (Hata et al., 1996, Biederer and Sudhof, 2000) (Fig.14). Both forms undergo extensive alternative splicing at five different sites (termed site 1-5) in α-nrxs, and two sites (sites 4-5) in β isoforms (Ichtchenko et al., 1996; Tabuchi and Sudhof, 2002; Ushkaryov and Sudhof, 1993). This gene organization generates a huge diversity of more than 2000 potential variants. Recent results have demonstrated that splicing controls the specificity of neurexin-neuroligin interactions as well as their activities in promoting excitatory and inhibitory synapse formation.

1.3.4.3 Neuroligins structure

Neuroligins (NLs) were initially identified as endogenous Nrx ligands (Ichtchenko et al 1995; Scheiffele et al 2000). They are type-I membrane proteins characterized by a simple domain structure. NLs are composed of an extracellular, N-linked glycosylated domain with strong sequence homology to acetylcholinesterase (AChE), a Serine-Threonine-rich stalk domain that carries both N- and O-linked oligosaccharides (Ichtchenko et al., 1996; Bolliger et al., 2001; Hoffman et al., 2004), a single transmembrane domain, and a small intracellular C-terminal domain. NLs are expressed from four genes in vertebrates (NL1 to NL4). Primates

contain non-recombining copies of NL4 on the X- and Y-chromosomes, with the Y-chromosomal copy often referred to as NL5. Alternative splicing in NLs occurs in the main functional domain, the acetylcholinesterase-homologous region (Fig. 14). Because NLs have two conserved splice sites in this region, sites A and B, up to four different isoforms are possible for each NL gene (Craig and Kang, 2007). Despite the high sequence conservation, the different NL isoforms differ notably in their subcellular distribution.

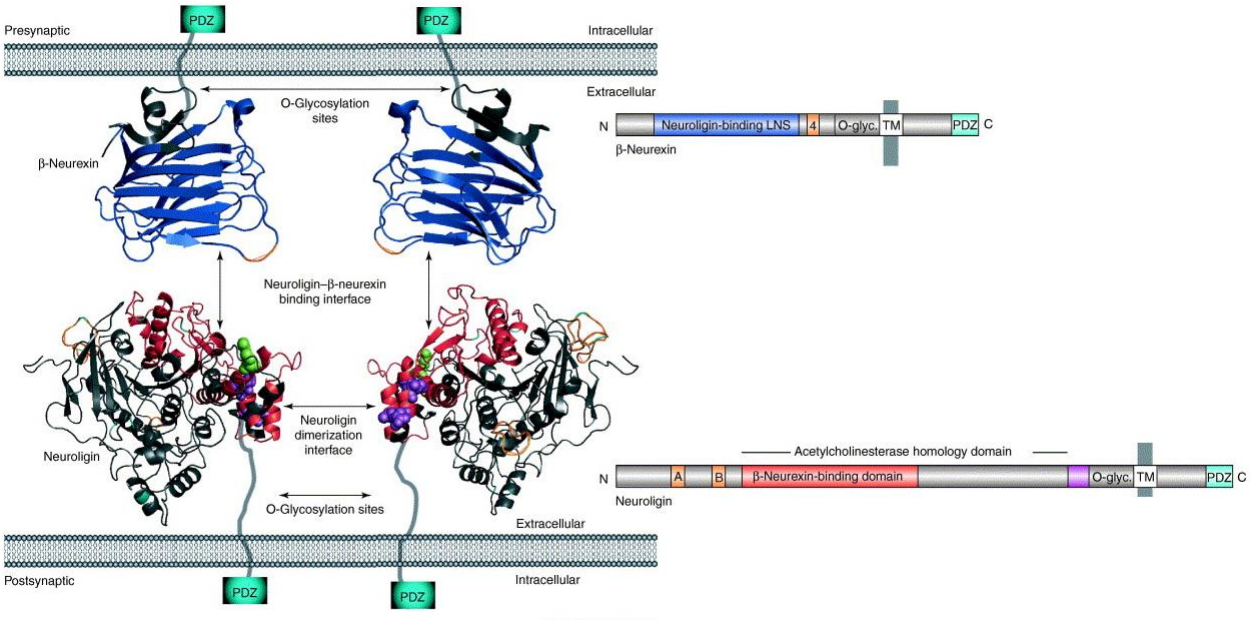

Figure 14. The structure of neuroligins and β-neurexins and their transynaptic interaction, β-Neurexins are composed of: an extracellular N-terminal sequence that is specific to β-neurexins, a single LNS domain that is essential for binding neuroligins (blue) an O-glycosylation (O-glyc.) region; a transmembrane (TM) domain; and (iv) a cytoplasmic tail that contains a PDZ-interaction site on the C-terminus. Neuroligins contain: two EF-hand motifs in this domain that bind Ca2; an O-glycosylation region; a transmembrane domain; and a cytoplasmic C-terminal tail that contains a PDZ-interaction site. A portion of the acetylcholinesterase homology domain shown in the neuroligin structure model is necessary for β-neurexin binding and synaptogenic activity (from Dean and Dresbach 2006).

NL1 is only present at excitatory synapses (Song et al., 1999), NL2 and NL4 at inhibitory synapses (Hoon et al., 2011; Varoqueaux et al. 2004; Graf et al. 2004) while NL3 is present at both inhibitory and excitatory synapses (Chih et al., 2005; Budreck & Scheiffele 2007). NLs exist natively as dimers and interact in vitro to both α- and β-neurexins in a Ca2+-dependent manner (Ichtchenko et al., 1995; Boucard et al., 2005). Dimer assembly takes place in early secretory pathway, and is a prerequisite for NLs to traffic delivery to the cell surface. This phenomenon represents a cellular quality control mechanism, which ensures that only fully

assembled functional complexes can reach their sites of action on the cell surface (Poulopoulos et al., 2012).

1.3.4.4 Neuroligin 2: the isoform enriched at GABAergic synapses

NL2 is the only member of the neuroligin family that interacts with gephyrin *in vivo* (Varoqueaux et al., 2004). For this reason it was assumed to function as a postsynaptic organizer that drives deposition of gephyrin and recruitment of $GABA_A$Rs at GABAergic post-synaptic sites during synaptogenesis. Interestingly, NL2 shares with all NL isoforms a highly conserved sequence of 15 amino acid residues in its cytoplasmic domain (768-782) that is sufficient to mediate gephyrin binding (Poulopoulos et al., 2009) (Fig. 15).

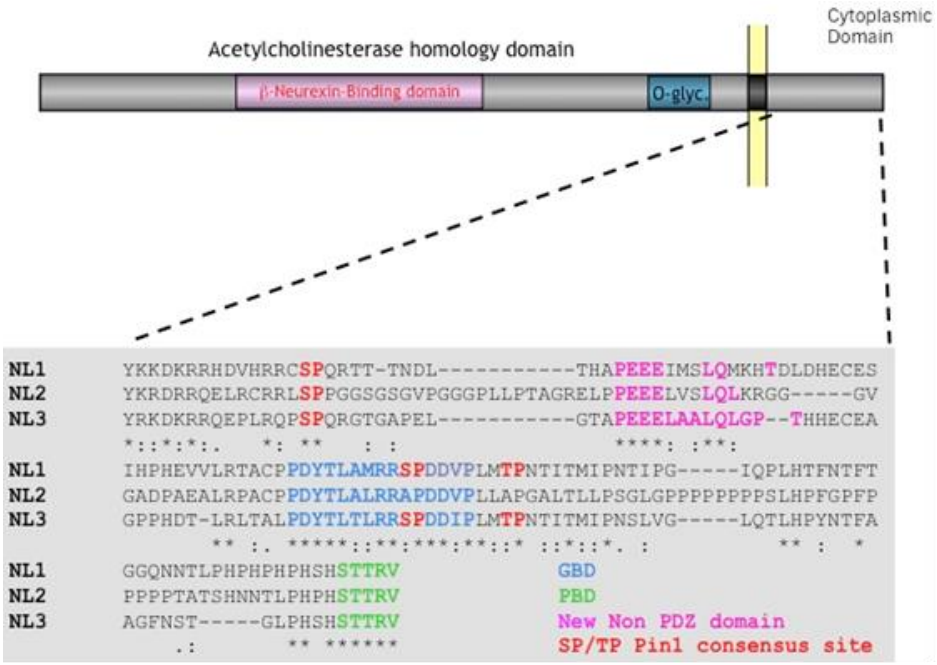

Figure 15. Sequence alignment of intracellular domains of mouse NLs. The well conserved gephyrin-binding and PDZ-binding regions are indicated in black and grey, respectively.

This sequence has been called gephyrin-binding domain (GBD). Nevertheless, NL2 is the sole isoform that recruits gephyrin *in vivo*, thus suggesting that other mechanisms contribute to determine such specificity. Poulopoulos and colleagues (2009) identified collybstin II as the key protein implicated in gephyrin recruitment by NL2. As discussed above collybistin is a gephyrin interactor that, by virtue of its phospholipid-binding domain (the PH domain), possesses the capacity to attach gephyrin to biological membranes (Papadopoulos and

Soykan, 2011). Only collybistin isoforms lacking the SH3 domain are able to redistribute gephyrin from large intracellular aggregates to small microclusters localized beneath the plasma membrane in non-neuronal cells (Papadopoulos et al., 2008; Soikan et al., 2014).

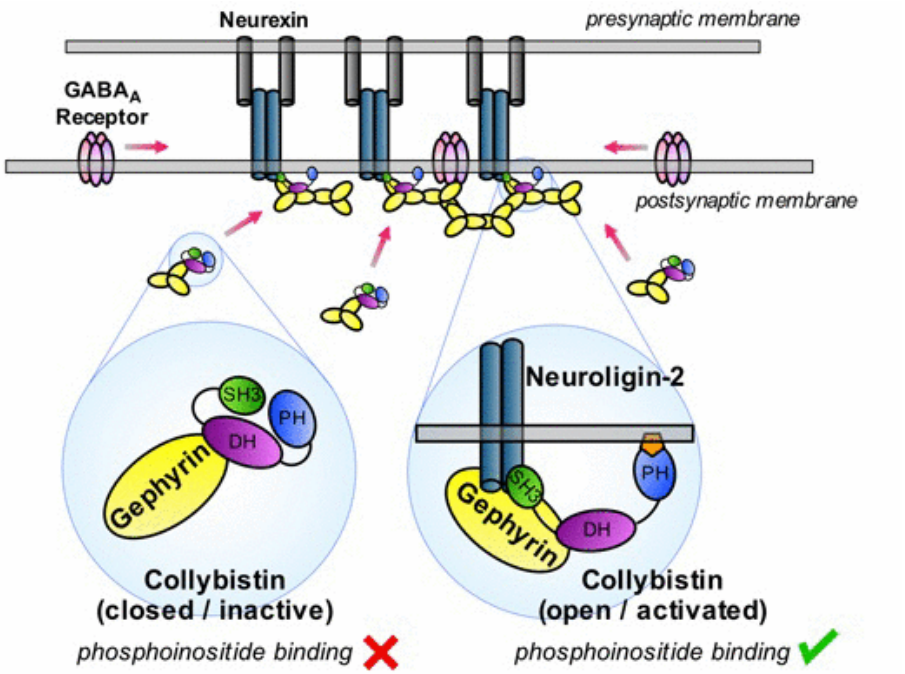

Figure 16. NL2 removes the collybistin inhibition to determine the differentiation of inhibitory post-synapses device: NL2 interacts with specific residues of the SH3 domain in this way collybistin shifts into an "open/active conformation" that can drive gephyrin deposition at inhibitory post-synaptic membranes (Soykan et al., 2014)

The SH3 domain indeed traps collybistin isoforms containing it in a so-called "close/inactive conformation" which makes the PH domain unavailable for lipid interaction due to intra-molecular interaction established between the SH3 domain itself and the PH domain of the protein (Soikan et al., 2014). Neuroligin 2, just like the α2 subunit of GABA$_A$Rs, was shown to absolve the role of neuron-specific activator of SH3-containing collybistin isoforms. NL2 has been shown to interact with specific residues of the SH3 domain not involved in collybistin auto-inhibition, shifting collybistin into an "open/active conformation" that can drive gephyrin deposition at inhibitory post-synaptic membranes (Fig. 16).

1.3.4.5 NL1 and NL2 phosphorylation in synapse specification and stabilization

Only recently evidences have been provided about the importance of phosphorylation in NL function. The site-directed mutagenesis approach , which has led to the identification of the GBD in the NL2 cytoplasmic tail, unveiled that Tyr-770 is essential for gephyrin recruitment. Substitution of tyrosine with alanine completely abolished gephyrin/NL2 interaction

(Poulopoulos et al 2009) raising the possibility that Tyrosine-phosphorylation would negatively modulate gephyrin recruitment at inhibitory synapses. Whether NL2 can undergo tyrosine phosphorylation *in vivo* is still an unexplored issue. Recently, Giannone and coauthors (2013) highlighted a key role played by NL1 phosphorylation at the corresponding Tyr-782 in selective scaffold recruitment. These authors demonstrated that the level of NL1 phosphorylation at this site dictates the strength of NL1/gephyrin interaction. NL1, like all other isoforms, can potentially recruit gephyrin as much as NL2, but phosphorylation at Tyr-782, promoted by neurexin-adhesion signaling, precludes such aberrant interaction while favoring the recruitment PSD-95, the scaffolding molecules of the excitatory synapses where NL1 is localized. Such a ligand-induced phospho-tyrosine ‘‘switch’’ could represent a very sensitive mechanism in synaptogenesis, during which early neuronal contacts that rely on Nrx/NL adhesion may be primed to assemble functional excitatory or inhibitory postsynapses (Giannone et al., 2013) .

The phosphorylation level of NLs may be implicated also at later stages of synapse stabilization and plasticity. Indeed, synaptic activity is required for NL-dependent synapse validation (Nam and Chen, 2005; Chubykin et al., 2007) and for the stabilization of scaffolding molecules at synapses (Mondin et al., 2011). Given the intrinsic turnover of scaffolding elements at synapses (Okabe et al., 1999; Sturgill et al., 2009), it is possible that the recurrent phosphorylation or dephosphorylation of NLs is involved in retaining PSD-95 and gephyrin at mature excitatory and inhibitory synapses, respectively.

NL1 has been also found heavily phosphorylated at Thr-739 by the CaMKII, a major component of the excitatory PSD and a critical mediator of synaptic plasticity. CaMKII-mediated phosphorylation of NL1 was shown to promote its surface expression level through a mechanism which is still unknown (Mukherjee et al., 2008).

1.4 Glutamatergic transmission

1.4.1 Glutamatergic synapses

The majority of excitatory synapses in the CNS are built at the tip of actin–rich micro-sized protrusions emanating from the dendritic shaft, called spines (Newpher and Ehlers, 2008; Sheng and Hoogenraad, 2007; Tada and Sheng, 2006). The postsynaptic membrane of each spine contains a high concentration of ionotropic glutamate receptors that detect the release of glutamate from the presynaptic terminal and host cytoplasmic scaffold proteins, associated signaling molecules and cytoskeletal elements that transduce glutamate binding into postsynaptic biochemical responses (Feng and Zhang, 2009; Newpher and Ehlers, 2008; Schoch and Gundelfinger, 2006; Sheng and Hoogenraad, 2007). This morphological and functional characterization of the post-synaptic membrane is also called postsynaptic density (PSD), due to its appearance as an electron-dense thickening of the membrane in electron micrographs (Fig. 17).

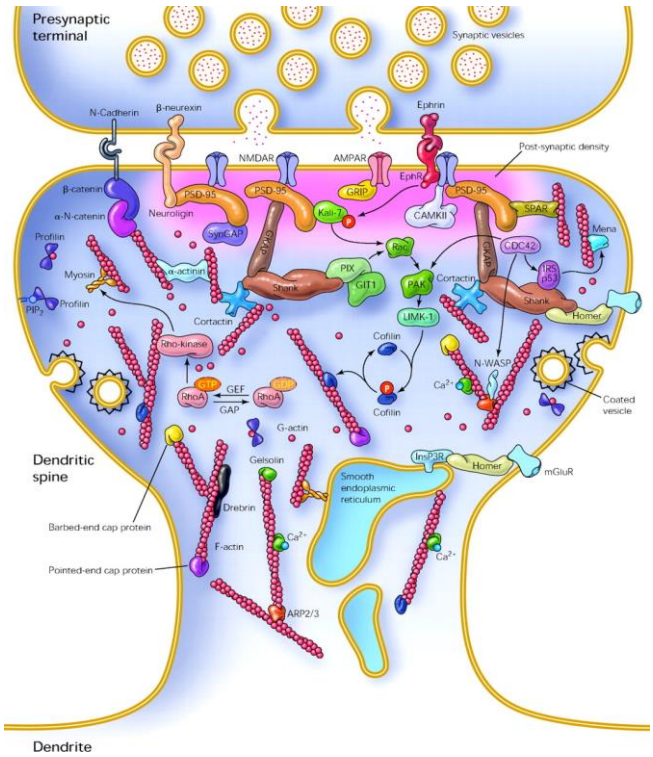

Figure 17. Excitatory PSD organization: the excitatory post synaptic density is composed by an incredible numbers of molecules that create an intricate proteins network (modified from Calabrese et al., 2006).

PSDs are highly heterogeneous in shape and dimensions (Sheng and Kim, 2011) with a diameter ranging from 200-800 nm and thickness from 30-60 nm (Carlin et al., 1980). The

structure and composition of PSDs is developmentally regulated (Petralia et al., 2005; Swulius et al. 2012) and generally, the expression level of many PSD proteins increase during development, reaching their peaks at about 2-4 week after birth and correlates with the formation and maturation of synapses within the brain. Dramatic changes in size, shape and composition are achieved in response to synaptic activity (Sheng and C. Hoogenraad, 2007).

1.4.2 Spines morphology

The morphology of dendritic spines is highly variable; imaging techniques have shown that number, size and shape of excitatory synapses undergo plastic changes during development and synaptic activity (Fischer et al., 2000; Star et al., 2002; Okamoto et al., 2004, Luebke et al., 2010). Spines have been generally classified into three morphological types: stubby, mushroom and thin (Peters and Kaiserman-Abramof, 1969). Mushroom spines have a large head that is connected to the parent dendrite through a narrow neck. Stubby spines do not have a noticeable neck and are most common during postnatal development (Rochefort and Konnerth, 2012). These two types of large spines are referred to as “memory spines,” because they are stable and persist for longer periods of time (Trachtenberg et al., 2002; Kasai et al., 2003). Conversely, thin spines have a thin, long neck, and a small bulbous head; they are highly motile, unstable, and often short-lived, usually representing weak or silent synapses (Rochefort and Konnerth, 2012). Because thin spines are more plastic than large spines and have the potential to become stable spines, they have been dubbed “learning spines” (Grutzendler et al., 2002; Trachtenberg et al., 2002; Kasai et al., 2003; Holtmaat et al., 2005). Thin protrusions longer than thin spines and without an obvious head are called dendritic filopodia. They are more abundant than spines in developing neurons. Dendritic filopodia are transient and highly motile protrusions that sample the extracellular space to detect presynaptic partners with to establish synaptic contacts and to develop into mature spines (Fiala et al., 1998; Luebke et al., 2010) (Fig. 18).

Also mature excitatory synapses are subjected to continuous refinement; this molecular turnover occurs under basal conditions and increases in response to synaptic activity (Inoue and Okabe, 2003). In this way the shape and size of synapses can change over time to allow fast and continuous neuronal circuits adaptation.

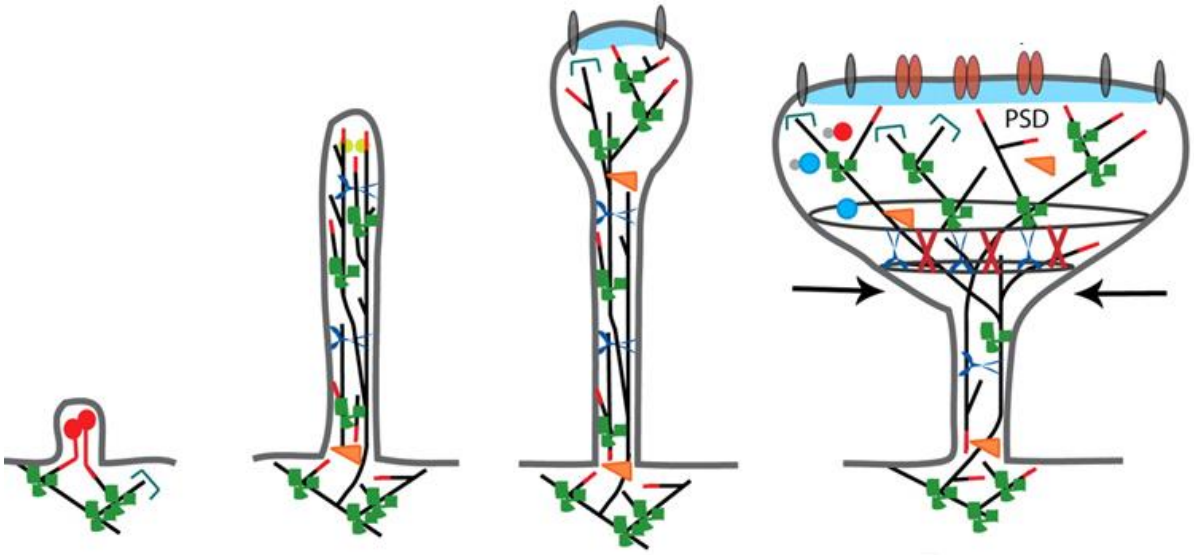

Figure 18. Spine maturation step: Spine development starts with the initiation of the dendritic filopodium and its elongation, extensive actin branching occurs at the filopodium tip and during the maturation the spine head enlarge (modified from Hotulainen, and Hoogenraad 2010).

1.4.3 Glutamate Receptors

1.4.3.1 Ionotropic glutamate receptors

The vast majority of excitation in the central nervous system is mediated by glutamate, a ubiquitous amino acid. In neurons, glutamate is packed within synaptic vesicles by dedicated vesicular transporters (VGluTs). Glutamate is released from presynaptic terminals into the the synaptic cleft in an activity dependent manner. Once liberated, glutamate acts on several structurally and pharmacologically different types of receptors: the ionotropic (iGluR) and the metabotropic receptors (mGluRs). The mGluRs are G-protein-linked receptors that couple to various intracellular signal transduction pathways. Ionotropic GluRs (iGluR) mediate fast excitatory synaptic transmission in the central nervous system and regulate a broad spectrum of processes in the brain, spinal cord, retina, and peripheral nervous system (Traynelis et al 2010). iGluRs are subdivided into three families according to their distinct responses to specific agonist molecules, namely α-amino-5-methyl-3-hydroxy-4-isoxazole propionic acid (AMPA), N-methyl-D-aspartate (NMDA), and kainate (Chua et al., 2010). A fourth family is represented by δ receptors, which seem not to form functional receptors (Traynelis et al. 2010).

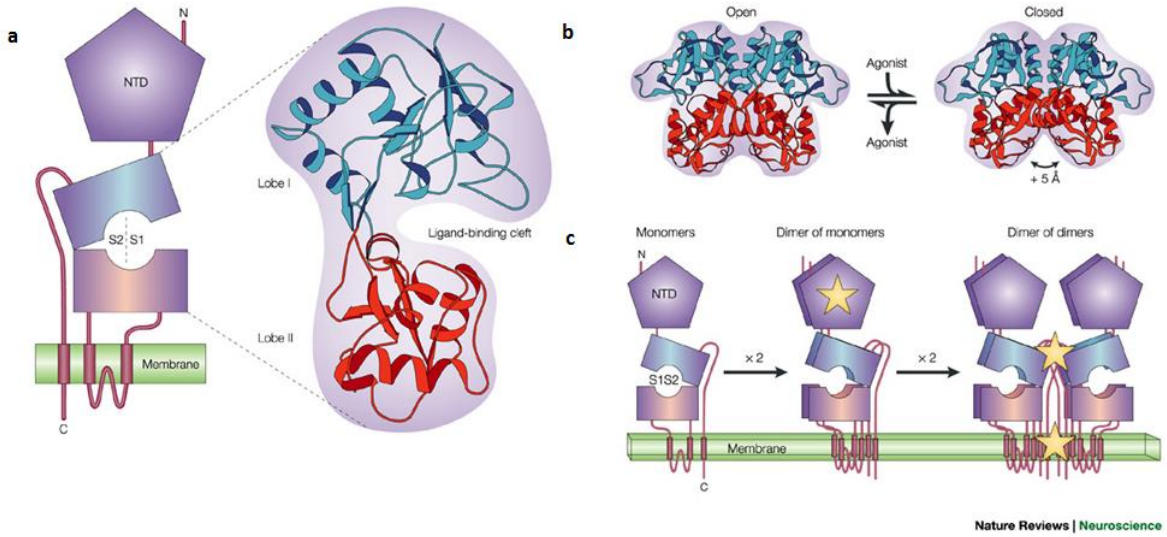

Figure 19. The structure of ionotropic glutamate receptors (iGluRs): a)The modular nature of iGluR subunits. The amino terminus of ionotropic glutamate receptor (iGluR) subunits is extracellular. An amino-terminal domain (NTD) is followed by the S1 half-domain, two transmembrane domains with an intervening re-entrant P loop, the S2 halfdomain and a third transmembrane domain. The carboxyl terminus is located in the cytoplasm, where it can interact with proteins of the postsynaptic density. The S1 and S2 half-domains form the iGluR ligand-binding domain, which is homologous to the bacterial glutamine-binding protein QBP. b)In the absence of ligand , the S1S2 domain of the glutamate receptor (GluR) probably exists in an open⇔closed equilibrium that is skewed towards the open form. Ligand can bind only to the open cleft (apo⇔bound equilibrium; left-hand side). In the presence of agonist (bottom), the closed conformation is stabilized relative to the open conformation, shifting the open⇔closed equilibrium towards the righ c) The assembly of tetrameric iGluR channels show a mechanism composed by two step 1) association of "dimer of monomers" 2) association of "dimer of dimers" to assembly a functional receptors. Modified (from Dean R. Madden et al., 2003).

All iGluR subunits show a characteristic modular organization consisting in a large extracellular domain (about 380 aminoacids), an agonist binding domain (about 300 aminoacids), a transmembrane domain formed by three membrane spanning-segment (M1, M2, M4), a membrane re-entrant loop (M2) which lines the channel pore and a cytoplasmic carboxy-terminal domain whose residues interact with numerous intracellular scaffolding and trafficking proteins. Sequence similarity among all known glutamate receptor subunits suggests they share a similar architecture. The main difference between iGluR subunits are in their amino acid sequence accommodating the binding pocket for specific agonists and in the length and sequence of their carboxyl-terminal domain, which interacts with intracellular proteins. Receptors of each class are formed by co-assembly of homologous subunits (Fig. 19).

1.4.3.2 AMPA receptors

AMPA receptors (AMPARs) mediate the majority of fast excitatory synaptic transmission in the brain. They are critically important for all aspects of brain function, including learning, memory, and cognition. These ligand-gated ion channels are composed of combinations of four separate subunits encoded by genes GluR1-4. They can form homo- and heteromer receptors but the latter constitute the majority of native AMPARs (Jonas and Burnashev, 1995; Rossmann et al., 2011). The different subunits composition determines the functional properties of the receptors; these properties can be modulated by protein–protein interaction (Gardner et al., 2005) and phosphorylation events (Roche et al., 1996; Carvalho et al., 1999). iGluRs respond relatively quickly to the binding of glutamate. This event allows a rapid Na+ inflow through the channel and a fast membrane depolarization. These receptors are characterized by a relatively low affinity for glutamate (Lisman and Raghavachari, 2006) therefore, to rapidly respond to glutamate release, they are positioned very close to the presynaptic release sites. They are highly dynamic and shuttle in and out of synapses in an activity-dependent fashion to alter synaptic transmission (Lüscher et al., 1999).

1.4.3.3 Kainate receptors

Kainate receptors are encoded by five different genes GluR5, GluR6, GluR7, KA1, and KA2. They are distributed on presynaptic and postsynaptic membranes. Presynaptic kainate receptors can be localized also on presynaptic inhibitory GABAergic terminals where they regulate transmitter release. In some cases, postsynaptic kainate receptors are co-localized with NMDA and AMPA receptors (Huettner 2003).

1.4.3.4 NMDA receptors

NMDARs exhibit several properties that are unique among iGluRs: i) they requires glutamate and a co-agonist, either glycine or D-serine, for the efficient opening of the ion channel (Johnson and Ascher, 1987; Kleckner and Dingledine, 1988; Lerma et al., 1990; Schell et al., 1995); ii) they are characterized by very slow deactivation kinetics (Forsythe and Westbrook, 1988; Lester et al., 1990; Partin et al., 1993; Swanson and Heinemann, 1998; Vicini et al., 1998); iii) they are highly permeable to Ca2+ (MacDermott et al., 1986; Burnashev et al., 1992, 1995; Schneggenburger et al., 1996); iiii) they are blocked by magnesium ions in a voltage-dependent manner (Mayer et al., 1984; Nowak et al., 1984; Ascher and Nowak, 1988). In other words NMDARs are activated by both ligand (glutamate) and by voltage (once

the Mg2+ block is relieved by membrane depolarization). NMDARs are tetrameric proteins, the majority of which comprise two obligatory GluN1 and two modulatory GluN2 subunits, and rarely GluN3 subunits (Cull-Candy and Leszkiewicz, 2004; Erreger et al*.,* 2004, Chen and Wyllie, 2006; Traynel*is* et al*.,* 2010). The GluN1 subunit exists in eight isoforms that are generated by alternative splicing (Sugihara et al*.,* 1992) while GluN2A-D and GluN3A and B subunits are encoded by separate genes (Monyer et al*.,* 1992). GluN1 is essential for ion selectivity and co-agonist binding (Cull-Candy and Leszkiewicz 2004); GluN2 control the electrophysiological properties of the NMDA receptor, being responsible of the Mg^{2+} blockade and Ca^{2+} permeability. Although the NMDARs are also found at extra-synaptic locations, they are highly concentrated at synaptic sites (Tovar and Westbrook 2002) and their synaptic clustering is promoted by a direct interaction of NMDAR subunits with the scaffolding elements of the PSDs (Roche et al., 2001; Xu et al., 2011).

The expression profile of GluN2A and GluN2B subunits is developmentally regulated. At birth, GluN2B mRNA and protein levels are present at near maximal amounts and may increase slightly during the first two postnatal weeks (Monyer et al., 1994; Sheng et al., 1994). In contrast, GluN2A mRNA and protein expression are low at birth and increase ubiquitously during the first three postnatal weeks. The adult synapse is thus composed of a mixture of GluN2A and GluN2B subunits, with GluN2A subunits predominating at the synapse and GluN2B subunits occupying extrasynaptic sites (Cull-Candy and Leszkiewicz, 2004). The up-regulation of GluN2A-containing NMDARs is believed to be the primary factor underlying the developmental increase in the decay of NMDAR-mediated synaptic currents (Carmignoto and Vicini, 1992; Quinlan et al., 1999b; Yoshimura et al., 2003; Paoletti et al., 2013).

1.4.3.5 Plasticity at glutamatergic synapses

As previously describe (Chapter 1.3) the efficacy of synaptic transmission is not fixed but can be modified in an activity-dependent manner. This phenomenon is known as synaptic plasticity. Synaptic transmission can be regulated at presynaptic site, by changes in the probability of transmitter release and/or the number of release sites, and at postsynaptic sites, by changes in the number and function of neurotransmitter receptors (Fig. 20). At glutamatergic synapses, long-term changes in synaptic efficacy (long-term potentiation or LTP and long term depression or LTD) are mainly due to postsynaptic mechanisms. These involve an increased (LTP) or decresed (LTD) in the number of functionally active AMPARs on the postsynaptic membrane. Glutamate release from presynaptic terminals acts on AMPARs

and NMDARs enriched at PSDs. As aforementioned, NMDARs at the normal resting membrane potential are blocked by Mg2+. Thus, membrane depolarization induced by repetitive activation of AMPARs causes the relieve of the Mg2+ block from NMDARs that open causing Ca2+ influx into the post-synaptic neuron. Increased intracellular Ca2+ triggers the activation of various downstream signalling pathways leading to changes in synaptic AMPARs content. In this context a key role is played by another category of molecules that are fundamental in trafficking, anchoring and clustering glutamate receptors at PSDs, the Discs-large (DLG)-MAGUKs.

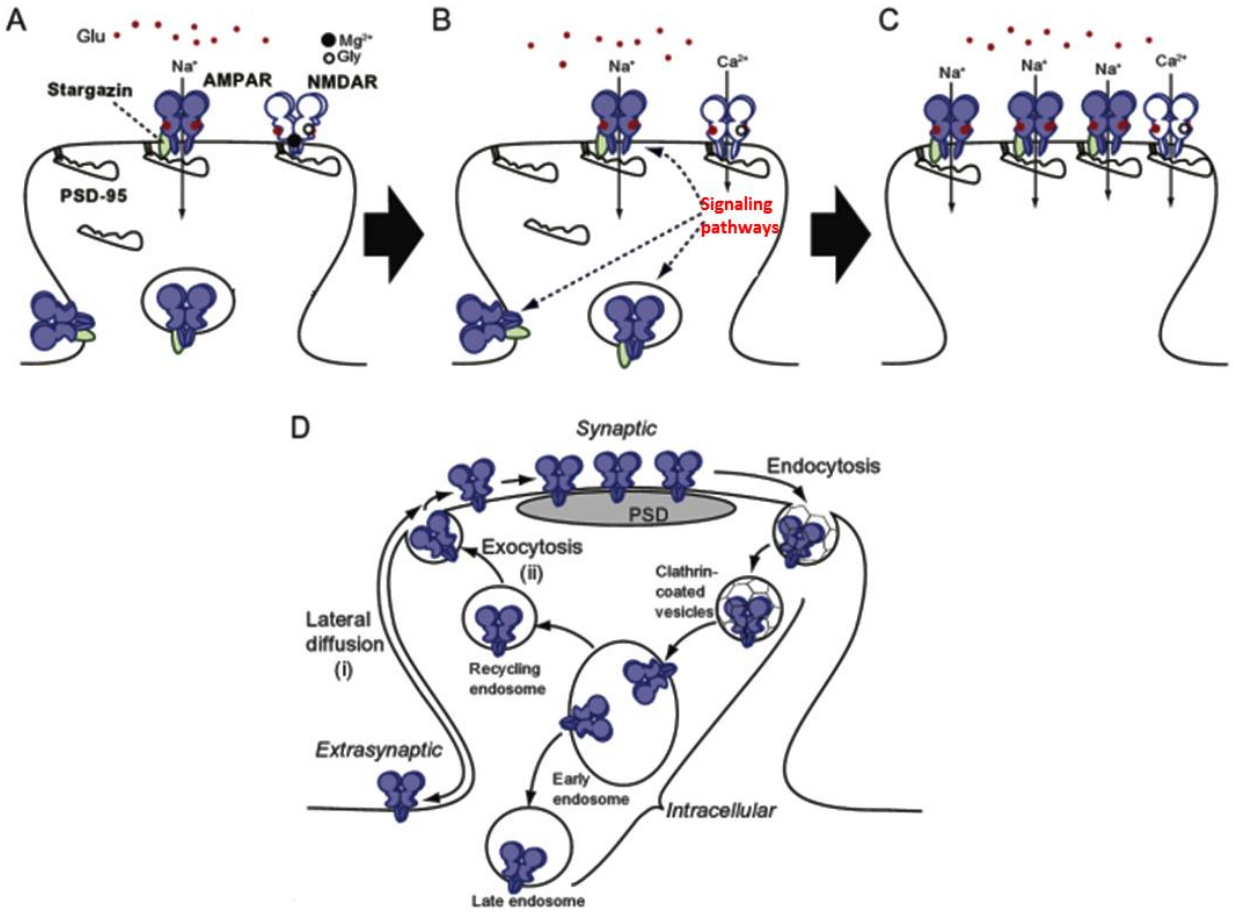

Figure 20. Receptor trafficking for synaptic plasticity: A) At the resting membrane potential synaptically released glutamate evokes excitatory post-synaptic currents that is mediated by AMPARs, while NMDARs are blocked by Mg2+. B) Upon AMPARs activation Mg2+ block of NMDARs is released. Glutamate-bound NMDARs allow Ca2+ entry into the neuron which triggers various signalling pathways. C) NMDARs-dependent signalling leads to recruitment of AMPARs at postsynapses and enhanced synaptic strength. D) Possible routes of AMPARs trafficking (lateral diffusion along the plasma membrane or local exocytosis) Modified from Yokoi et al., 2012.

1.4.4 Membrane-associated guanylate kinase (MAGUK)

1.4.4.1 MAGUKs structural organization

Discs-large (DLG)-MAGUKs are the major scaffolding proteins found in the PSD of excitatory synapses. Their role encompasses the tethering of ion channels and AMPAR to postsynaptic membrane, regulating the trafficking and functions of AMPA and NMDA receptors in addition to sustaining a very complex yet highly organized molecular network. The DLG-MAGUK protein family in mammals consists of four members, synapse associated protein-90 (SAP-90)/postsynaptic density protein 95 (PSD-95) (Cho et al., 1992), chapsyn-110 (PSD-93) (Brenman et al., 1996), synapse-associated protein 102 (SAP102) (Müller et al., 1996) and synapse-associated protein 97 (SAP97) (Lue et al., 1994). All four of these proteins share a common domain structure (Fig. 21). They consist of three PSD-95/Discs large/zona occludens-1 (PDZ) domains, one Src-homology 3 (SH3) domain and a catalytically inactive C-terminal guanylate kinase (GK) domain. PDZ domains are responsible for major protein-protein interactions involving binding to voltage- and ligand-gated ion channels as well as cell adhesion molecules.

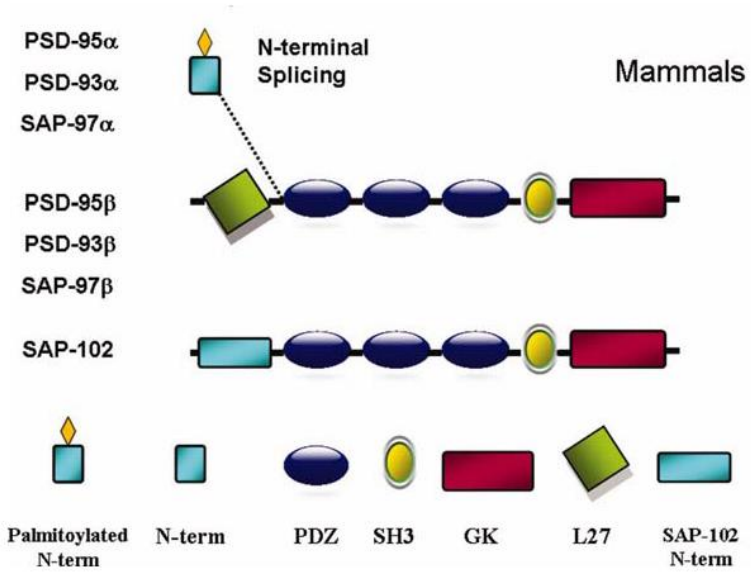

Figure 21. Domain organization and splice variants in the DLG subfamily: The member s of discs large (DLG) MAGUK family expressed in the brain present a common domain structure (From Oliva et al., 2012).

On the other hand, SH3 and GK domains contribute to intra-molecular and intermolecular connections besides mediating non-PDZ protein interactions (McGee et al. 2001;

Montgomery et al., 2004) (Fig. 22). Despite the fact that all MAGUKs share a common structure, the N-terminus of the proteins varies in a great extent, thus conferring them unique properties. Two isoforms of PSD-95 and SAP97 were identified, functioning in an activity-dependent and independent manner. Alpha isoforms work in an activity-independent fashion and possess two cysteine residues at their N-termini, which are accessible to palmitoylation (Schlüter et al., 2006). Particularly for PSD-95, the palmitoylation of these residues (C3 and C5) are crucial for synaptic targeting and clustering (Topinka and Bredt, 1998; Craven et al., 1999; El-Husseini et al., 2000).

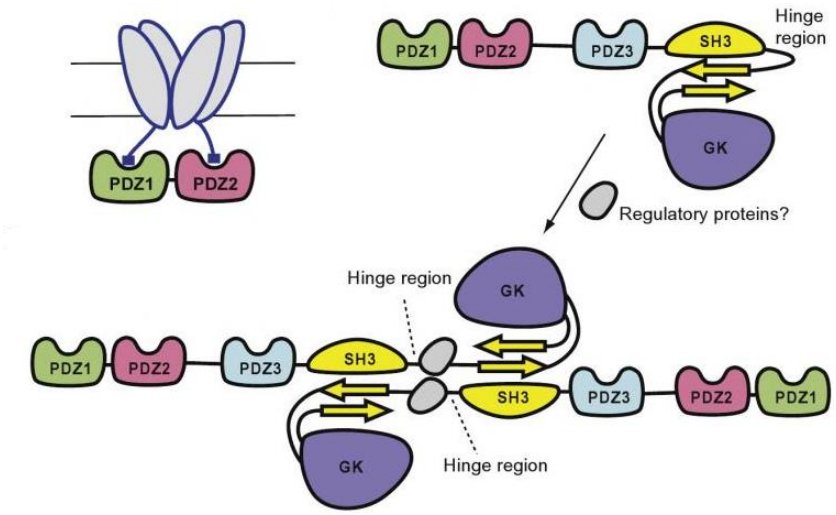

Figure 22. Model of SH3-GK interaction in PSD-95: The SH3 and GK domains of PSD-95 interact to create a supramodule structure. These events contribute to create intra-molecular and intermolecular connections that contribute to the formation of a MAGUK network. Modified from Yokoi et al., 2012.

On the other hand, beta isoforms are involved in the activity-dependent events and contain an L27 domain that does not undergo palmitoylation (Lee et al., 2002; Nakagawa et al., 2004; Schlüter et al., 2006). Even though both isoforms exist, PSD-95 is mainly expressed as the alpha isoform (Chetkovich et al., 2002).

1.4.4.2 PSD-95: functional role in synaptic clustering

PSD-95 is the most abundant and also the most studied member of the MAGUKs. PSD-95 can absolve its role as scaffolding device for stabilizing glutamate receptors, adhesion proteins and various signalling molecules at synaptic sites (Craven and Bredt, 1998; Kornau et al., 1997; Sheng and Sala, 2001; Sheng and Kim, 2002) because it is here targeted and clustered through several mechanisms (Fig. 23).

PSD-95 synaptic recruitment depends, as previously mentioned, on its N-terminal palmitoylation (Topinka et al., 1998 Craven et al., 1999; El-Husseini et al., 2002) while SH3-GK intra-molecular interactions were shown to contribute to PSD-95 self-assembly (McGee et al., 2001; Shin et al., 2000). Furthermore, the N-terminal segment of PSD-95 was shown to multimerize in a head-to-head fashion (Tomita et al., 2001).

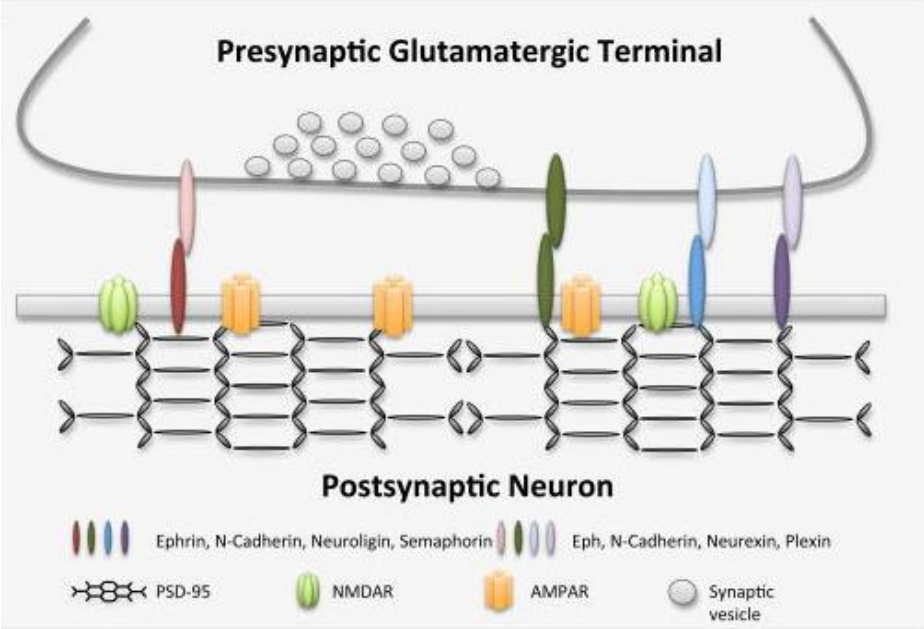

Figure 23. PSD-95 the core scaffold of glutamatergic synapse: schematic representation: PSD-95 directly and indirectly interacts with adhesion molecules and receptors to promote formation and maintenance of excitatory synapse. Modified Kuzirian and Paradis et al 2011)

PSD-95 anchors NMDARs in the PSDs by directly interacting with GluN2A/B cytosolic tails (Sheng, 2001). Mapping of the PSD-95/GluN2 protein-protein binding sites was carried out initially using yeast two-hybrid interaction assays. These studies led to the identification of the C-terminally located ES(E/D)V motif, found in all four GluN2 subunits, as the main site of association with PDZ1 and PDZ2 domains of PSD-95 (Kornau et al., 1997 , Schenker et al,. 1995). Interestingly casein kinase II (CK2)-dependent phosphorylation of Serine 1480 within the C-terminal motif of GluN2B was shown to negatively modulate PSD-95 interaction, leading to receptor internalization (Chung et al., 2004). Since deletion of the very last residues of GluN2 subunits did not completely block the interaction with PSD-95 (Bassand et al., 1999; Cousins et al., 2009; Kornau et al., 1995) these observations suggested that additional regions are involved. Indeed an SH3 domain-binding motif localized within the

GluN2 subunits has been recently identified that bind directly to PSD-95 (Cousins et al., 2012) (Fig. 24).

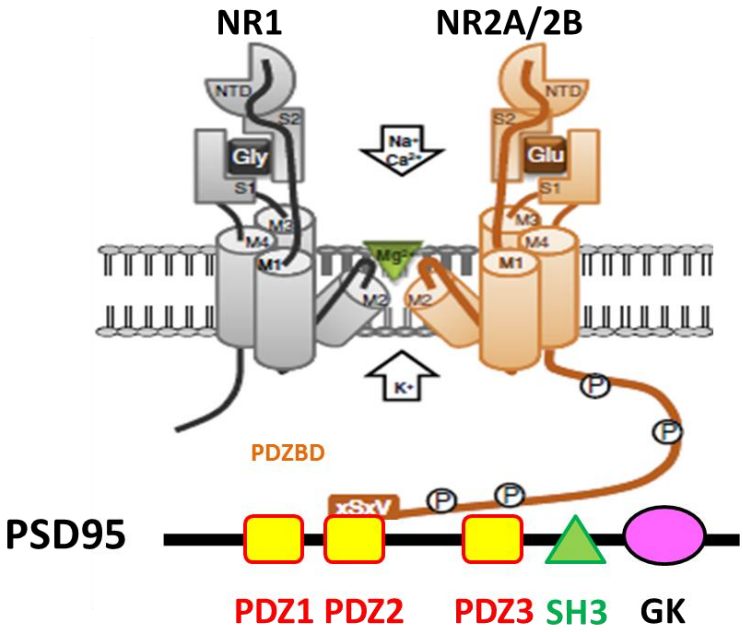

Figure 24. Schematic representation of PSD 95 interacting with GluN2 subunits of the NMDARs: The NMDAR and PSD-95 interact directly through the interaction with GluN2 . These subunits possess a large intracellular tail ended by a PDZ binding motif **xSxV** mediating the interaction with PSD-95 family proteins (modified from Bard and Groc 2011).

Synaptic localization of AMPARs is coupled to PSD-95 via transmembrane AMPAR regulatory proteins (TARPs) (Chen et al., 2000; Tomita et al., 2005). The first TARP found to interact with AMPA receptors is the tetra-spanning protein, stargazin (Chen et al., 2000), the protein mutated in stargazer mutant mice (Letts et al., 1998). TARPs mediate synaptic expression of AMPA receptors by virtue of their C-terminal PDZ binding motif that binds to all three PDZ domains of PSD-95 with similar affinities (Chen et al., 2000, Dakoji et al., 2003).

PSD-95 interacts directly, via its third PDZ domain, with the cell adhesion molecule predominantly localized at glutamatergic synapses, Neuroligin1. This interaction has emerged to be controlled by a specific tyrosine phosphorylation event occurring on NL1 gephyrin-binding domain, which abolishes the unwanted NL1 interaction with gephyrin, while favouring PSD-95 recruitment.

1.4.4.3 PSD-95: functional role in synaptic plasticity

The interaction between PSD-95 and glutamate receptors is known to be crucial for basal synaptic transmission as well as for the establishment of different forms of long-term plasticity. Focusing on the interplay between MAGUKs and glutamate receptors, several mechanisms promoting changes in receptor content rely on PSD-95 modification of its synaptic abundance and stability as well as on its ability to associate with glutamate receptors. In this context phosphorylation, occurring mainly on serine and threonine residues, has emerged as a key mechanism involved in orchestrating coordinated changes in protein-protein interaction (Thomas and Huganir 2004).

For instance, phosphorylation of PSD-95 at Serine 295 by Rac1-JNK1 pathway was shown to enhance the synaptic accumulation of phosphorylated PSD-95 and the ability of PSD-95 to recruit surface AMPARs, thus potentiating excitatory postsynaptic currents (Kim et al., 2007). Conversely, dephosphorylation of Ser-295 of PSD-95, mediated by PP1/PP2A phosphatases, has been associated with AMPAR internalization and long-term depression (LTD) (Kim et al., 2007). GSK-3β mediated phosphorylation of PSD-95 threonine 19 (Thr19) was shown to destabilize PSD-95 in spines, to reduce its membrane association, essential for AMPARs internalization and LTD induction (Nelson et al., 2013).

PSD-95 phosphorylation by cyclin-dependent kinase 5 (Cdk-5) at two out of three of the N-terminally localized putative consensus sites (Thr-19 and Ser-25) was shown to negatively regulate PSD-95 membrane association and synaptic clustering (Morabito et al., 2004). Cortical neurons derived from Cdk-5 knockout mice as well as rat hippocampal neurons over-expressing an inactive form of the kinase demonstrated PSD-95 clusters enlarged in size. This effect was associated with a concomitant increase in size of NMDAR clusters, thus indicating that scaffold phosphorylation provides a mechanism to promote rapid changes in the density and/or number of receptor at synapses. Cdk-5 dependent phosphorylation of PSD-95 affects synaptic NMDAR content by modulating the recruitment of Src kinase by PSD-95. This kinase phosphorylates Tyr-1472 of the GluN2B subunit and this event inhibits AP2-clathrin mediated endocytosis of GluN2B-containing NMDARs (Roche et al., 2001; Prybylowski et al., 2005) while promoting their surface expression (Zhang et al., 2008). Finally, CaMKII-dependent phosphorylation of PSD-95 at Ser-73, residue localized within the first PDZ domain of PSD-95, was shown to cause GluN2A dissociation from PSD-95, while it does not interfere with GluN2B binding to PSD-95 (Gardoni et al., 2006).

1.4.5 Pin1 at excitatory synapses

Most proteins found at PSD are heavily phosphorylated at Serine and Threonine-proline Pin1 consensus motifs, emphasizing the potential role of this signaling cascade at excitatory synaptic contacts. Even though nothing is known about the contribution of post-phosphorylation prolyl-isomerization in remodeling the excitatory post-synaptic device, Pin1 possess a recognized role as modulator of the late phase of LTP. LTP is defined temporally with respect to the requirement for new gene expression: Early-phase LTP (E-LTP) does not require new gene expression whereas Late-phase LTP (L-LTP) does. The regulation of dendritic translation occurs predominantly at the level of the initiation through the cap-binding protein eukaryotic translation initiation factor 4E (eIF4E). This molecule, as part of the multi subunit eIF4F complex, participates in the recruitment of mRNA to the ribosome, thus promoting translation initiation. eIF4F assembly is negatively regulated by eIF4E-binding proteins (4E-BPs) that, when hypo-phosphorylated, sequester eIF4E by directly binding to it (Provenzani et al., 2006; Loreni et al., 2000). Additional phosphorylation events of 4E-BPs by mammalian target of rapamycin (mTOR), S6 kinase p79 (S6K), MAPKs or PKC liberates the cap-binding protein eIF4E, thus allowing the proper assembly of the translation initiation complex (Sacktor at al., 1993; Hara et al., 1997). In this context Pin1 has been shown to interact with hypophosphorylated 4E-BP and eIF4E. By driven conformational changes on 4E-BP it prevents its further phosphorylation and facilitates 4E-BP inhibitory interaction with eIF4E. Signals mediated by glutamate release can promote dendritic translation by preventing Pin1 interactions with its targets.

2. AIM OF WORK

Synapses are highly dynamic structures that undergo continuous functional and structural changes in response to alterations of neuronal activity. This remodeling is critical for brain development, synaptic transmission and neuronal plasticity. At the post-synaptic site two classes of molecules play a crucial role in synaptic organization: scaffolding and cell adhesion proteins. Scaffolds ensure the accurate accumulation of neurotransmitter receptors in precise apposition to pre-synaptic release sites. In addition, they provide the physical constraints for maintaining a high concentration of receptors at synapses, and for regulating the constant flux of receptors and scaffolding elements in and out of post-synaptic sites. Scaffolds also regulate downstream signaling pathways to adjust the molecular composition of the post-synaptic devices necessary to sustain synaptic plasticity. Cell adhesion molecules bridge pre- and postsynaptic specializations through specific interactions of their extracellular domains. Such interactions do not simply provide a mechanical link between pre- and post-synaptic sites but are instrumental in activating transduction signals necessary for the recruitment of various synaptic components.

In this context phosphorylation processes are critical for modulating changes in the molecular composition of the post-synaptic device. While the impact of phosphorylation of neurotransmitter receptors has been extensively characterized much less is known about the effect of these post-translational modifications on scaffolding and cell adhesion molecules.

At GABAergic synapses specific phosphorylation events targeting the scaffolding molecule gephyrin were shown to alter its oligomerization properties, thus producing concomitant changes in the numbers of receptors trapped by the scaffold and synaptic strength. Most of these phosphorylation events occur at serine or threonine residues preceding a proline, underlying a potential role of proline-directed phosphorylation as modulator of synaptic strength. At excitatory synapses, mass spectrometric analysis performed on isolated postsynaptic density proteins (PSD) has led to the identification of a number of novel serine/proline phosphorylation sites on scaffolding MAGUKs. In addition the prolyl-isomerase activity of Pin1 has been shown to regulate protein synthesis necessary to sustain the late phase of long-term potentiation.

Based on these evidences, the aim of my thesis was to study the functional role of proline-directed phosphorylation in remodeling the post-synaptic devise of both inhibitory and excitatory systems by acting on pivotal constituents such as protein scaffolds and cell adhesion molecules.

By combining molecular biology, immunocytochemistry and electrophysiological recording I initially investigated the impact of Pin1-dependent signaling on GABAergic transmission. I found that Neuroligin2, the cell adhesion molecule constitutively present at GABAergic synapses, undergoes post-phosphorylation, prolyl-isomerization modulation of its activity. Proline-directed phosphorylation at Ser-714 of NL2 negatively impacts on NL2 ability to complex with gephyrin. As a consequence, an enhanced accumulation of NL2, gephyrin and $GABA_A$ receptors was detected at GABAergic synapses in the hippocampus of Pin1-knockout mice (Pin1−/−), which was accompanied by a concomitant increase in amplitude of spontaneous GABAA-mediated post-synaptic currents. These results suggest that Pin1-dependent signalling represents a mechanism to modulate GABAergic transmission by regulating NL2/gephyrin interaction.

Then I focused on the impact of Pin1-dependent signaling on excitatory glutamatergic transmission. In particular, I investigated whether the scaffolding molecule PSD-95, a member of the Disc-Large (DGL)-Membrane-associated guanylate kinase, and know to be phosphorylated by several proline-directed kinases, could be a target of Pin1-dependent modulation. I observed that Pin1 is recruited by PSD-95 at specific serine-threonine/proline consensus motifs localized in the linker region connecting PDZ2 to PDZ3 domains and exerts a negative control on PSD-95 ability to complex with NMDARs. Indeed an enhanced PSD-95/NMDA complex formation was detected in brain extracts derived from Pin1-/- mice. In electrophysiological experiments, larger NMDA-mediated synaptic currents were detected in CA1 principal cells in hippocampal slices obtained from Pin1-/- mice as compared to controls, an effect that was associated with an enhancement in spine density and size.

3. MATERIALS AND METHODS

3.1 Basic techniques for the construction of expression vectors

3.1.1 Cloning and plasmid constructs

The expression construct for HA-tagged human NL2 in pNice and HA-tagged human NL1 in pCAG were kindly provided by P. Scheiffele (Biozentrum, Basel). The amino acid sequence ranging from residues 768 to 782 was removed to generate the NL2HA lacking the gephyrin binding domain (pNice-NL2HA-ΔGBD). S714A mutation was also introduced into pNice-NL2HA-ΔGBD to remove the unique Pin1 consensus site (pNice-NL2HA-ΔGBDS714A pcDNA3-FLAG-Pin1 WT and pcDNA3-gephyrin-FLAG have been previously cloned in our laboratory. EGFP-tagged gephyrin point mutants (S270A and S319A), the WT and the truncated version ranging from amino acid 326 to 736 and 310 to 736, were PCR cloned into the *Xho*I/*Hin*dIII sites of pEFP-C1 (Clontech, Mountain View, CA). EGFP-tagged gephyrin GC (1–310) was kindly provided by G. Schwarz (University of Cologne, Germany). GFP-tagged PSD-95and FLAG-tagged GluN2B constructs were kindly provided by Dr Vicini (Geargetown, USA). GFP-PSD-95 mutagenesis of the several mutants and cloning of the C-terminus of the GluN2B subunit (amino acid 1086-1482) into pGEX-4T1 expression vector were performed by PCR amplification using Pfx DNA polymerase (Invitrogen) and the appropriate oligonucleotides. was kindly provided by Dr. Scheiffele (Biozentrum, Basel). All PCR-based mutagenesis were fully sequenced to exclude the possibility of second site mutations.

3.1.2 Polymerase Chain Reaction (PCR)

The amplification of DNA fragment by polymerase chain reaction (PCR) allows the use of a mixture containing a heat stable DNA polymerase, four deoxyribonucleoside tri phosphates (dATP, dCTP, dGTP, dTTP); a set of primers that are each complimentary to the DNA fragment and that acts as the precursor for DNA synthesis and the DNA template. The PCR reaction is generally composed of three steps namely denaturation, annealing and elongation or extension. During the elongation, the DNA polymerase attaches to the already annealed primers and uses the dNTPS to synthesize the new strand as it moves along the template strand. The elongation step is run at a temperature that is optimal for the polymerase (68-72°C) and the elongation time is dependent on the length of the fragment to be amplified with 1 minutes normally corresponding to 1000 base pairs. A typical PCR reaction is run for

25- 35 cycles. In order to monitor the performance of the PCR, both positive and negative controls should be included in the run as the first confirms that the PCR works and the later confirms that the amplification is free of contamination. Platinum Pfx DNA Polymerase (Invitrogen) was used for cloning while GoTaq DNA Polymerase (Promega) for routine screening.

3.1.3 Restriction enzyme for DNA digestion

DNA for downstream applications is usually digested with restriction endonucleases. Type II restriction enzymes are the most widely used in molecular biology applications. Digestions were performed using New England Biolab (NEB) enzymes, containing the optimal reaction conditions for each enzyme. The reactions were performed in 60µl (20µl for screening digestions), while the temperature and the duration of the digestions were chosen according to the characteristics of each enzyme following NEB instructions. The DNA fragments and plasmid vectors digest are purified using the PCR clean-up Gel extraction kit (Macherey-Nagel) and then combined and treated with DNA ligase. For the ligation reactions was used the T4 DNA ligase (Promega), which catalyzes the joining of two strands of DNA between the 5´-phosphate and the 3´-hydroxyl groups of adjacent nucleotides in either a cohesive-ended or blunt-ended configuration. The ratio a 3:1 insert to vector ratio will work just fine. The amount of insert (in ng) is calculated according the following formula:

ng (insert) = molar ratio insert/vector x 50ng (vector) x bp(insert)/bp (vector)

3.1.4 Bacterial Transformation

Digestion products and are transformate into a E.Coli DH5a, stored at –80°C are transform with heat shock. Thereafter 250 µL of SOC (20g/L Bacto-tryptone, 5g/L Bacto-yeast extract, 0,5g/L NaCL, 2,5ml KCL 1M, 20% glucose, $MgCl_2$ 10 mM) medium are added to the transformation mix and the bacteria are incubated for 1 hour at 37°C and 200 rpm to allow recovery from the heat shock and start expression of the selection gene. After that, the suspension is plated on appropriate prewarmed LB agar plates.

3.1.5 Growth and culture of bacteria

Bacterial transformation of Escherichia Coli (E. *Coli*) strains or BL21 were streaked on LB plates containing 1.5% agar supplemented with the appropriate antibiotic (Ampicillin 100µg/µl or Kanamycin 75µg/µl) and stored over-night in a 37°C incubator. Liquid culture of

E. *Coli* were grown in Luria-Bertani (LB) Medium (10g/L Trypton, 5g/L Yeast Extract, 10g/L NaCl), containing the proper antibiotic (Ampicillin 100ug/ul or Kanamycin 75μg/μl), according to the plasmid resistance, for 14 hours at 37°C in shaking. For long-term storage of bacteria, glycerol stocks were prepared and conserved at -80°C. The growth curve of a bacterial culture can be monitored photometrically by reading the optical density (OD) at 600 nm.

3.1.6 MINI and MIDI plasmid preparation

Plasmids are purified from liquid bacteria cultures, usually E. *Coli*, which have been transformed and isolated. The bacteria cultures were grown over night (o/n) at 37°C in shaking in LB, after the incubation they were pellet and small-scale isolation of plasmid DNA (MINI) or a medium isolation of plasmid DNA (MIDI) preparation were be performed according to the manufacturer's instructions of NucleoSpin Plasmid Kit and NucleoBond Xtra Midi Kit (Macherey-Nagel). MINI preparation can be used for digestion with restriction enzymes, sequencing or test of expression. A typical plasmid DNA yield of a mini preparation is 20 to 30 μg, depending on the cell strain. From a MIDI preparation is obtained a DNA of a higher quality and quantity, usually a yield of 100-300 μg, which can be used for transfection of eukaryotic cells.

3.1.7 Agarose gel electrophoresis

Gels allow separation and identification of nucleic acids based on charge migration. Migration of nucleic acid molecules in an electric field is determined by size and conformation, allowing nucleic acids of different sizes to be separated. The gel is obtained by dissolving the agarose in Tris-borate-EDTA (TBE) Buffer (5,4g/L Tris Base, 2,75g/L Boric Acid, 2% EDTA pH 8), adding intercalating agent to a final concentration of 0.5 μg/ml.

3.1.8 Preparation of chemically competent cells

E. *Coli* chemo-competent DH5-α bacterial were prepared as mentioned below. A single colony of DH5-α strain was incubated over night at 37°C in 5 ml of LB broth. The next day, the colture was diluted 1:50 in 100ml of SOB (20g/L Bacto-tryptone, 5g/L Bacto-yeast extract, 0,5g/L NaCL, 2,5ml KCL 1M) and the cells were grown until an OD 0.3 was reached at 600nm.The cells were incubated for 10 min on ice and centrifuged at 3500 rpm for 15 minutes at 4°C. The pellet was resuspended in about 30ml (1/3 of the volume of the initial solution) pre-iced CCMB80 buffer (10 mM KOAc pH 7.0, 80 mM $CaCl_2.2H_2O$, 20 mM

$MnCl_2.4H_2O$, 10 mM $MgCl_2.6H_2O$, 10% glycerol). The suspension was incubated for 10 min on ice followed by further centrifugation at the same conditions. Finally the pellet was resuspended in CCMB80 buffer (1/25 volume of the initial solution) and the competent bacteria were aliquoted and stored at -80°C indefinitely.The competence was measured by transforming 50µl of cells with 1µl of standard pUC19 plasmid (Invitrogen; 10 pg/µl). With this system the mean competence is about 10^6 colonies per µg plasmid.

3.1.9 Screening of positive colonies

The colonies appearing on the plate after the transformation must be checked for the presence of the plasmid, in which the insert has been cloned. In order to perform this, is possible to use a colony PCR or a digestion with restriction enzymes. The colony PCR is the fastest method to obtain information about the cloning, because it allows to detect the presence of the insert directly from the colonies. For this purpose, some individual colonies are selected and resuspended in 50µl of water. Then, 2µl of the resuspension are added to the mix for the PCR reaction, as described before. To confirm the result, it is possible to perform a digestion reaction, using the same enzyme used for the cloning. To do this, the DNA must first be extracted from the selected colonies by mini preparation and then purified.

3.1.10 DNA sequencing

The nucleotide sequence of a fragment of DNA can be determined using the DNA sequencing method developed by Sanger and colleagues. The principle was based on the generation of DNA fragments using a DNA polymerase in the presence of deoxynucleotide-triphosphates and fluorescent-labeled dideoxynucleotide-TP, which terminate the synthesis at nucleotide specific points along the target strand. A strand of DNA that is complementary to the template was synthesized by the extension of the primer that has attached to the template. During the extension, dNTPs were added or incorporated to form a fragment and this process continued until a dideoxynucleotide triphosphate (ddNTP) (Vander Horn et al., 1997). The ddNTPs did not poses the 3'-OH group that is required for chain elongation and the fragments ends at this point.

3.2 Analysis of proteins

3.2.1 SDS polyacrylamide gel electrophoresis

SDS polyacrylamide gel electrophoresis (SDS-PAGE) involves the separation of proteins based on their size. The concentration of acrylamide used for the gel depends on the size of the proteins to be analyzed. Low acrylamide concentrations are used to separate high molecular weight proteins, while high acrylamide concentrations are used to separate proteins of low molecular weight. The solutions were prepared following conventional protocols:

- *Stacking gel*: 5% acrylamide/bisacrylamide 29:1, 0.13M Tris-HCl pH 6.8, 0,1% SDS, 0,1% APS, 0,1% TEMED;
- *Separating* (Resolving) *gel*: 8-20% acrylamide/bisacrylamide 29:1, 0.13M Tris-HCl pH 8.8, 0,1% SDS, 0,1% APS, 0,1% TEMED;
- *Running Buffer*: Tris-Gycine 10x pH 8.3 (25mM Trizma Base, 250mM Glycine, 0.1%SDS)
- *Loading Buffer 2x*: 100mM Tris-HCl pH 6.8, 10% SDS, 10mM beta-mercapto-ethanol, 20% Glycerol, 0.05% Bromophenolblue.

3.2.1 Visualization of proteins in SDS-PAGE gels

Visualization of protein bands is carried out by incubating the gel with a staining solution. The two most commonly used methods are Coomassie. We used Coomassie staining (0.05% Coomassie Brilliant Blue R-250, 40% ethanol, 10% Glacial Acetic Acid, 50% Water), which is a quantitative method of visualization of proteins and Coomasie-stained proteins can be used for downstream applications.

3.2.2 Western blotting

Following electrophoresis, proteins in a polyacrylamide gel can be transferred to a positively charged membrane (typically nitrocellulose or positively-charged nylon), where they are stained with antibodies specific to the target protein. In wet transfer, the gel and membrane are sandwiched between sponge and paper (sponge/ 2 filters of 3MM paper/ gel/ nitrocellulose membrane/ 2 filters of 3MM paper/ sponge) and all are clamped tightly together after ensuring no air bubbles have formed between the gel and membrane. The

sandwich is submerged in transfer buffer to which an electrical field is applied. A standard buffer for wet transfer is the same as the 1X Tris-glycine buffer used for the running buffer without SDS, but with the addition of methanol to a final concentration of 20%. Transfer efficiency is than checked by staining proteins on the membrane using Ponceau S staining solution (0,2% Ponceau S, 1% glacial acetic acid), which is reversibly bound to proteins. The membrane is destained completely by repeated washing in TBST (50mM Tris-HCl pH 7.5, 200mM NaCl, 0.1% Tween 20) or water.

3.2.3 Protein quantification

The protein quantification was determined by using the BCA Protein Assay Kit (Pierce, Thermo Fisher Scientific, USA). This assay utilizes the biuret reaction, where cupric ions (Cu2+) are reduced to cuprous ions (Cu+) in the presence of protein, followed by a second reaction in which the resulting cuprous ions react and form complexes with bicinchoninic acid (BCA). The BCA-Cu+ proteins complexes were detect at 562 nm absorbance . A standard curve was prepared by diluting bovine serum albumine (BSA). The isolated protein homogenate was diluted 1:10. The mix BCA-Cu+ proteins complexes were incubated at 60 C^{o} 15 min. Absorption was then measured at 562 nm by the use of a Spectrophotometer **.**

3.2.4 Proteins detection with antibodies

The membranes are incubate in blocking solution composed by 5% non-fat milk in TBS-T buffer or 2.5% BSA solution in PBS-T for phospoantibodies. After blocking, the primary antibody (diluted in the blocking solution) is added and allowed to bind to the protein. The following primary antibodies were used: mouse monoclonal anti-FLAG M2 (Sigma Cat No F1804), mouse monoclonal anti-gephyrin 3B11 (Synaptic System Cat No 147111) and rabbit polyclonal anti-NL2 (Synaptic Systems Cat. No 129202), pS/pT-P (MPM2, Upstate Biotechnology Cat No 05-368), high affinity rat monoclonal anti-HA 3F10 (Roche), anti-GFP rabbit monoclonal (Life Technology, Cat No G10362) rabbit anti-GluN1 (Sigma), rabbit anti-GluN2B (Alomone), monoclonal anti-PSD95 (Abcam and NeuroMab). Validation of antibodies used in these assays can be found on the respective manufacturers' websites.

3.2.5 Images acquisition and quantification

Western blot image acquisition was performed using the ECL detection kit and the Alliance 4.7 software (UVITECH, Cambridge). Quantifications were performed using the UVIband

imager software (Amersham). The relative amount (Input, 1/20 of the total lysate) of the different antigens considered in this study and the immunoprecipitated fractions were determined by densitometry on the acquired images. The amount of immunoprecipitated and coimmunoprecipitated proteins are first normalized to their corresponding inputs and then the coimmunoprecipated value is additionally normalized on the immunoprecipitated antigen.

3.3 Protein assays

3.3.1 GST Pull-Down Assay

3.3.1.1 GST-tagged protein expression and purification

The pGEX series of vectors is designed for prokaryotic expression of proteins as fusion products with Glutathion-S-transferase (GST) from *Schistosoma japonicum*. Since GST binds to reduced glutathione with high affinity, the recombinant protein can be easily purified by chromatography using glutathione-coupled sepharose beads. All pGEX vectors carry a *lacI*^{q} gene coding for the *lac* repressor, which allows expression in all *E. coli* strains. Induction of promoter is achieved by Isopropyl β-D-1-thiogalactopyranoside (IPTG), 100µM final concentration. Plasmids pGEX4T1-NL290 aa-CD, pGEX4T1, Pin1WT,Pin1Y23A, pGEX4T-1 GluN2B aa1086-1482 were cloned into pGEX4T1 by PCR amplification and restriction enzymes digestion, as previously described. The expression of recombinant GST fusion proteins was performed in the *E. coli* strain BL21 competent cells, using a heat-shock transformation procedure. Colonies that carried a vector coding for recombinant protein were inoculated for overnight culture in 50 ml of LB medium containing the appropriate antibiotic (ampicillin), and incubated at 37°C with shaking at 220 rpm. After dilution to an optical density (OD 600nm) of 0.1 in LB medium, cultures were grown to an OD_{600} of 0.5-0.6. Expression of GST fusion genes from pGEX vectors, hat are under the control of the *tac* promoter, was induced by addition of 1 mM IPTG. After induction, cultures were further grown for 3 hours before harvesting the bacteria for protein isolation. Bacterial cultures were harvested by a centrifugation at 5000rpm for 20 minutes at 4°C. The resulting pellet was washed once with PBS to completely remove medium and resuspended in 1/10 of the original volume in Lysis Buffer (250mM Tris-HCl pH 7.8, 1% Triton x-100, 0.2% SDS, 0.5% NP40, 0.1% Tween 20). The lysis mixture was incubated in ice for 10-15 minutes and cells were disrupted by sonication (3x10 seconds). Insoluble material was then removed by a

centrifugation at 10000rpm for 30 minutes at 4°C, and the supernatant was used as the starting material for protein isolation. The clarified lysate was incubated with equilibrated Glutathione Sepharose 4B (GSH, GE Healthcare) for 3 hours at 4°C, in rocking. After the incubation time, the glutathione beads were gently pelleted and washed with the lysis buffer, in order to eliminate the unbound proteins. Finally, the beads was equilibrated and stored in an equal volume of PBS. To assay the amount of protein bound to the GSH, 5 to 20µl of sample (depending on the protein) were loaded onto a polyacrylamide gel, in parallel to a protein of known concentration, in order to perform quantification.

3.3.1.2 Pull-Down from overexpressed HEK293T cells

Hek293T cells transfected with the constructs of interest, were harvested 48 hours after transfection and lysed in 700µl of lysis buffer (50mM Tris-HCl pH 7.5, 100mM NaCl, 0.1% Tween 20, 10mM EDTA, 2mM $MgCl_2$, 10% glycerol, 25x protease inhibitors, 500x phosphatase Inhibitors) for 30 minutes at 4°C, in slow rocking. After a centrifugation of 15 minutes at 13000rpm at 4°C, the supernatant was recovered and a small amount (50µl) was used as input to control the expression. The rest of the lysis mixture was incubated with the GST alone (usually 5µl), as a negative control and the previously prepared GST-fused protein, in order to check the interaction between the overexpressed protein and the construct of interest. The incubation was performed for 3 hours at 4°C, in rocking. After that, the resin was washed several times with the lysis buffer, pelleted and the entire buffer is removed by an insulin syringe. Before being loaded on a SDS-page gel, 30µl of sample buffer were added to the resin, and the samples were boiled 5 minutes, allowing the proteins to become detached from the resin. The interaction was then checked with a Western Blot assay, as previously described.

3.3.2 Immunoprecipitation

3.3.2.1 Immunoprecipitation on HEK 293T cells

Immunoprecipitation for MPM2 experiments was performed using a lysis buffer containing 50 mM Tris–HCl, pH 7.5, 1% Nonidet P-40, 0.5% Triton X-100, 150 mM NaCl, 1 mM Na_3VO_4, 50 mM NaF and protease inhibitor mixture (Sigma). For NL2HA and gephyrin co-immunoprecipitation, HEK293 cells overexpressing NL2HA and gephyrin-FLAG were treated 48 h after transfection with 2.5 mM PiB or mock treated with DMSO as negative controls. Cells were lysed in 50 mM Tris-HCl, pH 7.5, 100 mM NaCl, 0.1% Tween 20, 10% glycerol,

10 mM EDTA, 2 mM $MgCl_2$ and protease inhibitor mixture and immunoprecipitated by either the anti-FLAG antibody or anti-HA agarose (Pierce). For Pin1-FLAG (wt and Y23A) and GFP-PSD-95 co-immunoprecipitation, transfected cells were lysed in a buffer containing 50 mM Tris-HCl, pH 7.5, 100 mM NaCl, 0.1% Tween 20, 10% glycerol, 10 mM EDTA, 2 mM $MgCl_2$ and protease inhibitor mixture. Extracts were incubated for 2 hours at 4^{o}C with the anti-FLAG antibody (Sigma, clone M2) and immunocomplexes captured using Protein G sepharose 4 fast Flow (Amersham). NL1-HA and GFP-PSD-95 transfected cells were lysate in buffer CHAPS containing 50 mM Tris–HCl, pH 7.5, 1 mM EDTA, 150 mM NaCl, 0.5% CHAPS, 10% glycerol and protease inhibitor mixture and immunoprecipitated with anti-HA affinity resin (Pierce).

3.3.2.2 Immunoprecipitation on brain and hippocampal tissue and chemical cross-linking

Co-immunoprecipitation of native gephyrin–NL2 complexes from p15 Pin1+/+ and Pin1−/− mouse brains or hippocampal tissues was performed using a chemical cross-linking approach on postnuclear homogenates using anti NL-2 SYSY (Synaptic Systems Cat. No 129202) . DSP (dithiobis[succinimidylpropionate], Thermo scientific) is a water-insoluble, homobifunctional *N*-hydroxysuccimide ester. This crosslinker is lipophilic and membrane-permeable, therefore it is useful for intracellular and intramembrane conjugation. DSP is dissolved in dry DMSO at a 10 mM and this Crosslinker Solution is then diluted in PBS to a final concentration of 1 mM (Reaction Mixture). Meanwhile the petri dishes with the cells are washed once with PBS to remove the media. The petri dishes are then incubated 30 minutes with the Reaction Mixture at room temperature or 2 hours on ice. After that, the Stop Solution (Tris or glycin 1 M can be used) is added to the cells to a final concentration of 10 mM and it is incubated for 15 minutes. Cells are then collected, centrifuged 7 minutes at 10.000 rpm at 4° C, washed once with PBS and finally centrifuged again. The supernatant is removed and the pellet of cells is now ready to be lysed. Co-immunoprecipitations of native PSD-95/Pin1 and PSD-95/NL1 complexes were obtain from p15 Pin1+/+ and Pin1−/− brain homogenates in buffer CHAPS (as above), while PSD-95/NMDA-R complexes were isolated using a chemical cross-linking approach describe above and the native complexes were immunoprecipitated using anti-PSD95 (Abcam).

3.3.3 Biotinylation of cell surface proteins

To examine changes in NL2 transported at the plasma membrane, we performed biotinylation assays on hippocampal neuronal cultures derived from Pin1+/+ and Pin1−/−

mice. Neuronal cells were incubated with 0.5 mg ml^{-1} EZ-Link -Sulfo-NHS-LC-Biotin (Pierce) in PBS at 4 °C for 30 min. To quench the reaction, cells were washed three times with cold PBS containing 0.1 M Tris-HCl pH 7.4. Cells were then lysed in lysis buffer containing protease inhibitor cocktail followed by centrifugation at 1,000*g* for 5 min. The collected lysate were incubated with streptavidin cross-linked to agarose beads (Pierce) for 2 h at 4 °C. The beads were then washed twice with lysis buffer, and eluted with SDS loading buffer. The amount of membrane protein loaded in each experiment was normalized to the amount of the glycophosphatidylinositol-anchored protein Flotilin1, whose expression levels are identical in both mouse genotypes.

3.3.4 Synaptic Protein Extraction

PSD enriched extracts were prepared by using the Syn-PER Synaptic Protein Extraction Reagent (ThermoScientific) following the manufacturer's instructions. Briefly, a pool of four hippocampi derived from the same genotypes were homogenized in the Extraction reagents (10 ml of reagent per g of tissue), centrifuged at 1,200*g* for 10 min. The pellet was discarded while the supernatant (homogenate) was additionally centrifuged at 15,000*g* for 20 min. The cytosolic fraction was discarded and the pellet containing the synaptosomes was resuspended in 400–500 µl of reagent and analysed by western blot analysis. The protein concentration of each sample was determined using the Pierce BCA Protein Assay to allow an equal loading of total protein.

3.4 Cell culture and transfection

3.4.1 Cell culture

HEK293T (human embryonic kidney 293T) cells were cultured in Dulbecco's modified Eagle's medium (DMEM, Sigma) supplemented with 10% heat-inactivated fetal bovine serum (FBS, Sigma), 100 units/ml penicillin and 100 µg/ml streptomycin at 37 °C under humidified air containing 5%CO_2. Primary cell cultures were prepared as previously described (Andjus et al., 1997). Briefly, 2-4 days old (P2-P4) Wistar rats were decapitated after being anesthetized with anintraperitoneal injection of urethane (2mg/kg). Hippocampi were dissected free, sliced, and digested with trypsin, mechanically triturated, centrifuged twice at 40 x g, plated in Petri dishes, and cultured for up to 14 days. Experiments were performed on cells cultured for at least 7 days. For paired recording experiments, neurons were plated at low density (~ 40000cells/ml).

3.4.2 Transfection methods

3.4.2.1 Transfection with Polyethylenimine (PEI) HEK293T cells

PEI is Polyethylenimine 25kD linear from Polysciences, stock solution is diluited in endotoxin-free dH2O that has been heated to ~80°C. Than it is needed to let it cool to room temperature, neutralize to pH 7.0, filter sterilize (0.22um), aliquot and store at -20°C; a working stock can be kept at 4°C the ratio DNA / Pei was 7:1. The mixture was incubated for 20 minutes at room temperature (RT) and then added drop by drop on the plate, where cells had already reached the 60-70% of confluence. The plates were incubated at 37°C in a CO2 incubator and collect after 24 or 48 hours after transfection.

3.4.2.2 Liposome transfection Hippocampal Neurons

Hippocampal neurons were transfected with Lipofectamine 2000 or Lipofectamine 3000 (Invitrogen), according to manufacturer's instructions. Neurons were transfected between 7 and 10 DIV (days in vitro) and they were fixed after 48-72 hours after transfection. Neuron medium was collected and a medium without serum and antibiotic was added. For each petri, 1- 1.5 mg of DNA was transfected in total and two solutions were prepared the same way as for HEK cells. After an incubation of 5 minutes, the two solutions were gently mixed and incubated 20 minutes at RT to form DNA-Lipofectamine complexes. After the incubation, the solution was added directly on each petri, which were then incubated at 37°C in CO2 incubator. 1.5 hours post-transfection, half of the medium was substituted with the neuron medium collected before and the neurons were incubated at 37°C in a CO2 incubator until assaying for expression.

3. 5 Immunofluorescence and Immunohistochemistry staining

3.5.1 Immunofluorescence staining

Hippocampal neurons from Pin +/+ or Pin1-/- mice or from rat neurons grown on glass coverslips were fixed with 4% paraformaldehyde and 4% sucrose in PBS. Unspecific binding was blocked by incubation with 10% normal goat serum in PBS. Primary and secondary antibodies were diluted in 5% normal goat serum/PBS. For PSD-95 staining the were fixed at DIV15 with cold methanol for 5 minutes, blocked by incubation with 10% normal goat serum in PBS. After fixation neurons were quenched in 0.1 M glycine in PBS for 5 min, and blocked

in 10% FCS in PBS for 30 min. They were then permeabilized with 0.1% Triton X-100 in PBS for 2 min and blocked again for 15 min. After incubation with primary antibodies for 2hour, cells were incubated with AlexaFluorophore-conjugated secondary antibodies for 45 min, Alexa-488, Alexa-594 and streptavidin-Alexa 405 at dilutions of 1:1,000 (Molecular Probes). In the case of double immunostaining, cells were incubated with biotinylated secondary antibodies (45 min) followed by Streptavidin-conjuaged fluorophores (30 min). The coverslips were washed in PBS, rinsed in water and mounted with VectaShield (Vector Labs). The primary antibodies used: anti-gephyrin Mab7a (Synaptic System Cat. No 147021), anti-VGAT rabbit or guinea pig (1:1,000, Synaptic System Cat. No 131004), anti-NL2 rabbit affinity purified (1:500, Synaptic system Cat, No 129203), mouse anti-PSD95 (Sigma), guinea pig anti-vGLUT1 (Chemicon), rabbit anti-GluN1 (Sigma).

3.5.2 Immunohistochemistry staining

Eight-week-old Pin1+/+ and Pin1−/− littermates (for each genotype, n=3) were anaesthetized and perfused transcardially with 0.1 M phosphate buffer, pH 7.4 (PB). Brains were quickly removed from the skull and frozen with isopentane cooled to −40 °C with liquid nitrogen. Ten to 12-µm thick cryostat sections were collected on Superfrost glass slides and further processed for immunostaining for combined detection of VGAT and GABAA γ2 or VGAT and gephyrin. Briefly, cryostat sections were fixed by immersion in 2% paraformaldehyde, and mildly treated with pepsin as antigen-retrieval procedure, and then incubated for 48 h with different combination of primary antibodies. The primary antibodies used: anti-gephyrin Mab7a (Synaptic System Cat. No 147021), anti-VGAT rabbit or guinea pig (1:1,000, Synaptic System Cat. No 131004), anti-NL2 rabbit affinity purified (1:500, Synaptic system Cat, No 129203). Secondary antibody staining was performed for 1 h at room temperature using anti-isotypic fluorophore-conjugated antibodies Alexa-488 and Alexa-594 at dilutions of 1:1,000 (Molecular Probes).

3.5.3 Confocal microscopy and image analysis

Fluorescence images were acquired on a TCS-SP confocal laser scanning microscope (Leica, Bensheim, Germany) with a × 40 1.4 NA or × 63 1.4 NA oil immersion objectives, additionally magnified fivefold with the pinhole set at 1 Airy unit. All the parameters used in confocal microscopy were consistent in each experiment, including the laser excitation power, detector and off-set gains and the pinhole diameter. Stacks of z-sections (12–13 optical

sections) with an interval of 0.3 µm were sequentially scanned three times for each emission line to improve the signal/noise ratio. The number of gephyrin, γ2 subunit and VGAT puncta was assessed in at least eight sections for each genotypes (Pin1+/+ and Pin1−/−), by taking at least four images of strata radiatum and oriens of the CA1 region of each hippocampus in each set of experiments (n=3). In the pyramidal cell layer, the high density and elongated shape of VGAT positive terminals precluded the determination of their numbers and their colocalization with the other two antigens investigated.For immunocitochemistry samples, at least 10 cells from at least three independent batches per condition were used for analysis. Images were acquired as a z-stack (six to seven optical sections, 0.25 µm step size). In each image, at least five dendritic segments were outlined and saved as regions of interest. Quantification of immunofluorescence data was performed using the Volocity3D Image Analysis Software (PerkinElmer, London, UK). Gephyrin, NL2, GABAAR γ2 and VGAT clusters or PSD95 , vGLUT1and GluN1 were determined after thresholding of images. Thresholds were determined using the 'voxel spy' facility of the software and chosen such that all recognizable punctuate structures were included into the analysis (minimal area, 0.1 µm2); colocalization was evaluated based on the determination of thresholded Pearson's correlation coefficient (PCC > 0,5) for each staining previously identified and quantified. NL2 colocalization with gephyrin puncta or PSD-95 with GluN1 were also quantified utilizing the software function 'intersect object' that measures size, volume and intensity values of intersecting objects identified by separate protocols in each channel. To determine the degree of apposition of NL2/gephyrin colabeled clusters with the presynaptic marker VGAT, we superimposed the mask of all identified overlapping puncta onto the third channel and count them manually.

3.6 Electrophysiological experiments

3.6.1 Hippocampal slice preparation and drug treatment

All experiments were performed in accordance with the European Community Council Directive of November 24, 1986 (86/609EEC) and were approved by the local authority veterinary service and by SISSA ethical committee. All efforts were made to minimize animal suffering and to reduce the number of animal used. Transverse hippocampal slices (300 µm thick) were obtained from postnatal (P) day P10–P13 mice (male and female) using a standard protocol45. Briefly, after being anaesthetized with CO_2, animals were decapitated.

The brain was quickly removed from the skull and placed in ice-cold artificial cerebrospinal fluid containing (in mM): 130 NaCl, 25 glucose, 3.5 KCl, 1.2 NaH_2PO_4, 25 $NaHCO_3$, 2 $CaCl_2$ and 1.3 $MgCl_2$, saturated with 95% O2 and 5% CO_2 (pH 7.3–7.4). Transverse hippocampal slices (300 µm thick) were cut with a vibratome and stored at room temperature (22–24 °C) in a holding bath containing the same solution as above. After incubation for at least 45 min, an individual slice was transferred to a submerged recording chamber and continuously superfused at 33–34 °C with oxygenated artificial cerebrospinal fluid at a rate of 3–4 ml min−1.

The following drugs were used: DNQX, PTX and bicuculline, purchased from Ascent Scientific; TPMPA purchased from Tocris Bioscence. DNQX and PTX were dissolved in DMSO. The final concentration of DMSO in the bathing solution was 0.1%. At this concentration, DMSO alone did not modify the membrane potential, input resistance or the firing properties of CA1 pyramidal neurons. Drugs were applied in the bath by gravity via a three-way tap system by changing the superfusion solution to one differing only in its content of drug(s). The ratio of flow rate to bath volume ensured a complete exchange within 2 min.

3.6.2 Electrophysiological recordings

Whole-cell patch-clamp recordings (in voltage clamp configuration) were performed from CA1 pyramidal cells, visualized with an upright microscope equipped with differential interference contrast optics and infrared video camera, using a patch-clamp amplifier (Axopatch 1D amplifier, Molecular Devices, Sunnyvale, CA, USA). Patched electrodes were pulled from borosilicate glass capillaries (Hingelberg, Malsfeld, Germany). They had a resistance of 4–6 MΩ when filled with the intracellular solution containing (in mM): 125 Cs-methanesulphonate, 10 CsCl, 10 HEPES, 0.3 EGTA, 2 MgATP, 0.3 NaGTP (pH adjusted to ~7.3 with CsOH; the osmolarity was adjusted to 290 mOsmol). The stability of the patch was checked by repetitively monitoring the input and series resistance during the experiment. Cells exhibiting >20% changes in series resistance were excluded from the analysis. The series resistance was <25 MΩ and was not compensated. Spontaneous GABAergic (sIPSCs) and glutamatergic (sEPSCs) post-synaptic currents were routinely recorded from a holding potential of −60 mV in the presence of DNQX (20 µM) and PTX (10 µM), respectively. While sEPSCs were recorded using patch pipettes filled with the above mentioned solution, sIPSCs were recorded using an intracellular solution containing (in mM): CsCl 137, Hepes 10, BAPTA 11, MgATP 2, $MgCl_2$ 2, $CaCl_2$ 1 and 5 QX-314 (pH adjusted to ~7.3 with CsOH). sIPSC were also

recorded from cultured hippocampal neurons co-transfected with GFP and NL2HA or NL2HA-S714A 24 h after transfection, at a holding potential of −60 mV in presence of DNQX (20 µM) with the same intracellular solution used for the acute slices experiment. The extracellular solution contained (in mM) 137 NaCl, 5 KCl, 2 $CaCl_2$, 1 $MgCl_2$, 20 glucose and 10 HEPES, pH 7.4 (corrected with NaOH).

AMPAR- and NMDAR- mediated EPSCs were evoked by stimulation of Schaffer collateral which was set at such intensity to produce half maximal responses. In cultured hippocampal cells, EPSCs were evoked by square pulses (5ms duration, 5–25µA amplitude) delivered through a glass electrode filled with extracellular solution positioned in the vicinity of the neuron to be stimulated. To establish the AMPA/NMDA ratio, AMPA-EPSCs were first recorded in the voltage-clamp mode at -60 mV in the presence of bicuculline (5µM) to block GABAergic transmission. NMDA-EPSCs were recorded by changing the membrane potential to +40mV. In slices the NMDA component was measured 50 ms post stimulus, when the AMPA-R contribution is negligible. In cultured neurons NBQX (10µM) was added to the extracellular solution to block the AMPA-mediated component. At the end of the experiment, AP-5 was added to confirm that, in these conditions, the recorded current was mediated by NMDA-Rs.

3.6.3 Data analysis

Data were acquired and digitized with an A/D converter (Digidata 1200, Molecular Device, Sunnyvale, CA, USA). Acquisition and analysis were performed with Clampfit 9 (Molecular Device, Sunnyvale, CA, USA). Data were acquired at 20 kHz , filtered with a cut-off frequency of 2 kHz and stored on computer hard disk in order to perform off-line analysis. The resting membrane potential (RMP) was measured immediately after break-in and establishing whole-cell recording. The membrane input resistance (R_{in}) was calculated by measuring the amplitude of voltage responses to steady hyperpolarizing current steps, using the Clampfit 10.0 program (Molecular Device, Sunnyvale, CA, USA).

Spontaneous AMPA and $GABA_A$-mediated postsynaptic currents were analyzed using Clampfit 10.0 (Molecular Device, Sunnyvale, CA, USA). This program uses a detection algorithm based on a sliding template. The template did not induce any bias in the sampling of events because it was moved along the data trace by one point at a time and was optimally scaled to fit the data at each position. The detection criterion was calculated from

the template-scaling factor and from how closely the scaled template fitted the data. Spontaneous GABAergic currents were analyzed with Mini Analysis program (version 6.0.1, Synaptosoft, Leonia, NJ) for their decay time constants. Only events with no deflections in the rising or decaying phases were included in the analysis. Low amplitude (< 5pA) events as well as events whose amplitude correlated with the rising or decaying time constants were discarded from the analysis because they were thought to be affected by dendritic filtering. The decay time of s IPSCs were fitted with a single exponential function as:

$$I(t) = Aexp(-t/\tau) \quad (1)$$

where *I(t)* is the current as a function of time, *A* is the amplitude at time 0, τ is the time constant.The Mini Analysis program was used to perform peak scaled non-stationary noise analysis according to Traynelis and co-workers[47]. Individual, not correlated events, were aligned to the point of steepest rise time. The peak of the mean current response waveform was scaled to the response value at the corresponding point in time of each individual event before subtraction to generate the difference waveforms. The ensemble mean post synaptic current was binned into 50 bins of equal amplitude to assign similar weights to all phases of ensemble mean waveform. Variance was plotted against amplitude and individual points were fitted with the equation:

$$\sigma^2(I) = iI - I^2/N + \sigma_b^2 \quad (2)$$

where *i* is the unitary single-channel current, *I* is the mean current, *N* is the number of channels open at the current peak and σ_b^2 is the variance of the background noise. The single-channel chord conductance (Υ) was calculated as:

$$\Upsilon = i/(E_m - E_{rev}) \quad (3)$$

from the holding potential (E_m) of −70 mV, assuming a reversal potential (E_{rev}) of 0 mV.

Amplitude distribution of sIPSCs amplitude was obtained fitting data with the following Gaussian function:

$$n(I) = \sum_{i=I}^{n} (a_i/\sqrt{2\ \pi\ \sigma^2})\ exp(-(I_i\text{-}I_{\sigma i})^2/2\ \sigma_i^2)$$

where I_σ is the mean current, a_i is the area and σ is the variance.

The amplitude of the tonic current was estimated by the outward shift of the baseline current after the application of the $GABA_A$ receptor-channel blocker picrotoxin (100µM). Only current recordings that exhibited a stable baseline were included in the analysis. Baseline currents were estimated by plotting 4-5 0.5 s periods in all point histograms. These were fitted with a Gaussian function. The peak of the fitted Gaussian was considered as the mean holding current.

3.7.Golgi staining and spine morphology

Five Pin-/- and Pin+/+ littermates were intracardially perfused with 0.9% saline solution. Brains were rapidly collected and immersed in Golgi solution (1% potassium dichromate, 1% mercuric chloride and 0.8% potassium chromate in distilled water) for 5 days at room temperature. After a rapid (24 hours) passage in 30% sucrose solution, 100 mm coronal sections were cut through a vibratome and then mounted on gelatined slides for staining according to the Gibb and Kolb method (Gibb and Kolb, 1998). Spine analysis was carried out on apical dendrites of neurons lying on the CA1 region in the ventral hippocampus using the public domain ImageJ software (NIH, USA) according to previously described protocols (Middei et al., 2012).

4. RESULTS AND DISCUSSION

PAPER 1

Pin1-dependent signalling negatively affects GABAergic transmission by modulating neuroligin2/gephyrin interaction

Roberta Antonelli[1] , Rocco Pizzarelli[1] , Andrea Pedroni[1] , Jean-Marc Fritschy[2], Giannino Del Sal3[4], Enrico Cherubini[1,5] & Paola Zacchi[1]

1 Department of Neuroscience, International School for Advanced Studies (SISSA), via Bonomea 265, 34136 Trieste, Italy
2 Institute of Pharmacology and Toxicology, University of Zurich, Winterthurerstrasse 190, 8057 Zurich, Switzerland
3 Laboratorio Nazionale del Consorzio Interuniversitario per le Biotecnologie (LNCIB), Padriciano 99, 34012 Trieste, Italy
4 Dipartimento di Scienze della vita, Universita' degli Studi di Trieste, Trieste, Italy
5 European Brain Research Institute (EBRI), via del Fosso di Fiorano 64, 00143 Rome, Italy

Nat Commun. 5:5066

ARTICLE Received 4 Jun 2014 | Accepted 25 Aug 2014 | Published 9 Oct 2014

nature COMMUNICATIONS

ARTICLE

Received 4 Jun 2014 | Accepted 25 Aug 2014 | Published 9 Oct 2014

DOI: 10.1038/ncomms6066 OPEN

Pin1-dependent signalling negatively affects GABAergic transmission by modulating neuroligin2/gephyrin interaction

Roberta Antonelli[1], Rocco Pizzarelli[1], Andrea Pedroni[1], Jean-Marc Fritschy[2], Giannino Del Sal[3,4], Enrico Cherubini[1,5] & Paola Zacchi[1]

The cell adhesion molecule Neuroligin2 (NL2) is localized selectively at GABAergic synapses, where it interacts with the scaffolding protein gephyrin in the post-synaptic density. However, the role of this interaction for formation and plasticity of GABAergic synapses is unclear. Here, we demonstrate that endogenous NL2 undergoes proline-directed phosphorylation at its unique S714-P consensus site, leading to the recruitment of the peptidyl-prolyl *cis–trans* isomerase Pin1. This signalling cascade negatively regulates NL2's ability to interact with gephyrin at GABAergic post-synaptic sites. As a consequence, enhanced accumulation of NL2, gephyrin and $GABA_A$ receptors was detected at GABAergic synapses in the hippocampus of Pin1-knockout mice (Pin1 $-/-$) associated with an increase in amplitude of spontaneous $GABA_A$-mediated post-synaptic currents. Our results suggest that Pin1-dependent signalling represents a mechanism to modulate GABAergic transmission by regulating NL2/gephyrin interaction.

[1] Department of Neuroscience, International School for Advanced Studies (SISSA), via Bonomea 265, 34136 Trieste, Italy. [2] Institute of Pharmacology and Toxicology, University of Zurich, Winterthurerstrasse 190, 8057 Zurich, Switzerland. [3] Laboratorio Nazionale del Consorzio Interuniversitario per le Biotecnologie (LNCIB), Padriciano 99, 34012 Trieste, Italy. [4] Dipartimento di Scienze della vita, Universita' degli Studi di Trieste, Trieste, Italy. [5] European Brain Research Institute (EBRI), via del Fosso di Fiorano 64, 00143 Rome, Italy. Correspondence and requests for materials should be addressed to P.Z. (email: zacchi@sissa.it).

Structural and functional changes of post-synaptic density (PSD) components contribute to regulate synapse formation and plasticity. These remodelling events can affect trafficking, lateral mobility and turnover of several classes of structural and signalling molecules. They often involve interactions among specific proteins regulated by post-translational modifications, such as phosphorylation. At GABAergic synapses, the impact of phosphorylation on the gating properties, surface mobility and trafficking of the gamma-aminobutyric acid A receptors ($GABA_A$Rs) has been extensively studied[1,2]. Much less is known about the effects of phosphorylation of other post-synaptic proteins functionally linked to $GABA_A$Rs.

An important class of molecules involved in synapse formation, maturation and stabilization comprizes the cell adhesion molecules of the neuroligin (NLs) family[3]. These post-synaptic proteins functionally coordinate pre and post-synaptic rearrangements by binding, via their extracellular domain, the presynaptically localized neurexins (NRXs) and via specific intracellular motifs, synapse-specific scaffolding molecules[4–6]. Neuroligin2 (NL2) isoform is the only known adhesion molecule constitutively present at GABAergic PSDs[7], where it drives the recruitment of inhibitory neurotransmitter receptors as well as the scaffolding molecule gephyrin[6]. Gephyrin, initially identified as a constituent of purified glycine receptor preparations (GlyR)[8,9], was soon recognized a key player in α2 and γ2 subunit-containing $GABA_A$Rs clustering[10,11] and to be a central component of the GABAergic (and glycinergic) PSD[8,12]. On the basis of its auto-oligomerization properties, gephyrin builds a bidimensional lattice underneath the synaptic membrane, which exposes a high number of binding sites to accumulate GlyR and $GABA_A$Rs in front of the presynaptic releasing sites[13–17].

NL2 interacts with gephyrin through a conserved stretch of amino acid residues highly conserved among all family members[6]. Site-directed mutagenesis within this binding module identified a specific tyrosine residue (Y770A) whose alanine substitution impairs NL2 ability to recruit recombinant and endogenous gephyrin to post-synaptic sites[6]. Notably, the corresponding tyrosine residue on NL1, the isoform enriched at excitatory synapses, was found to be phosphorylated *in vivo*, preventing NL1–gephyrin interaction while favouring PSD95 recruitment at excitatory synapses[18]. Altogether, these findings point to the existence of intracellular signalling mechanisms able to modulate NL-scaffolding protein interactions by modifying specifically NL properties, leading to alteration in excitatory and inhibitory synaptic transmission.

In the present study, we have investigated whether post-phosphorylation prolyl-isomerization may affect GABAergic transmission in a similar manner. This signalling cascade targets serine and threonine residues preceding a proline residue to promote conformational changes on its substrate[19]. This effect is achieved by a unique enzyme, peptidyl-prolyl isomerase Pin1, whose catalytic activity facilitates the *cis–trans* isomerization of the peptide bond[20,21]. Notably, Pin1 was found to interact with gephyrin and to alter its overall conformation, thus enhancing its ability to bind the GlyR[22].

Here, we provide evidence that endogenous NL2 can be phosphorylated at its unique Pin1 consensus motif thus rendering it able to physically recruit the phospho-specific effector Pin1. We show that post-phosphorylation prolyl-isomerization can regulate NL2's ability to complex with gephyrin. Specifically, Pin1-mediated propyl-isomerization of phosphorylated serine 714 negatively modulates NL2–gephyrin complex formation, down-regulating GABAergic synaptic transmission.

Results

Endogenous NL2 undergoes proline-directed phosphorylation. The cytoplasmic domain (CD) of NL2 possesses a unique consensus motif for proline-directed phosphorylation, S714-P, located 15 amino acids apart from the transmembrane domain (Fig. 1a). To assess whether this site can undergo phosphorylation *in vivo* we used the mitotic phosphoprotein monoclonal 2 (MPM2) antibody that specifically recognizes phosphorylated S/T-P motifs (Davis *et al.*[23]). Endogenous NL2 was therefore immunoprecipitated from mouse brain homogenates using an affinity-purified polyclonal antibody raised against its CD or normal mouse IgG as negative control. Western blotting using the MPM2 antibody revealed a band at around 120 kDa that corresponds to the upper band of the doublet recognized by the NL2 antibody in parallel immunoprecipitation experiments (Fig. 1b), suggesting that at least a fraction of NL2 can be phosphorylated at its unique Pin1 consensus motif. To demonstrate that phosphorylation at serine 714 is the event responsible for NL2 detection by the MPM2 antibody, we generated the phospho-defective point mutant NL2HA-S714A. This mutation was introduced into a NL2HA hampered in gephyrin binding (NL2HA-S714A-Δgephyrin-binding domain, GBD) (see Supplementary Fig. 1), to exclude the possibility that the MPM2 antibody would immune-react with phosphorylated Pin1 consensus motifs on endogenous gephyrin, which is, at the same time, a Pin1 target[22] and an interacting partner of NL2 (ref. 6). Under these conditions, the MPM2 antibody efficiently immunoprecipitated only NL2HA-ΔGBD but not the corresponding point mutant, as indicated by the anti-HA immunoblot (Fig. 1c), thus demonstrating that S714 can be found phosphorylated on NL2.

The essential feature of proline-directed phosphorylation as a signalling mechanism relies on the ability of phosphorylated S/T-P motifs to recruit the prolyl isomerase Pin1 (refs 19,24). To test whether this unique phospho-epitope is able to recruit the effector molecule of the signalling cascade, we performed co-immunoprecipitation experiments from Pin1 +/+ and Pin1 −/− brain lysates. This approach unveiled that Pin1 can be detected in NL2, but not in control, immunoprecipitates or in the absence of Pin1 expression (Fig. 1d). To exclude the possibility that Pin1 co-precipitated by NL2 is bound to endogenous gephyrin, these assays were performed on co-expression of NL2HA-ΔGBD and Pin1-FLAG in HEK293 cells. Cell lysates were immunoprecipitated with the anti-FLAG antibody and bound protein complexes analysed by western blotting using anti-HA and anti-FLAG antibodies for NL2 and Pin1 detection, respectively. As shown in Fig. 1e, while NL2HA-ΔGBD was still able to be immunoprecipitated from cells expressing Pin1-FLAG, S714 to alanine mutagenesis completely abolished such interaction, indicating that S714 represents a newly identified Pin1 target.

Pin1 modulates gephyrin–NL2 interaction. The observation that two fundamental components of the GABAergic PSD are both targets of proline-directed phosphorylation prompted us to investigate whether such signalling cascade would modulate their interaction. To this end, we initially co-expressed gephyrin-FLAG and NL2HA in HEK293 cells and examined the amount of NL2HA that complex with gephyrin-FLAG at 48 h after treating the cells with the selective and reversible inhibitor of Pin1 isomerase activity PiB (IC_{50} of approximately 1.5 μM) (ref. 25). As shown in Fig. 2a, even though the anti-FLAG antibody immunoprecipitated comparable amounts of gephyrin-FLAG, a significant increase (64%) in the amount of co-precipitated NL2HA was observed on PiB treatment as compared with

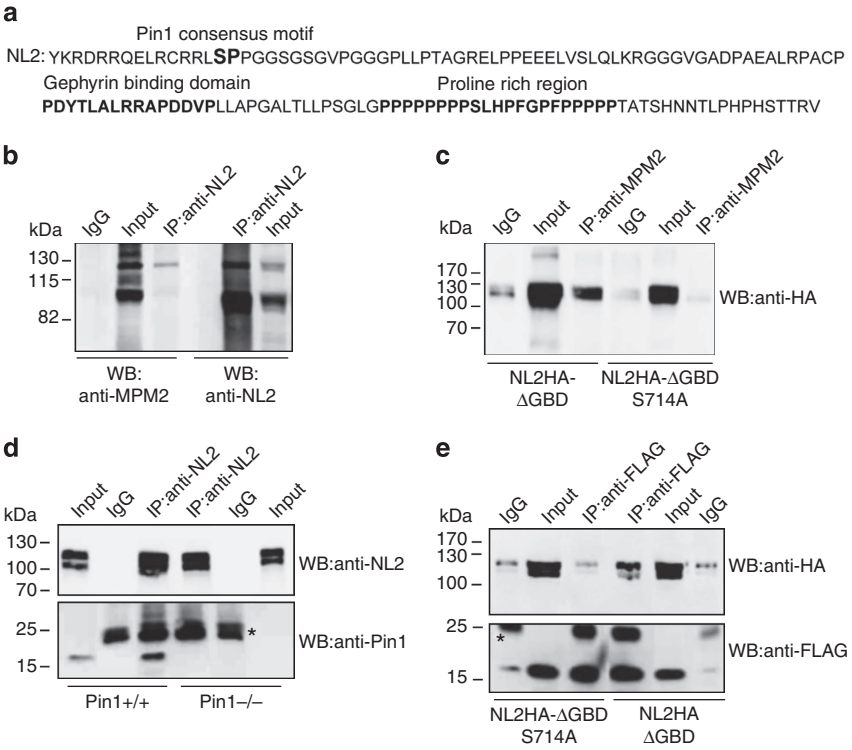

Figure 1 | NL2 is a proline-directed substrate. (**a**) Amino acid sequence of the NL2 CD. In bold is marked the unique Pin1 consensus motif (S714-P). The gephyrin-binding domain and the proline-rich region are highlighted in bold. (**b**) Representative immunoblotting of endogenous NL2 immunoprecipitated (IP) from mouse brain and probed with the anti-MPM2 that specifically recognizes phosphorylated S/T-P motifs and anti-NL2. Rabbit IgGs were used as negative control (IgG) ($n=4$). (**c**) Representative immunoblotting of overexpressed NL2HA lacking the gephyrin binding domain (NL2HA-ΔGBD) and the corresponding point mutant (NL2HA-ΔGBDSer714Ala) immunoprecipitated by the phospho-specific MPM2 antibody. Western blot analysis was carried out with anti-HA monoclonal antibody. Mouse IgGs were used as negative control ($n=5$). (**d**) Co-immunoprecipitation (Co-IP) of endogenous NL2 and Pin1 from DSP cross-linked brain homogenates of Pin1+/+ or Pin1−/− mice. Western blots were performed with anti-NL2 polyclonal and anti-Pin1 monoclonal antibodies. Mouse IgGs were used as negative control. Asterisk indicate the IgG light chains ($n=6$). (**e**) FLAG epitopes from cross-linked samples of HEK293 cells co-expressing Pin1-FLAG and NL2HA-ΔGBD or NL2HA-ΔGBDS714 were immunoprecipitated by anti-FLAG antibody. Western blot was performed with anti-HA and anti-FLAG monoclonal antibodies. Mouse IgGs were used as negative control ($n=4$). Full images of western blots are in Supplementary Fig. 5.

mock-treated cells (dimethylsulfoxide, DMSO). Interestingly, a marked increase (140%) was detected on gephyrin-FLAG co-precipitation by NL2HA-S714A as compared with NL2HA, indicating that Pin1 exerts a negative control on NL2–gephyrin complex formation, at least in part, through NL2 prolyl-isomerization (Fig. 2b).

This issue was then investigated using a source of native NL2–gephyrin complexes mouse brain homogenates from both genotypes. For these experiments, endogenous NL2 was immunoprecipitated using a rabbit polyclonal anti-NL2 antibody and the co-precipitated gephyrin fraction was visualized by the monoclonal 3B11 antibody (Fig. 2c). In the absence of Pin1 expression, the amount of gephyrin co-precipitated by NL2 was increased by 40% as compared with Pin1 expressing neurons. This approach was also applied on hippocampal tissues isolated from both mouse genotypes. Here, the enrichment of gephyrin co-precipitated by NL2 in the absence of Pin1 expression was even more dramatic as compared with the amount detected from whole brain (130% increase; Fig. 2d), suggesting a strong impact of such signalling pathway on GABAergic synapses of the hippocampus.

Characterization of gephyrin Pin1 sites S270-P and S319-P. The scaffolding molecule gephyrin possesses 10 putative Pin1 consensus motifs, the majority of them being concentrated in the central region (C-domain)[26]. To determine whether specific Pin1 sites may contribute to enhance NL2/gephyrin complex formation, we decided to focus on those located close to, or within, the NL2 binding site on gephyrin. A previous yeast two-hybrid screening identified a large portion of gephyrin encompassing the E-domain and part of the C-domain as the region involved in NL2 interaction[6]. We re-examine this issue by generating eGFP-tagged gephyrin truncated version to be tested in GST-NL2-CD pulldown assays. HEK293 cells transfected with different eGFP-gephyrin variants were incubated with GST-NL2-CD loaded beads or with GST alone as negative controls. As shown in Fig. 3a, while gephyrin 310–736 was recruited even better than the wild-type (WT) version, the mutants gephyrin 326–736 and gephyrin 1–310 (gephyrin GC) displayed a reduced binding activity as compared to both gephyrin full-length (FL) and the truncated version 310–736 (Fig. 3a). Since the two E-domain gephyrin versions, showing such a striking difference in the binding affinity, differ only for a short stretch of amino acids, we generated the deletion mutant removing, from the FL protein, only the residues contained in this region but belonging to the E-domain itself (gephyrinΔ319–329) and assayed it for NL2 binding. Interestingly, the lack of this short sequence almost completely abolished the interaction of gephyrin with NL2 (Fig. 3b), indicating that epitope(s) contained in the C-domain together with this minimal binding module are involved in gephyrin recruitment.

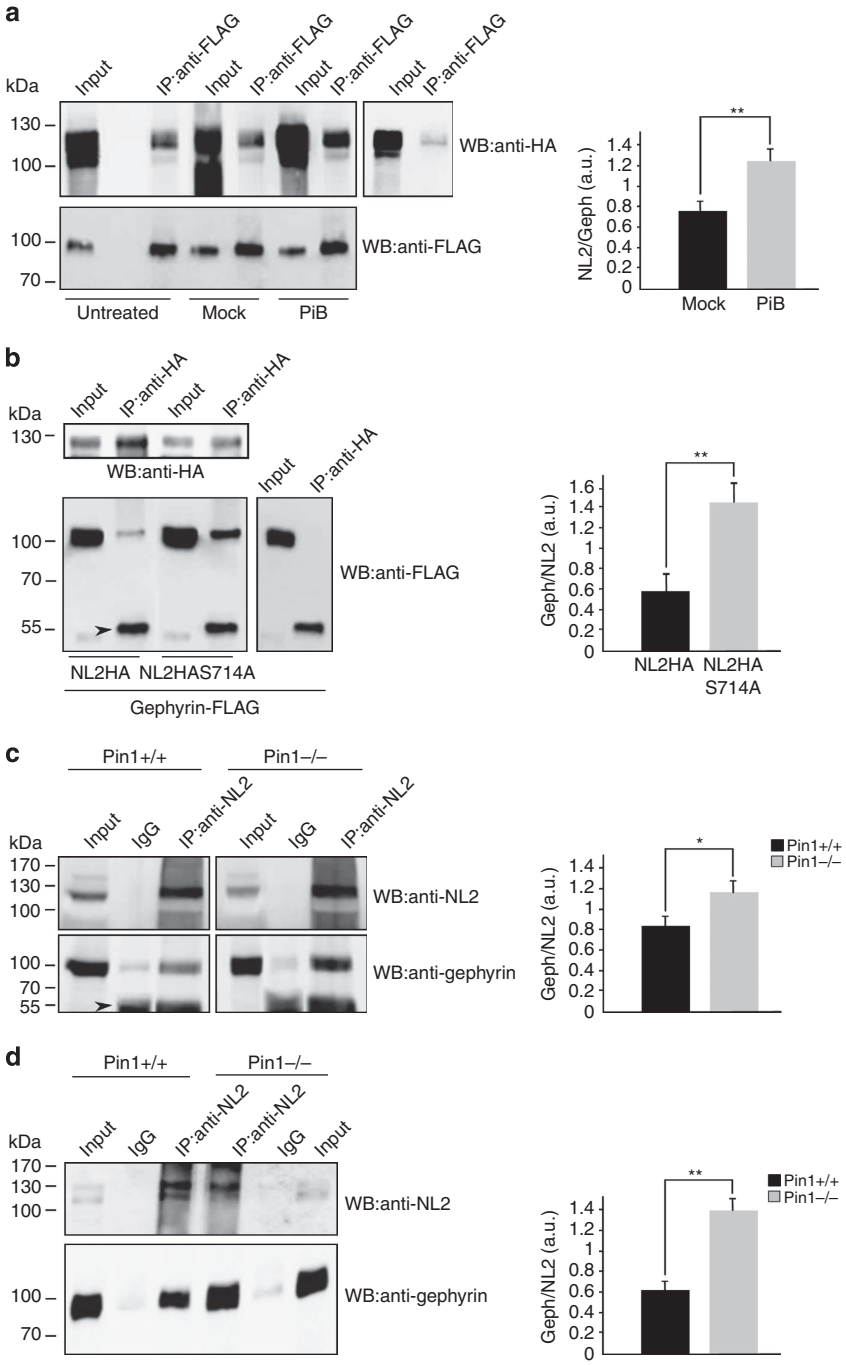

Figure 2 | Pin1 negatively modulates NL2/gephyrin interaction. (**a**) Representative IP of FLAG epitopes from samples of HEK293 cells co-expressing gephyrin-FLAG and NL2HA and treated for 48 h with PiB 2.5 μM, DMSO (mock) or untreated. IP was also performed on NL2HA single transfected cells as a negative control. Nitrocellulose membranes were probed with anti-HA and anti-FLAG antibodies. The histogram on the right shows the relative amount of NL2 co-precipitated by gephyrin-FLAG in control and PiB treated cells obtained from densitometric analysis ($n=5$, mean values ± s.d., $^{**}P<0.001$, Student's *t*-test). (**b**) Lysates of HEK cells transfected with gephyrin-FLAG in the presence of NL2HA or NL2HA-S714A or with gephyrin alone (as a negative control) were immunoprecipitated with anti-HA agarose. Immunoprecipitates were analysed by western blotting using anti-FLAG and anti-HA monoclonal antibodies. Arrowhead indicates the IgG heavy chains. The histogram on the right shows the relative amount of gephyrin-FLAG in complex with either NL2HA or NL2HA-S714A co-precipitated by anti-HA agarose obtained from densitometric analysis ($n=5$, mean values ± s.d., $^{**}P<0.001$, Student's *t*-test). (**c**) Co-IP of endogenous NL2/gephyrin complexes from DSP cross-linked brain homogenates of Pin1 + / + or Pin1 − / − mice. Western blots were performed with anti-NL2 polyclonal and anti-gephyrin monoclonal antibodies. Rabbit IgGs were used as negative control. An increased amount of gephyrin co-precipitates in complex with NL2 in the absence of Pin1 expression. Arrowhead indicates the IgG heavy chains. The histogram on the right shows the relative amount (obtained from densitometric analysis) of endogenous gephyrin co-precipitated by endogenous NL2 from both mouse genotypes ($n=8$, mean values ± s.d., $^{*}P<0.01$, Student's *t*-test). (**d**) A similar experiment described in **c** was carries out on hippocampus isolated from of Pin1 + / + or Pin1 − / − mice. The histogram on the right shows the relative amount (obtained from densitometric analysis) of endogenous gephyrin co-precipitated by endogenous NL2 from both mouse genotypes ($n=4$, mean values ± s.d., $^{**}P<0.001$, Student's *t*-test). Full images of western blots are in Supplementary Fig. 5.

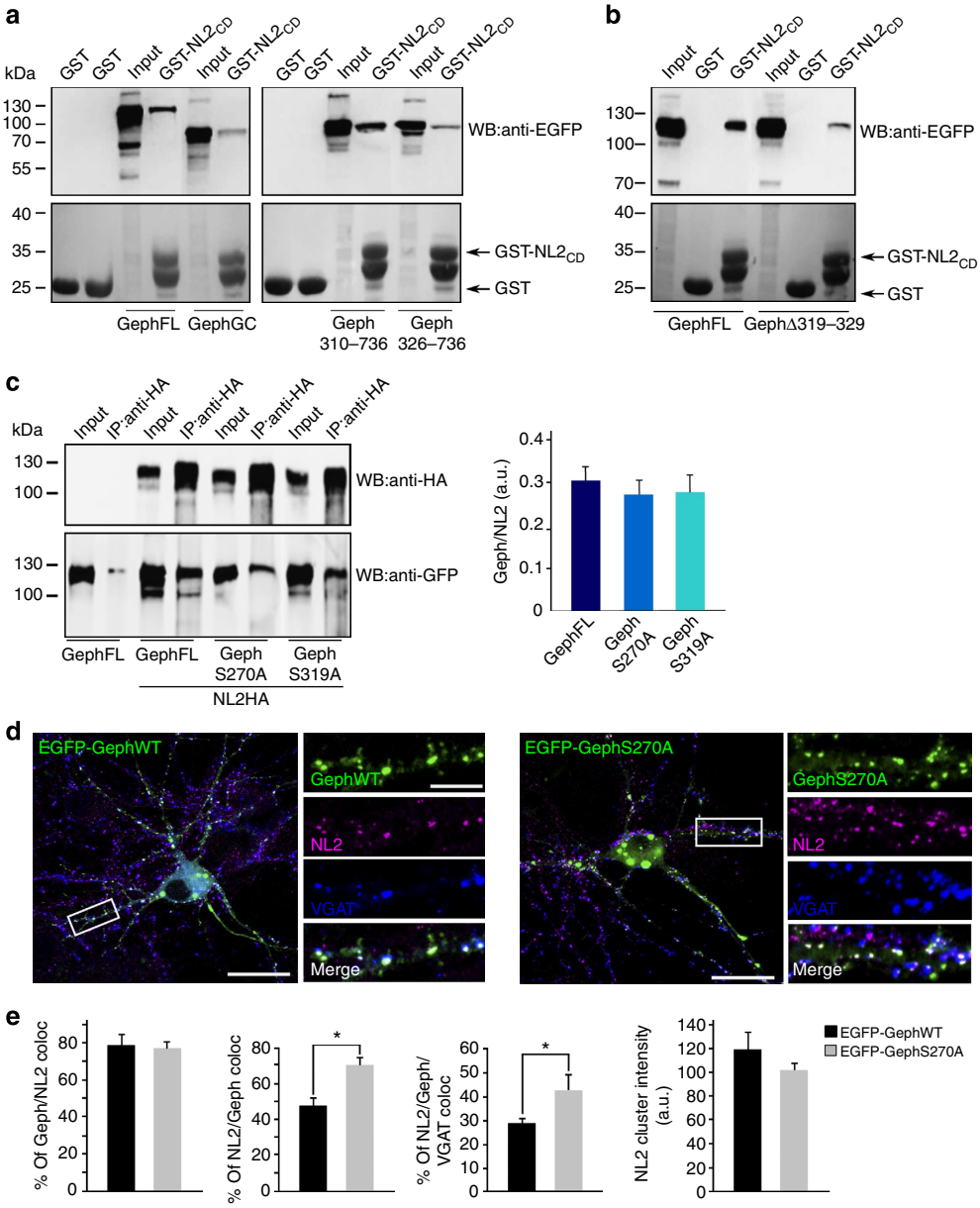

Figure 3 | Impact of gephyrin S270A and S319A in NL2/gephyrin interaction. (**a**) GST-NL2-CD pulldown from samples of HEK293 expressing EGFP-gephyrin full-length (FL), EGFP-gephyrin 310–736 (E-310), EGFP-gephyrin 326–736 (E-326) and EGFP-gephyrin GC. GST was used as negative control. Pulled down eGFPgephyrin variants were detected using an anti-GFP monoclonal antibody. The bottom panels show the levels of GST and GST-NL2-CD in the pulldown assays (Ponceau staining) ($n=8$). (**b**) EGFP-gephyrin Δ319 to 329 was tested in similar pulldown assays. Western blots in **a** and **b** were performed using anti-GFP antibody. Gephyrin requires amino acid sequence 319–329 for its efficient recruitment by NL2 ($n=6$). (**c**) Representative IP of HA epitopes from samples of HEK293 cells co-expressing NL2HA and EGFP-gephyrin WT, EGFP-gephyrinS270A or EGFP-gephyrinS319A. Nitrocellulose membranes were probed with anti-HA and anti-GFP antibodies. EGFP-gephyrin single transfected cells incubated with HA agarose were used as negative controls. The histogram on the right shows the relative amount of eGFP-gephyrinWT and point mutants co-precipitated by NL2HA ($n=4$, mean values ± s.d., $P>0.05$). (**d**) Representative images of hippocampal neurons transfected with EGFP-gephyrin and EGFP-gephyrinS270A point mutant immunolabeled for endogenous NL2 (magenta) and VGAT (blue) at DIV10. Enlarged boxed areas are shown aside to the corresponding full view image. Post-synaptic clustering is demonstrated by apposition of gephyrin/NL2 clusters to VGAT positive terminals on the merge window. Scale bars, 20 µm in full view images and 5 µm in enlarged panels. (**e**) Distribution histograms of the % of gephyrin clusters colabeled with NL2 (79 ± 5% in EGFP-gephyrinWT versus 77 ± 4% in EGFP-gephyrinS270A), % of NL2 clusters colabeled with gephyrin (48 ± 5% in EGFP-gephyrinWT versus 71 ± 4% in EGFP-gephyrinS270A), % of NL2 synaptically localized (29 ± 2% in EGFP-gephyrinWT versus 43 ± 6% in EGFP-gephyrinS270A) and NL2 clusters intensity (119 ± 15 a.u. in EGFP-gephyrinWT versus 102 a.u. ± 6 in EGFP-gephyrinS270A). The number of transfected hippocampal neurons investigated in each experiments (four independent experiments) were as follow: $n=15$ for eGFP-gephyrinWT, $n=10$ for eGFP-gepyrinS270A (for each neurons at least 4 dendritic regions of interests were measured, mean values ± s.d., $^*P<0.01$, Student's *t*-test).

On the basis of these results, two Pin1 consensus sites were further characterized, namely S319-P, located at the edge of the minimal binding module, and S270-P, positioned in its proximity, still contained, in the C-domain participating in NL2 binding. To this end, we introduced point mutations in eGFP-gephyrin to create S319A and S270A mutants and tested them for their ability

to interact with NL2HA. As judged by co-immunoprecipitation experiments, no significant differences were observed in binding capacity of the mutants as compared with gephyrin WT (Fig. 3c). These constructs were also overexpressed in cultured hippocampal neurons to analyse and quantify their impact on endogenous NL2 distribution using immunofluorescence staining and confocal microscopy. As previously reported, neurons expressing the S270A mutants had an increased number, unchanged in size, of gephyrin clusters compared with eGFP-gephyrin WT[27] (18.9 ± 1.7 per 20 µm dendritic segment versus 6.5 ± 0.6, $P = 0.00015$). The expression of the S319A construct produced a dramatic decrease in cluster density associated with a diffuse cytoplasmic staining. This latter effect seems to correlate with the intrinsic instability of the mutant protein that undergoes a high rate of degradation on neuronal expression (data not shown), hampering its further characterization. Clusters formed by gephyrin S270A co-localized with NL2 at the same extent as the WT protein (around 78%; Fig. 3d,e). The fraction of NL2 clusters co-localizing with S270A mutant as well as their synaptic localization were increased as compared with gephyrin WT but their intensity values (calculated by normalizing cluster fluorescence intensity to cluster area and expressed in a.u.: 119 a.u. ± 15.2 versus 102 ± 6.3) were unchanged (Fig. 3e). These data indicate that the increase in NL2/gephyrin S270 interaction observed by immunoprecipitation is simply due to the augmented S270A cluster density and not to an enhance affinity of the mutant for NL2.

Pin1 selectively controls NL2 synaptic enrichment. Pin1 has emerged as a negative regulator of gephyrin–NL2 interaction. Since these protein complexes are mainly localized at the plasma membrane, we tested whether Pin1 affects the amount of NL2 transported to, or maintained at, the neuronal plasma membrane. To this end, cultured hippocampal neurons derived from Pin1 +/+ and Pin1 −/− mice were subjected to surface biotinylation assay. Cell surface proteins were treated with the membrane-impermeant sulfo-NHS-biotin reagent, then isolated by binding to Streptavidin beads and probed with anti-NL2 antibody. To check for unspecific protein binding during surface biotinylation experiments, hippocampal neurons not labelled with biotin were processed with biotinylated samples. Western blot detecting the intracellular glycophosphatidylinositol-anchored protein Flotilin1 was included to ensure that similar amount of associated membrane proteins, biotinylated or not, where incubated with Streptavidin beads. No major differences on the total content of membrane localized NL2 were observed between Pin1 +/+ and Pin1 −/− (Fig. 4a).

These results allow excluding the involvement of Pin1 in NL2 transport and/or turnover at the plasma membrane. Surface biotinylation represents an experimental approach that cannot provide an accurate analysis of protein distributions among different membrane domains. Since NL2 is enriched at GABAergic synapses, but is also distributed on extrasynaptic sites[28], with

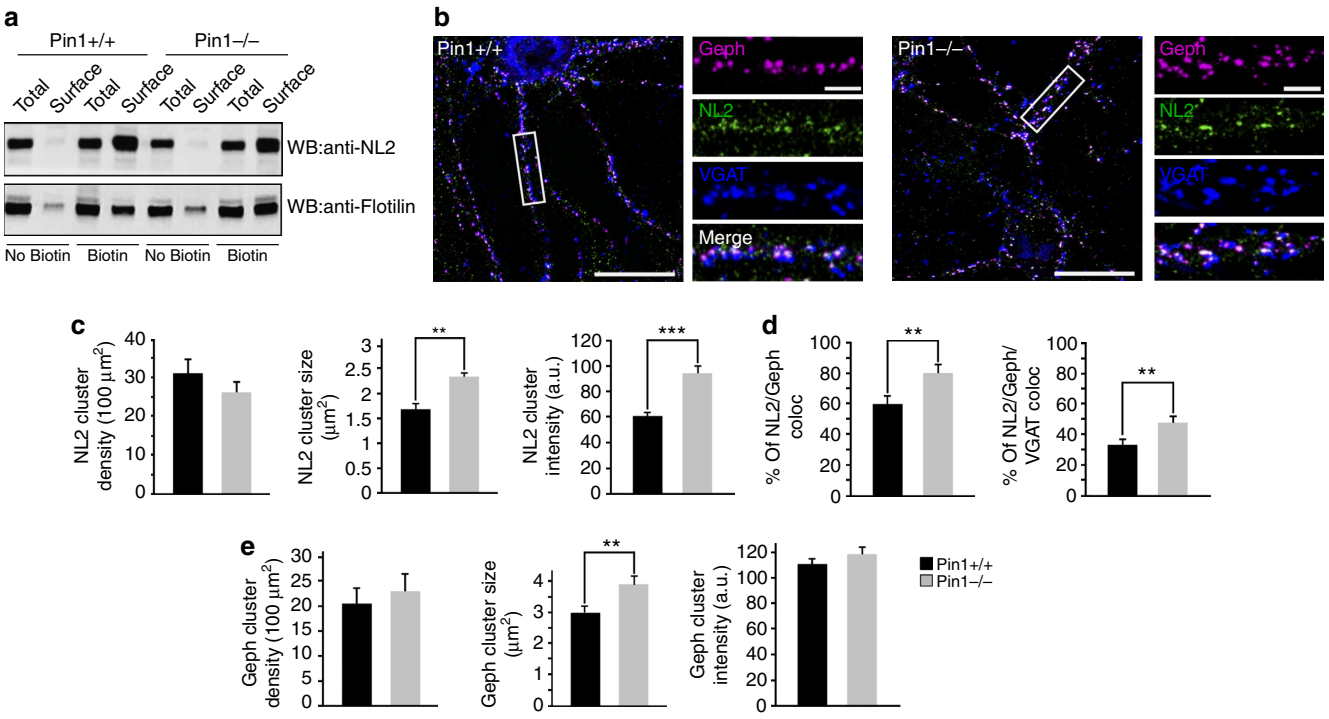

Figure 4 | Pin1 enhances NL2 synaptic content not its surface abundance. (**a**) Surface NL2 derived from cultured hippocampal neurons of Pin1 +/+ and Pin1 −/− mice was isolated by biotinylation assay and detected by anti-NL2 antibody. No biotinylated neuronal cells were processed in parallel to evaluate unspecific NL2 binding. Western blot detecting glycophosphatidylinositol-anchored Flotilin was used as loading control ($n = 4$). Full images of western blots are in Supplementary Fig. 5. (**b**) Typical examples of hippocampal neurons from Pin1 +/+ and Pin1 −/− immunolabeled for endogenous gephyrin (magenta), NL2 (green) and VGAT (blue) at DIV10. Enlarged boxed areas are shown aside to the corresponding full view image. Post-synaptic clustering is demonstrated by apposition of gephyrin/NL2 clusters to VGAT positive terminals on the merge window. Scale bars, 20 µm in full view images and 5 µm in enlarged panels. (**c**) Distribution histograms of NL2 cluster density (normalized to 100 µm^2), the average cluster size and intensity in Pin1 +/+ and Pin1 −/− hippocampal neurons. (**d**) Distribution histograms of the percentage of NL2 co-localizing with gephryin and the percentage of double labelled NL2/gephyrin puncta overlapping with the presynaptic marker VGAT. (**e**) Distribution histograms of gephyrin cluster density (normalized to 100 µm^2), the average cluster size and intensity (calculated as described in **c**) in both mouse genotypes. The number of hippocampal neurons investigated in each experiments (three independent experiments) were as follows: $n = 10$ for Pin1 +/+, $n = 12$ for Pin1 −/−. For each neurons, at least five dendritic regions of interests were measured, mean values ± s.d., $^{**}P < 0.001$, $^{***}P < 0.0001$, Student's t-test).

this approach differences in NL2 partitioning between these two compartments might have been missed.

To this aim, immunocytochemical experiments were performed in dissociated Pin1 +/+ and Pin1 −/− hippocampal neurons co-labelled for NL2, gephyrin and VGAT, a specific marker of GABAergic innervations[29] (Fig. 4b). In the absence of Pin1 expression a significant increase in NL2 cluster size (2.4 μm² ± 0.2 versus 1.7 μm² ± 0.2, $P = 0.00044$) and intensity (92 a.u. ± 4.0 versus 58 a.u. ± 2, $P < 0.00048$) was observed as compared with WT neurons, while no major changes in NL2 cluster density were detected (Fig. 4c). The fraction of NL2-positive clusters co-localized with endogenous gephyrin puncta was also enhanced in Pin1 −/− cells (80 ± 3.0% versus 60 ± 5%, $P = 0.00013$) and found enriched at post-synaptic sites, as demonstrated by the higher percentage of NL2/gephyrin co-stained puncta overlapping with the presynaptic marker VGAT (48 ± 4% versus 33 ± 4%, $P = 0.0008$; Fig. 4d). Gephyrin puncta appeared slightly, but significantly, increased in size while their density and intensity values were unchanged as compared with Pin1 +/+ (Fig. 4e). These observations suggest that the absence of Pin1 promotes the formation and/or stabilization of NL2/gephyrin complexes at GABAergic post-synaptic sites.

NL2/gephyrin complex modulates synaptic abundance of $GABA_A$Rs. The recruitment of $GABA_A$Rs at synaptic sites is functionally coupled to NLs expression levels as well as to the gephyrin scaffold[6]. To assess whether the enhanced NL2/gephyrin complex formation detected at GABAergic synapses similarly affects the distribution of synaptic γ2 subunit-containing $GABA_A$Rs, we performed a quantitative evaluation of the γ2 subunit present in synaptosome suspensions isolated from the hippocampus of Pin1 +/+ and Pin1 −/− mice. Quantitative immunoblot analysis was also extended to NL2 and gephyrin to further verify their synaptic enrichment. As shown in Fig. 5a, the amount of all three markers investigated was significant increased in Pin1 −/− mice as compared with Pin1 +/+. The synaptic enrichment (synaptic fraction versus homogenate) was 35 ± 5% for the NL2, 30 ± 6% for the γ2 subunit and 20 ± 4% for gephyrin.

We also examined the number of puncta labelled for gephyrin and γ2 subunit-specific antibodies, as well as their levels of colocalization with the presynaptic marker VGAT, in the CA1 region of the hippocampus of both genotypes. The staining pattern of gephyrin in Pin1 −/− demonstrated a slight increase in the number of clusters both in the stratum oriens (SO) and stratum radiatum (SR) as compared with Pin1 +/+ (SO 16 ± 3 clusters per 100 μm² and SR 28 ± 3 clusters per 100 μm² versus SO 10 ± 2 clusters per 100 μm² and SR 19 ± 3 clusters per 100 μm²; $P < 0.05$; Fig. 5b,c). This increase was paralleled by a small increase (around 6–8%) in gephyrin puncta co-localized with presynaptic VGAT (SO 30 ± 2% and SR 39 ± 1.4% versus SO 24 ± 2% and SR 31 ± 2%; $P < 0.05$; Fig. 5b,c). The average cluster size and intensity were similar in both genotypes (3.6 μm² ± 0.2 versus 3.5 μm² ± 0.3 and 61 ± 7 versus 65 ± 4 a.u. for cluster size and intensity in Pin1 −/− versus Pin1 +/+, respectively).

The γ2 subunit staining pattern exhibited a similar cluster density in the two strata analysed in both genotypes (SO 8 ± 2 and SR 18 ± 2 versus SO 8 ± 1 and SR 17 ± 1.2; $P > 0.05$; Fig. 5d,e). A small, although significant, increase in their intensity was evident (120 ± 3 RFU versus 106 ± 2 RFU in Pin1 −/− versus Pin1 +/+; $P < 0.05$) but they were similar in size (4.3 μm² ± 0.5 versus 3.7 μm² ± 0.5). VGAT colocalization was increased by 10–15% in tissue from knockout animals (SO 38.9 ± 2.7% and SR 52 ± 3% versus SO 29 ± 2% and SR 36 ± 3%; $P < 0.05$; Fig. 5d,e). The changes in gephyrin and γ2 subunit synaptic fraction are not due to an increase in synapses numbers, the density of inhibitory terminals being unaltered between the two genotypes, as assessed by quantification of VGAT immunolabeling (SO 14 ± 2% and SR 22 ± 3% versus SO 13 ± 2% and SR 21 ± 3%; $P > 0.05$).

Altogether, these data indicate that the enhanced interaction between gephyrin and NL2 observed in the absence of Pin1 is associated with a concomitant increase in the synaptic recruitment of γ2 subunit-containing $GABA_A$Rs.

Pin1 signalling affects the number of synaptic $GABA_A$Rs. To functionally explore whether the enrichment of γ2 subunit-containing $GABA_A$Rs in Pin1 −/− mice affects GABAergic transmission, whole-cell recordings in voltage clamp configuration were performed from CA1 principal cells in hippocampal slices obtained from Pin1 +/+ and Pin1 −/− mice at postnatal (P) day P10–P13. These neurons presented similar resting membrane potential (V_{rest}) and input resistance (R_{in}) values (data not shown), thus indicating that Pin1 does not affect the passive membrane properties of principal cells. Spontaneous $GABA_A$-mediated inhibitory post-synaptic currents (sIPSCs) were then recorded from both genotypes in the presence of 6,7-dinitroquinoxaline-2,3-dione (DNQX; 20 μM) to block AMPA-mediated excitatory post-synaptic currents (sEPSCs). As shown in Fig. 6a, recordings from Pin1 −/− mice exhibited sIPSCs of higher amplitude values compared with control littermates (106 ± 12 pA versus 62 ± 8 pA; $P < 0.05$), in the absence of any significant change in frequency (4.2 ± 0.5 Hz versus 3.6 ± 0.6 Hz; $P > 0.05$; Fig. 6b). The amplitude distribution histogram of sIPSCs recorded in Pin1 −/− unveiled a clear peak at ∼200 pA (Fig. 6c). The observed effects were selective for sIPSCs since no significant differences in amplitude (22 ± 2 pAin Pin1 −/− mice and 27 ± 4 pA in Pin1 +/+; $n = 6$ for both genotypes; $P > 0.05$) or frequency (1.7 ± 0.3 Hz in Pin1 −/− mice and 1.3 ± 0.4 Hz in Pin1 +/+ mice; $P > 0.05$) of sEPSCs (recorded in the presence of picrotoxin, PTX, 100 μM) were detected between the two genotypes (Supplementary Fig. 2a,b).

Spontaneous inhibitory events from hippocampal neurons in culture overexpressing the NL2HA-S714A mutation exhibited, compared with NL2HA-transfected cells, a significant increase in amplitude (but not frequency), which in part mimicked the phenotype observe in Pin1 −/− mice, suggesting that the interaction of Pin1 with NL2 is critical for this effect (Fig. 7a). As shown in the cumulative amplitude plot (Fig. 7b), the curve obtained from NL2HA-S714A transfected cells was shifted to the right as compared with cells expressing NL2HA ($P < 0.05$).

The selective increase in amplitude of sIPSCs detected in Pin1 −/− mice suggest a post-synaptic site of action. This may involve an increase in the number of active $GABA_A$Rs or changes in single-receptor channel conductance. To distinguish between these two possibilities, peak-scaled non-stationary fluctuations analysis of sIPSCs was performed only on stable recordings with no time-dependent changes in either peak amplitude, 10–90% rise time and decay time (Fig. 8a) (electrotonic filtering was excluded on the basis of no correlation between 10–90% rise time and decay time[30]). Plotting the mean current amplitude versus variance and fitting individual points with the parabolic equation (equation (2) in the methods; Fig. 8b), allowed estimating single-channel conductance and the number of channels open at the peak of spontaneous IPSCs. The single-channel conductance was calculated according to equation (3), assuming a reversal potential for chloride equal to 0. Interestingly, while the values of single-channel conductance were similar in both genotypes (Fig. 8c), the average number of active channels open at the peak of sIPSCs (Np) was significantly increased in Pin1 −/− mice compared with controls (53 ± 11 versus 26 ± 5; $P = 0.03$; Fig. 8c).

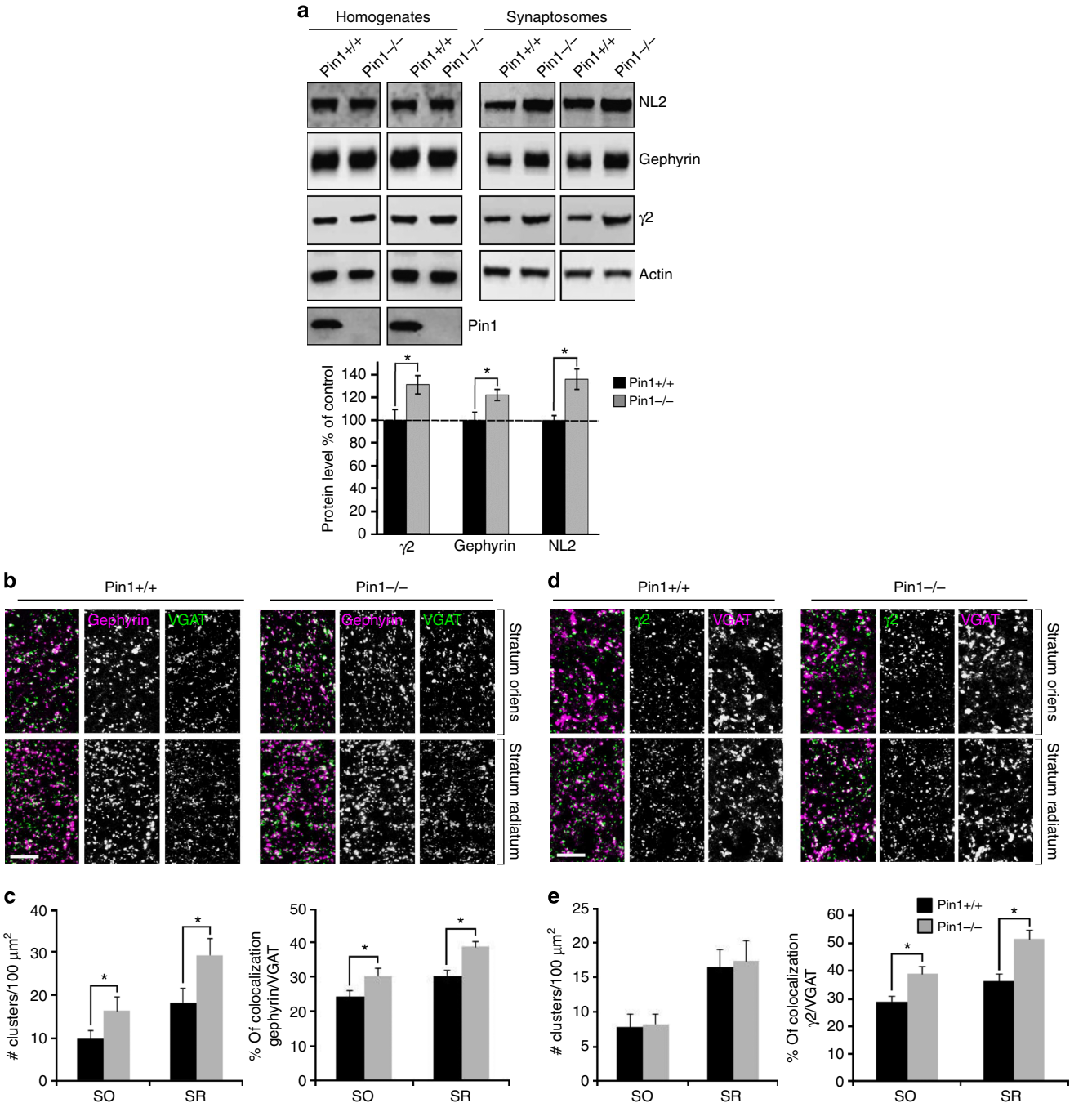

Figure 5 | Synaptic enrichment of $GABA_ARs$ is achieved in Pin1 −/−. (**a**) Representative immunoblots of NL2, gephyrin and γ2 subunit of $GABA_A$ receptor extracted from the hippocampus of Pin1+/+ and Pin1−/− mice (littermates) in two different sets of experiments. Total proteins from the homogenates and synaptosome suspension fractions were analysed by western blotting. Below: quantification of the indicated antigens extracted from hippocampal tissues of Pin1+/+ and Pin1−/− mice. All markers analysed are enriched at inhibitory synapses. Western blot to actin was done as loading control. Pin1 immunoblot indicates hyppocampus from Pin1+/+ and Pin1−/− ($n=6$ littermate pairs, mean values ± s.d, $^*P<0.05$, Student's *t*-test) Full images of western blots are in Supplementary Fig. 5. (**b**) Representative confocal micrographs of frontal brain sections showing segments of the SR and SO of the CA1 region of the hippocampus from adult Pin1+/+ and Pin1−/− mice immunolabeled for gephyrin (magenta) and VGAT (green). Scale bar, 5 µm. (**c**) Quantification of gephyrin punctum density (normalized to 100 μm^2) and their percentage of colocalization with the presynaptic marker VGAT in both mouse genotypes. (**d**) Confocal micrographs as in **a** immunolabeled for $GABA_A$ receptor γ2 subunit (green) and VGAT (magenta). (**e**) Quantification of γ2 subunit punctum and their percentage of colocalization with VGAT in both mouse genotypes. The number of gephyrin, γ2, gephyrin and VGAT puncta was assessed in at least eight sections for each genotypes (Pin1+/+ and Pin1−/−), by taking at least four images of SR and SO of the CA1 region of each hippocampus in each set of experiments ($n=3$). Mean values ± s.d., $^*P<0.05$, Student's *t*-test. Scale bar, 5 µm.

To further evaluate the possibility that higher amplitude inhibitory events recorded in Pin1−/− mice may originate from $GABA_ARs$ containing different subunits, we measured in both genotypes the decay time constants of small and large amplitude events. Spontaneous IPSCs were plotted against their decay half-widths and arbitrarily divided in two main classes whose

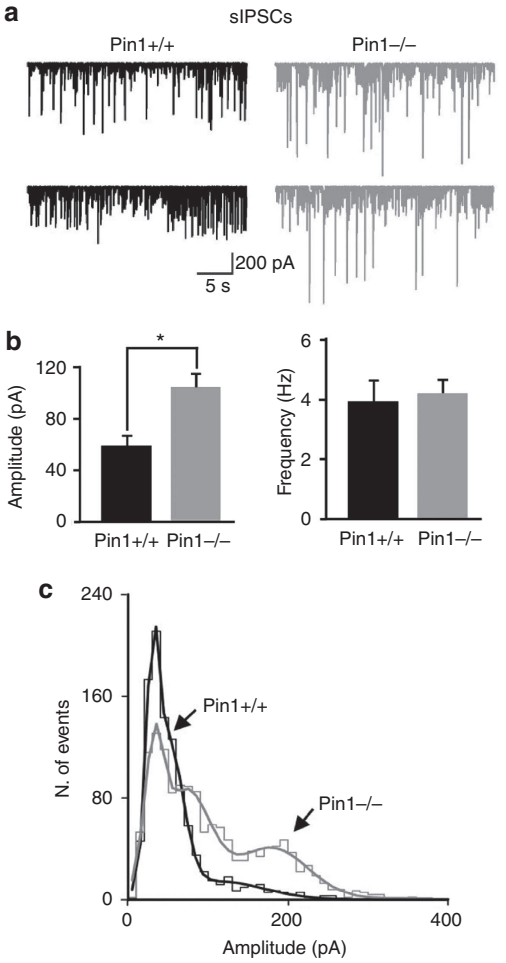

Figure 6 | Pin1 affects the amplitude but not the frequency of sIPSCs. (**a**) Representative traces of sIPSCs recorded from CA1 principal cells at P11 in hippocampal slices from Pin1+/+ (black) and Pin1−/− mice (grey). Note higher amplitude events in Pin1−/− mice. (**b**) Each column represents the mean frequency and amplitude values of sIPSCs recorded from Pin1+/+ (black, $n=9$) and Pin−/− mice (grey, $n=8$). *$P<0.05$, Student's t-test). (**c**) Amplitude distribution histograms of sIPSCs recorded in Pin1+/+ (1,030 events; black) and in Pin1−/− mice (1,412 events; grey). Note the appearance of a clear peak at ~200 pA in Pin1−/− mice.

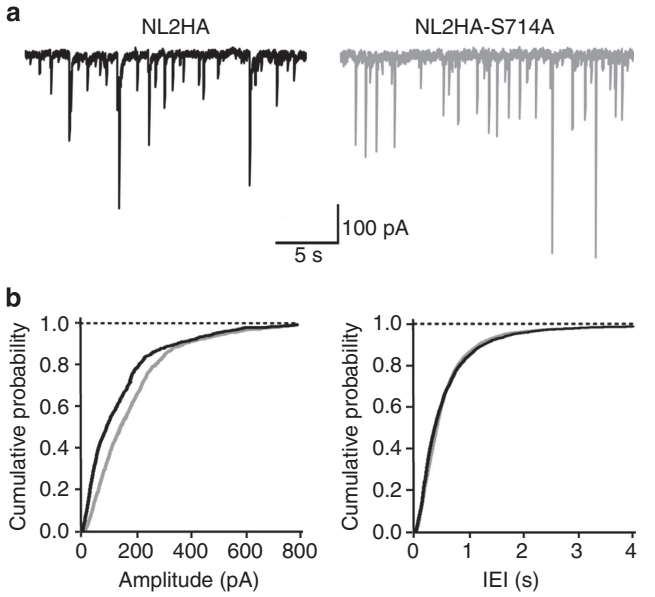

Figure 7 | Changes in amplitude of sIPSCs involve the interaction of Pin1 with NL2. (**a**) Samples traces of sIPSCs recorded from hippocampal neurons in culture expressing either the NL2HA or the NL2HA-S714A mutation. (**b**) Amplitude and inter-event interval (IEI) plots of sIPSCs recorded in cells transfected either with the NL2HA (black; $n=7$) or the NL2HA-S714A point mutant (grey; $n=12$). $P<0.05$; Kolmogorov–Smirnov test. Note the shift to the right of the cumulative amplitude distribution curve obtained from cells transfected with the mutant as compared to controls.

amplitude was <or>150 pA (Fig. 9a, in green and blue, respectively). Notably, larger amplitude events (>150 pA) prevailed in Pin1−/− mice. No differences in decay of sIPSCs <or>150 pA were observed between Pin1+/+ and Pin1−/− mice, thus excluding the involvement of multiple receptor subtypes with different kinetics (the 90–10% decay (τ) of sIPSCs <150 pA was 9±1 ms in Pin−/− mice and 11±2 ms in Pin1+/+; $P>0.05$; τ of sIPSCs >150 pA was 11±2 ms in Pin−/− mice and 10±2 ms in Pin1+/+; $P>0.05$. The 90–10% decay time ($\tau_{90-10\%}$) of all sIPSCs was 11±2 ms and 10±2 ms in Pin1+/+ and Pin1−/− mice, respectively; Fig. 9b,c, P>0.05). These data altogether suggest that the observed increase in amplitude of sIPSCs in Pin1−/− mice is exclusively due a genuine increase in number of $GABA_A$Rs composed of the same subunits.

GABA release and tonic inhibition are unaltered in Pin1−/−. In a previous study, we demonstrated that the functional knockdown of NL2 was accompanied by a reduction in the probability of GABA release[31], thus underlying the role of NLs as retrograde regulators of presynaptic function. Therefore, we evaluated here whether Pin1-dependent modulation of NL2–gephyrin interaction could also affect GABA release from presynaptic nerve terminals. To this end, we used 1,2,5,6-tetrahydropyridin-4-yl methylphosphinic acid (TPMPA), a low affinity competitive $GABA_A$R antagonist[32]. This approach allowed to compare differences in presynaptic GABA transients between Pin1+/+ and Pin1−/− mice. Similar reduction of sIPSCs amplitude in both genotypes (51±6% versus 54±8%, $P>0.05$, Supplementary Fig. 3a,b) was detected on bath application of TPMPA (200 µM), thus excluding a transsynaptic action of Pin1 on GABA release.

Part of GABA released during synaptic activity may escape the cleft and invade the extracellular space to activate extrasynaptic high affinity $GABA_A$Rs. This feature generates a persistent $GABA_A$-mediated conductance[33] that is involved in a number of physiological processes[34]. To determine whether Pin1 signalling affects extrasynaptic $GABA_A$Rs, we analysed the tonic $GABA_A$-mediated conductance in both Pin1+/+ and Pin1−/− mice. The tonic conductance was assessed by the shift of the holding current induced by application of the $GABA_A$R channel blocker PTX (100 µM) (Supplementary Fig. 4a). This drug caused a similar shift in holding current in Pin1−/− and Pin1+/+ mice (Supplementary Fig. 4b,c), indicating that extrasynaptic $GABA_A$ receptors are not influenced by Pin1-mediated signalling.

Discussion

The present study shows that NL2 is a newly identified substrate of proline-directed phosphorylation. This post-translational modification, acting on its unique Pin1 consensus motif localized within the CD (S714-P), modulates the amount of NL2–gephyrin

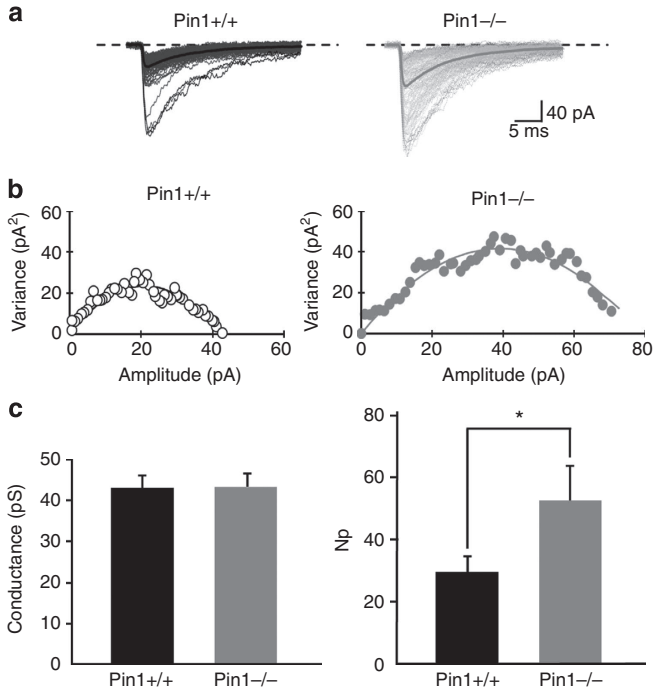

Figure 8 | Pin1 controls the number of active receptor channels at GABAergic synapses. (**a**) Individual sIPSCs from Pin1+/+ (black) and Pin1−/− mice (grey) are shown with the average currents (thick lines). (**b**) Current/variance relationships for sIPSCs shown in **a** (**c**) Summary plots of weighted mean channel conductance (43 ± 3 pS and 43 ± 3 pS, $P = 0.9$, Student's *t*-test) and number of $GABA_A$ receptor channels (Np) in wt (black; $n = 8$) and in Pin1−/− mice (gray; $n = 5$). *$P = 0.03$, Student's *t*-test.

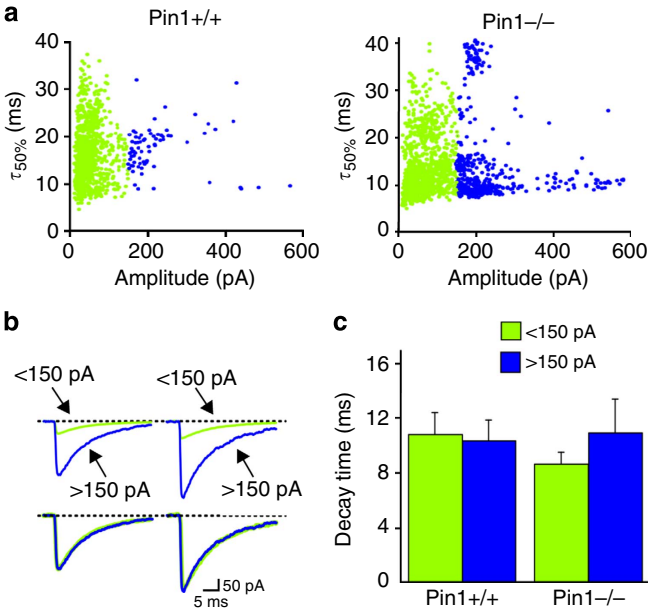

Figure 9 | Pin1 does not affect the decay kinetics of spontaneous IPSCs. (**a**) The peak amplitude of individual sIPSCs <150 pA (green) and >150 pA (blue) is plotted against their decay half-widths (τ_{50}%) in Pin1+/+ and in Pin1−/− mice. (**b**) In the upper part, average traces of spontaneous IPSCs shown in **a**. In the lower part, average traces are normalized and superimposed. (**c**) Each column represents the mean 90–10% decay time constant of spontaneous IPSCs in Pin1+/+ and Pin1−/− mice, <150 pA (green), $n = 8$ and 7, respectively and >150 pA (blue), $n = 6$ and 7, respectively. For all comparisons, $P > 0.05$, Student's *t*-test.

complexes at synaptic sites. This modulation impacts on GABAergic transmission, by selectively affecting the total number of synaptic $GABA_A$Rs. On the basis of these findings, post-phosphorylation prolyl-isomerization can play a crucial role in remodelling the GABAergic PSD to sustain plasticity processes.

Protein phosphorylation on serine and threonine residues preceding a proline, the so-called proline-directed phosphorylation, has emerged as a mechanism regulating signalling events through conformational changes that are catalysed by the phospho-dependent recruitment of the peptidyl-prolyl isomerase Pin1. While the different roles of Pin1 in dividing cells have long been established and characterized[19], its function in post-mitotic neurons in general and at synapses in particular is still poorly understood. In a previous study, we identified gephyrin, the main scaffolding protein of inhibitory PSD, as a new target of post-phosphorylation prolyl-isomerization[22].

Here, by inspecting the protein sequence of NL CDs, we identified S/T-P motifs that may provide Pin1 binding sites if phosphorylated *in vivo*. In particular, NL2 presents a unique Pin1 consensus site in its cytoplasmic region, S714-P, which is located 15 amino acids apart from the transmembrane domain. Even though this proximity to the plasma membrane raises doubts about its accessibility by a proline-directed kinase, several lines of evidence suggest that endogenous NL2 can undergo proline-directed phosphorylation. First, this isoform was recognized by the MPM2 antibody on NL2 immunoprecipitation from mouse brain homogenates. Second, MPM2-mediated NL2 immunoprecipitation was still maintained on removal of the NL2–gephyrin-binding domain, excluding the possibility of an indirect recognition mediated by endogenous gephyrin. Third, such detection was completely lost on NL2HA-S714A mutagenesis. This phosphorylation event is then able to directly recruit the effector molecule of the signalling cascade Pin1, as shown by co-immunoprecipitation experiments with endogenous neuronal proteins. Also in this case, Pin1 binding to NL2 was still maintained on the removal of the GBD, while it was completely abolished by mutating S714 to alanine, thus suggesting that the prolyl isomerase can be directly recruited by the unique NL2 Pin1 consensus motif in a phosphorylation-dependent manner. These results altogether indicate that NL2 represents a newly identified substrate for proline-directed signalling cascade *in vivo*.

Our biochemical data demonstrate that NL2–gephyrin interaction is negatively regulated by proline-directed phosphorylation. Co-immunoprecipitation experiments on recombinantly expressed gephyrin-FLAG and NL2HA unveiled an enhanced complex formation on pharmacological inhibition of Pin1 catalytic activity. Similarly, endogenous NL2/gephyrin complexes pulled down from whole brain or hippocampal tissues of Pin1−/− animals were significantly augmented as compared with the corresponding WT tissues. These biochemical findings were also validated by immunocytochemistry performed on cultured hippocampal neurons, where we could detect a high number of clusters co-labelled for NL2 and gephyrin as well as their increased apposition to presynaptic GABAergic inputs in the absence of Pin1 expression. Interestingly, the NL2 point mutant unable to undergo prolyl-isomerization was capable to recruit gephyrin even more efficiently as compared with the WT form, whereas gephyrin mutagenesis at two putative Pin1 consensus motifs, S270A and S319A, located within, or close to, the minimal NL2 binding domain, was completely ineffective. The fact that this post-translational modification seems to control the strength of NL2 association with gephyrin by acting mainly on NL2, and not *vice versa*, further reinforces the emerging idea

that cell adhesion molecules are key determinant in regulating synapse function. In a recent study by Giannone *et al.*[18], it has been demonstrated that the level of NL1 phosphorylation at a specific tyrosine residue located within the GBD dictates the strength of NL1/gephyrin interaction. In other words, NL1, the isoform enriched at excitatory synapses and therefore mostly associated with PSD95, can potentially recruit gephyrin as well as NL2, but its phosphorylation, promoted by neurexin–adhesion signalling, precludes such interaction while favouring PSD95 binding. Our experimental data indicate that proline-directed phosphorylation is acting similarly to tyrosine phosphorylation signalling. Since NL2 S714 is not positioned within the GBD, but is located just 50 amino acid upstream, it is reasonable to believe that Pin1-driven conformational changes, by affecting the overall folding of the CD, will induce gephyrin release (Fig. 10a). Alternatively, these conformational changes may promote NL2 tyrosine phosphorylation, an event shown to impede NLs/gephyrin interaction[18] (Fig. 10b). Interestingly, tyrosine to alanine mutagenesis on NL2 was shown to completely abolish recombinant gephyrin recruitment by the mutant protein or to strongly reduce its interaction with endogenous gephyrin[6]. Whether NL2 phosphorylation occurs at tyrosine 770 and whether this event is able to hamper gephyrin binding is still unknown.

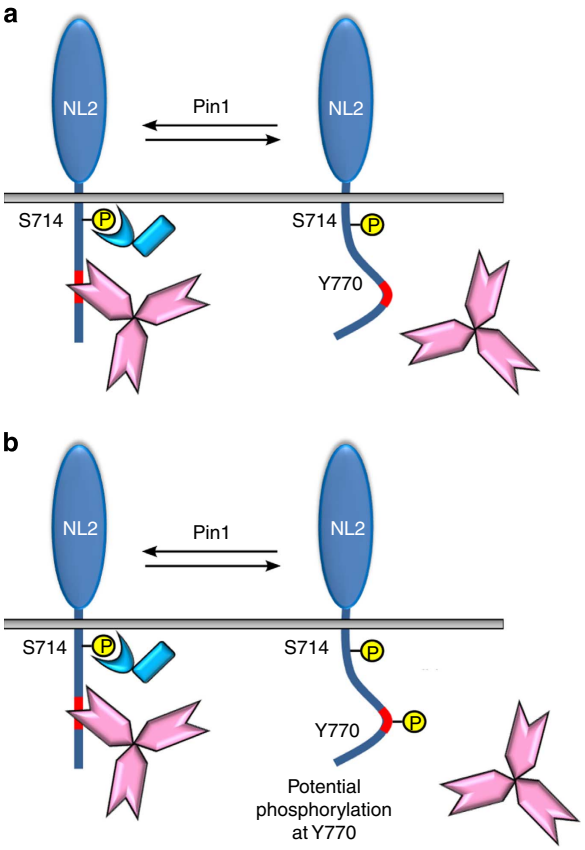

Figure 10 | Model of the putative cross-talk between proline-directed phosphorylation and tyrosine phosphorylation. Phosphorylation of NL2 CD at S714 by a proline-directed kinase allows the recruitment of the proly isomerase Pin1. Pin1-driven conformational changes, by altering the folding of the NL2 CD, may represent the main cause responsible for gephyrin detachment (**a**). Alternatively, Pin1-mediated structural rearrangement may render the conserved tyrosine residue of the GBD (Y770) susceptible to phosphorylation, an event shown to prevent NL1/gephyrin interaction (**b**).

The other partner of the complex is represented by gephyrin, a recognized target of Pin1 (ref. 22). Gephyrin contains 10 consensus motifs mostly concentrated in its C-domain, and all of them found to be phosphorylated *in vivo*[35,36]. This region of the protein is positioned between the amino-terminal G- and carboxyl-terminal E-domains, which are directly involved in gephyrin multimerization. Conformational changes induced by phosphorylation, possibly followed by prolyl-isomerization, are expected to alter the conformation of the gephyrin C-domain and in turn, regulate specific functional properties of gephyrin, in particular its binding to interacting proteins, including possibly NL2. However, the complexity of the system under investigation makes it very difficult to determine whether and how a specific phosphorylation event can contribute, directly or indirectly, to enhance gephyrin association to NL2. Nevertheless, it should be emphasized that gephyrin is robustly phosphorylated at several residues *in vivo*, thus suggesting that a specific pattern of phosphorylation, rather than a single post-translational modification, is functionally determinant. In contrast, NL2 possesses a unique target for prolyl-isomerization suggesting that it could represent the master switch of the signalling cascade.

Our electrophysiological experiments clearly demonstrate that deletion of Pin1 specifically affects GABAergic transmission, causing a dramatic increase in amplitude, but not in frequency, of sIPSCs due to an increase in the number of $GABA_A$Rs at post-synaptic sites. Notably, such enhancement was detected on neuronal overexpression of the NL2 mutant unable to undergo prolyl-isomerization, suggesting a functional link between the signalling cascade strengthening NL2/gephyrin interaction and the increased synaptic recruitment of $GABA_A$Rs. There is a large body of evidence underlying the key role played by NL2 in promoting clustering and/or stabilization of $GABA_A$Rs at post-synaptic sites. By employing a heterologous expression system, it was shown that $GABA_A$Rs are able to co-aggregate with NL2 and only the presence of this isoform can induce strong GABAergic presynaptic differentiation from co-cultured neurons and promote the establishment of fully functional hemi-synapses[37]. In NL2-deficient mice, the number of functional $GABA_A$Rs detected in the retina was shown to be drastically reduced[38]. Furthermore, targeting of $GABA_A$Rs and gephyrin scaffold appeared severely compromised in the pyramidal cell layer of the CA1 region of the hippocampus, a morphological phenotype accompanied by a strong deficit in synaptic inhibition[6].

The increased recruitment of synaptic $GABA_A$ receptors in Pin1 −/− mice may simply depend on the enhanced gephyrin targeting at synaptic sites. More scaffold deposition should offer a high number of binding sites available for the transient immobilization of $GABA_A$Rs at inhibitory synapses. In addition, or alternatively, we cannot exclude the possibility that the extracellular domain of NL2 could also participate in $GABA_A$Rs receptor recruitment. The unique S714-P consensus motif, located very close to the NL2 transmembrane domain, could influence the folding of the extracellular domain of NL2, rendering it incapable to interact in *cis* with $GABA_A$R subunits. This type of mechanism has been shown to operate at excitatory synapses, where the abundance of NMDARs is controlled by the interaction occurring between the GluN1 subunit with NL1-specific sequences located in its extracellular domain[39].

In conclusion, our findings unveil the existence of a new signalling pathway operating at GABAergic synapses to alter the efficacy of GABAergic transmission by modulating NL2/gephyrin interaction. Although a comprehensive understanding of the molecular mechanisms underlying the action of Pin1 on NL2/gephyrin interaction is still lacking, we believe that our study further emphasizes the key role played by NL2 in organizing and stabilizing GABAergic synapses.

Methods

Plasmid constructs. The expression construct for HA-tagged human NL2 in pNice was kindly provided by P. Scheiffele (Biozentrum, Basel). The amino acid sequence ranging from residues 768 to 782 was removed to generate the NL2HA lacking the gephyrin binding domain (pNice-NL2HA-ΔGBD). S714A mutation was also introduced into pNice-NL2HA-ΔGBD to remove the unique Pin1 consensus site (pNice-NL2HA-ΔGBDS714A). All PCR-based mutagenesis were fully sequenced to exclude the possibility of second site mutations. pcDNA3-FLAG-Pin1 WT and pcDNA3-gephyrin-FLAG have been previously described[22]. EGFP-tagged gephyrin point mutants (S270A and S319A), the WT and the truncated version ranging from amino acid 326 to 736 and 310 to 736, were PCR cloned into the *Xho*I/*Hin*dIII sites of pEFP-C1 (Clontech, Mountain View, CA). EGFP-tagged gephyrin GC (1–310) was kindly provided by G. Schwarz (University of Cologne, Germany)[40].

Cell cultures and transfections. HEK-293-T cells were cultured at 37 °C under a 5% CO2 atmosphere in Dulbecco's modified Eagle's medium supplemented with 10% fetal bovine serum. They were transiently transfected with various plasmid constructs using Lipofectamine 2000 (Invitrogen) according to the manufacturer's protocol. Cells were collected 24–48 h after transfection.

Primary hippocampal neurons from P0 Pin1 +/+ and Pin1 −/− littermates and rat hippocampal neurons were prepared as previously described[41]. Being Pin1 −/− mice infertile, Pin1 +/+ and Pin1 −/− littermates for neuronal cultures were routinely obtained by mating heterozygous mice[42]. Each hippocampus derived from single newborn littermate was processed and plated separately and identified by tail genotyping. Neurons were Lipofectamine transfected after 8 DIV with 1 μg of EGFP-gephyrinWT or EGFP-gephyrinS270A and processed for immunofluorescence 2–3 days later. For electrophysiological recordings, neurons were co-transfected with 1 μg NL2HA/NL2HA-S714A and 500 ng of green fluorescent protein (GFP) to visualize transfected cells.

PiB treatments. To inhibit Pin1 catalytic activity, the chemical inhibitor PiB (diethyl-1,3,6,8-tetrahydro-1,3,6,8-tetraoxobenzol-phenanthroline-2,7-diacetate) was added to the culture medium for 24 h at a concentration of 2.5 μm. PiB was purchased from Calbiochem and resuspended in DMSO.

Immunoprecipitation and chemical cross-linking. Immunoprecipitation for MPM2 experiments was performed using a lysis buffer containing 50 mM Tris–HCl, pH 7.5, 1% Nonidet P-40, 0.5% Triton X-100, 150 mM NaCl, 1 mM Na_3VO_4, 50 mM NaF and protease inhibitor mixture (Sigma). For NL2HA and gephyrin co-immunoprecipitation, HEK293 cells overexpressing NL2HA and gephyrin-FLAG were treated 48 h after transfection with 2.5 mM PiB or mock treated with DMSO as negative controls. Cells were lysed in 50 mM Tris-HCl, pH 7.5, 100 mM NaCl, 0.1% Tween 20, 10% glycerol, 10 mM EDTA, 2 mM $MgCl_2$ and protease inhibitor mixture and immunoprecipitated by either the anti-FLAG antibody or anti-HA agarose (Pierce).

Co-immunoprecipitation of native gephyrin–NL2 complexes from p15 Pin1 +/+ and Pin1 −/− mouse brains or hippocampal tissues was performed using a chemical cross-linking approach on postnuclear homogenates as previously described[6]. Primary antibodies were revealed by HRP-conjugated secondary antibodies (Sigma) followed by ECL (Amersham Biosciences).

Biotinylation assay and analysis on synaptosomes. To examine changes in NL2 transported at the plasma membrane, we performed biotinylation assays on hippocampal neuronal cultures derived from Pin1 +/+ and Pin1 −/− mice. Neuronal cells were incubated with 0.5 mg ml^{-1} EZ-Link Sulfo-NHS-LC-Biotin (Pierce) in PBS at 4 °C for 30 min. To quench the reaction, cells were washed three times with cold PBS containing 0.1 M Tris-HCl pH 7.4. Cells were then lysed in lysis buffer containing protease inhibitor cocktail followed by centrifugation at 1,000*g* for 5 min. The collected lysate were incubated with streptavidin cross-linked to agarose beads (Pierce) for 2 h at 4 °C. The beads were then washed twice with lysis buffer, and eluted with SDS loading buffer. The amount of membrane protein loaded in each experiments was normalized to the amount of the glycophosphatidylinositol-anchored protein Flotilin1, whose expression levels are identical in both mouse genotypes.

PSD enriched extracts were prepared by using the Syn-PER Synaptic Protein Extraction Reagent (ThermoScientific) following the manufacturer's instructions. Briefly, a pool of four hippocampi derived from the same genotypes were homogenized in the Extraction reagents (10 ml of reagent per g of tissue), centrifuged at 1,200*g* for 10 min. The pellet was discarded while the supernatant (homogenate) was additionally centrifuged at 15,000*g* for 20 min. The cytosolic fraction was discarded and the pellet containing the synaptosomes was resuspended in 400–500 μl of reagent and analysed by western blot analysis. The protein concentration of each sample was determined using the Pierce BCA Protein Assay to allow an equal loading of total protein.

Western blot analysis. Western blot image acquisition was performed using the ECL detection kit and the Alliance 4.7 software (UVITECH, Cambridge). Quantifications were performed using the UVIband imager software (Amersham). The relative amount (Input, 1/20 of the total lysate) of the different antigens considered in this study and the immunoprecipitated fractions were determined by densitometry on the acquired images. The amount of immunoprecipitated and coimmunoprecipitated proteins are first normalized to their corresponding inputs and then the coimmunoprecipated value is additionally normalized on the immunoprecipitated antigen. Full images of western blots are in Supplementary Fig. 5.

Antibodies. The following antibodies were used in immunohistochemistry and immunocitochemistry: anti-gephyrin Mab7a (Synaptic System Cat. No 147021), anti-VGAT rabbit or guinea pig (1:1,000, Synaptic System Cat. No 131004), anti-NL2 rabbit affinity purified (1:500, Synaptic system Cat, No 129203), guinea pig anti-$GABA_A$ γ2 subunit (1:2,000 (ref. 43)), biotinylated anti-guinea pig (1:200, Vector Laboratories, Cat No BA-7000). The following primary antibodies were used in immunoprecipitation and western blot analysis: mouse monoclonal anti-FLAG M2 (Sigma Cat No F1804), mouse monoclonal anti-gephyrin 3B11 (Synaptic System Cat No 147111) and rabbit polyclonal anti-NL2 (Synaptic Systems Cat. No 129202), pS/pT-P (MPM2, Upstate Biotechnology Cat No 05-368), high affinity rat monoclonal anti-HA 3F10 (Roche), anti-GFP rabbit monoclonal (Life Technology, Cat No G10362). Validation of antibodies used in these assays can be found on the respective manufacturers' websites.

Immunohistochemistry and immunocytochemistry. Eight-week-old Pin1 +/+ and Pin1 −/− littermates (for each genotype, $n=3$) were anaesthetized and perfused transcardially with 0.1 M phosphate buffer, pH 7.4 (PB). Brains were quickly removed from the skull and frozen with isopentane cooled to −40 °C with liquid nitrogen. Ten to 12-μm thick cryostat sections were collected on Superfrost glass slides and further processed for immunostaining for combined detection of VGAT and GABAA γ2 or VGAT and gephyrin. Briefly, cryostat sections were fixed by immersion in 2% paraformaldehyde, and mildly treated with pepsin as antigen-retrieval procedure, and then incubated for 48 h with different combination of primary antibodies. Secondary antibody staining was performed for 1 h at room temperature using anti-isotypic fluorophore-conjugated antibodies Alexa-488 and Alexa-594 at dilutions of 1:1,000 (Molecular Probes).

Hippocampal neurons grown on glass coverslips were fixed with 4% paraformaldehyde and 4% sucrose in PBS. Unspecific binding was blocked by incubation with 10% normal goat serum in PBS. Primary and secondary antibodies were diluted in 5% normal goat serum/PBS. Secondary antibodies included anti-isotypic fluorophore conjugated antibodies Alexa-488, Alexa-594 and streptavidin-Alexa 405 at dilutions of 1:1,000 (Molecular Probes).

Confocal microscopy and image analysis. Fluorescence images were acquired on a TCS-SP confocal laser scanning microscope (Leica, Bensheim, Germany) with a ×40 1.4 NA or ×63 1.4 NA oil immersion objectives, additionally magnified fivefold with the pinhole set at 1 Airy unit. All the parameters used in confocal microscopy were consistent in each experiment, including the laser excitation power, detector and off-set gains and the pinhole diameter. Stacks of z-sections (12–13 optical sections) with an interval of 0.3 μm were sequentially scanned three times for each emission line to improve the signal/noise ratio. The number of gephyrin, γ2 subunit and VGAT puncta was assessed in at least eight sections for each genotypes (Pin1 +/+ and Pin1 −/−), by taking at least four images of strata radiatum and oriens of the CA1 region of each hippocampus in each set of experiments ($n=3$). In the pyramidal cell layer, the high density and elongated shape of VGAT positive terminals precluded the determination of their numbers and their colocalization with the other two antigens investigated.

For immunocitochemistry samples, at least 10 cells from at least three independent batches per condition were used for analysis. Images were acquired as a *z*-stack (six to seven optical sections, 0.25 μm step size). In each image, at least five dendritic segments were outlined and saved as regions of interest.

Quantification of immunofluorescence data was performed using the Volocity3D Image Analysis Software (PerkinElmer, London, UK). Gephyrin, NL2, $GABA_AR$ γ2 and VGAT clusters were determined after thresholding of images. Thresholds were determined using the 'voxel spy' facility of the software and chosen such that all recognizable punctuate structures were included into the analysis (minimal area, 0.1 μm^2); colocalization was evaluated based on the determination of thresholded Pearson's correlation coefficient (PCC > 0,5) for each gephyrin and γ2 cluster previously identified and quantified[44]. NL2 colocalization with gephyrin puncta was also quantified utilizing the software function 'intersect object' that measures size, volume and intensity values of intersecting objects identified by separate protocols in each channel. To determine the degree of apposition of NL2/gephyrin colabeled clusters with the presynaptic marker VGAT, we superimposed the mask of all identified overlapping puncta onto the third channel and count them manually.

Hippocampal slice preparation and drug treatment. All experiments were performed in accordance with the European Community Council Directive of November 24, 1986 (86/609EEC) and were approved by the local authority veterinary service and by SISSA ethical committee. All efforts were made to

minimize animal suffering and to reduce the number of animal used. Transverse hippocampal slices (300 μm thick) were obtained from postnatal (P) day P10–P13 mice (male and female) using a standard protocol[45]. Briefly, after being anaesthetized with CO_2, animals were decapitated. The brain was quickly removed from the skull and placed in ice-cold artificial cerebrospinal fluid containing (in mM): 130 NaCl, 25 glucose, 3.5 KCl, 1.2 NaH_2PO_4, 25 $NaHCO_3$, 2 $CaCl_2$ and 1.3 $MgCl_2$, saturated with 95% O_2 and 5% CO_2 (pH 7.3–7.4). Transverse hippocampal slices (300 μm thick) were cut with a vibratome and stored at room temperature (22–24 °C) in a holding bath containing the same solution as above. After incubation for at least 45 min, an individual slice was transferred to a submerged recording chamber and continuously superfused at 33–34 °C with oxygenated artificial cerebrospinal fluid at a rate of 3–4 ml min^{-1}.

The following drugs were used: DNQX, PTX and bicuculline, purchased from Ascent Scientific; TPMPA purchased from Tocris Bioscence. DNQX and PTX were dissolved in DMSO. The final concentration of DMSO in the bathing solution was 0.1%. At this concentration, DMSO alone did not modify the membrane potential, input resistance or the firing properties of CA1 pyramidal neurons. Drugs were applied in the bath by gravity via a three-way tap system by changing the superfusion solution to one differing only in its content of drug(s). The ratio of flow rate to bath volume ensured a complete exchange within 2 min.

Electrophysiological recordings. Whole-cell patch-clamp recordings (in voltage clamp configuration) were performed from CA1 pyramidal cells, visualized with an upright microscope equipped with differential interference contrast optics and infrared video camera, using a patch-clamp amplifier (Axopatch 1D amplifier, Molecular Devices, Sunnyvale, CA, USA). Patched electrodes were pulled from borosilicate glass capillaries (Hingelberg, Malsfeld, Germany). They had a resistance of 4–6 MΩ when filled with the intracellular solution containing (in mM): 125 Cs-methanesulphonate, 10 CsCl, 10 HEPES, 0.3 EGTA, 2 MgATP, 0.3 NaGTP (pH adjusted to ~7.3 with CsOH; the osmolarity was adjusted to 290 mOsmol). The stability of the patch was checked by repetitively monitoring the input and series resistance during the experiment. Cells exhibiting >20% changes in series resistance were excluded from the analysis. The series resistance was <25 MΩ and was not compensated.

Spontaneous GABAergic (sIPSCs) and glutamatergic (sEPSCs) post-synaptic currents were routinely recorded from a holding potential of −60 mV in the presence of DNQX (20 μM) and PTX (10 μM), respectively. While sEPSCs were recorded using patch pipettes filled with the above mentioned solution, sIPSCs were recorded using an intracellular solution containing (in mM): CsCl 137, Hepes 10, BAPTA 11, MgATP 2, $MgCl_2$ 2, $CaCl_2$ 1 and 5 QX-314 (pH adjusted to ~7.3 with CsOH).

sIPSC were also recorded from cultured hippocampal neurons co-transfected with GFP and NL2HA or NL2HA-S714A 24 h after transfection, at a holding potential of −60 mV in presence of DNQX (20 μM) with the same intracellular solution used for the acute slices experiment. The extracellular solution contained (in mM) 137 NaCl, 5 KCl, 2 $CaCl_2$, 1 $MgCl_2$, 20 glucose and 10 HEPES, pH 7.4 (corrected with NaOH).

Data analysis. Data were acquired and digitized with an A/D converter (Digidata 1,200, Molecular Devices) and stored on a computer hard disk. Acquisition and analysis were performed with Clampfit 9 (Molecular Devices).

Data were acquired at 20 kHz, filtered with a cut-off frequency of 2 kHz and stored on computer hard disk to perform off-line analysis. The resting membrane potential was measured immediately after break-in and establishing whole-cell recording. The membrane input resistance (R_{in}) was calculated by measuring the amplitude of voltage responses to steady hyperpolarizing current steps, using the Clampfit 10.0 program (Molecular Devices).

Spontaneous AMPA- and $GABA_A$-mediated post-synaptic currents were analysed using Clampfit 10.0 (Molecular Devices). This programme uses a detection algorithm based on a sliding template. The template did not induce any bias in the sampling of events because it was moved along the data trace by one point at a time and was optimally scaled to fit the data at each position. The detection criterion was calculated from the template-scaling factor and from how closely the scaled template fitted the data.

Spontaneous GABAergic currents were analysed with Mini Analysis program (version 6.0.1, Synaptosoft, Leonia, NJ) for their decay time constants. Only events with no deflections in the rising or decaying phases were included in the analysis. Low amplitude (<5 pA) events as well as events whose amplitude correlated with the rising or decaying time constants were discarded from the analysis because they were thought to be affected by dendritic filtering. The decay time of s IPSCs were fitted with a single exponential function as:

$$I(t) = Aexp(-t/\tau) \quad (1)$$

where $I(t)$ is the current as a function of time, A is the amplitude at time 0, τ is the time constant.

The Mini Analysis programme was used to perform peak-scaled non-stationary noise analysis according to Traynelis and co-workers[46]. Individual, not correlated, events were aligned to the point of steepest rise time. The peak of the mean current response waveform was scaled to the response value at the corresponding point in time of each individual event before subtraction to generate the difference waveforms. The ensemble mean post-synaptic current was binned into 50 bins of equal amplitude to assign similar weights to all phases of ensemble mean waveform. Variance was plotted against amplitude and individual points were fitted with the equation:

$$\sigma^2(I) = iI - I^2/N + \sigma_b^2 \quad (2)$$

where i is the unitary single-channel current, I is the mean current, N is the number of channels open at the current peak and σ_b^2 is the variance of the background noise. The single-channel chord conductance (γ) was calculated as:

$$\gamma = i/(E_m - E_{rev}) \quad (3)$$

from the holding potential (E_m) of −60 mV, assuming a reversal potential (E_{rev}) of 0 mV.

Amplitude distribution of sIPSCs amplitude was obtained fitting data with the following Gaussian function:

$$n(I) = \sum_{i=1}^{n} (a_i/\sqrt{2\pi\sigma^2})\ exp(-(I_i - I_{\sigma i})^2/2\sigma_i^2) \quad (4)$$

where I_σ is the mean current, a_i is the area and σ is the variance.

The amplitude of the tonic current was estimated by the outward shift of the baseline current after the application of the $GABA_A$ receptor channel blocker PTX (100 μM). Only current recordings that exhibited a stable baseline were included in the analysis. Baseline currents were estimated by plotting four to five 0.5 s periods in all point histograms. These were fitted with a Gaussian function. The peak of the fitted Gaussian was considered as the mean holding current[47].

Statistics. Statistical analyses for Co-IP, PSD enriched extracts fractions analyses were performed by using Microsoft Excel. Comparisons were performed by Student's t-test two-tailed distribution unequal variance. Deviation and error bars were calculated using the same software. Statistical significance was defined as $P<0.05$.

Statistical analyses of morphological data (NL2 and gephyrin cluster size and density) were performed pair-wise (Pin1 −/− versus Pin1 +/+) using unpaired, two-tailed Student's t-test. Bars indicate (s.d.)

Statistical analyses for electrophysiological experiments were performed by using pClamp 10 and Microsoft Excel. Comparison were perfomed by Student's t-test unless otherwise stated. Statistical significance was defined as $P<0.05$.

References

1. Vithlani, M. & Moss, S. J. The role of $GABA_AR$ phosphorylation in the construction of inhibitory synapses and the efficacy of neuronal inhibition. *Biochem. Soc. Trans.* **37,** 1355–1358 (2009).
2. Jacob, T. C., Moss, S. J. & Jurd, R. GABA(A) receptor trafficking and its role in the dynamic modulation of neuronal inhibition. *Nat. Rev. Neurosci.* **9,** 331–343 (2008).
3. Südhof, T. C. Neuroligins and neurexins link synaptic function to cognitive disease. *Nature* **455,** 903–911 (2008).
4. Levinson, J. N. *et al.* Neuroligins mediate excitatory and inhibitory synapse formation: involvement of PSD-95 and neurexin-1beta in neuroligin-induced synaptic specificity. *J. Biol. Chem.* **280,** 17312–17319 (2005).
5. Craig, A. M. & Kang, Y. Neurexin-neuroligin signalling in synapse development. *Curr. Opin. Neurobiol.* **17,** 43–52 (2007).
6. Poulopoulos, A. *et al.* Neuroligin2 drives postsynaptic assembly at perisomatic inhibitory synapses through gephyrin and collybistin. *Neuron* **63,** 628–642 (2009).
7. Varoqueaux, F., Jamain, S. & Brose, N. Neuroligin 2 is exclusively localized to inhibitory synapses. *Eur. J. Cell Biol.* **83,** 449–456 (2004).
8. Pfeiffer, F., Graham, D. & Betz, H. Purification by affinity chromatography of the glycine receptor of rat spinal cord. *J. Biol. Chem.* **257,** 9389–9393 (1982).
9. Prior, P. *et al.* Primary structure and alternative splice variants of gephyrin, a putative glycine receptor-tubulin linker protein. *Neuron* **8,** 1161–1170 (1992).
10. Essrich, C., Lorez, M., Benson, J. A., Fritschy, J. M. & Luscher, B. Postsynaptic clustering of major GABAA receptor subtypes requires the gamma2 subunit and gephyrin. *Nat. Neurosci.* **1,** 563–571 (1998).
11. Kneussel, M. *et al.* Loss of postsynaptic GABA(A) receptor clustering in gephyrin-deficient mice. *J. Neurosci.* **19,** 9289–9297 (1999).
12. Tretter, V. *et al.* Gephyrin, the enigmatic organizer at GABAergic synapses. *Front. Cell. Neurosci.* **6,** 1–16 (2012).
13. Schwarz, G., Schrader, N., Mendel, R. R., Hecht, H. J. & Schindelin, H. Crystal structures of human gephyrin and plant Cnx1 G domains: comparative analysis and functional implications. *J. Mol. Biol.* **312,** 405–418 (2001).
14. Sola, M., Kneussel, M., Heck, I. S., Betz, H. & Weissenhorn, W. X-ray crystal structure of the trimeric N-terminal domain of gephyrin. *J. Biol. Chem.* **276,** 25294–25301 (2001).
15. Sola, M. *et al.* Structural basis of dynamic glycine receptor clustering by gephyrin. *EMBO J.* **23,** 2510–2519 (2004).
16. Maric, H. M., Mukherjee, J., Tretter, V., Moss, S. J. & Schindelin, H. Gephyrin-mediated GABA(A) and glycine receptor clustering relies on a common binding site. *J. Biol. Chem.* **286,** 42105–42114 (2011).

17. Kowalczyk, S. *et al.* Direct binding of GABAA receptor β2 and β3 subunits to gephyrin. *Eur. J. Neurosci.* **37,** 544–554 (2013).
18. Giannone, G. *et al.* Neurexin-1β binding to neuroligin-1 triggers the preferential recruitment of PSD-95 versus gephyrin through tyrosine phosphorylation of neuroligin-1. *Cell Rep.* **3,** 1996–2007 (2013).
19. Lu, K. P. & Zhou, X. Z. The prolyl isomerase PIN1: a pivotal new twist in phosphorylation signaling and disease. *Nat. Rev. Mol. Cell. Biol.* **8,** 904–916 (2007).
20. Ranganathan, R., Lu, K. P., Hunter, T. & Noel, J. P. Structural and functional analysis of the mitotic rotamase Pin1 suggests substrate recognition is phosphorylation dependent. *Cell* **89,** 875–886 (1997).
21. Shen, M., Stukenberg, P. T., Kirschner, M. W. & Lu, K. P. The essential mitotic peptidyl-prolyl isomerase Pin1 binds and regulates mitosis-specific phosphoproteins. *Genes Dev.* **12,** 706–720 (1998).
22. Zita, M. M. *et al.* Post-phosphorylation prolyl isomerisation of gephyrin represents a mechanism to modulate glycine receptors function. *EMBO J.* **26,** 1761–1771 (2007).
23. Davis, F. M., Tsao, T. Y., Fowler, S. K. & Rao, P. N. Monoclonal antibodies to mitotic cells. *Proc. Natl Acad. Sci. USA* **80,** 2926–2930 (1983).
24. Lu, K. P. Pinning down cell signaling, cancer and Alzheimer's disease. *Trends Biochem. Sci.* **29,** 200–209 (2004).
25. Uchida, T. *et al.* Pin1 and Par14 peptidyl prolyl isomerase inhibitors block cell proliferation. *Chem. Biol.* **10,** 15–24 (2003).
26. Zacchi, P., Antonelli, R. & Cherubini, E. Gephyrin phosphorylation in the functional organization and plasticity of GABAergic synapses. *Front. Cell. Neurosci.* **8,** 103 (2014).
27. Tyagarajan, S. K. *et al.* Regulation of GABAergic synapse formation and plasticity by GSK3beta-dependent phosphorylation of gephyrin. *Proc. Natl Acad. Sci. USA* **108,** 379–384 (2011).
28. Levinson, J. N. *et al.* Postsynaptic scaffolding molecules modulate the localization of neuroligins. *Neuroscience* **165,** 782–793 (2010).
29. Dumoulin, A., Lévi, S., Riveau, B., Gasnier, B. & Triller, A. Formation of mixed glycine and GABAergic synapses in cultured spinal cord neurons. *Eur. J. Neurosci.* **12,** 3883–3892 (2000).
30. Momiyama, A. *et al.* The density of AMPA receptors activated by a transmitter quantum at the climbing fibre-Purkinje cell synapse in immature rats. *J. Physiol.* **549,** 75–92 (2003).
31. Varley, Z. K. *et al.* Gephyrin regulates GABAergic and glutamatergic synaptic transmission in hippocampal cell cultures. *J. Biol. Chem.* **286,** 20942–20951 (2011).
32. Barberis, A., Petrini, E. M. & Cherubini, E. Presynaptic source of quantal size variability at GABAergic synapses in rat hippocampal neurons in culture. *Eur. J. Neurosci.* **20,** 1803–1810 (2004).
33. Farrant, M. & Nusser, Z. Variations on an inhibitory theme: phasic and tonic activation of GABA(A) receptors. *Nat. Rev. Neurosci.* **6,** 215–229 (2005).
34. Brickley, S. G. & Mody, I. Extrasynaptic GABA(A) receptors: their function in the CNS and implications for disease. *Neuron* **73,** 23–34 (2012).
35. Herweg, J. & Schwarz, G. Splice-specific glycine receptor binding, folding, and phosphorylation of the scaffolding protein gephyrin. *J Biol Chem.* **287,** 12645–12656 (2012).
36. Tyagarajan, S. K. *et al.* Extracellular signal-regulated kinase and glycogen synthase kinase 3β regulate gephyrin postsynaptic aggregation and GABAergic synaptic function in a calpain-dependent mechanism. *J. Biol. Chem.* **288,** 9634–9647 (2013).
37. Dong, N., Qi, J. & Chen, G. Molecular reconstitution of functional GABAergic synapses with expression of neuroligin-2 and GABAA receptors. *Mol. Cell. Neurosci.* **35,** 14–23 (2007).
38. Hoon, M. *et al.* Neuroligin 2 controls the maturation of GABAergic synapses and information processing in the retina. *J. Neurosci.* **29,** 8039–8050 (2009).
39. Budreck, E. C. *et al.* Neuroligin-1 controls synaptic abundance of NMDA-type glutamate receptors through extracellular coupling. *Proc. Natl Acad. Sci. USA* **110,** 725–730 (2013).
40. Lardi-Studler, B. *et al.* Vertebrate-specific sequences in the gephyrin E-domain regulate cytosolic aggregation and postsynaptic clustering. *J. Cell Sci.* **120,** 1371–1382 (2007).
41. Andjus, P. R., Stevic-Marinkovic, Z. & Cherubini, E. Immunoglobulins from motoneurone disease patients enhance glutamate release from rat hippocampal neurones in culture. *J. Physiol.* **504,** 103–112 (1997).
42. Atchison, F. W., Capel, B. & Means, A. R. Pin1 regulates the timing of mammalian primordial germ cell proliferation. *Development* **130,** 3579–3586 (2003).
43. Mohler, H. *et al.* Heterogeneity of $GABA_A$-receptors: cell-specific expression, pharmacology, and regulation. *Neurochem. Res.* **20,** 631–636 (1995).
44. Barlow, A. L., MacLeod, A., Noppen, S., Sanderson, J. & Guérin, C. J. Colocalization analysis in fluorescence micrographs: verification of a more accurate calculation of Pearson's correlation coefficient. *Microsc. Microanal.* **16,** 710–724 (2010).
45. Griguoli, M. *et al.* Nicotine blocks the hyperpolarization-activated current Ih and severely impairs the oscillatory behavior of oriens-lacunosum moleculare interneurons. *J. Neurosci.* **30,** 10773–10783 (2010).
46. Traynelis, S. F., Silver, R. A. & Cull-Candy, S. G. Estimated conductance of glutamate receptor channels activated during EPSCs at the cerebellar mossy fiber-granule cell synapse. *Neuron* **11,** 279–289 (1993).
47. Glykys, J. & Mody, I. The main source of ambient GABA responsible for tonic inhibition in the mouse hippocampus. *J. Physiol.* **582,** 1163–1178 (2007).

Acknowledgements

We are grateful to Dr P. Scheiffele (Biozentrum, University of Basel, Basel, Switzerland) for kindly providing us NL2HA cDNA. We thank B. Pastore for her excellent technical support with neuronal cultures. We are extremely grateful to L. Gasperini, E. Meneghetti and F. Ruggeri for their help and for critical discussion during experiments and to E. Grdina for managing the animal house facility. This work was partially supported by grants from Telethon (GGP11043), Human Brain Project (Neuroantibodies #604102) and MIUR (PRIN 2012) to E.C.

Author contributions

R.A., E.C. and P.Z. conceived the project. R.A. performed most of the molecular biology experiments; R.P. and A.P. performed the electrophysiological experiments; G.D.S. and J.-M.F. supplied some reagents; E.C. and P.Z. wrote the manuscript, which was revised by all authors in collaboration.

Additional information

Supplementary Information accompanies this paper at http://www.nature.com/naturecommunications

Competing financial interests: The authors declare no competing financial interests.

Reprints and permission information is available online at http://npg.nature.com/reprintsandpermissions/

How to cite this article: Antonelli, R. *et al.* Pin1-dependent signalling negatively affects GABAergic transmission by modulating neuroligin2/gephyrin interaction. *Nat. Commun.* 5:5066 doi: 10.1038/ncomms6066 (2014).

Supplementary Information

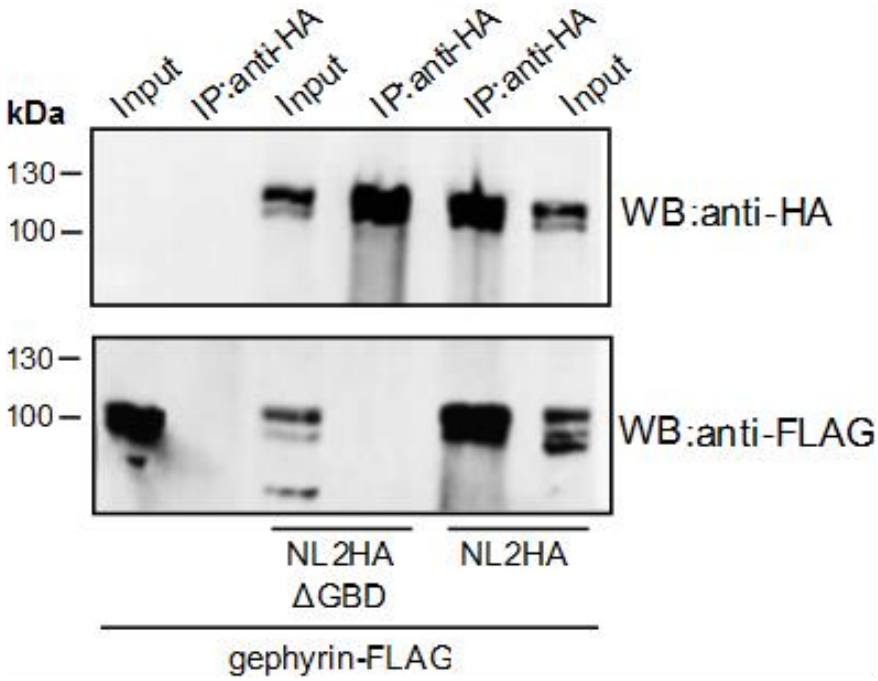

Supplementary Figure 1. NL2 lacking the gephyrin binding domain does not interact with gephyrin. Representative IP of HA epitopes from samples of HEK293 cells co-expressing gephyrin-FLAG and NL2HA or NL2HA-ΔGBD. IP was also performed on gephyrin-FLAG single transfected cells as a negative control. Nitrocellulose membranes were probed with anti-HA and anti-FLAG antibodies. Gephyrin-FLAG interaction with NL2HA is completely abolished upon removal of the GBD.

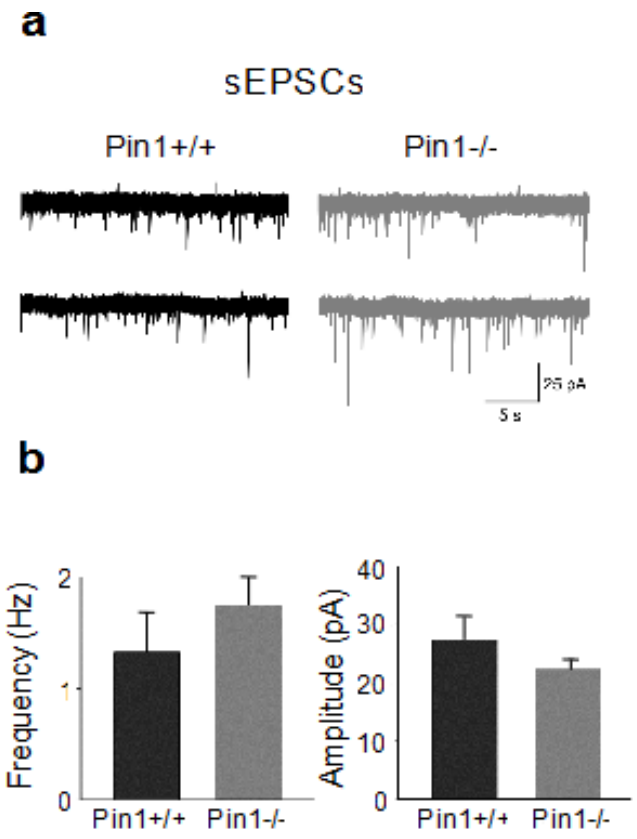

Supplementary Figure 2. Pin1 does not affect the amplitude or frequency of sEPSCs. **a)** Samples traces of sEPSCs recorded in the presence of the $GABA_A$ receptor antagonist PTX 100 μM from a CA1 principal cells at P11 in hippocampal slices from Pin1+/+ (black) and Pin1-/- mice (gray), n=6 for both genotypes. **b)** Each column represents the mean frequency and amplitude values of sEPSCs recorded from WT (black, n=6) and Pin-/- mice (gray, n= 6). $P > 0.05$, Student's *t*-test.

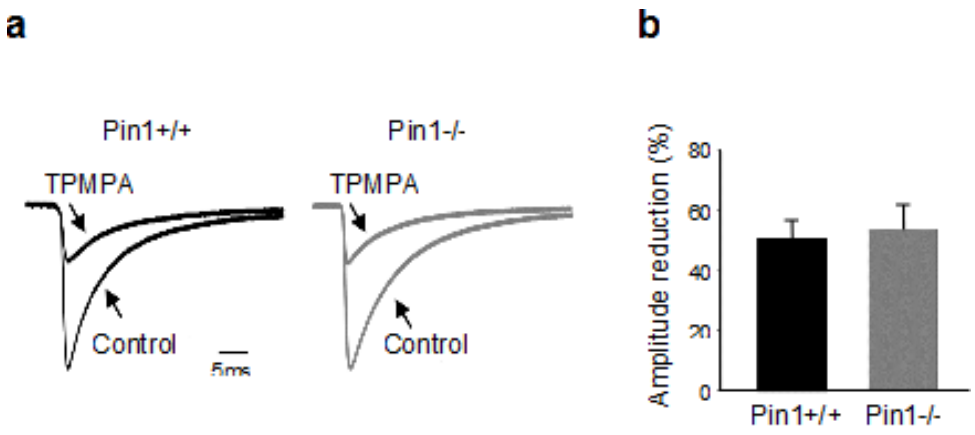

Supplementary Figure 3. Pin1 does not affect GABA transient in the cleft. a) Sample traces of sIPSCs recorded from Pin1+/+ (black) and Pin1-/- mice (gray), in the absence (Control) and in the presence of TPMPA (200 μM). The amplitudes of sIPSCs from Pin1-/- mice were normalized to those obtained from control littermates. **b**) Each column represents the mean TPMPA-induced reduction of sIPSCs amplitude in Pin1+/+ (black; n=4) and Pin1-/- mice (gray; n=5). $P > 0.05$; one-way ANOVA and Bonferroni post test for multi comparison analysis between groups

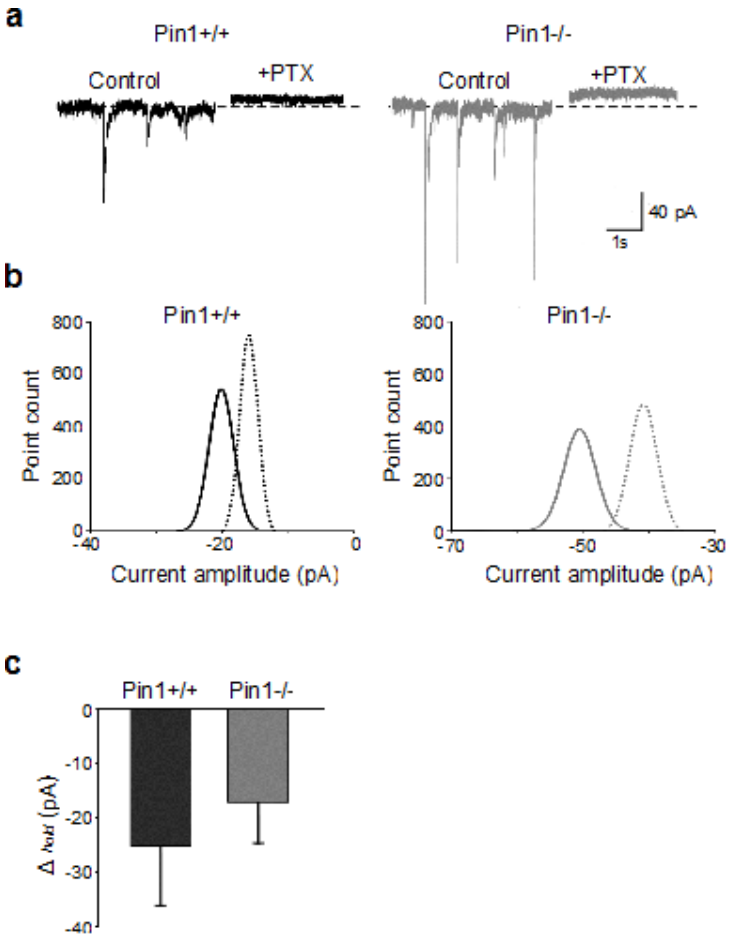

Supplementary Figure 4. Pin does not affect extrasynaptic $GABA_A$ Receptors. a) Representative traces of spontaneous IPSCs recorded from a CA1 pyramidal cell in hippocampal slice obtained from Pin1+/+ (black) and Pin1-/- mice (gray) before and during application of picrotoxin (PTX, 100 μM). **b)** All-point histogram of 5 ms traces from the cells recorded in a, before (dotted lines) and during (continuous lines) bath application of PTX in Pin1+/+ (black) and Pin1-/- mice (gray). Pin1+/+ n=6 and Pin1-/- mice n= 7. $P > 0.05$, Mann-Whitney test **. c)** Summary data of tonic currents obtained from both genotyping.

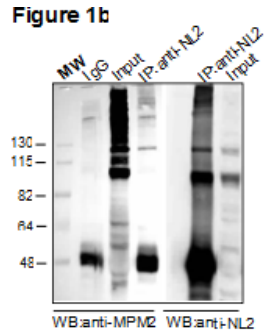

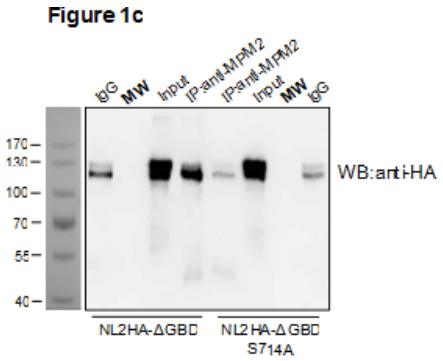

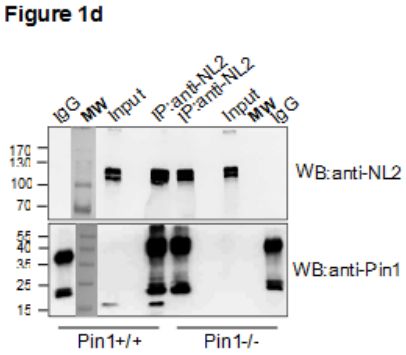

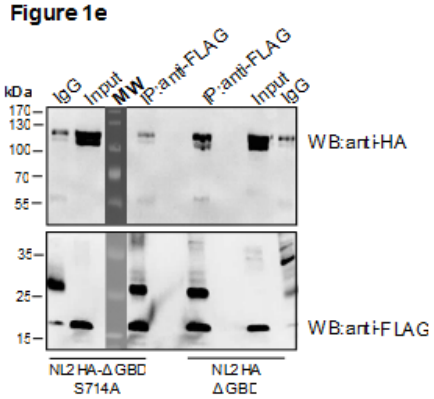

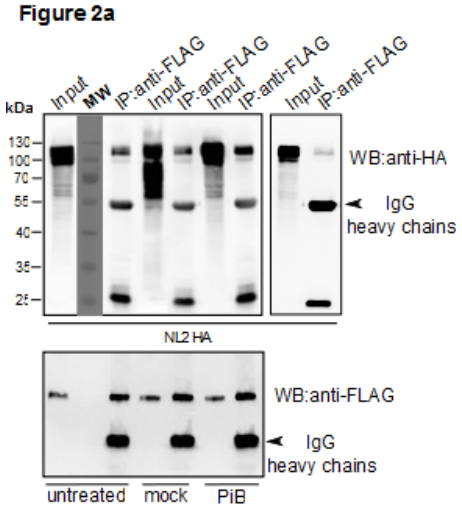

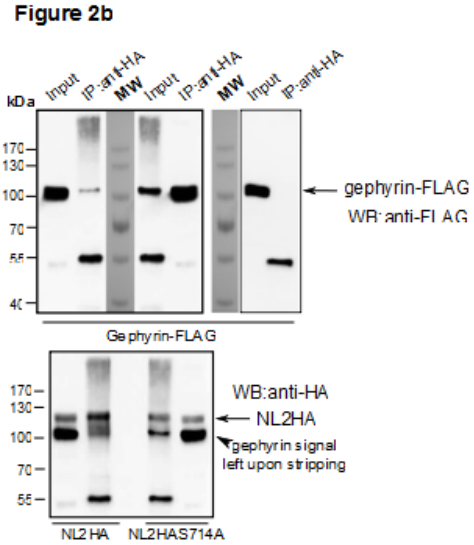

Supplementary Figure 5. Full images of western blot displayed in cropped format in figures 1, 2, 3, 4 and 5 (continued below)

Figure 2c

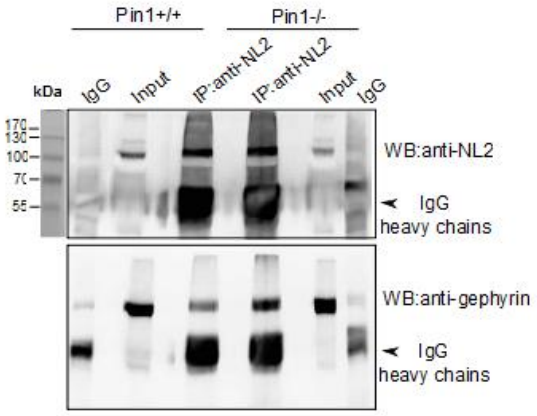

Figure 2d

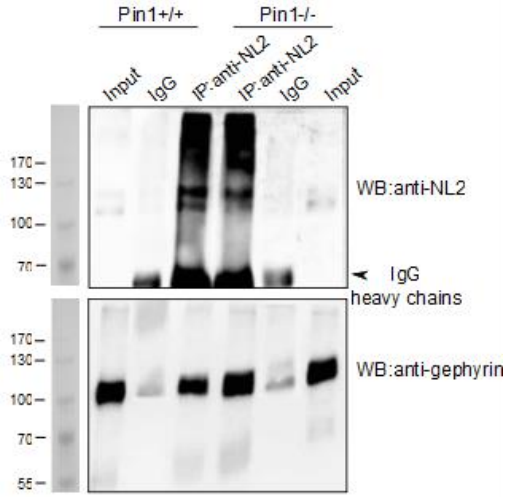

Figure 3c

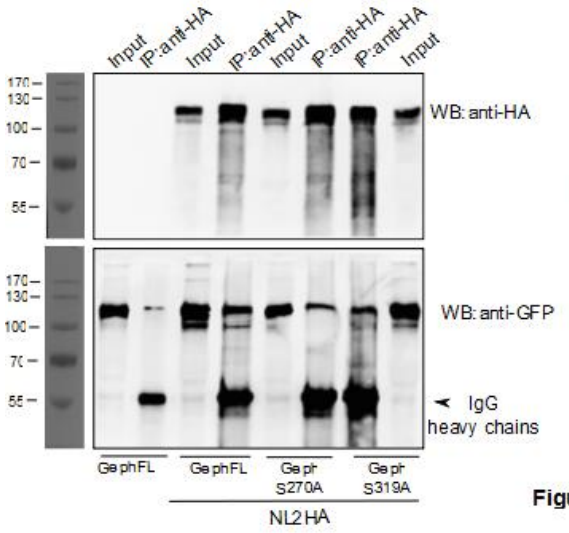

Figure 4a

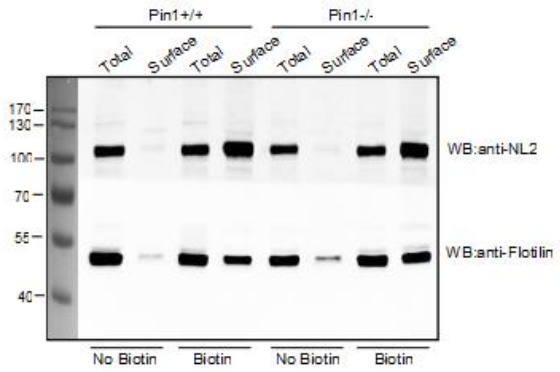

Figure 5a

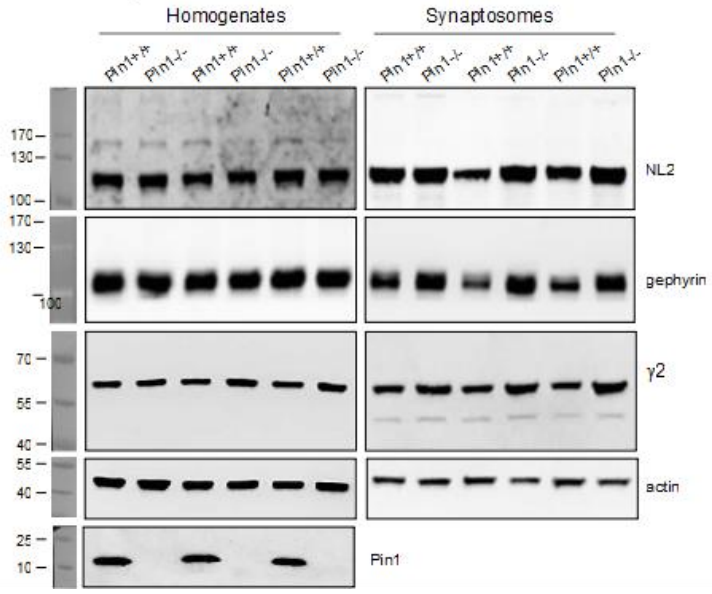

PAPER 2

Pin1 modulates the synaptic content of NMDA receptors via prolyl-isomerization of PSD-95

Roberta Antonelli[1], Roberto De Filippo[1], Silvia Middei[2], Stefka Stancheva[3], Beatrice Pastore[1], Martine Ammassari-Teule[2], Andrea Barberis[3], Enrico Cherubini[1-4], Paola Zacchi[1-4]

1. International School for Advanced Studies, via Bonomea 265, 34136 Trieste, Italy
2. National Research Council Institute of Cell Biology and Neurobiology, Santa Lucia Foundation, via del Fosso di Fiorano 64, 00143 Rome, Italy
3. Istituto Italiano di Tecnologia, Via Morego 30, 16163 Genoa, Italy
4. European Brain Research Institute, via del Fosso di Fiorano 64, 00143 Rome, Italy

SUBMITTED

Pin1 modulates the synaptic content of NMDA receptors *via* prolyl-isomerization of PSD-95

Roberta Antonelli[1], Roberto De Filippo[1], Silvia Middei[2], Stefka Stancheva[3], Beatrice Pastore[1], Martine Ammassari-Teule[2], Andrea Barberis[3], Enrico Cherubini[1-4], Paola Zacchi [1-4]

1. International School for Advanced Studies, via Bonomea 265, 34136 Trieste, Italy
2. National Research Council Institute of Cell Biology and Neurobiology, Santa Lucia Foundation, via del Fosso di Fiorano 64, 00143 Rome, Italy
3. Istituto Italiano di Tecnologia, Via Morego 30, 16163 Genoa, Italy
4. European Brain Research Institute, via del Fosso di Fiorano 64, 00143 Rome, Italy

Abstract

Phosphorylation of serine/threonine residues preceding a proline regulates the fate of its targets through post-phosphorylation conformational changes catalyzed by the peptidyl-prolyl *cis/trans* isomerase Pin1. By flipping the substrate between two different functional conformations, this enzyme exerts a fine tuning of phosphorylation signals. Pin1 has been detected in dendritic spines and shafts where it regulates protein synthesis required to sustain the late phase of long-term potentiation. Here, we demonstrate that Pin1 not only resides in post-synaptic structures but it can also interact with postsynaptic density protein-95 (PSD-95), a key scaffold protein that anchors N-methyl-D-aspartate receptors (NMDA-R) in PSD *via* GluN2-type receptor subunits. Pin1 recruitment by PSD-95 occurs at specific serine-threonine/proline consensus motifs localized in the linker region connecting PDZ2 to PDZ3 domains, thus negatively affecting PSD-95 ability to interact with NMDA-Rs.

In electrophysiological experiments, larger NMDA-mediated synaptic currents, evoked in CA1 principal cells by Schaffer collateral stimulation, were detected in hippocampal slices obtained from Pin1-/- mice as compared to controls. Similar results were obtained in cultured hippocampal cells expressing a PSD-95 mutant unable to undergo prolyl-isomerization, thus indicating that the action of Pin1 on PSD-95 is critical for this effect. In addition, an enhancement in spine density and size was detected in CA1 principal cells by Golgi staining.

Our data indicate that Pin1 controls the synaptic content of NMDA-Rs *via* PSD-95 prolyl-isomerization and the expression of dendritic spines, both required for the maintenance of long-term potentiation.

Significance Statement

PSD-95, a membrane-associated guanylate kinase, is the major scaffolding protein at excitatory postsynaptic densities and a potent regulator of synaptic strength and plasticity. The activity of PSD-95 is tightly controlled by several post-translational mechanisms including proline-directed phosphorylation. This signaling cascade regulates the fate of its targets through post-phosphorylation conformational

modifications catalyzed by the peptidyl-prolyl cis/trans isomerase Pin1. Here, we uncover a new role of Pin1 in glutamatergic signaling. By physically interacting with PSD-95, Pin1 dampens PSD-95 ability to complex with NMDA-Rs, thus negatively affecting NMDA-R signaling and spine morphology. Our findings further emphasize the emerging role of Pin1 as key modulator of synaptic transmission.

Introduction

PSD-95 represents a major core scaffolding protein enriched at post-synaptic densities (PSD) of excitatory synapses (Chen et al., 2005) which regulates several aspects of synapse dynamics, from synapse maturation to synaptic strength and plasticity (Kim and Shen, 2004; Elias and Nicoll, 2007; Xu 2011). This scaffolding molecule is one of the earliest proteins detected in the PSD (Rao et al., 1998) and regulation of its synaptic clustering is essential for proper synapse formation and maturation. PSD-95 shares with other membrane-associated guanylate kinases (MAGUK)-family members a multi-modular structure composed of three PDZ [PSD-95/Discs large (Dlg)/zona occludens-1 (ZO-1)] domains, a Src homology 3 (SH3) domain and a catalytically inactive guanylate kinase domain (Kim and Sheng, 2004). This structural architecture allows anchoring NMDA- and α-amino-3-hydroxy-5-methyl-4-isoxazolepropionic acid (AMPA)-types of glutamate receptors at postsynapses, and tethering them to intracellular signaling complexes and cytoskeletal elements responsible for their dynamic changes (Opazo et al., 2012).

Several post-translational modifications have been shown to control the dynamic deposition of PSD-95 at synapses such as palmitoylation (Craven et al., 1999), Serine/Threonine phosphorylation (Morabito et al., 2004; Gardoni et al., 2006; Kim et al., 2007) and Tyrosine phosphorylation (Du et al., 2009). Phosphorylation on certain serine or threonine residues preceding a proline regulates the fate of its targets through post-phosphorylation conformational modifications catalyzed by the peptidyl-prolyl *cis/trans* isomerase (PPIase) Pin1 (Lu et al., 2007). This enzyme acts by flipping the substrate between two different conformations that are functionally diverse, thus exerting a fine-tuning of phosphorylation signals (Liou et al., 2011). At inhibitory synapses, Pin1-dependent isomerization of gephyrin, the functional homologue of PSD-95 at inhibitory synapses, affects GlyRs function (Zita et al., 2007). At GABAergic synapses, Pin1 recruitment by the cell adhesion molecule neuroligin2 negatively modulates its ability to complex with gephyrin, leading to a down-regulation of GABAergic transmission (Antonelli et al., 2014). At glutamatergic synapses Pin1 has been detected in dendritic shafts and spines where it acts by suppressing protein synthesis required to sustain late long-term potentiation (Westmark et al., 2010).

The high abundance of Pin1 at excitatory synaptic contacts and the observation that PSD-95 bears potential recognition sites for prolyl-isomerization prompted us to investigate

whether such MAGUK member may undergo post-phosphorylation modulation of its activity. Here we provide evidence that endogenous PSD-95 can recruit Pin1 at consensus motifs located between the second and third PDZ domains. We show that post-phosphorylation prolyl-isomerization negatively regulate PSD-95's ability to complex with NMDA-Rs, leading to a down-regulation of the NMDA-R-mediated synaptic transmission associated with a decrease in dendritic spines density.

Materials and Methods

Constructs. GFP-tagged PSD-95and FLAG-tagged GluN2B constructs were kindly provided by Dr Vicini (Geargetown, USA, (Craven et al., 1999; Prybylowski et al., 2002). GFP-PSD-95 mutagenesis and cloning of the C-terminus of the GluN2B subunit (amino acid 1086-1482) into pGEX-4T1 expression vector were performed by PCR amplification using Pfx DNA polymerase (Invitrogen) and the appropriate oligonucleotides. All mutations were fully sequenced to exclude the possibility of second site mutations. HA-tagged human NL1 in pCAG was kindly provided by Dr. Scheiffele (Biozentrum, Basel). pGEX4T1 plasmids containing Pin1WT and Pin1Y23A and FLAG-tagged version were previously described (Zacchi et al., 2002).

Cell culture. HEK293T cells were cultured at 37^{o}C under a 5% CO2 atmosphere in Dulbecco's modified Eagle's medium supplemented with 10% fetal bovine serum. They were transiently transfected with various plasmids using Polyethylenimine linear (Polysciences) and collected 24–48 h after transfection. Pin1+/+ and Pin1-/- primary hippocampal neurons were prepared as previously described (Antonelli et al., 2014) from either sex. For transfection experiments mouse hippocampal neurons were transiently transfected with the indicated plasmids using Effectene (Qiagen) according to the manufacturer's protocol.

GST-Pull Down, Co-immunoprecipitation, Western blot analysis and Synaptic Protein Extraction.

GST pull-down and MPM2-mediated immunoprecipitation were performed as previously described (Zita et al., 2007; Zacchi et al., 2002). For Pin1-FLAG (wt and Y23A) and GFP-PSD-95 co-immunoprecipitation, transfected cells were lysed in a buffer containing 50 mM Tris-HCl, pH 7.5, 100 mM NaCl, 0.1% Tween 20, 10% glycerol, 10 mM EDTA, 2 mM $MgCl_2$ and protease inhibitor mixture. Extracts were incubated for 2 hours at 4^{o}C with the anti-FLAG antibody (Sigma, clone M2) and immunocomplexes captured using Protein G sepharose 4 fast Flow (Amersham). NL1-HA and GFP-PSD-95 transfected cells were lysate in buffer CHAPS containing 50 mM Tris–HCl, pH 7.5, 1 mM EDTA, 150 mM NaCl, 0.5% CHAPS, 10% glycerol and protease inhibitor mixture and immunoprecipitated with anti-HA affinity resin (Pierce). Co-immunoprecipitations of native PSD-95/Pin1 and PSD-95/NL1 complexes were obtain from p15 Pin1+/+ and Pin1−/− brain homogenates (from either sex) in buffer CHAPS (as above), while PSD-95/NMDA-R complexes were isolated using a chemical cross-linking approach (Poulopoulos et al., 2009). In all experiments native complexes were immunoprecipitated

using the anti-PSD95 (Abcam). The following antibodies were used in western blot analysis: rabbit anti-GluN1 (Sigma), rabbit anti-GluN2B (Alomone), monoclonal anti-PSD95 (Abcam and NeuroMab), monoclonal anti-FLAG M2 (Sigma), monoclonal anti-GFP (NeuroMab). Western blot image acquisition was performed using the ECL detection kit and the Alliance 4.7 software (UVITECH, Cambridge). Quantifications were performed using the UVI band imager software (Amersham) as described (Antonelli et al., 2014). PSD enriched extracts were prepared by using the Syn-PER Extraction Reagent (ThermoScientific) as previously described (Antonelli et al., 2014). P-values were calculated using the Student's t-Test with a two-tailed distribution on samples.

Immunocytochemistry, Confocal microscopy and image analysis. Hippocampal neurons grown on glass coverslips were fixed at DIV15 with cold methanol for 5 minutes, blocked by incubation with 10% normal goat serum in PBS. Antibodies were diluted in 5% normal goat serum/PBS. Secondary antibodies included anti-isotypic fluorophore conjugated antibodies Alexa-488, Alexa-594 and streptavidin-Alexa 405 at dilutions of 1:1,000 (Molecular Probes). The following commercially available antibodies were used in immunocytochemistry: mouse anti-PSD95 (Sigma), guinea pig anti-vGLUT1(Chemicon), rabbit anti-GluN1 (Sigma). Fluorescence images were acquired on a TCS-SP confocal laser scanning microscope (Leica, Bensheim, Germany) with a 40X 1.4 NA oil immersion objective, additionally magnified fivefold with the pinhole set at 1 Airy unit. All the parameters used in confocal microscopy were consistent in each experiment, including the laser excitation power, detector and off-set gains and the pinhole diameter. Quantification of immunofluorescence data was performed using the Volocity3D Image Analysis Software (PerkinElmer, London, UK) (Antonelli et al., 2014).

Hippocampal slice preparation. All experiments were performed in accordance with the European Community Council Directive of November 24, 1986 (86/609EEC) and approved by the local authority veterinary service and by SISSA ethical committee. Transverse hippocampal slices (300µM thick), were obtained from postnatal (P) day P10-P15 mice using a standard protocol (Gasparini et al., 2000). Drugs used were: 6,7-dinitroquinoxaline-2,3-dione (DNQX), bicuculline methiodide, and threo-ifenprodil-hemitartrate, all purchased from Tocris Bioscence (Bristol, UK). Drugs were applied in the bath by gravity *via* a three-way tap system.

Electrophysiological recordings and Data analysis. In acute slices whole-cell patch-clamp recordings (in voltage clamp configuration) were performed from CA1 pyramidal cells. AMPAR- and NMDAR- mediated EPSCs were evoked by stimulation of Schaffer collateral which was set at such intensity to produce half maximal responses. In cultured hippocampal cells, EPSCs were evoked by square pulses (5ms duration, 5–25μA amplitude) delivered through a glass electrode filled with extracellular solution positioned in the vicinity of the neuron to be stimulated. To establish the AMPA/NMDA ratio, AMPA-EPSCs were first recorded in the voltage-clamp mode at -60 mV in the presence of bicuculline (5μM) to block GABAergic transmission. NMDA-EPSCs were recorded by changing the membrane potential to +40mV. In slices the NMDA component was measured 50 ms post stimulus, when the AMPA-R contribution is negligible. In cultured neurons NBQX (10μM) was added to the extracellular solution to block the AMPA-mediated component. At the end of the experiment, AP-5 was added to confirm that, in these conditions, the recorded current was mediated by NMDA-Rs. Data from acute slices were acquired and digitized with an A/D converter (Digidata 1200, Molecular Device) and analysed with Clampfit 9. Currents from transfected neurons were acquired and analyzed using Clampex and Clampfit software (Molecular Devices). Data are presented as mean ± S.E.M. Statistical comparison was performed using the unpaired t-test.

Golgi staining and spine morphology assessment. Five Pin-/- and Pin+/+ littermates were intracardially perfused with 0.9% saline solution. Brains were rapidly collected and immersed in Golgi solution (1% potassium dichromate, 1% mercuric chloride and 0.8% potassium chromate in distilled water) for 5 days at room temperature. After a rapid (24 hours) passage in 30% sucrose solution, 100 μm coronal sections were cut through a vibratome and then mounted on gelatined slides for staining according to the Gibb and Kolb method (Gibb and Kolb, 1998). Spine analysis was carried out on apical dendrites of neurons lying on the CA1 region in the ventral hippocampus using the public domain ImageJ software (NIH, USA) according to previously described protocols (Middei et al., 2012).

Results

PSD-95 recruits Pin1 at consensus sites located between PDZ2 and PDZ3 domains

PSD-95 phosphorylation, and in particular proline-directed phosphorylation, represents one of the key mechanisms controlling its synaptic targeting and clustering (El-Husseini et al., 2000; Elias et al., 2006). In line with these findings we were able to immunoprecipitate endogenous PSD-95 from mouse brain by using the anti-phospho-Ser/Thr-Pro MPM-2 antibody (Davis et al., 1983) (Fig1A, left panel) and to detect GFP-PSD-95 upon its ectopic expression in HEK293 cells (Fig 1A, right panel). If PSD-95 can undergo post-phosphorylation prolyl-isomerization, it should be able to bind the rotamase Pin1. Indeed co-immunoprecipitation assays demonstrated the presence of native PSD-95/Pin1 complexes in Pin1+/+ mouse brain (Fig 1B).

Figure 1

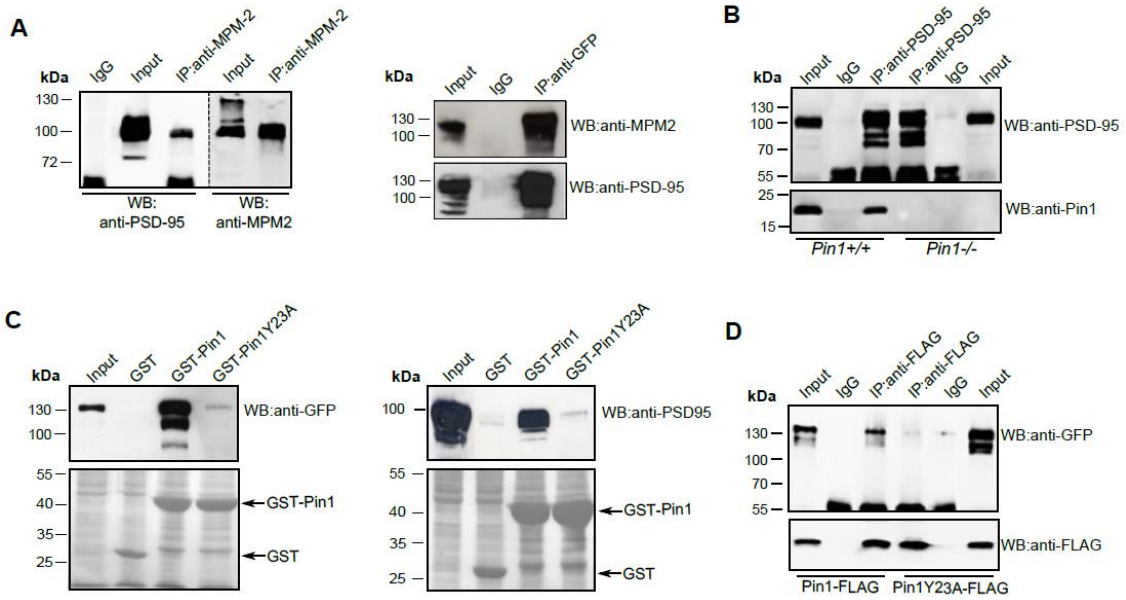

Pin1 interacts with PSD-95. (**A**) PSD-95 was precipitated from brain extracts using the anti-MPM2 antibody. Each sample was run twice to perform immunoblots with anti-PSD-95 and anti MPM2 antibodies (left panel). HEK293T extracts expressing GFP-PSD-95 were immunoprecipitated with anti-GFP antibody and immunoblotted with anti-MPM2 and anti-PSD-95 antibodies (right panel). (B) Brain extracts from Pin1+/+ and Pin1-/- were immunoprecipitated with anti-PSD-95 antibody and immunoblotted with anti-PSD-95 and anti-Pin1. (C) Extracts of HEK293 cells transfected GFP-PSD-95WT (left panel) or mouse brain homogenates (right panel) were incubated with GST, GST-Pin1 and GFT-Pin1Y23A and immunoblotted with anti-PSD-95 and anti-GFP antibodies. (D) Extracts of HEK293 cells co-transfected with Pin1-FLAG and GFP-PSD-95WT were immunoprecipitated with anti-FLAG and immunoblotted with anti-FLAG or anti-GFP. Mouse IgG were used as negative control.

The interaction of Pin1 with PSD-95 and its phospho-dependency were further examined in GST-Pin1 pull-down, either upon ectopic expression of GFP-PSD-95 (Fig 1C, left panel) or

on endogenous protein levels (Fig 1C, right panel), and in co-immunoprecipitation experiments (Fig 1D).Both approaches clearly unveiled that only Pin1wt efficiently associates with PSD-95 while the Pin1Y23A, a mutant impaired in phospho-Ser/Thr-binding activity (Lu et al., 1999), interacts only weakly with it, indicating that PSD-95 recruits Pin1 in a phosphorylation-dependent manner.

PSD-95 contains six potential Pin1 recognition motifs organized in two clusters, one located on the N-terminal (T19/ S25/ S35) while the other on the linker region connecting PDZ2 to PDZ3 domains (T287/ S290/ S295) (Fig 2A). To identify the Pin1 binding sites on PSD-95, we initially generated PSD-95 deletion constructs lacking either the first cluster (PSD-95Δ19-35), the second (PSD-95Δ287–295) or both and tested them for interaction with GST-Pin1. PSD-95Δ19-35 was associated with Pin1 to the same extent as wild-type PSD-95, while PSD-95Δ287–295 only poorly interacted with the chaperone molecule (Fig 2B, left panel) and its binding capacity was not further dampened upon the additional removal of the N-terminal sites (Fig 2B, right panel).

Figure 2

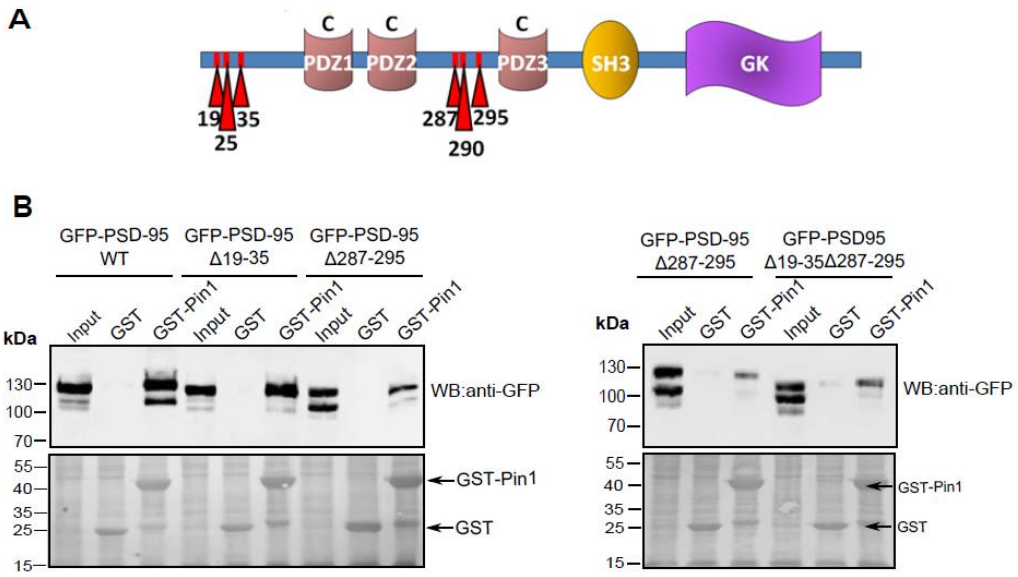

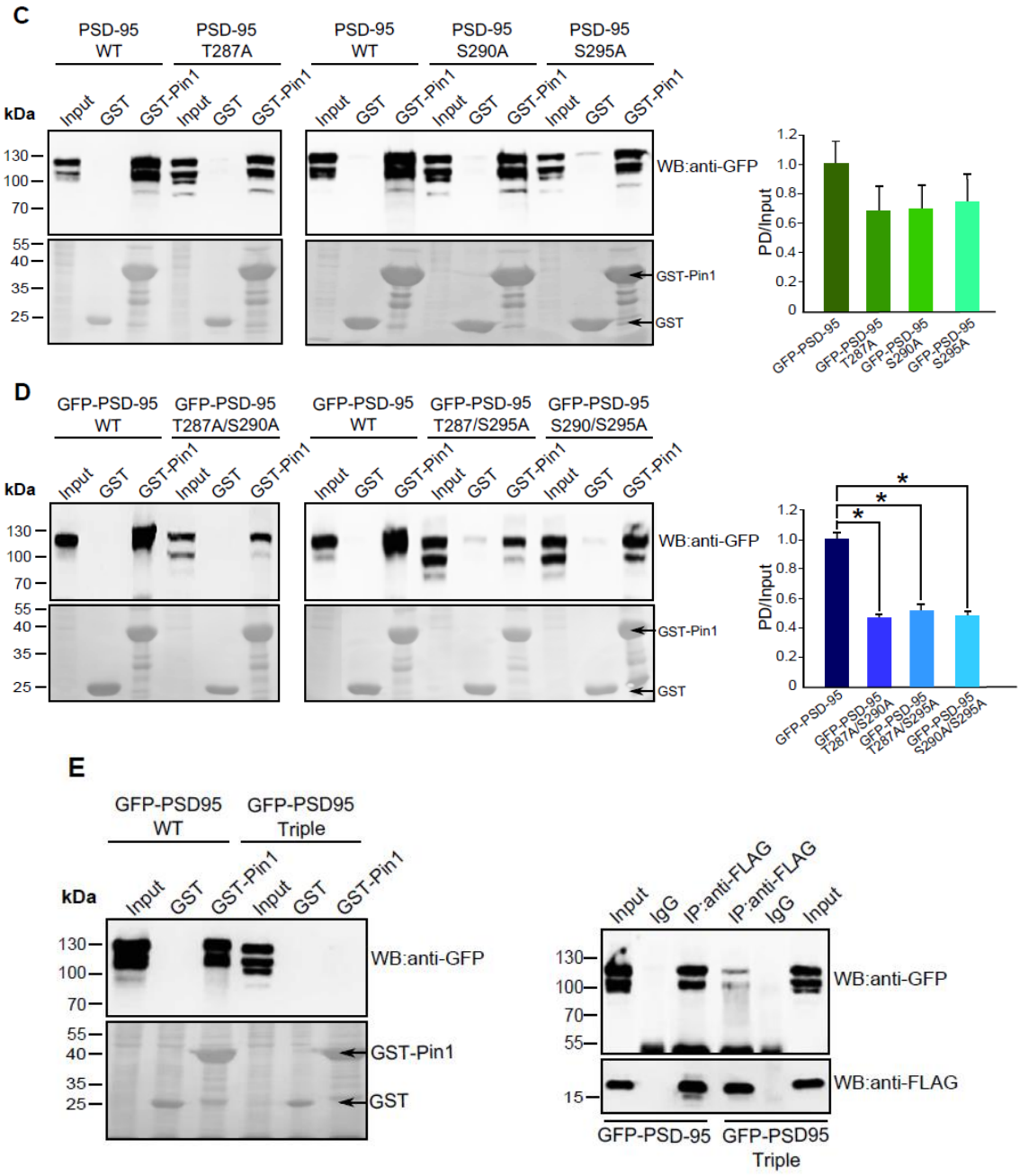

Pin1 interacts with PSD-95 at T287, S290 and S295 consensus motifs. (A) Schematic representation of PSD-95 domains (PDZs in brown; SH3 in yellow; GK in purple). Putative Pin1 sites are indicated by red arrows. **(B)** Extracts of HEK293 cells transfected GFP-PSD-95WT or the indicated deletion mutants were incubated with GST or GST-Pin1 and immunoblotted with anti-GFP antibody. **(C, D and E)** Extracts of HEK293 cells transfected GFP-PSD-95WT and the indicated single, double and triple point mutants were incubated and processed as in B. Histograms represent the amount of PSD-95 mutants pulled-down (PD) by equal amount of GST-fusion probe normalized to their expression level (Input). (n=4; mean values±s.d., *P*>0.05 for single mutants and **P*<0.05 for double mutants). **(F)** Extracts of HEK293 cells co-transfected with Pin1-FLAG and GFP-PSD-95 or PSD-95 Triple mutant were immunoprecipitated with anti-FLAG or mouse IgG as negative control and immunoblotted with anti-GFP or anti-FLAG. Bottom panels in B, C, D and E show levels of GST fusion proteins (Ponceau staining)

To further validate the importance of this short stretch of amino acid residues (287-295) as Pin1 recruitment domain, we performed a serine/threonine to alanine scan mutagenesis at each putative Pin1 consensus site to generate singles (PSD-95T287A, PSD-95S290A, PSD-95S295A), doubles (PSD-95S287A/S290A) and the triple (PSD-95S287A/S290A/S295A)

mutants to be tested in the GST-Pin1 pull-down assays. Under these conditions, while single point mutants exhibited a similar affinity for Pin1 as the wild-type protein (Fig 2C), double mutants showed a significant reduction in binding (Fig 2D), which was almost abolished upon alanine substitution at all three sites both in GST-Pin1 pull down (Fig 2E, left panel) and in co-immunoprecipitation (Fig 2E, right panel), thus suggesting that all of them contribute to Pin1 recruitment.

Pin1 action on PSD-95 alters the ability of the scaffold molecule to interact with the NMDA receptors

The close proximity of the identified Pin1 recruitment motifs to PSD-95 PDZ domains known to be involved in GluN2A/B and neuroligin1 (NL1) interaction raises the possibility that a conformational shift in this region may affect the PDZ binding affinity for the corresponding binders. The first two PDZ domains are known to directly interact with the C-terminal of the GluN2A and/or GluN2Bsubunits of NMDA-Rs (Kornau et al., 1995; Niethammer et al., 1996) while PDZ3 with the cell adhesion molecule NL1 (Irie et al., 1997). Neither detectable differences in NL1-HA precipitated by GFP-PSD-95wt and PSD-95 triple mutant were found (Fig 3A) nor in endogenous NL1 pulled down by PSD-95 in the presence or absence of Pin1 expression (Fig 3B), indicating that PDZ3 was not involved. By contrast, PSD-95 triple mutant showed an enhanced association with the GluN2B as compared to PSD-95wt (Fig 3C) in GST-based pull-down assays (only the C-terminus of GluN2B). This observation prompted us to investigate how endogenous PSD-95 complexes with NMDA-Rs in the presence or in the absence of Pin1. As shown in Figure 3D, in Pin1-/- hippocampal extracts, the amount of GluN2B receptor subunit co-precipitated by PSD-95 was increased by 20.9% ± 2.02 as compared to Pin1 expressing neurons (Fig 3D).

To test whether the enhanced PSD-95/GluN2B complex formation occurs at synaptic sites, we analyzed the expression levels of PSD-95, GluN1 (the obligatory subunit of all NMDA-Rs

Figure 3

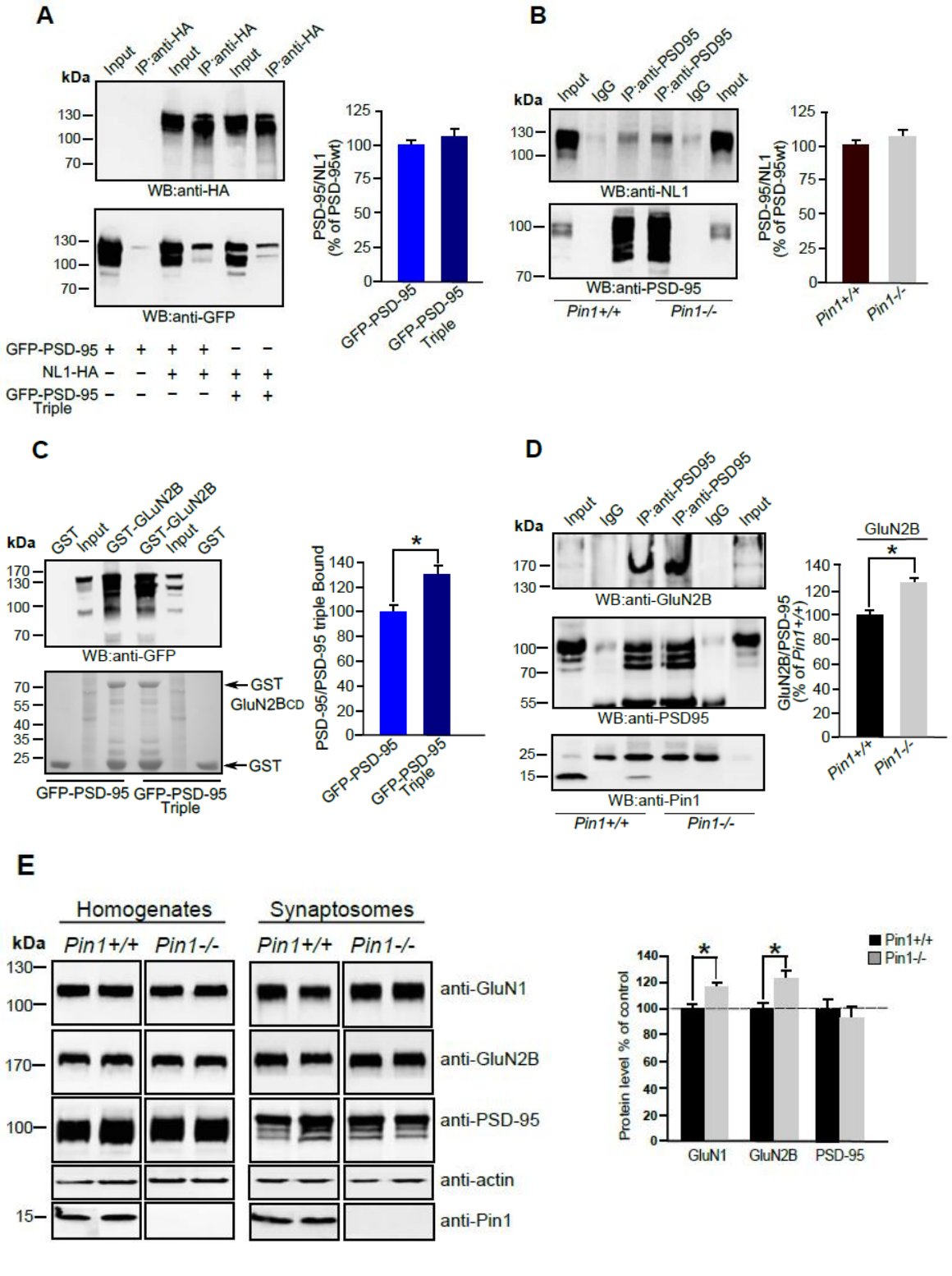

Figure 3. Pin1 modulates PSD-95's ability to complex with NMDARs at synapse. (**A**) Extracts of HEK293 cells transfected with the indicated plasmids were immunoprecipitated with anti-HA antibody and immunoblotted with anti-GFP and anti-HA. Histogram shows the relative amount of PSD-95 or Triple mutant in complex with NL1HA obtained from densitometric analysis (n=4, mean values±s.d., *P*>0.05). (**B**) Brain extracts from Pin1+/+ and Pin1-/- were immunoprecipitated with anti-PSD-95 antibody and immunoblotted with anti-PSD-95 and anti-NL1. Histogram shows the relative amount of NL1 in complex with PSD-95 obtained as in (A) (n=4, mean values±s.d. *P*>0.05). (**C**) Extracts of HEK293 cells transfected with GFP-PSD-95 were incubated with

GST and GST-GluN2B and immunoblotted with anti-GFP antibody. Bottom panel show levels of GST fusion proteins (Ponceau staining). Histogram shows the amount of PSD-95 or PSD-95 Triple pulled-down as % of PSD-95WT (n=5; mean values±s.d., **P*<0.05). (**D**) Brain extracts from Pin1+/+ and Pin1-/- were immunoprecipitated with anti-PSD-95 antibody and immunoblotted with anti-GluN2B, anti-PSD-95 and anti-Pin1. Histogram shows the amount of GluN2B in complex with PSD-95 quantify as in C (n=5;mean values±s.d., **P*<0.05).**(E)** Representative immunoblots of the indicated antigens extracted from the hippocampus of Pin1+/+ and Pin1-/- mice (littermates) in two different sets of experiments. On the right quantification of the indicated antigens. Actin represents loading control. (n=6 littermate pairs, mean values±s.d, **P*<0.05)

(Paoletti et al., 2013)), and GluN2B in synaptosomal fractions isolated from Pin1+/+ and Pin1-/- hippocampus. As shown in Figure 3E, quantitative immunoblot analysis unveiled that the amount of GluN1 and GluN2B subunits was significant increased in Pin1-/- mice, being the synaptic enrichment (synaptic fraction *vs* homogenate) for GluN1 of 18 ± 3% and GluN2B of 23 ± 4% . Altogether these data indicate that Pin1 negatively modulates the synaptic enrichment of NMDA-Rs *via* PSD-95 prolyl-isomerization.

Pin1 affects NMDA-mediated synaptic signaling

To investigate the functional consequences of Pin1-dependent regulation of NMDA-Rs signaling at excitatory synapses, the NMDA/AMPA ratio of synaptic currents evoked in CA1 principal cells by Schaffer collateral stimulation were analyzed in both genotypes. In comparison with control littermates, Pin1-/- mice exhibited larger NMDA-mediated synaptic responses (Fig 4A). On average, the peak amplitudes of AMPA-R-mediated excitatory postsynaptic currents (EPSCs) were similar in both genotypes (103 ± 10 pA and 107 ± 12 pA in Pin+/+, n=17 and Pin1-/- mice, n=16, respectively; *P* = 0.8), while NMDA-mediated EPSCs were enhanced in Pin1-/- mice (48 ± 5 pA and 71±13 pA in Pin1+/+ and Pin1-/- mice, respectively; *P*<0.05). As expected, the NMDA/AMPA ratio was significantly increased in Pin1-/- mice respect to controls (0.49 ± 0.04 and 0.66 ± 0.07 in Pin+/+ and Pin1-/- mice, respectively, *P*<0.05; Fig 4B) as well as the charges transfer through synaptic NMDA-Rs (Figure 4C), thus suggesting modifications in amplitude and/or shape.

Figure 4

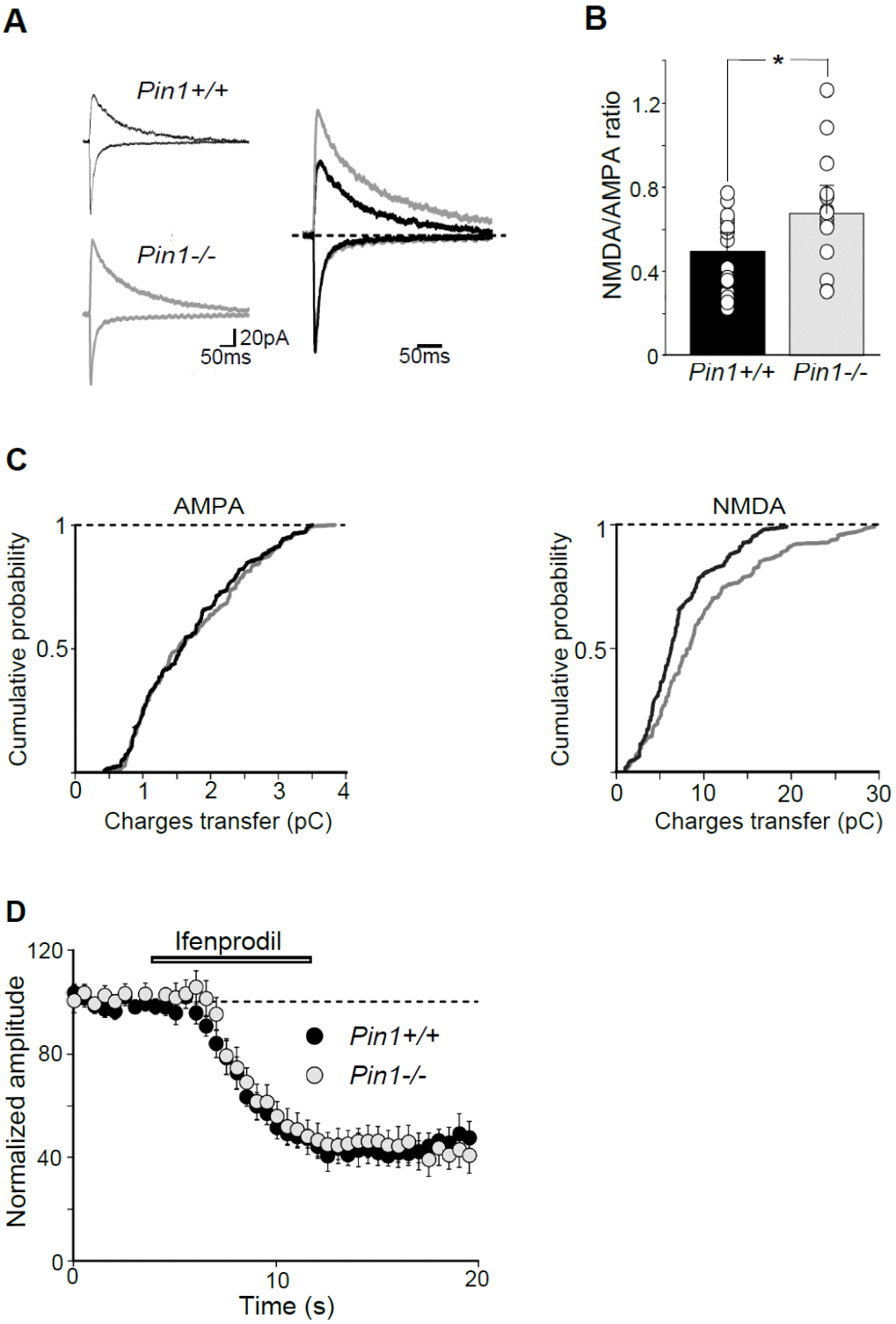
A
Pin1+/+
Pin1-/-
20pA
50ms
50ms
B
NMDA/AMPA ratio
1.2
0.8
0.4
0
*
Pin1+/+
Pin1-/-
C
AMPA
Cumulative probability
1
0.5
0
1
2
3
4
Charges transfer (pC)
NMDA
Cumulative probability
1
0.5
0
10
20
30
Charges transfer (pC)
D
Ifenprodil
Normalized amplitude
120
80
40
0
Pin1+/+
Pin1-/-
0
10
20
Time (s)

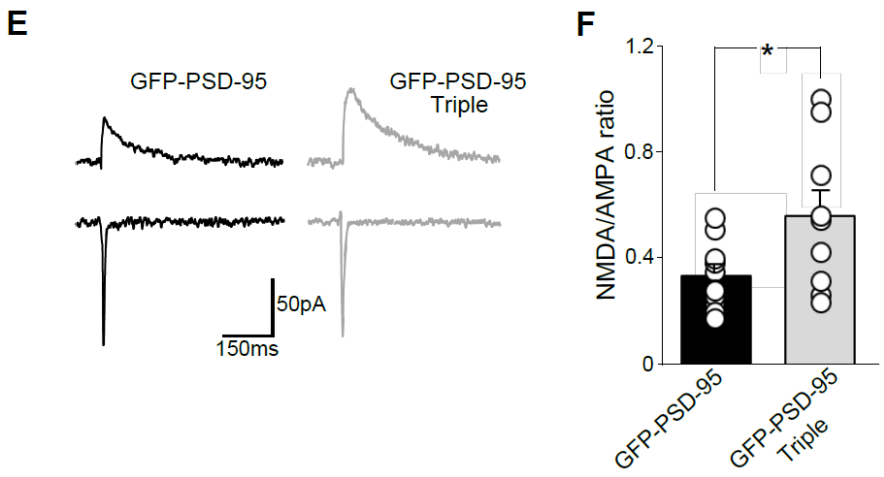

Pin1 controls synaptic signaling *via* NMDA receptors and regulates spine number and size. (**A**) Sample traces of NMDA-R- and AMPA-R-mediated EPSCs recorded from CA1 principal cells in hippocampal slices of Pin1+/+ and Pin1-/- at holding potentials of −60 and +40 mV, respectively. Each trace is the average of ten responses. On the right, the traces normalized to those mediated by AMPA-R are superimposed. (**B**) Summary graphs of the NMDA/AMPA-mediated receptor response ratios. Data represent means ± SEMs. Open symbols are individual values; * P<0.05, Student's t-test. (**C**) Cumulative probability plots of charge transfers through AMPAR (left) and NMDAR (right) receptors mediated currents. The NMDA curves are significantly different (P=0.003; KS test). (**D**) Time course of ifenprodil action (open bar) on NMDAR-mediated synaptic currents from Pin1+/+ (n=12) and Pin1-/- mice (n=10). Each point represents the mean ± SEM. (**E**) Examples of evoked AMPA- and NMDA-mediated EPSCs in cultured hippocampal cells from GFP-PSD-95wt (black) and GFP-PSD-95 triple mutant (grey) transfected cells. (**F**) Summary graphs of the NMDA/AMPA ratios of transfected neurons. Open symbols are individual values; * P<0.05.

NMDA-Rs are assembled as heteromers that differ in subunits composition, giving rise to NMDA-Rs with different biophysical and functional properties (Paoletti et al., 2013). In particular, NMDA-Rs containing GluN2B-D subunits, exhibit slower deactivation kinetics respect to those containing GluN2A (Vicini et al., 1998). Therefore, to investigate whether Pin1 may alter the subunits composition of NMDA-Rs, we measured the deactivation kinetics of NMDA- and AMPA-mediated synaptic currents in both genotypes. While the decay of AMPA-mediated EPSCs could be fitted by a single exponential (τ_{fast}: 11±1 ms and 13±1 ms in Pin1+/+, n=16 and Pin1-/- mice, n=11, respectively, P=0.21), that of NMDAR-mediated currents by two exponentials (τ_{fast}: 55±4 ms and 42±6 ms in Pin1 +/+, n=16 and Pin1-/-mice, n=13, respectively; τ_{slow} : 243±27 ms and 218±32 ms in Pin1 +/+ and Pin1-/- mice, respectively). Despite a certain degree of variability between the two genotypes, no significant differences in the decay time constants were observed (P=0.1 and P=0.8 for τ_{fast} ans τ_{slow}, respectively), suggesting that Pin1 does not affect the composition of synaptic NMDA-R subtypes. Moreover, treatment with ifenprodil, a selective antagonist of GluN2B containing receptors (Williams, 1993), produced a similar depression of NMDA-mediated

synaptic currents in both genotypes (Fig 4D), further indicating that Pin1 does not alter the subunits composition of NMDA receptors but it exerts its control on their total number. It is interesting to note that the NMDA/AMPA ratio was also increased in cultured hippocampal neurons transfected with GFP-PSD-95 triple mutant as compared to GFP-PSD-95wt (Fig 4E and F), thus further indicating that the action of Pin1 on PSD-95 is critical for this effect.

Pin1 regulates the number and the morphology of dendritic spines

NMDA-Rs have been reported to play a key role in dendritic spines formation and morphology (Lamprecht and LeDoux, 2004; Rao and Finkbeiner, 2007). Since in the absence of Pin1 NMDA-Rs appear enriched at PSD, we tested whether this effect may impact on dendritic spines dynamics. Spines number and morphology were evaluated in Golgi-stained CA1 pyramidal neurons from both mouse genotypes (Fig 5A).

Figure 5

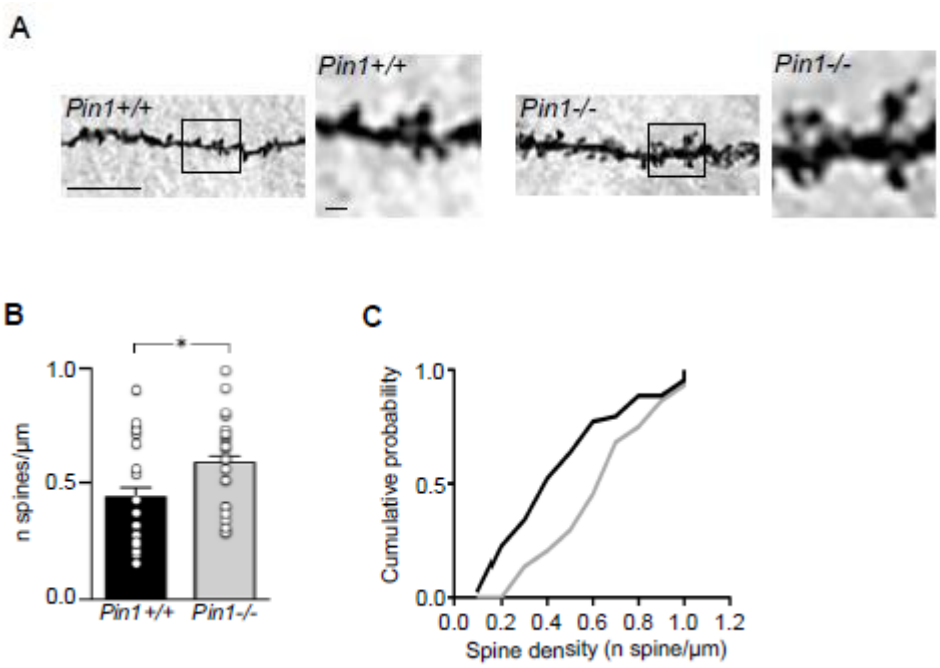

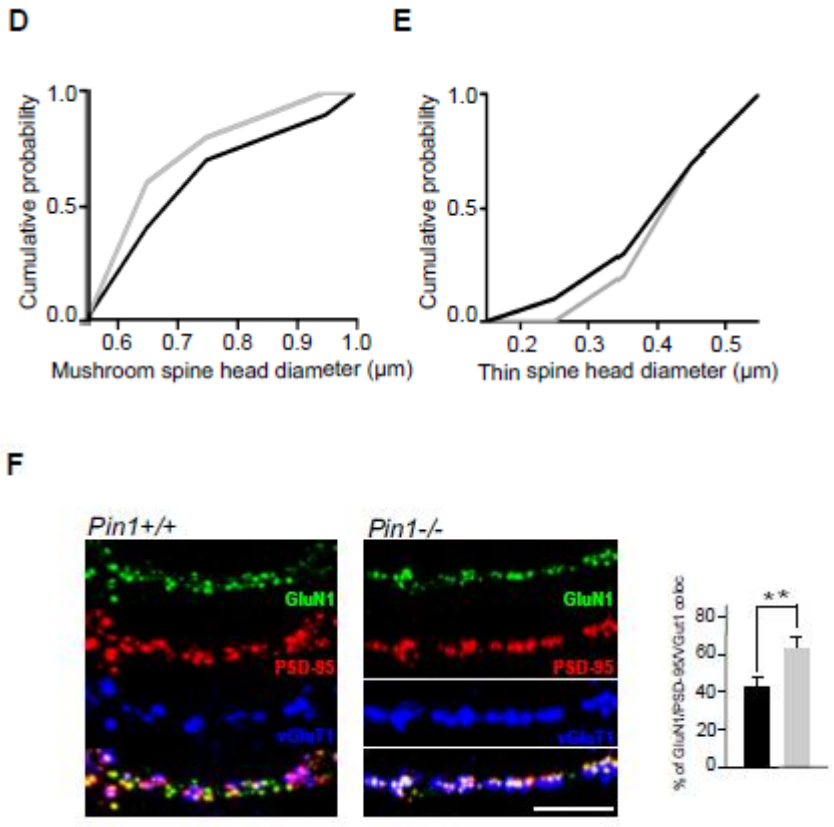

Figure 5 Pin1 regulates spine number and size. (**A**) Representative segments of CA1 pyramidal neurons dendrites (scale bar 10 µm). Selected area are reported in right panels (scale bar 1µm). (**B**) Histograms showing mean spine density ± SEM, along apical CA1 dendrites of Pin+/+ and Pin-/-. **P*<0.05. n=5 mice for each genotype; 5 to 6 neurons for each mouse. (**C**) Cumulative probability plots of spine density values along 20-dendritic segments in the two groups (Pin1+/+ black line, Pin1-/- grey line) (*P*= 0,003 KS–test, n=5 mice for each genotype; 8 to 9 segments for each mouse. (**D**, **E**) Cumulative probability plots for head width of mushroom (D) and thin (E) spines along apical CA1 dendrites in Pin+/+ (black line) and Pin-/- mice (grey line). **P*<0.05 Kolmogorov–Smirnov (KS) test. n=5 mice for each genotype; 1016 spines. (**F**) Example of hippocampal neurons from Pin1+/+ and Pin1-/- immunolabeled for endogenous PSD-95 (red), GluN1 (green) and vGlut1 (blu). On the right distribution histograms of the % of clusters co-labeled with PSD-95, GluN1 and VGLUT1. Scale bar, 5 m. The number of hippocampal neurons investigated in each experiment (three independent experiments) were as follows: n=10 for Pin+/+, n=13 for Pin1-/-.** *P*=0.00057.

As compared to control, neurons from Pin1-/- mice showed a significant increase in spines density along *stratum radiatum* apical dendrites (Fig 5B; One-way ANOVA F1,46=4,30, *P*=0.043), leading to a rightward shift of the cumulative distribution curve of spine density per dendritic segment as compared to Pin1+/+ mice (Fig 5C, *P* = 0.003; KS test). A significantly larger proportion of mushroom spines was observed in Pin1-/- as demonstrated by the respective cumulative frequency plots (Fig 5D, *P* = 0.001; KS test) while the proportion of thin spines did not significantly differ (Fig 5E; left panel; *P* = 0.142; KS test). To evaluate whether the increased spines density in Pin1-/- neurons is associated with an enhanced recruitment of NMDA-Rs clusters at synapses, immunocytochemical experiments were performed on

cultured hippocampal neurons co-labeled for PSD-95, GluN1 and VGLUT1, a presynaptic marker of glutamatergic innervation. As shown in Figure 5F, a significant increase in the number of GluN1 co-localized with PSD-95 and juxtaposed to VGLUT1 clusters was detected in Pin1-/- mice respect to controls (63.1±6.5% and 41.2±5.4%, Pin1+/+ and Pin1-/- neurons, respectively, *P*=0.00057). Altogether, these data suggest that Pin1 negatively regulates the number of spines and NMDA-Rs recruitment at excitatory synapses.

Discussion

Here we provide evidence that PSD-95 represents a newly identified target of Pin1-dependent signaling cascade. This scaffold molecule becomes competent to recruit the rotamase upon phosphorylation at specific consensus motifs localized just before the third PDZ domain. Pin1 activity impacts on the ability of PSD-95 to interact with NMDA-Rs. In particular, Pin1 negatively influences PSD-95/GluN2B complex formation, an effect associated with a decrease in spine density and NMDA-R-mediated synaptic transmission.

It is well established that PSD-95 exerts a tight control on post-synaptic maturation and synaptic transmission (El-Husseini et al., 2000; Elias et al., 2006) and its regulated phosphorylation represents one of the key mechanism controlling synaptic targeting and clustering. Phosphorylation can either facilitate PSD-95 delivery to the synapse *via* association with motor protein complexes or increase its stability at synapses *via* interaction with other PSD components, including NMDA-Rs. PSD-95 is a recognized target of proline-directed phosphorylation: while cyclin-dependent kinase 5 (Cdk5) phosphorylates Thr19/Pro and Ser25/Pro N-terminal motifs leading to a down-regulation of PSD-95 and NMDA-Rs at synapses (Morabito et al., 2004), JKN1 heavily modify Ser295/Pro site, thus promoting PSD-95 synaptic targeting (Kim et al., 2007). Interestingly, all these phosphorylated forms of PSD-95 are enriched at postsynaptic densities, underlying the importance of this mechanism in controlling the amount of synaptic PSD-95.

Overall, PSD-95 possesses six potential Pin1 consensus motifs clustered at the N-terminus and at the linker region connecting PDZ2 to PDZ3. Our study points to the second cluster for the phosphorylation-dependent recruitment of Pin1 by PSD-95. Indeed, only the removal of the domain encompassing Ser287 to Ser295, or the sequential disruption of each Pin1 consensus motif here located, drastically abolished Pin1/PSD-95 interaction. The N-terminal deletion mutant was instead completely ineffective either alone or in conjunction with the linker deletion mutant. The close proximity of these sites to PDZ domains known to be involved in GluN2A/B and NL1 interactions raises the possibility that a conformational shift in this region affects the PDZ binding affinity for the corresponding interactors. Our data demonstratethat Pin1-driven conformational rearrangements mainly impacts on PDZ2, the domain involved in NMDA-R recruitment. In co-immunoprecipitation experiments from

hippocampus and brain extracts, we consistently detected an enhanced GluN2B/PSD-95 complex formation in the absence of Pin1 expression while PSD-95/NL1 interaction was quantitatively similar in both genotypes. We also found an overall increase in the amount of GluN2B and GluN1 receptor subunits in synaptosomal preparations derived from Pin1-/- hippocampal tissues as compared to Pin1+/+, further emphasizing the role of Pin1 as negative modulators of PSD-95/NMDA-R interaction. Unexpectedly, PSD-95 total protein levels did not parallel the NMDA-Rs increase. A plausible interpretation of this apparent discrepancy may rely on the fact that PSD-95 at synapses is present in large excess as compared to glutamate receptors (Chen et al., 2005). Therefore, just by increasing the fraction of PSD-95 undergoing proly-isomerization can render PSD-95 based scaffold more efficient in trapping NMDA-Rs at post-synapses. These results were validated by immunocytochemical experiments, where a higher number of synaptic PSD-95/GluN1 co-labeled clusters was detected in Pin1-/- neurons. In addition electrophysiological data demonstrated an enhanced NMDA-R-mediated synaptic transmission in the absence of Pin1 expression. Notably, a similar increase in NMDA-R mediated currents was uncovered upon ectopic expression of GFP-PSD-95 mutant unable to undergo prolyl-isomerization, indicating that Pin1 action on PSD-95 represent a key event in boosting its ability to trap NMDA-Rs at synapses. We can exclude that modifications in NMDA-R subunits composition (Monyer et al., 1991) contribute to the observed effect since no significant changes in the kinetics of NMDA-mediated synaptic responses or in the ifenprodil-induced depression of synaptic currents emerged between two genotypes.

In line with these results, a higher amount of dendritic spines was unveiled in Golgi stained pyramidal neurons lacking Pin1 expression. It is interesting to note that the observed increase in spine density in Pin1-/- mice is due to a selective gain in mushroom spines, being thin spines content similar in both genotypes. Thin spines are regarded as transient, learning spines, highly dynamic and plastic, that can rapidly form or disappear in response to different levels of synaptic activity (Sala and Segal, 2014). Mushroom spines, instead, are more stable structures, characterized by larger PSDs, accommodating a higher number of glutamate receptors as well as organelles required to sustain local protein synthesis (Hering and Sheng, 2001). It worth noting that the conversion of "learning spines" into "memory spines" (Bourne and Harris, 2007) strengthens activity-dependent synaptic plasticity processes such as long-

term potentiation, a phenomenon known to be controlled by Pin1 activity (Westmark et al., 2010). Indeed, Pin1 has emerged to negatively regulate the induction of dendritic translation required for late LTP maintenance. By combining those evidences with our data it is tempting to speculate that Pin1 may affect plasticity not only by regulating *de novo* protein synthesis necessary to express it, but also by determining the amount of NMDA-Rs initiating plasticity, *via* PSD-95 prolyl-isomerization.

In conclusion, Pin1 has clearly emerged as key regulator of synaptic transmission. Previous studies identified gephyrin, the core scaffold at GABAergic synapses, and NL2 as the functional transducers of this post-translational mechanism to achieve changes in inhibitory transmission (Zita et al., 2007; Antonelli et al., 2014). The uncovered function of Pin1 as modulator of PSD-95/NMDA-R interaction not only strengthen its pivotal contribution in modulating synaptic signaling but also assign to Pin1 a role in the cross-talk between excitatory and inhibitory transmission, which is of fundamental importance to modulate network activity.

References

Antonelli R, Pizzarelli R, Pedroni A, Fritschy JM, Del Sal G, Cherubini E, Zacchi P (2014) Pin1-dependent signalling negatively affects GABAergic transmission by modulating neuroligin2/gephyrin interaction. Nat Commun. 5:5066

Bourne J and Harris KM (2007) Do thin spines learn to be mushroom spines that remember? Current Opinion in Neurobiology 2007, 17:1–6.

Chen X, Vinade L, Leapman RD, Petersen JD, Nakagawa T, Phillips TM, Sheng M, Reese TS (2005) Mass of the postsynaptic density and enumeration of three key molecules. Proc Natl Acad Sci USA. 102:11551–11556.

Craven SE, El-Husseini AE, Bredt DS (1999) Synaptic targeting of the postsynaptic density protein PSD-95 mediated by lipid and protein motifs. Neuron 22:497–509.

Davis FM, Tsao TY, Fowler SK, Rao PN (1983) Monoclonal antibodies to mitotic cells. Proc Natl Acad Sci USA 80: 2926–293

Du CP, Gao J, Tai JM, Liu Y, Qi J, Wang W, Hou XY (2009) Increased tyrosine phosphorylation of PSD-95 by Src family kinases after brain ischaemia. Biochem J. 417:277-285.

El-Husseini AE, Schnell E, Chetkovich DM, Nicoll RA, Bredt DS (2000) PSD-95 involvement in maturation of excitatory synapses. Science 290:1364-8.

Elias GM, Funke L, Stein V, Grant SG, Bredt DS, Nicoll R (2006) Synapse-specific and developmentally regulated targeting of AMPA receptors by a family of MAGUK scaffolding proteins. Neuron 52, 307–320

Elias GM, Nicoll RA (2007) Synaptic trafficking of glutamate receptors by MAGUK scaffolding proteins. Trends Cell Biol. 17:343-52

Gardoni F, Polli F, Cattabeni F, Di Luca M (2006) Calcium–calmodulin-dependent protein kinase II phosphorylation modulates PSD-95 binding to NMDA receptors. European Journal of Neuroscience, 24:2694–2704.

Gasparini S, Saviane C, Voronin LL, Cherubini E (2000) Silent synapses in the developing hippocampus: Lack of functional AMPA receptors or low probability of glutamate release. PNAS 97:9741-9746.

Gibb R and Kolb B(1998) A method for vibratome sectioning of Golgi-Cox stained whole rat brain. J Neurosci Methods. 79:1-4.

Hering H and Sheng M (2001) Dentritic spines: structure, dynamics and regulation. Nature Reviews Neuroscience 2, 880-888.

Irie M, Hata Y, Takeuchi M, Ichtchenko K, Toyoda A, Hirao K, Takai Y, Rosahl TW, Südhof TC (1997) Binding of neuroligins to PSD-95. Science 27:1511-1515

Kim E and Sheng M (2004) PDZ domain proteins of synapses. Nature Reviews Neuroscience 5:771-781

Kim MJ, Futai K, Jo J, Hayashi Y, Cho K, Sheng M (2007) Synaptic accumulation of PSD-95 and synaptic function regulated by phosphorylation of serine-295 of PSD-95. Neuron 56:488-502.

Kornau HC, Schenker LT, Kennedy MB, Seeburg PH (1995) Domain interaction between NMDA receptor subunits and the postsynaptic density protein PSD-95. Science 269:1737–1740

Lamprecht R and LeDoux J. (2004) Structural plasticity and memory. Nat Rev Neurosci. 5:45-54

Liou YC, Zhou XZ, Lu KP (2011) Prolyl isomerase Pin1 as a molecular switch to determine the fate of phosphoproteins. Trends Biochem Sci. 36:501-514.

Lu PJ, Zhou XZ, Shen M, Lu KP (1999) Function of WW domains as phosphoserine- or phosphothreonine-binding modules. Science 283: 1325–1328

Lu KP and Zhou XZ (2007) The prolyl isomerase PIN1: a pivotal new twist in phosphorylation signaling and disease. Nature Reviews Molecular Cell Biology 8:904-916.

Middei S, Spalloni A, Longone P, Pittenger C, O'Mara SM, Marie H, Ammassari-Teule M (2012) CREB selectively controls learning-induced structural remodeling of neurons. Learn Mem. 19:330-336

Monyer H, Seeburg PH, Wisden W (1991) Glutamate-operated channels: developmentally early and mature forms arise by alternative splicing. Neuron. 1991; 6: 799–810.

Morabito MA, Sheng M, Tsai LH (2004) Cyclin-Dependent Kinase 5 phosphorylates the N-terminal domain of the Postsynaptic Density Protein PSD-95 in neurons J Neurosci. 24:865–876 -865.

Niethammer M, Kim E, Sheng M (1996) Interaction between the C terminus of NMDA receptor subunits and multiple members of the PSD-95 family of membrane-associated guanylate kinases. J Neurosci. 16:2157-2163

Opazo P, Sainlos M, Choquet D (2012) Regulation of AMPA receptor surface diffusion by PSD-95 slots. Curr Opin Neurobiol. 22:453-60.

Paoletti P, Bellone C, Zhou Q (2013). NMDA receptor subunit diversity: impact on receptor properties, synaptic plasticity and disease. Nat Rev Neurosci. 14:383-400

Poulopoulos A, Aramuni G, Meyer G, Soykan T, Hoon M, Papadopoulos T, Zhang M, Paarmann I, Fuchs C, Harvey K, Jedlicka P, Schwarzacher SW, Betz H, Harvey RJ, Brose N, Zhang W, Varoqueaux F (2009) Neuroligin2 drives postsynaptic assembly at perisomatic inhibitory synapses through gephyrin and collybistin. Neuron 63:628-642

Prybylowski K, Fu Z, Losi G, Hawkins LM, Luo J, Chang K, Wenthold RJ, Vicini S (2002) Relationship between availability of NMDA receptor subunits and their expression at the synapse. J Neurosci.22:8902–8910

Rao A, Kim E, Sheng M, Craig AM (1998) Heterogeneity in the molecular composition of excitatory postsynaptic sites during development of hippocampal neurons in culture. The Journal of Neuroscience 18:1217–1229.

Rao VR and Finkbeiner S (2007) NMDA and AMPA receptors: old channels, new tricks. Trends Neurosci. 30:284-291.

Sala C and Segal M (2014) Dendritic spines: the locus of structural and functional plasticity. Physiol Rev. 94:141-188.

Vicini S, Wang JF, Li JH, Zhu WJ, Wang YH, Luo JH, Wolfe BB, Grayson DR. (1998) Functional and pharmacological differences between recombinant N-methyl-D-aspartate receptors. J Neurophysiol. 79:555-566.

Vithlani M, Terunuma M, Moss SJ. (2011) The Dynamic Modulation of GABAA Receptor Trafficking and Its Role in Regulating the Plasticity of Inhibitory Synapses. Physiological Reviews 3:1009-1022.

Westmark PR, Westmark CJ, Wang S, Levenson J, O'Riordan KJ, Burger C, Malter JS. (2010) Pin1 and PKMzeta sequentially control dendritic protein synthesis. Sci Signal. 3:ra18.

Williams K (1993) Ifenprodil discriminates subtypes of the N-methyl-D-aspartate receptor: selectivity and mechanisms at recombinant heteromeric receptors. Mol Pharmacol. 44:851-859.

Xu W (2011) PSD-95-like membrane associated guanylate kinases (PSD-MAGUKs) and Synaptic Plasticity. Curr Opin Neurobiol. 21: 306–312

Zacchi P, Gostissa M, Uchida T, Salvagno C, Avolio F, Volinia S, Ronai Z, Blandino G, Schneider C, Del Sal G (2002) The prolyl isomerase Pin1 reveals a mechanism to control p53 functions after genotoxic insults. Nature 419:853-857

Zita MM, Marchionni I, Bottos E, Righi M, Del Sal G, Cherubini E, Zacchi P (2007) Post-phosphorylation prolyl isomerisation of gephyrin represents a mechanism to modulate glycine receptors function. EMBO J. 26, 1761–1771

5. CONCLUSIONS AND FUTURE PROSPECTIVES

In this thesis I have investigated the impact of proline-directed phosphorylation signaling cascade on the remodeling of the post-synaptic device at both GABAergic and glutamaterigc synapses.

Impact of Pin1 on GABAergic synapses

At inhibitory synapses I focused on the cell adhesion molecule NL2, given its emerging role as central organizer of inhibitory synapses. Several experimental evidences support this notion:
i. the ectopic expression of NL2 together with the different GABAAR subunits in transfected HEK293 cells is sufficient to allow the detection of spontaneous and action potential-evoked synaptic events, sign of reconstitution of functional GABAergic synapses in non-neuronal cells (Dong et al., 2007); ii. the NL2 knock-out mouse is characterized by a strong and selective deficit in both GABAergic and glycinergic neurotransmission in several brain areas, including the brainstem and the retina (Chubykin et al., 2007; Poulopoulos et al., 2009; Hoon et al., 2009); iii. these deficits are usually accompanied by a reduced neurotransmitter receptors clustering and gephyrin recruitment, underlying the key role played by NL2 in organizing inhibitory synapses.
If NL2 is so fundamental for inhibitory synapse assembly and function, any signaling able to modulate its ability to interact with its postsynaptic partners is expected to strongly impact on the organization of the synapse and therefore the strength of inhibitory transmission.
I decided to investigate the involvement of proline-directed phosphorylation on NL2 functions since this protein possess, in its cytoplasmic domain, the consensus motifs able to recruit, once phosphorylated, the effector molecule of the signaling cascade, the prolyl-isomerase Pin1. NL2 is provided by a unique Pin1 consensus site, serine 714 proline, located very close to the transmembrane domain. I was able to demonstrate that this site is phosphorylated in vivo and it can recruit the prolyl-isomerase Pin1. Pin1 action on NL2 manifests in negatively modulating its ability to interact with the gephyrin scaffold at postsynapses. Thus, under conditions of pharmacological inhibition of Pin1 catalytic activity or in its absence (Pin1 knock-out mice), I could detect an increase in NL2/gephyrin complex formation.

The functional consequences of the above-mentioned events were an increased enrichment of NL2, gephyrin and GABAARs at inhibitory synapses, as assessed by immunohistochemistry and quantitative western blot analysis on synapotosomal fractions derived from Pin1-/- mice. In agreement with these data, electrophysiological experiments demonstrated an increase in amplitude, but not in frequency, of inhibitory post synaptic currents in the CA1 hippocampal region in slices obtained from Pin1-/- mice, indicating an increase number of postsynaptic GABAARs in the absence of Pin1. Interestingly a similar result was obtained upon over-expression, in cultured hippocampal neurons, of a NL2 point mutant unable to undergo prolyl-isomerization, emphasizing the key role played by NL2 proline-directed phosphorylation in modulating GABAergic transmission.

The possibility that the action of Pin1 on gephyrin, an already recognized target of the signaling cascade under investigation, participates in controlling the strength of NL2/gephyrin interaction cannot be excluded. Gephyrin possesses ten putative Pin1 consensus sites in its sequence and three of them, localized in the Proline rich region, have been shown to be involved in modulating gephyrin's ability to interact with the beta subunit of glycine receptors (Zita et al., 2007). In the present experiments, I have just excluded the contribution of Serine270-Proline and Serine319-Proline motifs, which are located in proximity or within the newly identified minimal NL2 binding module on gephyrin, respectively. This is based on the fact that the corresponding serine to alanine variants, which make them unable to undergo prolyl-isomerization, did not show any increased capacity to interact with NL2 in co-immunoprecipitation experiments nor to sequester endogenous NL2 upon over-expression in cultured hippocampal neurons. It is worth mentioning that GABA and glycine binding overlap on gephyrin. Therefore, it is possible to assume that Pin1-mediated actions on gephyrin may have similar effects on GABAergic clustering (Zita et al., 2007)It remains to be evaluated the contribution of the remaining gephyrin consensus sites, following similar experimental settings.

In addition, the mechanistic details explaining how Pin1 prevents NL2 binding to gephyrin are still unknown. One possibility is that Pin1, by altering the folding of the NL2 cytoplasmic domain, destabilizes the NL2/gephyrin interaction. Alternatively, Pin1, by acting on Ser-714 may induce a conformational change of the NL2 tail, thus facilitating phosphorylation at specific Tyrosine residue (Tyrosine 770), embedded in the gephyrin-binding domain. This is

expected to uncouple NL2-gephyrin interaction. This mechanism has been recently identified at excitatory synapses, where the corresponding tyrosine residue on NL1, upon neurexin-induced phosphorylation, precludes gephyrin recruitment while favoring PSD-95 binding (Giannone et al., 2013). Even though no evidence has been provided that NL2 can undergo tyrosine phosphorylation in vivo, tyrosine to alanine mutation at this site is sufficient to completely abolish NL2/gephyrin interaction, similarly to NL-1Y770A point mutant (Poulopoulos et al., 2009). In future experiments, to explore this possibility, we are planning to perform phospho-tyrosine (pTyr) immunoblots on immunoprecipitated NL2-HA and on endogenous NL2 derived from Pin1+/+ and Pin1-/- neuronal tissues.

It is worth noticing that the molecular mechanism controlling GABAARs recruitment on NL2 prolyl-isomerization are still unknown. At glutamatergic synapses, Budreck and colleagues (2013) demonstrated that NL1 controls the density of postsynaptic NMDARs via an interaction with specific sequences between the extracellular domain of NL1 and the GluN1 subunit of NMDAR. If a similar mechanism takes place also at GABAergic synapses, it should be hypothesized that Pin1-dependent conformational changes, occurring very close to the NL2 transmembrane domain, are able to influence the folding of NL2 extracellular domain, thus modulating its capacity to interact in cis with GABAAR subunits. To explore this option, I plan to test whether NL2 can directly interact with any of the subunits of GABAAR. This can initially be explored by performing co-immunoprecipitation experiments on ectopically expressed NL2 and GABAARs subunits and consequentially should be performed on brain tissues derived from Pin 1 wt and ko mouse genotypes to evaluated the impact of Nl2 isomerization on Nl2/GABAARs subunits interaction.

In an alternative scenario, the observed quantitative changes in postsynaptic GABAARs density observed in the absence of Pin1, could simply depend on the amount of gephyrin recruited by NL2, which is indeed modulated by NL2 prolyl-isomerization. It has been extensively demonstrated that changes in gephyrin deposition at post synapses produce parallel changes in the number of receptors trapped by the scaffold, leading to corresponding alterations in the strength of synaptic transmission.

The rate of receptor trapping is influenced by the affinity of gephyrin for inhibitory neurotransmitter receptors (Fritschy et al., 2008). Since Pin1 action on gephyrin has been shown to modulate its binding affinity for GlyR (Zita et al. 2007), and the binding site for GABAARs overlap the binding site for GlyR, I should explore whether this type of modulation

occurs also at GABAARs. Recently, synaptic GABAARs have been shown to directly interact with gephyrin and interaction sites have been identified and mapped within the intracellular loops of the GABAAR α1, α2, α3 and β2, β3, respectively (Tretter et al., 2008; Saiepour et al., 2010; Tretter et al., 2011, Kowalczyk et al., 2013). Interestingly, Pin1 activity on gephyrin could also affect its clustering properties. Most of the Pin1 consensus motifs on gephyrin are concentrated in the C-domain, which is positioned between the highly conserved G- and E domains directly involved in gephyrin multimerization.

Impact of Pin1 on glutamatergic synapses

At glutamatergic synapses, Westmark and coworkers (2010) have demonstrated the presence of Pin1 in dendritic spines and shafts where it exerts a key role in suppressing protein synthesis required to sustain the late phase of long-term potentiation.

I turned my interest on scaffolding molecules of the MAGUK family, in particular PSD-95, for several reasons. PSD-95 represents the functional homologue of gephyrin at excitatory synaptic contacts. Due to its central role in organizing and trapping ionotropic glutamate receptors, PSD-95 regulates NMDAR-dependent plasticity at several levels: i. PSD-95 is itself a recognized target of phosphorylation (and palmitoylation) signaling, and these post-traslational modifications have been shown to influence its synaptic abundance and consequentially the levels of synaptic AMPAR on the postsynaptic membrane surface (Kim et al., 2007; Nelson et al., 2013); ii. PSD-95, as a signaling scaffold, can recruit intracellular signaling complexes close to NMDAR channels, coupling calcium influx to specific downstream signaling events (Sheng 2001). All these features render PSD-95 an attractive candidate for being regulated by post-phosphorylation prolyl-isomerization.

I showed that PSD-95 interacts with Pin1 in a phosphorylation-dependent manner and this recruitment occurs at three specific consensus sites localized between the second and third PDZ domains. Pin1-driven structural rearrangement at this locus indeed impacted on the ability of PSD-95 to interact with the NMDAR, mediated by PDZ1 and PDZ2, while the binding of PSD-95 to interact with NL1, mediated by PDZ3, was unaffected. At excitatory connections, Pin1 emerged as a negative modulator of the interaction between the scaffold and the receptor, leading, in the absence of Pin1, to an enhanced content of PSD-95/NMDA complexes at post-synaptic sites.

In agreement with biochemical data, electrophysiological recordings from CA1 principal cells in acute hippocampal slices obtained from Pin1-/- mice unveiled, in comparison to controls, larger NMDA-mediated synaptic currents. Larger NMDA-mediated synaptic currents could be recorded also from cultured hippocampal neurons, over-expressing a PSD-95 mutant unable to recruit Pin1, indicating that Pin1-dependent signaling exerts a control on the synaptic content of NMDA-Rs via PSD-95 prolyl-isomerization. In this way, Pin1 could affect synaptic plasticity processes not only by regulating de novo protein synthesis necessary for the maintenance of LTP, but also by determining the amount of postsynaptic NMDA-Rs and associated signaling pathways necessary for LTP induction.

Based on our biochemical mapping, Pin1 is recruited at three consensus sites, namely Thr287-proline, Ser290-proline and Ser295-proline, but nothing is known about the endogenous level of phosphorylation of these residues. This aspect should be carefully addressed by using phospho-specific antibodies on immunoprecipitated PSD-95 and by performing quantitative western blot analysis on synaptoneurosomes derived from both mouse genotypes.

Since NMDAR clustering and stability at post-synapses depend on the amount of PSD-95 here localized and stabilized via palmitoylation and self-assembly, it will be interesting to know whether Pin1 may affect PSD-95 multimerization. This possibility can be addressed by performing co-immunoprecipitation experiments using PSD-95 constructs of different size (given by a different epitope tags: PSD-95 FLAG and PSD-95 GFP). To test the influence that Pin1 might exerts on this interaction we have generated, in collaboration with Dr. Del Sal (LNCIB, Area Science Park, Trieste), immortalized mouse embryo fibroblasts derived from Pin1+/+ and Pin1-/- littermates to use as recipient cell lines.

As already mentioned, in basic conditions, Pin1 exerts a negative regulation on the NMDAR content at postsynaptic sites. However, it is still unclear whether this effect involves a reduction of the interaction PSD-95/NMDAR and /or an acceleration of NMDAR turnover. To address this issue I plan to combine surface thrombin cleavage and immunocytochemistry assays as designed by Lavezzari and colleagues (2004).

It would also be interesting to elucidate whether in the CA1 region of the hippocampus Pin1 alters, via PSD-95/NMDAR, not only LTP maintenance (Westmark et al., 2010) but also LTP induction. In our experiments, the observation that, under basal physiological conditions, Pin1 signaling affects only NMDAR- and not AMPAR-mediated synaptic currents, suggest a

clear postsynaptic type of action and allows excluding a concomitant change in the probability of glutamate release that should have altered synaptic events mediated by both receptor subtypes. However, whether this occurs during activity-dependent plasticity processes (i.e. LTP or LTD) cannot be excluded. Hence, Pin1 may affect NMDA-dependent insertion (LTP) or removal (LTD) of AMPA receptors into or from the postsynaptic membrane, respectively, an effect that could be associated to changes in the probability of glutamate release and/or glutamatergic innervation. This could be assessed by examining, in immunocytochemical experiments (performed on both mouse genotypes), changes in AMPAR and NMDAR clusters associated with LTP or LTD. In addition, a careful quantal analysis of spontaneous and evoked AMPA-mediated postsynaptic currents (recorded in different extracellular calcium concentration) would allow examining whether possible activity-dependent changes in postsynaptic receptors density are associated to modification in the probability of glutamate release and/or in the number of releases sites. Behavioral tests will permit to explore, in Pin1+/+ and Pin1-/- mice, whether LTP or LTD are accompanied by modifications in spatial memory, contextual fear memory, and social behavior.

Post-phosphorylation prolyl-isomerization signaling cascade has been extensively studied in proliferating cells and in the field of cancer, while most studies addressing the role of Pin1 in a neuronal context have focused on unraveling its contribution to the pathogenesis of Alzheimer's disease and other tauopathies, where spurious cell-cycle events are observed. The work I performed assigns to Pin1 a novel role as key modulator of synaptic transmission at both inhibitory and excitatory system.

6. REFERENCES

Akert K., Pfenninger K., Sandri C. and MoorH. (1972) Freeze-etching and the cytochemistry ofvesicles and membrane complexes in synapses of the central nervous system. In: Structure and Function of Synapses Pappas, pp. 67–86.

Arancibia-Cárcamo I.L., Kittler J.T (2009) Regulation of GABA(A) receptor membrane trafficking and synaptic localization. Pharmacol Ther.; 123:17-31.

Ascher P. and Nowak L. (1988) The role of divalent cations in the N-methylD-aspartate responses of mouse central neurones in culture. J Physiol.; 399:247–266.

Atchison F.W., Capel B., Means A.R. (2003) Pin1 regulates the timing of mammalian primordial germ cell proliferation. Development; 130: 3579–3586.

Banke T.G., Bowie D., Lee H., Huganir R.L., Schousboe A., Traynelis S.F. (2000) Control of GluR1 AMPA receptor function by cAMP-Dependent protein kinase. J. Neurosci.; 20: 89-102.

Bard L. and Groc L. (2011) Glutamate receptor dynamics and protein interaction: lessons from the NMDA receptor. Mol. Cell Neurosci.; 48:298-307.

Bassand P., Bernard A., Rafiki A., Gayet D., Khrestchatisky M. (1999) Differential interaction of the tSXV motifs of the NR1 and NR2A NMDA receptor subunits with PSD-95 and SAP97. Eur. J. Neurosci.; 11:2031-43.

Bausen M., Fuhrmann J.C, Betz H., O'sullivan G.A. (2006) The state of the actin cytoskeleton determines its association with gephyrin: role of ena/VASP family members. Mol. Cell Neurosci.; 31:376-386.

Bedford F.K., Kittler J.T, Muller E., Thomas P., Uren J.M., Merlo D., Wisden W.,Triller A., Smart T.G., Moss S.J, (2001) GABA(A) receptor cell surface number and subunit stability are regulated by the ubiquitin-like protein Plic-1. Nat Neurosc.; 4:908-916.

Behrsin C.D., Bailey M.L., Bateman K.S., Hamilton K.S., Wahl L.M., Brandl C.J. (2007) Functionally important residues in the peptidyl-prolyl isomerase Pin1 revealed by unigenic evolution. J. Mol. Biol.; 365:1143–1162.

Biederer T., Südhof T.C. Mints as adaptors. (2000) Direct binding to neurexins and recruitment of munc18. J. Biol. Chem.; 275:39803-39806.

Blume-Jensen P., Hunter T. (2001) Oncogenic kinase signalling. Nature; 411: 355–365.

Bolliger M.F., Frei K., Winterhalter K.H., Gloor S.M. (2001) Identification of a novel neuroligin in humans which binds to PSD-95 and has a widespread expression. Biochem. J.; 356:581-8.

Boucard A.A, Chubykin A.A, Comoletti D., Taylor P., Südhof T.C. (2005) A splice code for trans-synaptic cell adhesion mediated by binding of neuroligin1 to alpha- and beta-neurexins Neuron; 48:229-36.

Branco T. and Staras K. (2009) The probability of neurotransmitter release: variability and feedback control at single synapses. Nature Reviews Neuroscience; 10:373-383.

Brandon N.J., Delmas P., Kittler J.T., McDonald B.J., Sieghart W., Brown D.A., Smart T.G., Moss S.J. (2000) $GABA_A$ receptor phosphorylation and functional modulation in cortical neurons by a protein kinase C-dependent pathway. J. Biol. Chem.; 275:38856–38862.

Brandon N.J., Jovanovic J.N., Moss S.J. (2002) Multiple roles of protein kinases in the modulation of GABA(A) receptor function and cell surface expression. Pharmacol Ther.; 94:113–122.

Budreck E.C., Scheiffele P. (2007) Neuroligin-3 is a neuronal adhesion protein at GABAergic and glutamatergic synapses. Eur. J. Neurosci.; 26:1738-48.

Burnashev N., Khodorova A., Jonas P., Helm P.J., Wisden W., Monyer H., Seeburg P.H., Sakmann B. (1992) Calcium permeable AMPA-kainate receptors in fusiform cerebellar glial cells. Science; 256:1566–1570.

Burnashev N., Zhou Z., Neher E., Sakmann B. (1995) Fractional calcium currents through recombinant GluR channels of the NMDA, AMPA and kainate receptor subtypes. J. Physiol., 485:403–418.

Carlin R.K., Grab D.J., Cohen R.S., Siekevitz P. (1980) Isolation and characterization of postsynaptic densities from various brain regions: enrichment of different types of postsynaptic densities. J. Cell. Biol.; 86:831-45.

Carmignoto G., Vicini S. (1992) Activity-dependent decrease in NMDA receptor responses during development of the visual cortex. Science; 258:1007–1011.

Carvalho A.L., Kameyama K., Huganir R.L. (1999) Characterization of phosphorylation sites on the glutamate receptor 4 subunit of the AMPA receptors. J. Neurosci.; 19:4748-54.

Chen L., Chetkovich D.M., Petralia R.S., Sweeney N.T., Kawasaki Y., Wenthold R.J., Bredt D.S., Nicoll R.A. (2000) Stargazin regulates synaptic targeting of AMPA receptors by two distinct mechanisms. Nature; 408:936-43.

Chen P.D., Wyllie D.J. (2006). Pharmacological insights obtained from structure-function studies of ionotropic glutamate receptors. Br. J. Pharmacol.; 147: 839–853.

Chetkovich D.M., Chen L., Stocker T.J., Nicoll R.A., Bredt D.S. (2002) Phosphorylation of the Postsynaptic Density-95 (PSD-95)/Discs Large/Zona Occludens-1 Binding Site of Stargazin Regulates Binding to PSD-95 and Synaptic Targeting of AMPA Receptors. J. Neurosci.; 22:5791–5796.

Chih B., Engelman H., Scheiffele P. (2005) Control of excitatory and inhibitory synapse formation by neuroligins. Science; 307:1324–1328.

Chubykin A.A., Atasoy D., Etherton M.R., Brose N., Kavalali E.T., Gibson, J.R., Südhof T.C. (2007) Activity-dependent validation of excitatory versus inhibitory synapses by neuroligin-1 versus neuroligin-2. Neuron; 54:919-931.

Chung H.J., Huang Y.H., Lau L.F., Huganir R.L. (2004) Regulation of the NMDA receptor complex and trafficking by activity-dependent phosphorylation of the NR2B subunit PDZ ligand. J. Neurosci.; 24:10248–10259.

Colonnier M. (1968) Synaptic patterns on different cell types in the different laminae of the cat visual cortex. An electron microscope study. Brain Res.; 9 (268-287).

Comenencia-Ortiz E., Moss S.J., Davies P.A. (2014) Phosphorylation of $GABA_A$ receptors influences receptor trafficking and neurosteroid actions. Psychopharmacology; 231:3453–3465.

Connolly C.N., Wafford K.A. (2004) The Cys-loop superfamily of ligand-gated ion channels: the impact of receptor structure on function. Biochemical Society transactions; 32:529–34.

Cousins S.L and Stephenson F.A. (2012) Identification of N-methyl-D-aspartic acid (NMDA) receptor subtype-specific binding sites that mediate direct interactions with scaffold protein PSD-95. J. Biol. Chem.; 287:13465-76.

Cousins S.L., Kenny A.V., Stephenson F.A. (2009) Delineation of additional PSD-95 binding domains within NMDA receptor NR2 subunits reveals differences between NR2A/PSD-95 and NR2B/PSD-95 association. Neuroscience; 158:89-95.

Craig A.M. and Kang Y. (2007) Neurexin-neuroligin signaling in synapse development. Curr. Opin. Neurobiol.; 17:43-52.

Craven S.E., Bredt D.S. (1998) PDZ proteins organize synaptic signaling pathways. Cell; 93:495-498.

Craven S.E., El-Husseini A.E., Bredt D.S. (1999) Synaptic targeting of the postsynaptic density protein PSD-95 mediated by lipid and protein motifs. Neuron; 22:497–509.

Cull-Candy S.G., Leszkiewicz D.N. (2004) Role of distinct NMDA receptor subtypes at central synapses. Sci STKE.; 255:re16.

Dakoji S., Tomita S., Karimzadegan S., Nicoll R.A, Bredt D.S. (2003) Interaction of transmembrane AMPA receptor regulatory proteins with multiple membrane associated guanylate kinases. Neuropharmacology; 45:849-856.

Dalva M.B., McClelland A.C., Kayser M.S. (2007) Cell adhesion molecules: signalling functions at the synapse. Nat. Rev. Neurosci.; 8:206-20.

Dean C., Dresbach T. (2006) Neuroligins and neurexins: linking cell adhesion, synapse formation and cognitive function. Trends Neurosci.; 29:21-29.

Derkach V., Barria A., and Soderling T. (1999) Ca2+/calmodulin-kinase II enhances channel conductance of α-amino-3-hydroxy-5-methyl-4-isoxazolepropionate type glutamate receptors. Proc. Natl. Acad. Sci.; 96: 3269-3274.

Ehrensperger M., Hanus C., Vannier C., Triller A., Dahan M. (2007) Multiple association states between glycine receptors and gephyrin identified by SPT analysis. Biophys. J.; 92:3706-3718.

El-Husseini A.D., Bredt D.S. (2002) Protein palmitoylation: a regulator of neuronal development and function. Nat. Rev. Neurosci ; 3:791-802.

El-Husseini A.E., Craven S.E., Chetkovich D.M., Firestein B.L., Schnell E., Aoki C., Bredt D.S. (2000) Dual Palmitoylation of PSD-95 Mediates Its Vesiculotubular Sorting, Postsynaptic Targeting, and Ion Channel Clustering. Cell Biol.; 148: 159–172.

Erreger K., Chen P.E., Wyllie D.J., Traynelis S.F. (2004).Glutamate receptor gating. Crit Rev Neurobiol.; 16**:** 187–224.

Essrich C., Lorez M., Benson J. A., Fritschy J. M., Luscher B. (1998). Postsynaptic clustering of major $GABA_A$ receptor subtypes requires the gamma 2 subunit and gephyrin. Nat. Neurosci.; 1:563–571.

Feng W. and Zhang M. (2009) Organization and dynamics of PDZ-domain-related supramodules in the postsynaptic density. Nat. Rev. Neurosci.; 10:87-99.

Feng, G., Tintrup, H., Kirsch, J., Nichol, M. C., Kuhse, J., Betz, H., and Sanes, J. R. (1998). Dual requirement for gephyrin in glycine receptor clustering and molybdoenzyme activity. Science; 282:1321–1324.

Fiala J.C., Feinberg M., Popov V., Harris K. M. (1998) Synaptogenesis via dendritic filopodia in developing hippocampal area CA1. J. Neurosci.; 18:8900–8911.

Fischer F., Kneussel M., Tintrup H., Haverkamp S., Rauen T., Betz H., Wassle H. (2000). Reduced synaptic clustering of GABA and glycine receptors in the retina of the gephyrin null mutant mouse. J. Comp. Neurol.; 427:634–64810.

Fischer G., Aumuller T. (2003) Regulation of peptide bond *cis/trans* isomerization by enzyme catalysis and its implication in physiological processes. Rev. Physiol. Biochem. Pharmacol.; 148:105–5010.

Fischer M., Kaech S., Wagner U., Brinkhaus H., Matus A. (2000) Glutamate receptors regulate actin-based plasticity in dendritic spines. Nat. Neurosci.; 3:887-894.

Forsythe I.D., Westbrook G.L. (1988) Slow excitatory postsynaptic currents mediated by N-methyl-D-aspartate receptors on cultured mouse central neurons. J. Physiol.; 396:515-33.

Foster (1897) A text – Book of physiology 7^{th} edition part III The central nervous system . London

Fritschy J.M., Harvey R.J., Schwarz G. (2008) Gephyrin: where do we stand, where do we go? Trends Neurosci.; 31:257–264.

Fritschy J.M., Panzanelli P. (2014) $GABA_A$ receptors and plasticity of inhibitory neurotransmission in the central nervous system. Eur. J. Neurosci.; 39:1845-65.

Fuhrmann J.C., Kins S., Rostaing, P., El Far O., Kirsch J., Sheng M., Triller A., Betz H.,Kneussel M., (2002) Gephyrin interacts with Dynein light chains 1 and 2, components of motor protein complexes. J. Neurosci.; 22:5393-5402.

Gardner S.M., Takamiya K., Xia J., Suh J.G., Johnson R., Yu S., Huganir R.L. (2005) Calcium-permeable AMPA receptor plasticity is mediated by subunit-specific interactions with PICK1 and NSF. Neuron.; 45:903-15.

Gardoni F., Polli F., Cattabeni F., Di Luca M. (2006) Calcium–calmodulin-dependent protein kinase II phosphorylation modulates PSD-95 binding to NMDA receptors. Eur. J. Neurosci.; 24:2694–2704.

Garner C.C., Nash J., Huganir R.L. (2000) PDZ domains in synapse assembly and signaling, Trends in cell biology; 10:274-80.

Giannone G., Mondin M., Grillo-Bosch D., Tessier B., Saint-Michel E., Czöndör K., Sainlos M., Choquet D., Thoumine O. (2013) Neurexin-1β binding to neuroligin-1 triggers the preferential recruitment of PSD-95 versus gephyrin through tyrosine phosphorylation of neuroligin-1. Cell Rep.; 3(6).

Giesemann T., Schwarz G., Nawrotzki R., Berhörster K., Rothkegel M., Schlüter K., Schrader N., Schindelin H., Mendel R.R, Kirsch J., Jockusch B.M. (2003) Complex formation between the postsynaptic scaffolding protein gephyrin, profilin, and Mena: a possible link to the microfilament system. J. Neurosci.; 23:8330-8339.

Graf E.R., Zhang X., Jin S.X., Linhoff M.W., Craig A.M. (2004) Neurexins induce differentiation of GABA and glutamate postsynaptic specializations via neuroligins. Cell; 119:1013–1026.

Gray E.G. (1959) Axo-somatic and axo-dendritic synapses of the cerebral cortex: an electron microscope study. J. Anat.; 93:420–433.

Grison A., Mantovani F., Comel A., Agostoni E., Gustincich S., Persichetti F., Del Sal G.(2011) Ser46 phosphorylation and prolyl-isomerase Pin1-mediated isomerization of p53 are key events in p53-dependent apoptosis induced by mutant huntingtin. Proc. Natl. Acad. Sci. U. S. A. 108:17979-84.

Grutzendler J., Kasthuri N., Gan W. B. (2002). Long-term dendritic spine stability in the adult cortex. Nature; 420 812–816.

Hamdane M., Dourlen P., Bretteville A., Sambo A.V., Ferreira S., Ando K., Kerdraon O., Bégard S., Geay L., Lippens G., Sergeant N., Delacourte A., Maurage C.A., Galas M.C., Buée L. (2006) Pin1 allows for differential Tau dephosphorylation in neuronal cells. Mol. Cell Neurosci.; 32:155-60.

Hara K., Yonezawa K., Kozlowski M.T., Sugimoto T., Andrabi K., Weng Q.P., Kasuga M., Nishimoto I., Avruch J. (1997) Regulation of eIF-4E BP1 phosphorylation by mTOR. J. Biol. Chem. ; 272:26457-63.

Harris K.M. and Weinberg R. J. (2012) Ultrastructure of Synapses in the Mammalian Brain Cold Spring Harb Perspect Biol. 4(5).

Harvey K., Duguid I. C., Alldred M. J., Beatty S. E., Ward H., Keep N. H., Lingenfelter S. E., Pearce B. R., Lundgren J., Owen M. J., Smart T. G., Luscher B., Rees M. I., Harvey R. J. (2004) The GDP-GTP exchange factor collybistin: an essential determinant of neuronal gephyrin clustering. J. Neurosci. 24:5816-5826.

Hata Y., Butz S., Südhof T.C. (1996) CASK: a novel dlg/PSD95 homolog with an N-terminal calmodulin-dependent protein kinase domain identified by interaction with neurexins. J. Neurosci.; 16:2488-2494.

Herring D., Huang R., Singh M., Robinson L.C., Dillon G.H., Leidenheimer N.J. (2003) Constitutive $GABA_A$ receptor endocytosis is dynamin-mediated and dependent on a dileucine AP2 adaptin-binding motif within the beta 2 subunit of the receptor. J. Biol. Chem.; 278:24046-24052.

Herweg J. and Schwarz G. (2012) Splice-specific glycine receptor binding, folding and phosphorylation of the scaffolding protein gephyrin. J. Biol. Chem.; 287:12645–12656.

Hoffman R.C, Jennings L.L., Tsigelny I., Comoletti D., Flynn R.E., Sudhof T.C., Taylor P. (2004) Structural characterization of recombinant soluble rat neuroligin 1: mapping of secondary structure and glycosylation by mass spectrometry. Biochemistry; 43:1496-506.

Holtmaat A. J., Trachtenberg J. T., Wilbrecht L., Shepherd G. M., Zhang X., Knott G. W., et al. (2005) Transient and persistent dendritic spines in the neocortex in vivo. Neuron; 45:279–291.

Hoogenraad C.C., Milstein A.D., Ethell I.M., Henkemeyer M., Sheng M. (2005) GRIP1 controls dendrite morphogenesis by regulating EphB receptor trafficking. Nat. Neurosci.; 8:906-915.

Hoon M., Soykan T., Falkenburger B., Hammer M., Patrizi A., Schmidt K.F., Sassoè-Pognetto M., Löwel S., Moser T., Taschenberger H., Brose N., Varoqueaux F. (2011) Neuroligin-4 is localized to glycinergic postsynapses and regulates inhibition in the retina. Proc. Natl. Acad. Sci. U. S. A.; 108:3053-8.

Hrabetova S., Sacktor T.C. (1996) Bidirectional regulation of protein kinase M zeta in the maintenance of long-term potentiation and long-term depression. J. Neurosci; 16:5324-33.

Huang Z.J. and Scheiffele P. (2008) GABA and neuroligin signaling: linking synaptic activity and adhesion in inhibitory synapse development. Curr. Opin. Neurobiol.; 18:77-83.

Huettner J.E. (2003) Kainate receptors and synaptic transmission. Prog. Neurobiol.; 70:387-407.

Hyvonen M., Macias M. J., Nilges M., Oschkinat H., Saraste M., Wilmanns M. (1995) Structure of the binding site for inositol phosphates in a PH domain. EMBO J.; 14:4676–4685.

Ichtchenko K., Hata Y., Nguyen T., Ullrich B., Missler M., Moomaw C., Südhof T.C. (1995) Neuroligin 1: a splice site-specific ligand for beta-neurexins.; 81:435-443.

Ichtchenko K., Nguyen T., Südhof T.C. (1996) Structures, alternative splicing, and neurexin binding of multiple neuroligins. J. Biol. Chem.; 271:2676-2682.

Innes B.T., Bailey M.L., Brandl C.J, Shilton B.H., Litchfield D.W. (2013) Non-catalytic participation of the Pin1 peptidyl-prolyl isomerase domain in target binding. Front. Physiol.; 4:18.

Inoue A., Okabe S. (2003) The dynamic organization of postsynaptic proteins: translocating molecules regulate synaptic function. Curr. Opin. Neurobiol.; 13: 332–340.

Jacob T.C., Bogdanov Y.D., Magnus C., Saliba R.S., Kittler J.T., Haydon P.G., Moss S.J. (2005) Gephyrin regulates the cell surface dynamics of synaptic GABAA receptors. J. Neurosci.;25:10469-78.

Jacob T.C., Moss S.J., Jurd R. (2008) GABA(A) receptor trafficking and its role in the dynamic modulation of neuronal inhibition. Nat. Rev. Neurosci.; 9:331–343.

Jacob T.C., Wan Q., Vithlani M., Saliba R.S., Succol F., Pangalos M.N., Moss S.J. (2009) GABA(A) receptor membrane trafficking regulates spine maturity. Proc. Natl. Acad. Sci. U. S. A.; 106:12500-12505.

Jacobs D.M., Saxena K., Vogtherr M., Bernado P., Pons M., Fiebig K.M. (2003) Peptide binding induces large scale changes in inter-domain mobility in human Pin1. J. Biol. Chem.; 278:26174–26182.

Jaffe H., Vinade L., Dosemeci A. (2004) Identification of novel phosphorylation sites on postsynaptic density proteins. Biochem. Biophys. Res. Commun.; 321: 210–218.

Johnson J.W., Ascher P. (1987) Glycine potentiates the NMDA response in cultured mouse brain neurons. Nature; 325:529-31.

Jonas P., Burnashev N., (1995) Molecular mechanisms controlling calcium entry through AMPA-type glutamate receptor channels. Neuron ; 15:987-990.

Jordens J., Janssens V., Longin S., Stevens I., Martens E., Bultynck G., Engelborghs Y., Lescrinier E., Waelkens E., Goris J., Van Hoof C. (2006) The protein phosphatase 2A phosphatase activator is a novel peptidyl-prolyl cis/trans-isomerase. J. Biol. Chem.;281:6349-57.

Kalscheuer V.M., Musante L., Fang C., Hoffmann K., Fuchs C., Carta E., Deas E., Venkateswarlu K., Menzel C., Ullmann R., Tommerup N., Dalpra L., Tzschach A., Selicorni A., Luscher B., Ropers H. H., Harvey K., Harvey R.J. (2009) A balanced chromosomal translocation disrupting ARHGEF9 is associated with epilepsy, anxiety, aggression, and mental retardation. Hum. Mutat.; 30:61–68.

Kandel E.R., Schwartz J.H., Jessell T.M. (2000) Principles of Neural Science. New York: McGraw-Hill.

Kasai H., Matsuzaki M., Noguchi J., Yasumatsu N., Nakahara H. (2003) Structure-stability-function relationships of dendritic spines. Trends Neurosci.; 26:360–368.

Keller C.A., Yuan X., Panzanelli P., Martin M.L, Alldred M., Sassoè-Pognetto M., Lüscher B. (2004) The gamma2 subunit of GABA(A) receptors is a substrate for palmitoylation by GODZ. J Neurosci.; 24:5881-5891.

Kim M.J., Futai K., Jo J., Hayashi Y., Cho K., Sheng M. (2007) Synaptic accumulation of PSD-95 and synaptic function regulated by phosphorylation of serine-295 of PSD-95. Neuron; 56:488–502.

Kins S., Betz H., Kirsch J., (2000) Collybistin, a newly identified brain-specific GEF, induces submembrane clustering of gephyrin. Nat. Neurosci.; 3:22-29.

Kirsch J., Langosch D., Prior P., Littauer U.Z, Schmitt B., Betz H. (1991) The 93-kDa glycine receptor-associated protein binds to tubulin. J. Biol. Chem.; 266:22242-22245.

Kittler J., Chen G., Kukhtina V., Vahedi-Faridi A., Gu Z., Tretter V., Smith K., McAinsh K., Arancibia-Carcamo I., Saenger W., Haucke V., Yan Z., Moss S. (2008). Regulation of synaptic inhibition by phospho-dependent binding of the AP2 complex to a YECL motif in the GABAA receptor gamma2 subunit. Proc. Natl. Acad. Sci. USA; 105:3616–3621.

Kittler J., Delmas P., Jovanovic J., Brown D., Smart T., Moss S. (2000) Constitutive endocytosis of GABAA receptors by an association with the adaptin AP2 complex modulates inhibitory synaptic currents in hippocampal neurons. J. Neurosci.; 20:7972–7977.

Kittler J., Thomas P., Tretter V., Bogdanov Y.D., Haucke V., Smart T.G., Moss S.J. (2004) Huntingtin-associated protein 1 regulates inhibitory synaptic transmission by modulating gamma-aminobutyric acid type A receptor membrane trafficking. Proc. Natl. Acad. Sci. U. S. A.; 101:12736-12741.

Kleckner N.W., Dingledine R. (1988) Requirement for glycine in activation of NMDA-receptors expressed in Xenopus oocytes. Science; 241:835-837.

Kneussel M. and Betz H. (2000) Clustering of inhibitory neurotransmitter receptors at developing postsynaptic sites: the membrane activation model. Trends Neurosci.; 23:429–435.

Kneussel M., Brandstatter J.H., Gasnier B., Feng G., Sanes J.R., Betz H. (2001) Gephyrin-independent clustering of postsynaptic GABAA receptor subtypes. Mol. Cell. Neurosci.; 17: 973–982.

Kneussel M., Brandstätter J.H., Laube B., Stahl S., Müller U., Betz H. (1999). Loss of postsynaptic GABA(A) receptor clustering in gephyrin-deficient mice. J. Neurosci.; 19:9289–9297.

Kneussel M., Loebrich S. (2007) Trafficking and synaptic anchoring of ionotropic inhibitory neurotransmitter receptors. Biol. Cell.; 99:297-309.

Kornau H.C., Schenker L.T., Kennedy M.B., Seeburg P.H. (1995) Domain interaction between NMDA receptor subunits and the postsynaptic density protein PSD-95. Science; 269:1737-40.

Kornau H.C., Seeburg P.H., Kennedy M.B. (1997) Interaction of ion channels and receptors with PDZ domain proteins. Curr. Opin. Neurobiol.; 7:368-373.

Kowalczyk S., Winkelmann A., Smolinsky B., Förstera B., Neundorf I., Schwarz G., Meier J.C. (2013) Direct binding of GABAA receptor β2 and β3 subunits to gephyrin. Eur. J. Neurosci.; 37:544-54.

Lardi-Studler B., Smolinsky B., Petitjean C.M., Koenig F., Sidler C., Meier J.C, Fritschy J., Schwarz G. (2007) Vertebrate-specific sequences in the gephyrin E-domain regulate cytosolic aggregation and postsynaptic clustering. J. Cell Sci.; 120:1371-1382.

Lavezzari G., McCallum J., Dewey C.M., K.W. Roche. (2004) Subunit-Specific Regulation of NMDA Receptor Endocytosis. J. Neurosci.; 24:6383-6391.

Lee M.S., Kao S.C., Lemere C.A., Xia W., Tseng H.C. Zhou Y., Neve R., Ahlijanian M.K., Tsai L.H. (2003). APP processing is regulated by cytoplasmic phosphorylation. J. Cell Biol.; 163:83-95.

Lee S., Fan S., Makarova O., Straight S., Margolis B. A (2002) Novel and conserved protein-protein interaction domain of mammalian Lin-2/CASK binds and recruits SAP97 to the lateral surface of epithelia. Mol. Cell Biol.; 22:1778–1791.

Lerma J., Zukin R.S., Bennett M.V. (1990) Glycine decreases desensitization of N-methyl-D-aspartate (NMDA) receptors expressed in Xenopus oocytes and is required for NMDA responses. Proc. Natl. Acad. Sci. U. S. A.; 87:2354–2358.

Lester R.A.J., Clements J.D., Westbrook G.L., Jahr C.E. (1990) Channel kinetics determine the time course of NMDA receptor-mediated synaptic currents. Nature; 346:565–567.

Levi S., Logan S.M., Tovar K.R., Craig A.M. (2004) Gephyrin is critical for glycine receptor clustering but not for the formation of functional GABAergic synapses in hippocampal neurons. J. Neurosci.; 24:207–217.

Li R., Serwanski D.R., Miralles C.P., Li X., Charych E., Riquelme R., Huganir R.L., de Blas A.L. (2005) GRIP1 in GABAergic synapses. J. Comp. Neurol.; 488:11-27.

Liou, Y.C., Sun A., Ryo A., Zhou X.Z., Yu Z.X., Huang H.K., Uchida T., Bronson R., Bing G., Li X., Hunter T., Lu K.P. (2003) Role of the prolyl isomerase Pin1 in protecting against age-dependent neurodegeneration. Nature; 424:556–561.

Lisman J. Raghavachari S. (2006) A unified model of the presynaptic and postsynaptic changes during LTP at CA1 synapses. S. Sci STKE.; (356):re11.

Loreni F., Thomas G., Amaldi F. (2000) Transcription inhibitors stimulate translation of 5' TOP mRNAs through activation of S6 kinase and the mTOR/FRAP signalling pathway. Eur. J. Biochem.; 267:6594-6601.

Lu K.P., Liou Y.C., Zhou X. Z. (2002a) Pinning down proline-directed phosphorylation signalling. Trends Cell Biol.; 12:164–172 .

Lu K.P., Hanes S.D., Hunter T.A. (1996) human peptidyl-prolyl isomerase essential for regulation of mitosis. Nature; 380:544-547.

Lu P.J., Zhou X.Z., Liou Y.C., Noel J.P., Lu K.P. (2002b) Critical role of WW domain phosphorylation in regulating its phosphoserine-binding activity and the Pin1 function. J. Biol. Chem.; 277:2381–2384.

Lu P.J., Zhou X.Z., Shen M., Lu K.P. (1999) A function of WW domains as phosphoserine- or phosphothreonine-binding modules. Science; 283:1325-1328.

Lu Z. and Hunter T. (2014) Prolyl isomerase Pin1 in cancer Cell Research; 24:1033–1049.

Luebke J.I., Weaver C.M., Rocher A.B., Rodriguez A., Crimins J.L., Dickstein D. L., Wearne S.L., Hof P.R. (2010) Dendritic vulnerability in neurodegenerative disease: insights from analyses of cortical pyramidal neurons in transgenic mouse models. Brain Struct. Funct.; 214:181–199.

Luscher B., Fuchs T., Kilpatrick C.L (2011) GABAA receptor trafficking-mediated plasticity of inhibitory synapses. Neuron; 385-409.

Lüscher C., Xia H., Beattie E.C., Carroll R.C., von Zastrow M., Malenka R.C., Nicoll R.A. (1999) Role of AMPA receptor cycling in synaptic transmission and plasticity. Neuron; 24:649-58.

Ma S.L., Pastorino L., Zhou X.Z., Lu K.P. (2012) Prolyl isomerase Pin1 promotes amyloid precursor protein (APP) turnover by inhibiting glycogen synthase kinase-3beta (GSK3beta) activity: novel mechanism for Pin1 to protect against Alzheimer disease. J. Biol. Chem.; 287:6969–6973.

Maas C., Belgardt D., Lee H. K., Heisler F.F., Lappe-Siefke C., Magiera M.M., van Dijk J., Hausrat T.J., Janke C., Kneussel M. (2009) Synaptic activation modifies microtubules underlying transport of postsynaptic cargo. Proc. Natl. Acad. Sci. U.S.A; 106:8731-6.

Maas C., Tagnaouti N., Loebrich S., Behrend B., Lappe-Siefke C., Kneussel M. (2006) Neuronal cotransport of glycine receptor and the scaffold protein gephyrin. J. Cell Biol.; 172:441–451.

MacDermott A.B., Mayer M.L., Westbrook G.L., Smith S.J., Barker J.L. (1986) NMDA-receptor activation increases cytoplasmic calcium concentration in cultured spinal cord neurones. Nature; 321:519-522.

Mammoto A., Sasaki T., Asakura T., Hotta I., Imamura H., Takahashi K., Matsuura Y., Shirao T., Takai Y. (1998) Interactions of drebrin and gephyrin with profilin. Biochem. Biophys. Res. Commun.; 243:86-89.

Marchionni I., Kasap Z., Mozrzymas J.W., Sieghart W., Cherubini E., Zacchi P. (2009) New insights on the role of gephyrin in regulating both phasic and tonic GABAergic inhibition in rat hippocampal neurons in culture. Neuroscience;164:552-62.

Marsden K.C., Beattie J.B., Friedenthal J., Carroll R.C. (2007) NMDA receptor activation potentiates inhibitory transmission through GABA receptor-associated proteindependent exocytosis of GABA(A) receptors. J Neurosci.; 27:14326-14337.

Mayer M.L., Westbrook G.L., Guthrie P.B. (1984) Voltage-dependent block by Mg2+ of NMDA responses in spinal cord neurones. Nature; 309:261–26.

Mayer S., Kumar R., Jaiswal M., Soykan T., Ahmadian M.R., Brose N., Betz H., Rhee J.S., Papadopoulos T. (2013) Collybistin activation by GTP-TC10 enhances postsynaptic gephyrin clustering and hippocampal GABAergic neurotransmission. Proc. Natl. Acad. Sci. U. S. A.; 110:20795-800.

McGee A.W., Dakoji S.R., Olsen O., Bredt D.S., Lim W.A., Prehoda K.E. (2001) Structure of the SH3-guanylate kinase module from PSD-95 suggests a mechanism for regulated assembly of MAGUK scaffolding proteins. Mol. Cell; 8: 1291–1301.

Meier J., Vannier C., Sergé A., Triller A., Choquet D. (2001) Fast and reversible trapping of surface glycine receptors by gephyrin. Nat. Neurosci.; 4:253–260.

Meyer G., Kirsch J., Betz H., Langosch D., (1995) Identification of a gephyrin binding motif on the glycine receptor beta subunit. Neuron; 15:563-572.

Middei S., Spalloni A., Longone P., Pittenger C., O'Mara S.M., Ammassari-Teule M. (2012) CREB selectively controls learning-induced structural remodeling of neurons. Learn. Mem. 19:330-336.

Mondin M., Labrousse V., Hosy E., Heine M., Tessier B., Levet F., Poujol C., Blanchet C., Choquet D., Thoumine O. (2011) Neurexin-neuroligin adhesions capture surface-diffusing AMPA receptors through PSD-95 scaffolds. J Neurosci.; 31:13500-13515.

Montgomery J.M., Zamorano P.L, Garner C.C. (2004). MAGUKs in synapse assembly and function: an emerging view. Cell. Mol. Life Sci.; 61:911–929.

Monyer H., Sprengel R., Schoepfer R., Herb A., Higuchi M., Lomeli H., Burnashev N., Sakmann B., Seeburg P.H. (1992) Heteromeric NMDA receptors: molecular and functional distinctions of subtypes. Science; 256:1217–1221.

Monyer H., Burnashev N., Laurie D.J., Sakmann B., Seeburg P.H. (1994) Developmental and regional expression in the rat brain and functional properties of four NMDA receptors. Neuron; 12:529–540.

Morabito M.A., Sheng M., Tsai L.H. (2004) Cyclin-Dependent Kinase 5 phosphorylates the N-terminal domain of the Postsynaptic Density Protein PSD-95 in neurons. J. Neurosci.; 24:865–876.

Moretto Zita M., Jin H., Shen Z., Zhao T., Briggs S.P., Xu Y. (2010) Phosphorylation stabilizes Nanog by promoting its interaction with Pin1. Proc. Natl. Acad. Sci. U. S. A.; 107:13312-13317.

Mukherjee K., Sharma M., Urlaub H., Bourenkov G.P., Jahn R., Sudhof T.C., Wahl M.C. (2008) CASK Functions as a Mg2+-independent neurexin kinase. Cell; 133:328–339.

Nakagawa T., Futai K., Lashuel H.A., Lo I., Okamoto K., Walz T., Hayashi Y., Sheng M. (2004) Quaternary structure, protein dynamics, and synaptic function of SAP97 controlled by L27 domain interactions. Neuron; 44:453–467.

Nakamura K., Kosugi I., Lee D.Y, Hafner A., Sinclair D.A., Ryo A., Lu K.P. (2012) Prolyl isomerase Pin1 regulates neuronal differentiation via β-catenin. Mol. Cell Biol.; 32:2966-2978.

Nam C.I., Chen L. (2005) Postsynaptic assembly induced by neurexin-neuroligin interaction and neurotransmitter. Proc. Natl. Acad. Sci. U. S. A.; 102:6137-6142.

Nelson C.D., Kim M.J., Hsin H., Chen Y., Sheng M. (2013) Phosphorylation of threonine-19 of PSD-95 by GSK-3β is required for PSD-95 mobilization and long-term depression. J. Neurosci.; 33:12122-12135.

Newpher T.M., Ehlers M.D. (2008) Glutamate receptor dynamics in dendritic microdomains. Neuron; 58:472–497.

Nowak L., Bregestovski P., Ascher P., Herbert A., Prochiantz A. (1984) Magnesium gates glutamate-activated channels in mouse central neurones. Nature; 307:462–465.

Nusbaum M.P, Blitz D.M, Swensen A.M., Wood D., Marder E. (2001) The roles of co-transmission in neural network modulation. TRENDS in Neurosciences; 24:146-154.

Okabe S., Kim H.D., Miwa A., Kuriu T., and Okado H. (1999) Continual remodeling of postsynaptic density and its regulation by synaptic activity. Nat. Neurosci; 2: 804–811.

Okamoto K., Nagai T., Miyawaki A., Hayashi Y. (2004) Rapid and persistent modulation of actin dynamics regulates postsynaptic reorganization underlying bidirectional plasticity. Nat. Neurosci.;7:1104-1112.

Oliva C., Escobedo P., Astorga C., Molina C., Sierralta J. (2012) Role of the MAGUK protein family in synapse formation and function. Dev Neurobiol; 72:57–72.

Paarmann I., Schmitt B., Meyer B., Karas M., Betz H. (2006) Mass Spectrometric Analysis of Glycine Receptor-associated Gephyrin Splice Variants. J. Biol. Chem.; 281:34918-25.

Paoletti P., Bellone C.and Zhou Q. (2013) NMDA receptor subunit diversity: impact on receptor properties, synaptic plasticity and disease. Nature Reviews Neuroscience; 14-383-400.

Papadopoulos T. and Soykan T. (2011) The role of collybistin in gephyrin clustering at inhibitory synapses: facts and open questions. Front. Cell Neurosci.; 5:11.

Papadopoulos T., Eulenburg V., Reddy-Alla S., Mansuy I. M., Li Y., Betz H. (2008). Collybistin is required for both the formation and maintenance of GABAergic postsynapses in the hippocampus. Mol. Cell. Neurosci.; 39:161–169.

Partin K.M., Patneau D.K., Winters C.A., Mayer M.L., Buonanno A. (1993) Selective modulation of desensitization at AMPA *versus* kainate receptors by cyclothiazide and concanavalin A. Neuron; 11:1069–1082.

Pastorino L., Sun A., Lu P.J., Zhou X.Z., Balastik M., Finn G., Wulf G., Lim J., Li S.H., Li X., Xia W., Nicholson L.K., Lu K.P. (2006) The prolyl isomerase Pin1 regulates amyloid precursor protein processing and amyloid-beta production. Nature; 440:528-34.

Peters A. and Kaiserman-Abramof I.R. (1969) The small pyramidal neuron of the rat cerebral cortex The synapses upon dendritic spines. Zeitschrift für Zellforschung und Mikroskopische Anatomie; 100:487-506.

Peters A., Palay S.L. (1996) The morphology of synapses. J. Neurocytol.; 25:687–700.

Petralia R.S., Sans N., Wang Y.X., Wenthold R.J. (2005) Ontogeny of postsynaptic density proteins at glutamatergic synapses. Mol. Cell Neurosci.; 29:436-452.

Petrini E.M. and Barberis A. (2014) Diffusion dynamics of synaptic molecules during inhibitory postsynaptic plasticity. Front. Cell Neurosci.; 8:300.

Petrini E.M., Ravasenga T., Hausrat T.J., Iurilli G., Olcese U., Racine V., Sibarita J.B., Jacob T.C., Moss S.J., Benfenati F., Medini P., Kneussel M., Barberis A. (2014) Synaptic recruitment of gephyrin regulates surface GABAA receptor dynamics for the expression of inhibitory LTP. Nat. Commun.; 5:3921.

Pfeiffer F., Graham D., Betz H. (1982) Purification by affinity chromatography of the glycine receptor of rat spinal cord. J. Biol. Chem.; 257:9389–9393.

Polonio-Vallon T., Krüger D., Hofmann T.G. (2014) ShaPINg Cell Fate Upon DNA Damage: Role of Pin1 Isomerase in DNA Damage-Induced Cell Death and Repair. Front. Oncol.; 4:148.

Poulopoulos A., Aramuni G., Meyer G., Soykan T., Hoon M., Papadopoulos T., Zhang M., Paarmann I., Fuchs C., Harvey K., Jedlicka P., Schwarzacher S. W., Betz H., Harvey R. J., Brose N., Zhang W., Varoqueaux F. (2009) Neuroligin 2 drives postsynaptic assembly at perisomatic inhibitory synapses through gephyrin and collybistin. Neuron; 63:628–642.

Prior P., Schmitt B., Grenningloh G., Pribilla I., Multhaup G., Beyreuther K., Maulet Y., Werner P., Langosch D., Kirsch J., Betz H. (1992) Primary structure and alternative splice variants of gephyrin, a putative glycine receptor-tubulin linker protein. Neuron; 8:1161–1170.

Provenzani A., Fronza R., Loreni F., Pascale A., Amadio M., Quattrone A. (2006) Global alterations in mRNA polysomal recruitment in a cell model of colorectal cancer progression to metastasis. Carcinogenesis; 1323-1333.

Prybylowski K., Fu Z., Losi G., Hawkins L.M., Luo J., Chang K., Wenthold R.J., Vicini S. (2002) Relationship between availability of NMDA receptor subunits and their expression at the synapse. J. Neurosci.; 22:8902–8910.

Pulikkan J.A., Dengler V., Peer Zada A.A., Kawasaki A., Geletu M., Pasalic Z., Bohlander S.K., Ryo A., Tenen D.G., Behre G. (2010) Elevated PIN1 expression by C/EBPalpha-p30 blocks C/EBPalpha-induced granulocytic differentiation through c-Jun in AML. Leukemia; 24:914-923.

Quinlan E.M., Philpot B.D., Huganir R.L., Bear M.F. (1999) Rapid, experiencedependent expression of synaptic NMDA receptors in visual cortex in vivo. Nat. Neurosci.; 2:352–357.

Ranganathan R., Lu K.P., Hunter T., Noel J.P. (1997). Structural and functional analysis of the mitotic rotamase Pin1 suggests substrate recognition is phosphorylation dependent. Cell; 89: 875–886.

Reid T., Bathoorn A., Ahmadian M.R., Collard J.G. (1999) Identification and characterization of hPEM-2, a guanine nucleotide exchange factor specific for Cdc42. J. Biol. Chem.; 274:33587-33593.

Roche K.W., O'Brien R.J., Mammen A.L., Bernhardt J., Huganir R.L.(1996) Characterization of multiple phosphorylation sites on the AMPA receptor GluR1 subunit.Neuron; 16:1179-88.

Roche K.W, Standley S., McCallum J., Dune Ly C, Ehlers M.D., Wenthold R.J . (2001) Molecular determinants of NMDA receptor internalization. Nat. Neurosci.; 4:794–802.

Rochefort N.L., Konnerth A. (2012) Dendritic spines: from structure to in vivo function. EMBO Rep.; 13:699-708.

Rossmann M., Sukumaran M., Penn A.C., Veprintsev D.B., Babu M.M, Greger I. H (2011) Subunit-selective N-terminal domain associations organize the formation of AMPA receptor heteromers EMBO J.; 30:959–971.

Ryo A., Liou Y.C., Lu K.P., Wulf G. (2003) Prolyl isomerase Pin1: a catalyst for oncogenesis and a potential therapeutic target in cancer. J. Cell Sci.; 116:773-83.

Ryo, A., Nakamura, N., Wulf, G., Liou, Y. C. & Lu, K. P. (2001) Pin1 regulates turnover and subcellular localization of beta-catenin by inhibiting its interaction with APC. Nature Cell Biol.; 3:793–801.

Ryo A., Togo T., Nakai T., Hirai A., Nishi M., Yamaguchi A., Suzuki K., Hirayasu Y., Kobayashi H., Perrem K., Liou Y.C., Aoki I.(2006) Prolyl-isomerase Pin1 accumulates in lewy bodies of parkinson disease and facilitates formation of alpha-synuclein inclusions. J. Biol. Chem.; 281:4117-4125.

Sabatini D.M., Barrow R.K, Blackshaw S., Burnett P.E, Lai M.M., Field M.E., Bahr B.A., Kirsch J., Betz H., Snyder S.H. (1999) Interaction of RAFT1 with gephyrin requiredfor rapamycin-sensitive signaling. Science; 284:1161-1164.

Saiepour L., Fuchs C., Patrizi A., Sassoè-Pognetto M., Harvey R.J., Harvey K. (2010) Complex role of collybistin and gephyrin in GABAA receptor clustering. J. Biol. Chem.; 285:29623-31.

Saiyed T., Paarmann I., Schmitt B., Haeger S., Sola M., Schmalzing G., Weissenhorn W., Betz H., (2007) Molecular basis of gephyrin clustering at inhibitory synapses: role of G- and E-domain interactions. J. Biol. Chem.; 282:5625-5632.

Scannevin R.H and Huganir R.L. (2000) Postsynaptic organization and regulation of excitatory synapses. Nat. Rev. Neurosci.;1:133-41.

Scheiffele P. (2003) Cell-cell signaling during synapse formation in the CNS. Annu. Rev. Neurosci.; 26:485–508.

Scheiffele P., Fan J., Choih J., Fetter R., Serafini T. (2000) Neuroligin expressed in non-neuronal cells triggers presynaptic development in contacting axons. Cell; 101:657-669.

Schell M.J., Molliver M.E, Snyder S.H., (1995) Neurobiology D-Serine, an endogenous synaptic modulator: Localization to astrocytes and glutamate-stimulated release. Proc. Natl. Acad. Sci. U. S. A.; 92:3948-3952

Schluter O.M., Xu W., Malenka R.C. (2006) Alternative N-terminal domains of PSD-95 and SAP97 govern activity-dependent regulation of synaptic AMPA receptor function. Neuron; 51:99 –111.

Schmitt B., Knaus P., Becker C.M., Betz H. (1987) The Mr 93000 polypeptide of the postsynaptic glycine receptor complex is a peripheral membrane protein. Biochemistry; 26:805–811.

Schneggenburger R. (1998) Altered voltage dependence of fractional Ca2+ current in N-methyl-D-aspartate channel pore mutants with a decreased Ca2+ permeability. Biophys. J.; 74:1790–1794.

Schoch S., Gundelfinger E.D. (2006) Molecular organization of the presynaptic active zone. Cell Tissue Res.; 326:379-91.

Schonbrunner E.R and Schmid F.X. (1992) Peptidyl-prolyl cis-trans isomerase improves the efficiency of protein disulfide isomerase as a catalyst of protein folding. Proc. Natl. Acad. Sci. U. S. A.; 89:4510-3.

Schrader N., Kim E. Y., Winking J., Paulukat J., Schindelin H., Schwarz G. (2004) Biochemical characterization of the high affinity binding between the glycine receptor and gephyrin. J. Biol. Chem.; 279:18733–18741 .

Schwarz G., Schrader N., Mendel R.R., Hecht H.J., Schindelin H. (2001) Crystal structures of human gephyrin and plant Cnx1 G domains: comparative analysis and functional implications. J. Mol. Biol.;312:405-418.

Segat L., Pontillo A., Annoni G., Trabattoni D., Vergani C., Clerici M., Arosio B., Crovella S., (2007) Pin1 promoter polymorphisms are associated with Alzheimer's disease. Neurobiol. Aging; 28:69-74.

Sheng M (2001) The postsynaptic NMDA-receptor--PSD-95 signaling complex in excitatory synapses of the brain. J. Cell Sci.; 114(Pt 7):1251.

Shen M., Stukenberg P.T., Kirschner M.W., Lu K.P. (1998) The essential mitotic peptidyl-prolyl isomerase Pin1 binds and regulates mitosis-specific phosphoproteins. Genes Dev.; 12:706–720.

Sheng M., Cummings J., Roldan L.A., Jan Y.N, Jan LY (1994) Changing subunit composition of heteromeric NMDA receptors during development of rat cortex. Nature; 368:144–147.

Sheng M., Hoogenraad C.C. (2007) The postsynaptic architecture of excitatory synapses: a more quantitative view. Annu. Rev. Biochem.; 76:823-847.

Sheng M., Kim E. (2011) The postsynaptic organization of synapses. Cold Spring Harb Perspect Biol.; 1;3 (12).

Sheng M., Sala C. (2001) PDZ domains and the organization of supramolecular complexes. Annu Rev Neurosci ;24:1-29

Shin H., Hsueh Y.P., Yang F.C., Kim E., Sheng M. (2000) An intramolecular interaction between Src homology 3 domain and guanylate kinase-like domain required for channel clustering by postsynaptic density-95/SAP90. J. Neurosci.; 20:3580-7.

Sieghart W. and Sperk G. (2002) Subunit composition, distribution and function of GABA-A receptor subtypes. Curr. Top. Med. Chem.; 2795–816.

Smet C., Wieruszeski J.M., Buee L., Landrieu I., Lippens G. (2005) Regulation of Pin1 peptidyl-prolyl *cis*/*trans* isomerase activity by its WW binding module on a multi-phosphorylated peptide of Tau protein. FEBS Lett.; 579:4159–4164.

Smith K.S., Engin E., Meloni E.G., Rudolph U. (2012) Benzodiazepine-induced anxiolysis and reduction of conditioned fear are mediated by distinct GABAA receptor subtypes in mice. Neuropharmacology.; 63:250-258.

Sola M., Bavro V.N., Timmins J., Franz T., Ricard-Blum S., Schoehn G., Ruigrok R.W., Paarmann I., Saiyed T., O'Sullivan G.A. (2004) Structural basis of dynamic glycine receptor clustering by gephyrin. EMBO J.; 23:2510–2519.

Sola M., Kneussel M., Heck I.S., Betz H., Weissenhorn W., (2001) X-ray crystal structure of the trimeric N-terminal domain of gephyrin. J. Biol. Chem.; 276:25294-25310.

Song J.Y., Ichtchenko K., Sudhof T.C., Brose N. (1999) Neuroligin 1 is a postsynaptic celladhesion molecule of excitatory synapses. Proc. Natl. Acad. Sci. U.S.A.; 96:1100–1105.

Sontag E., Nunbhakdi-Craig V., Lee G., Bloom G.S., Mumby M.C. (1996) Regulation of the phosphorylation state and microtubule-binding activity of Tau by protein phosphatase 2A. Neuron; 17:1201–1207.

Soykan T., Schneeberger D., Tria G., Buechner C., Bader N., Svergun D., Tessmer I., Poulopoulos A., Papadopoulos T., Varoqueaux F., Schindelin H., Brose N. (2014) A conformational switch in collybistin determines the differentiation of inhibitory postsynapses. EMBO J.; 33:2113-2133.

Specht C.G., Grunewald N., Pascual O., Rostgaard N., Schwarz G., Triller A. (2011) Regulation of glycine receptor diffusion properties and gephyrin interactions by protein kinase C. EMBO J.; 30:3842–3853.

Specht C.G., Izeddin I., Rodriguez P.C., El Beheiry M., Rostaing P., Darzacq X., Dahan M., Triller A. (2013). Quantitative nanoscopy of inhibitory synapses: counting gephyrin molecules and receptor binding sites. Neuron; 79, 308–321.

Stallmeyer B., Schwarz G., Schulze J., Nerlich, A., Reiss J., Kirsch J., Mendel R.R. (1999) The neurotransmitter receptor-anchoring protein gephyrin reconstitutes molybdenum cofactor biosynthesis in bacteria, plants, and mammalian cells. Proc. Natl. Acad. Sci. U.S.A.; 96:1333–1338.

Star E.N., Kwiatkowski D.J., Murthy V.N. (2002) Rapid turnover of actin in dendritic spines and its regulation by activity. Nat. Neurosci.; 5:239-246.

Sturgill J.F., Steiner P., Czervionke B.L., Sabatini, B.L. (2009) Distinct domains within PSD-95 mediate synaptic incorporation, stabilization, and activity-dependent trafficking. J. Neurosci.; 29:12845–12854.

Sugihara H., Moriyoshi K., Ishri T., Masu M., Nakanishi S. (1992) Structures and properties of seven isoforms of the NMDA receptor generated by alternative splicing. Biochem. Biophys. Res. Commun.; 185:826–832.

Sultana R., Boyd-Kimball D., Poon H.F., Cai J., Pierce W.M., Klein J.B., Markesbery W.R., Zhou X.Z., Lu K.P., Butterfield D.A. (2006) Oxidative modification and down-regulation of Pin1 in Alzheimer's disease hippocampus: A redox proteomics analysis. Neurobiol Aging; 27:918-25.

Swanson G.T., Heinemann S.F. (1998) Heterogeneity of homomeric GluR5 kainate receptor desensitization expressed in HEK293 cells. J Physiol.; 513:639–646.

Swulius M.T., Farley M.M., Bryant M.A., Waxham M.N. (2012) Electron cryotomography of postsynaptic densities during development reveals a mechanism of assembly. Neuroscience; 212:19-29.

Tabuchi K. and Südhof T.C. (2002) Structure and evolution of neurexin genes: insight into the mechanism of alternative splicing. Genomics.; 79:849-859.

Tada T. and Sheng M. (2005) Molecular mechanisms of dendritic spine morphogenesis. Curr. Opin. Neurobiol.; 16:95-101.

Thomas G.M. and Huganir R.L. (2004) MAPK cascade signalling and synaptic plasticity. Nat. Rev. Neurosci.; 5:173-83.

Thorpe J.R., Morley S.J., Rulten S.L., (2001) Utilising the peptidyl prolyl *cis –trans* isomerase Pin1 as a probe of its phosphorylated target proteins: examples of binding to nuclear proteins in a human kidney cell line and to Tau in Alzheimer's diseased brain. J. Histochem. Cytochem.; 49:97–108.

Tomita S., Nicoll R.A., Bredt D.S. (2001) PDZ protein interactions regulating glutamate receptor function and plasticity. J. Cell Biol.; 153: F19-F23.

Topinka J.R. and Bredt D.S. (1998) N-terminal palmitoylation of PSD-95 regulates association with cell membranes and interaction with K+ channel Kv1.4. Neuron; 20:125-134.

Tovar K.R. and Westbrook G.L. (2002) Mobile NMDA receptors at hippocampal synapses. Neuron; 34:255-64.

Trachtenberg J.T., Chen B.E., Knott G.W., Feng G., Sanes J.R., Welker E., Svoboda K. (2002) Long-term in vivo imaging of experience-dependent synaptic plasticity in adult cortex. Nature; 420:788-94.

Traynelis S.F., Wollmuth L.P., McBain C.J., Menniti F.S., Vance K.M., Ogden K.K., (2010) Glutamate receptor ion channels: structure, regulation and function. Pharmacol. Rev.; 62:405–496.

Tretter V., Mukherjee J., Maric H.-M., Schindelin H., Sieghart W., Moss S.J. (2012) Gephyrin, the enigmatic organizer at GABAergic synapses. Front. Cell. Neurosci.; 6:23.

Triller A. and Choquet D. (2005) Surface trafficking of receptors between synaptic and extrasynaptic membranes: and yet they do move!. Trends Neurosci.; 28:133-139.

Triller A., Cluzeaud F., Korn H. (1987) Gamma-aminobutyric acid-containing terminals can be apposed to glycine receptors at central synapses. J. Cell Biol.; 104:947–956.

Triller A., Cluzeaud F., Pfeiffer F., Betz H., Korn H. (1985) Distribution of glycine receptors at central synapses: an imunoelectron microscopy study. J Cell Biol.; 101:683–688.

Turrigiano G.G. and Nelson S.B. (2004) Homeostatic plasticity in the developing nervous system, Nature Reviews Neuroscience; 5:97-107.

Tyagarajan S. K., Ghosh H., Yévenes G. E., Nikonenko I., Ebeling C., Schwerdel C., Sidler C., Zeilhofer H.U., Gerrits B., Muller D., Fritschy J.M. (2011) Regulation of GABAergic synapse formation and plasticity by GSK3beta-dependent phosphorylation of gephyrin. Proc. Natl. Acad. Sci. U. S. A.; 108:379–384.

Tyagarajan S.K., Ghosh H., Yévenes G.E., Imanishi S.Y., Zeilhofer H U., Gerrits B., Fritschy J.M. (2013). Extracellular signal-regulated kinase and glycogen synthase kinase 3β regulate gephyrin postsynaptic aggregation and GABAergic synaptic function in a calpain-dependent mechanism. J. Biol. Chem.; 288:9634– 9647.

Unwin N. (1989) The structure of ion channels in membranes of excitable cells Neuron; 3:665–676.

Ushkaryov Y.A. and Sudhof T.C. (1993) Neurexin III alpha: extensive alternative splicing generates membrane-bound and soluble forms. Proc. Natl. Acad. Sci. U. S. A.; 90:6410-6914.

Ushkaryov Y.A., Hata Y., Ichtchenko K., Moomaw C., Afendis S., Slaughter C.A., Südhof T.C. (1994) Conserved domain structure of beta-neurexins. Unusual cleaved signal sequences in receptor-like neuronal cell-surface proteins. J. Biol. Chem. 269:11987-11992.

Ushkaryov Y.A., Petrenko A.G., Geppert M., Südhof T.C. (1992) Neurexins: synaptic cell surface proteins related to the alpha-latrotoxin receptor and laminin. Science ; 257:50-56.

Van Spronsen M. and Hoogenraad C.C. (2010) Synapse Pathology in Psychiatric and Neurologic Disease. Curr. Neurol. Neurosci. Rep.; 10:207–214.

Vander Horn P.B., Davis M.C., Cunniff J.J., Ruan C., McArdle B.F, Samols S.B., Szasz J., Hu G., Hujer K.M., Domke S.T., Brummet S.R., Moffett R.B., Fuller C.W. (1997) Thermo Sequenase DNA Polymerase and T. acidophilum Pyrophosphatase: New Thermostable Enzymes for DNA Sequencing. Bio.Techniques; 22:758-765.

Varoqueaux F., Jamain S., Brose N. (2004) Neuroligin 2 is exclusively localized to inhibitory synapses. Eur. J. Cell Biol.; 83:449–456.

Verdecia M.A., Bowman M.E., Lu K.P., Hunter T., Noel J.P. (2000) Structural basis for phosphoserine-proline recognition by group IV WW domains. Nat. Struct. Biol.; 7:639–643.

Vicini S., Wang J.F., Li J.H., Zhu W.J., Wang Y.H., Luo J.H., Wolfe B.B., Grayson D.R. (1998) Functional and pharmacological differences between recombinant N-methyl-D-aspartate receptors. J. Neurophysiol.; 79:555-66.

Vithlani M., Terunuma M., Moss S.J. (2011) The dynamic modulation of GABA(A) receptor trafficking and its role in regulating the plasticity of inhibitory synapses. Physiol. Rev.; 91:1009-1022.

Wang J., Liu S., Haditsch U., Tu W., Cochrane K., Ahmadian G., Tran L., Paw J., Wang Y., Mansuy I., Salter M., Lu Y. (2003) Interaction of calcineurin and type-A GABA receptor gamma 2 subunits produces long-term depression at CA1 inhibitory synapses. J. Neurosci.; 23:826–836.

Wang J.Z., Gong C.X., Zaidi T., Grundke-Iqbal I., Iqbal K. (1995) Dephosphorylation of Alzheimer paired helical filaments by protein phosphatase-2A and -2B. J. Biol. Chem.; 270:4854–4860.

Weiwad M., Kullertz G., Schutkowski M., Fischer G. (2000). Evidence that the substrate backbone conformation is critical to phosphorylation by p42 MAP kinase. FEBS Lett.; 478, 39-42.

Westmark P.R., Westmark C.J., Wang S., Levenson J., O'Riordan K.J., Burger C., Malter J.S. (2010) Pin1 and PKMzeta sequentially control dendritic protein synthesis. Sci. Signal.; 3(112):ra18.

Whiting P.J. (1999) The GABA-A receptor gene family: new targets for therapeutic intervention. Neurochem. Int.; 34:387-390.

Whiting P.J. (2003) GABA-A receptor subtypes in the brain: a paradigm for CNS drug discovery?. Drug Discov. Today; 8:445-450.

Wintjens R., Wieruszeski J. M., Drobecq H., Rousselot-Pailley P., Buee L., Lippens G., Landrieu I. (2001) 1H NMR study on the binding of Pin1 Trp-Trp domain with phosphothreonine peptides. J. Biol. Chem.; 276:25150–25156 .

Wisden W., Laurie D.J, Monyer H., Seeburg P.H. (1992) The distribution of 13 $GABA_A$ receptor subunit mRNAs in the rat brain. I. Telencephalon, diencephalon, mesencephalon. J. Neurosci.; 12:1040-1062.

Wulf G.M., Ryo A., Wulf G.G., Lee S.W., Niu T., Petkova V., Lu K.P. (2001) Pin1 is overexpressed in breast cancer and cooperates with Ras signaling in increasing the transcriptional activity of c-Jun towards cyclin D1. EMBO J.; 20:3459–3472.

Xiang S., Nichols J., Rajagopalan K.V., Schindelin H. (2001) The crystal structure of Escherichia coli MoeA and its relationship to the multifunctional protein gephyrin. Structure; 9:299-310.

Xu Y.X. and. Manley J.L. (2007) Pin1 modulates RNA polymerase II activity during the transcription cycle. Genes Dev.; 21:2950–2962.

Xu Y.X., Hirose Y., Zhou X.Z., Lu K.P., Manley J.L. (2003) Pin1 modulates the structure and function of human RNA polymerase II. Genes & Dev.; 17:2765–2776.

Xu W.(2011) PSD-95-like membrane associated guanylate kinases (PSD-MAGUKs) and synaptic plasticity. Curr. Opin. Neurobiol.; 21:306–312.

Yaffe M.B., Schutkowski M., Shen M., Zhou X. Z., Stukenberg P.T., Rahfeld J.U., Xu J., Kuang J., Kirschner M.W., Fischer G., Cantley L.C., Lu K.P. (1997) Sequence-specific and phosphorylation-dependent proline isomerization: a potential mitotic regulatory mechanism. Science; 278:1957–1960.

Yeh E.S. and Means A.R. (2007) Pin1, the cell cycle and cancer. Nature Rev. Cancer; 7:381–388.

Yokoi N., Fukata M., Fukata Y. (2012) Synaptic plasticity regulated by protein-protein interactions and posttranslational modifications. Int. Rev. Cell Mol. Biol.; 297:1-43.

Yoshimura Y., Ohmura T., Komatsu Y. (2003) Two forms of synaptic plasticity with distinct dependence on age, experience, and NMDA receptor subtype in rat visual cortex. J. Neurosci.; 23:6557–6566.

Yu W., Charych E.I, Serwanski D.R, Li R., Ali R., Bahr B.A., De Blas A.L., (2008) Gephyrin interacts with the glutamate receptor interacting protein 1 isoforms at GABAergic synapses. J. Neurochem.; 105:2300-2314.

Yu W., Jiang M., Miralles C.P., Li R.W., Chen, G., de Blas, A.L. (2007) Gephyrin clustering is required for the stability of GABAergic synapses. Mol. Cell. Neurosci.; 36:484–500.

Yuan X., Yao J., Norris D., Tran D.D., Bram R.J., Chen G., Luscher B. (2008) Calcium-modulating cyclophilin ligand regulates membrane trafficking of postsynaptic GABA(A) receptors. Mol. Cell Neurosci.; 38:277-289.

Zacchi P., Gostissa M., Uchida T., Salvagno C., Avolio F., Volinia S., Ronai Z., Blandino G., Schneider C., Del Sal G. (2002) The prolyl isomerase Pin1 reveals a mechanism to control p53 functions after genotoxic insults. Nature; 419:853-857.

Zhang W., Howe J.R., Popescu G.K. (2008) Distinct gating modes determine the biphasic relaxation of NMDA receptor currents. Nat. Neurosci.; 1:1373–1375.

Zhang Y., Daum S., Wildemann D., Zhou X.Z., Verdecia M.A., Bowman M.E., Lücke C., Hunter T., Lu K.P., Fischer G., Noel J.P. (2007) Structural basis for high-affinity peptide inhibition of human Pin1. ACS Chem. Biol.; 2:320–328.

Zheng H., You H., Zhou X.Z., Murray S.A., Uchida T., Wulf G., Gu L., Tang X., Lu K.P., Xiao Z.X. (2002) The prolyl isomerase Pin1 is a regulator of p53 in genotoxic response. Nature; 419:849-853.

Zita M.M., Marchionni I., Bottos E., Righi M.,, Del Sal G., Cherubini E., Zacchi P. (2007) Post-phosphorylation prolyl isomerisation of gephyrin represents a mechanism to modulate glycine receptors function. EMBO J.; 26:1761–1771.

7. APPENDIX

REVIEW

Gephyrin phosphorylation in the functional organization and plasticity of GABAergic synapses

Paola Zacchi,[1,*] Roberta Antonelli,[1] and Enrico Cherubini[1,2]

1Department of Neurosciences, Scuola Internazionale Superiore di Studi Avanzati, Trieste, Italy
2European Brain Research Institute, Roma, Italy

Front Cell Neurosci. 2014; 8: 103.
Published online 2014 Apr 9.

frontiers in
CELLULAR NEUROSCIENCE

REVIEW ARTICLE
published: 09 April 2014
doi: 10.3389/fncel.2014.00103

Gephyrin phosphorylation in the functional organization and plasticity of GABAergic synapses

Paola Zacchi[1]*, Roberta Antonelli[1] and Enrico Cherubini[1,2]

[1] *Department of Neurosciences, Scuola Internazionale Superiore di Studi Avanzati, Trieste, Italy*
[2] *European Brain Research Institute, Roma, Italy*

Edited by:
Andrea Barberis, Fondazione Istituto Italiano di Tecnologia, Italy

Reviewed by:
Annalisa Scimemi, University at Albany, State University of New York, USA
Nils Brose, Max-Plank-Institute for Experimental Medicine, Germany

***Correspondence:**
Paola Zacchi, Department of Neurosciences, Scuola Internazionale Superiore di Studi Avanzati, via Bonomea 265, 34136 Trieste, Italy
e-mail: zacchi@sissa.it

Gephyrin is a multifunctional scaffold protein essential for accumulation of inhibitory glycine and $GABA_A$ receptors at post-synaptic sites. The molecular events involved in gephyrin-dependent $GABA_A$ receptor clustering are still unclear. Evidence has been recently provided that gephyrin phosphorylation plays a key role in these processes. Gephyrin post-translational modifications have been shown to influence the structural remodeling of GABAergic synapses and synaptic plasticity by acting on post-synaptic scaffolding properties as well as stability. In addition, gephyrin phosphorylation and the subsequent phosphorylation-dependent recruitment of the chaperone molecule Pin1 provide a mechanism for the regulation of GABAergic signaling. Extensively characterized as pivotal enzyme controlling cell proliferation and differentiation, the prolyl-isomerase activity of Pin1 has been shown to regulate protein synthesis necessary to sustain the late phase of long-term potentiation at excitatory synapses, which suggests its involvement at synaptic sites. In this review we summarize the current state of knowledge of the signaling pathways responsible for gephyrin post-translational modifications. We will also outline future lines of research that might contribute to a better understanding of molecular mechanisms by which gephyrin regulates synaptic plasticity at GABAergic synapses.

Keywords: gephyrin, phosphorylation, $GABA_A$ receptors, GSK-3β signaling, ERK signaling, Pin1

INTRODUCTION

Post-synaptic scaffolding molecules are key factors for the functional organization of synapses. They ensure the accurate accumulation of neurotransmitter receptors in precise apposition to pre-synaptic release sites as required for a reliable synaptic transmission. Scaffolding molecules also interact with cytoskeletal anchoring elements and these interactions are thought not only to provide the physical constraints for maintaining receptors at synapses, but also for regulating the constant flux of receptors and scaffolding elements in and out of post-synaptic sites (Choquet and Triller, 2003; Hanus et al., 2006). They can also regulate downstream signaling pathways to adjust the molecular composition of the post-synaptic devices necessary to sustain synaptic plasticity. At inhibitory post-synaptic densities (PSDs) a single protein, gephyrin, builds the major scaffold for the transient immobilization of inhibitory glycine receptors (GlyRs) and α2-γ2 subunits containing $GABA_A$ receptors ($GABA_A$Rs; Tretter et al., 2012). The formation and maintenance of gephyrin clusters rely mostly on gephyrin-gephyrin interactions (reviewed in Fritschy et al., 2008). Gephyrin is a 93-kDa protein that consists of three major domains: an N-terminal G-domain, a C-terminal E-domain and a connecting central linker region (C-domain) (Prior et al., 1992). Crystal structure studies have demonstrated that while the G-domain has an intrinsic tendency to trimerize the E-domain dimerizes (Schwarz et al., 2001; Sola et al., 2001, 2004). These oligomerization features suggest a model for cluster formation whereby gephyrin builds a bidimensional hexagonal lattice underneath the synaptic membrane (Kneussel and Betz, 2000; Schwarz et al., 2001; Sola et al., 2001, 2004; Xiang et al., 2001) which exposes a high number of binding sites for GlyR β subunits and for $GABA_A$Rs α1, α2, α3, β2 and β3 subunits (Maric et al., 2011; Kowalczyk et al., 2013).

Recently, an elegant study based on quantitative three-dimensional nanoscopic imaging, has not only confirmed that gephyrin clusters are indeed bidimensional planar structures lying underneath the synaptic plasma membrane but has also provided evidence that all gephyrin molecules in the cluster are potentially capable to interact with neurotransmitter receptors localized in the synaptic membrane in a stoichiometry ratio gephyrin-receptor of approximately 1:1 (Specht et al., 2013).

A consequence of this organization is that changes in gephyrin clustering could produce parallel changes in the number of receptors trapped by the scaffold, and thus lead to corresponding alteration of the strength of synaptic transmission. This may vary with age and in different cell compartments as suggested by the transient expression of gephyrin clusters co-localized with $GABA_A$Rs at immature perisomatic but not dendritic basket-Purkinje cell synapses (Viltono et al., 2008). The loss of gephyrin and the consequent re-organization of perisomatic $GABA_A$R clusters in more mature neurons may affect their trafficking and stability.

Another important element in the functional organization of inhibitory synapses is represented by the affinity of gephyrin for neurotransmitter receptors (Fritschy et al., 2008). Mechanisms that are able to alter these parameters could uncouple gephyrin clustering and the number of receptors that can be effectively accommodated within the cluster itself. This mechanism would be well suited for the complex and still poorly understood dynamics of gephyrin-dependent $GABA_A$Rs (Tretter et al., 2012). In contrast to GlyRs that interact with gephyrin only through the β subunits, $GABA_A$Rs interact *via* their large intracellular loops with several subunits of the α and β families such α1, α2, α3 and β2, β3, respectively (Tretter et al., 2008, 2011; Saiepour et al., 2010; Mukherjee et al., 2011; Kowalczyk et al., 2013). These subunits utilize the same binding site as GlyR (Maric et al., 2011) but display a binding affinity at least one order of magnitude lower. The γ2 subunit, initially thought to be implicated in controlling gephyrin-dependent $GABA_A$Rs clustering (Essrich et al., 1998), as its gene deletion strongly affects both receptor and gephyrin synaptic accumutation (Günther et al., 1995), was never identified as direct interactor of gephyrin (Tretter et al., 2012). The α4, α5 and δ subunits present mainly on extrasynaptic $GABA_A$Rs lack of co-localization with gephyrin (Farrant and Nusser, 2005). While each $GABA_A$R is a pentamer, it is still not known which available binding sites are actively involved in gephyrin interaction and whether and how they cooperate to increase the overall binding affinity for gephyrin. Finally, gephyrin dynamics rely on its availability for cluster formation which depends on its regulated transport to post-synaptic sites and degradation. Degradation requires mainly the activity of the Ca^{2+}-dependent cysteine protease calpain-1 (Kawasaki et al., 1997; Tyagarajan et al., 2011).

The recruitment of gephyrin to GABAergic synapses needs the contribution of at least two classes of interactors: the cell adhesion molecules of the neuroligin (NL) family (Südhof, 2008) and the guanine nucleotide exchange factor for the monomeric GTPase Cdc42 collybistin (Kins et al., 2000). In particular NL2, the isoform constitutively localized at inhibitory GABAergic synapses (Varoqueaux et al., 2004), interacts with both gephyrin and collybistin forming a ternary complex able to activate collybistin-driven gephyrin tethering to the plasma membrane followed by receptors recruitment (Poulopoulos et al., 2009).

In summary, several gephyrin-dependent mechanisms affect the number of $GABA_A$Rs at synaptic sites at any given time, and thereby may influence the strength of synaptic transmission: gephyrin-gephyrin interaction, gephyrin-receptor (neurotransmitters or other synaptically localized membrane proteins) binding affinities, gephyrin turnover and synaptic transport. Recently new mechanistic insights on the regulation of gephyrin oligomerization, stability and receptor binding capability have been provided. They suggest that phosphorylation, (a versatile mechanism for regulating protein activity in a specific and controlled manner), already involved in the functional modulation of receptors at synapses, is determinant for all aspect of gephyrin dynamics. Interestingly, the signaling pathways altering the phosphorylation status of gephyrin have been previously identified as modulator of glutamatergic signaling. The functional cross-talk between excitatory and inhibitory transmission may have important implications for the long-term stability of neuronal networks.

SIGNALING PATHWAYS INVOLVED IN GEPHYRIN CLUSTERING

A recent genome-wide siRNA screening aimed at identifying protein kinases stabilizing gephyrin clustering revealed a contribution of Receptor Tyrosine Kinases (RTKs) signaling; in particular the tropomyosin-related kinase B (Trk-B) and its ligand the brain-derived neurotrophic factor (BDNF; Wuchter et al., 2012). The BDNF-TrkB system is required for multiple aspects of neuronal functions including neuronal survival and differentiation during development as well as synaptic plasticity of mature neurons (Thoenen et al., 1987; Tanaka et al., 2000; Poo, 2001). The activation of TrkB by BDNF triggers various signaling cascades including the Ras/mitogen-activated protein (MAP) kinase (Ras/MAPK) pathway, the phosphatidylinositol 3-kinase (PI3-Kinase)/Akt pathway and the phospholipase C gamma (PLCγ) pathway (Arévalo and Wu, 2006). At glutamatergic synapses, the activation of MAPK and PI3K pathways plays a crucial role in synaptic plasticity. This occurs not only *via de novo* regulation of protein synthesis but also *via* trafficking of pre-existing synaptic proteins. Therefore, it is not surprising that these signaling pathways contribute to regulate gephyrin transport at synapses (**Figure 1**). The BDNF-dependent activation of the PI3K/Akt pathway leads to the activation of rapamycin (mTOR), a regulator of mRNA translation (Sarbassov et al., 2005). Sabatini et al. (1999) demonstrated that mTOR interacts with gephyrin and this interaction is fundamental for mTOR-dependent signaling to the translational repressor 4E-BP1 (Sabatini et al., 1999). Upon BDNF treatment mTOR decreases its association with gephyrin, thus releasing gephyrin for membrane transport and cluster assembly. In addition PI3K activation, by promoting an increase in phosphatidylinositol (3,4,5)-triphosphate (PIP3) membrane content, may enhance collybistin-mediated gephyrin recruitment at GABAergic synapses (Reddy-Alla et al., 2010). In parallel, BDNF-dependent activation of Akt was shown to promote the inactivation of the serine/threonine kinase glycogen synthase kinase 3β (GSK-3β), a recently indentified negative regulator of gephyrin clustering (Tyagarajan et al., 2011). The authors of the wide-genome screening (Wuchter et al., 2012) also provided evidence for a contribution of the MAPK signaling cascade to gephyrin clustering, independent of mTOR activation, and controlled by the negative regulators of RTKs signaling sprouty proteins (Kim and Bar-Sagi, 2004).

The screening identified two siRNA directed against testicular protein kinase 1 (Tesk1) and Dual specificity tyrosine-phosphorylation-regulated kinase 1A (Dyrk1A), two protein kinases implicated in the inhibitory phosphorylation of sprouty proteins, in particular sprouty2, that specifically inhibit the Ras-Raf-MAPK pathway triggered by BDNF (Aranda et al., 2008; Chandramouli et al., 2008). This study, while revealing mechanisms involved in the control of gephyrin clustering, did not address the possibility that such signaling cascade may also affect gephyrin phosphorylation. Tyagarajan et al. (2013) were able to demonstrate that some of the kinases belonging to the MAPK and

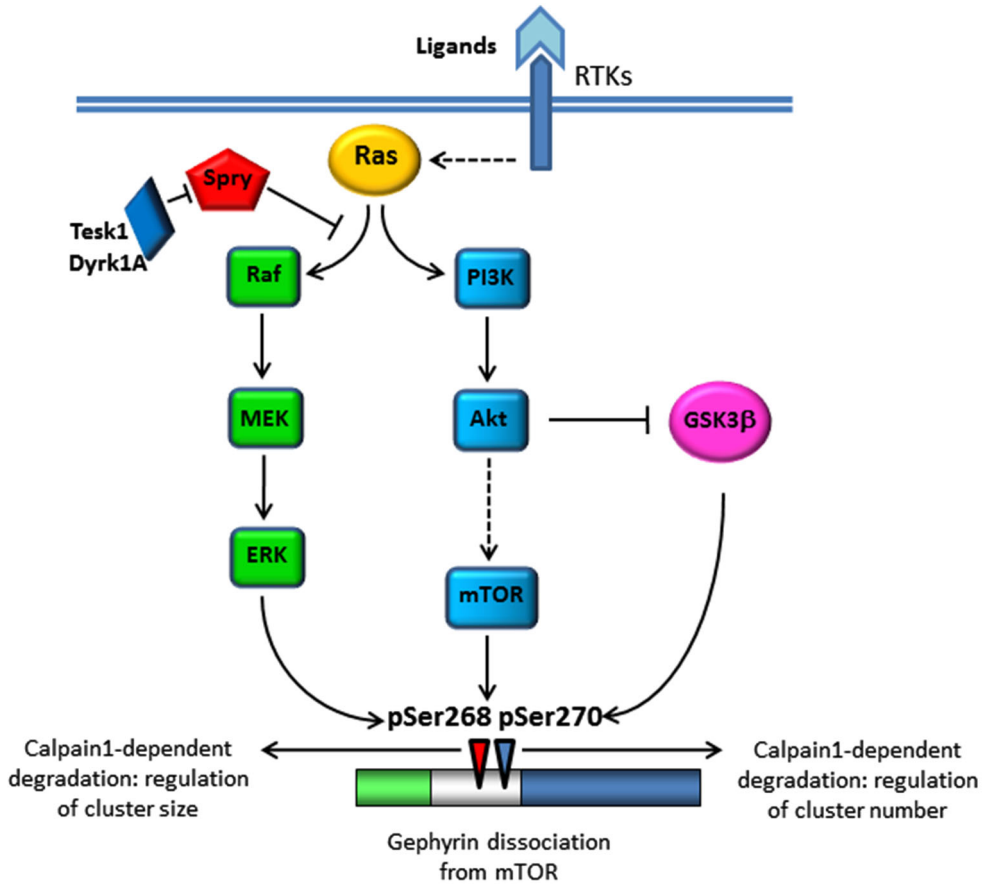

FIGURE 1 | Schematic representation of signaling pathways affecting gephyrin clustering. Stimulation of RTKs by ligand binding or activity-dependent increase in calcium levels activates Ras and its downstream signaling cascades Ras/MAPK and PI3K/Akt leading to gephyrin phosphorylation at Ser268 by ERK and gephyrin dissociation from mTOR. Akt also inhibits GSK-3β activity, the kinase responsible of Ser270 phosphorylation. Gephyrin phosphorylated by these two kinases becomes substrate of calcium-dependent calpain degradation.

PI3K/Akt signaling pathways influence gephyrin dynamics and GABAergic transmission right through direct gephyrin phosphorylation (see below).

PHOSPHORYLATION OF GEPHYRIN C-DOMAIN ALTERS ITS OLIGOMERIZATION AND STABILITY PROPERTIES

Gephyrin has been known to be a phosphoprotein since 1992, when Langosh and colleagues discovered that this protein co-purified with GlyR preparations has a kinase activity capable of promoting the incorporation of phosphate groups into serine and threonine residues (Langosch et al., 1992). The functional relevance of these post-translational modifications was neglected for long time, possibly because gephyrin was considered to be just a mere tubulin-binding protein, therefore a simple structural component of the inhibitory PSD.

Mass spectrometry analysis performed on gephyrin isolated from either mouse or rat brain homogenates or purified upon its overexpression in eukaryotic cells, has identified 22 phosphorylation sites, all located within the C-domain of gephyrin, except the threonine 324 (Thr324) site that lies in the C-terminal E-domain (**Figure 2**; Herweg and Schwarz, 2012; Kuhse et al., 2012; Tyagarajan et al., 2013). The C-domain is positioned between the highly conserved G- and E-domains that are directly involved in gephyrin multimerization. Based on its sensitivity to proteolytic cleavage (Schrader et al., 2004), the C-domain is the most exposed to the surrounding environment, making it a suitable substrate for post-traslational modifications. This domain also mediates the phosphorylation-dependent recruitment of the peptidyl prolyl *cis-trans* isomerase Pin1 (discussed below) (Zita et al., 2007), the interaction with dynein light chain (Fuhrmann et al., 2002) and contributes to the recruitment of collybistin (Zacchi et al., personal communication).

In this region, conformational changes induced by phosphorylation could affect the folding of the C-domain itself and of the neighboring G- and E-domains, thus altering gephyrin clustering properties. A recent study (Herweg and Schwarz, 2012) has demonstrated that gephyrin, once expressed in a system that allows post-translational modifications, behaves quite differently in terms of oligomerization, folding stability and receptor binding. Gephryn expressed in Spodoptera frugiperda (Sf9) insect cells shows a diffuse distribution in the cytosol instead of the characteristic "aggregates" observed in HEK293 (Meier et al.,

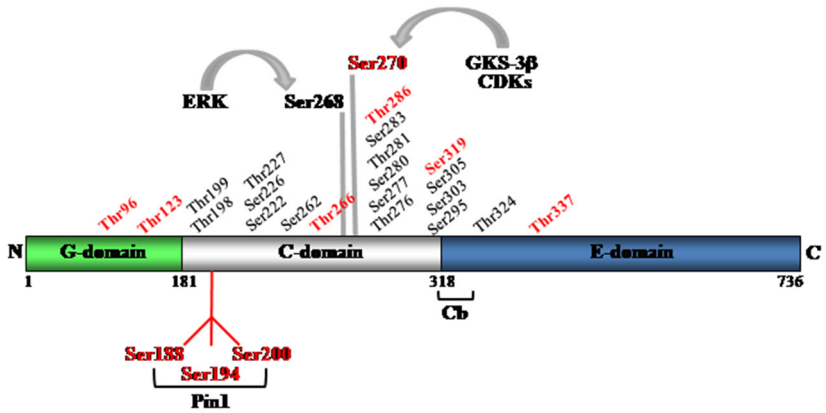

FIGURE 2 | Schematic representation of gephyrin domains and the identified phosphorylation sites. Mass spectrometry has allowed identifying 22 serine and threonine residues within the C-domain and one (threonine 324), in the E-domain. In red are highlighted all putative Pin1 consensus motifs. Ser270 and Ser268 are recognized targets of GSK-3β and ERK kinase activities, respectively.

2000) or COS7 cells (Kirsch and Betz, 1995). The basic building blocks are formed by hexamers instead of trimers; in addition, G- and C-domains form a complex with increased overall stability while E-domains are stabilized upon receptor interaction. These parameters are also sensitive to changes in the amino acid sequence of gephyrin due to alternative splicing of the gene that, interestingly, impacts mostly on its C-domain organization, further underlying the contribution of this region in determining gephyrin folding and clustering (Herweg and Schwarz, 2012). It is therefore not surprising that most of the signaling pathways able to affect gephyrin clustering are represented by serine/threonine kinases targeting specific residues embedded in the C-domain of the protein.

PHOSPHORYLATION OF GEPHYRIN AT SERINE 270 IS AT THE CROSS-ROAD OF DIFFERENT SIGNALING PATHWAYS

One of the first gephyrin residues identified as the target of specific kinases was serine 270 (Ser270; Tyagarajan et al., 2011). Interestingly, the first kinase found to promote post-translational modifications was a serine/threonine kinase belonging to the family of Glycogen Synthase Kinase 3 (GSK3), enzymes originally identified as key regulators of glucose metabolism (Woodgett and Cohen, 1984; Wang and Roach, 1993). GSK3 signaling cascades have clearly recognized roles in neurodevelopmental processes such as neurogenesis, neuronal migration, neuronal polarization and axonal growth and guidance (reviewed in Hur and Zhou, 2010). Recently they have been implicated in N-methyl-D-aspartate receptors (NMDARs)-dependent long-term depression at glutamatergic synapses (Bradley et al., 2012). Even though the underlying molecular mechanisms are still not understood, GSK-3β–dependent phosphorylation of PSD-95, the major scaffold protein of excitatory PSD, functionally homologue of gephyrin, was found to destabilize the scaffold molecule thus allowing AMPA receptors internalization and LTD induction (Nelson et al., 2013).

Like PSD-95, GSK-3β appears to exert a negative effect on gephyrin clustering at GABAergic synapses (Tyagarajan et al., 2011). Several lines of evidence support this notion. Overexpression of a gephyrin phosphodeficient mutant (Ser270Ala) in cultured hippocampal neurons promotes the formation of supernumerary gephyrin clusters similar in size to those obtained upon wild-type gephyrin overexpression. Functionally, alanine mutation at this site selectively enhances the frequency of miniature inhibitory post-synaptic currents (mIPSC), a result which is in line with the increased density of functional GABAergic synapses. Additionally, a similar phenotype was observed upon pharmacological inhibition of GSK-3β activity both *in vitro* and *in vivo*. The authors of this study also provided mechanistic insights on how GSK-3β dependent phosphorylation of Ser270 can negatively regulate gephyrin clustering. They were able to demonstrate that phosphorylated gephyrin becomes substrate of the Ca^{2+}-dependent protease calpain-1, possibly because at this location the phosphorylation-dependent conformational change may expose the sequence rich in proline (P), glutamic acid (E), serine (S) and threonine (T) (PEST sequence; Rechsteiner, 1990) that acts as a signal peptide for protein degradation. It is interesting to note that Ser270 lies also within a putative Pin1 consensus motif, raising the intriguing possibility that prolyl-isomerase may also participate in the conformational changes required to drive gephyrin proteolytic degradation. Since rises in calcium and GSK-3β activation are coupled to neuronal activity, the identified mechanisms are well suited to mediate plasticity-related changes at GABAergic synapses. Several issues remain to be unraveled regarding the functional consequences of this phosphorylation event. It will be interesting to understand how Ser270 phosphorylation destabilizes gephyrin assembled into a crowded lattice, where gephyrin is engaged in several protein-protein interactions with itself, neurotransmitter receptors and other transmembrane proteins (e.g., NL2). All these interactions represent potential targets of the signaling cascade. The fact that gephyrin phosphodeficient mutants possess synaptogenic activity further supports the notion that this site may regulate gephyrin binding to proteins important for building and maintaining functional GABAergic synapses. By converging on both scaffold

molecules PSD-95 and gephyrin, GSK-3β signaling cascade, coordinates changes at both glutamatergic and GABAergic synapses, thus allowing to maintain an appropriate excitatory/inhibitory (E/I) balance.

The picture became even more complicated by the discovery that other kinases of the CDK family, in particular Cyclin-dependent kinase 5 (Cdk5), can target the same site, making this residue at the cross-road of different signaling pathways (Kuhse et al., 2012). Cdk5 is a proline-directed serine/threonine kinase with high activity in the central nervous system. Based on sequence homology, Cdk5 belongs to a class of kinases operating in the cell cycle, even though it is not activated by traditional cyclins and it plays critical roles in several aspect of brain development and neuronal functions including neuronal migration, differentiation, synapse development and plasticity (Lai and Ip, 2009; Su and Tsai, 2011).

The precise role of Cdk5 in activity-dependent synaptic plasticity is still not understood but the identification of novel substrates and interacting molecules has provided significant mechanistic insights. At glutamatergic synapses, Cdk5 has been shown to affect NMDA receptors-dependent plasticity through several mechanisms: (i) by altering NMDA receptor channel conductance upon Cdk5-depenent phosphorylation of certain receptor subunits (Li et al., 2001); (ii) by down-regulating in an activity-dependent manner NMDA receptors number *via* a calpain-dependent proteolytic degradation (Hawasli et al., 2007); and (iii) by regulating the endocytosis of NMDA receptor *via* phosphorylation of the scaffolding molecule PSD-95 (Morabito, 2004; Zhang et al., 2008).

Members of Cdk family, in particular Cdk5, contribute to gephyrin posphorylation at Ser270. Interestingly, this event seems to be tightly controlled by the level of expression of collybistin, being its down-regulation associated with a loss of gephyrin immunoreactivity as detected by the widely used monoclonal antibody mAb7a (Kuhse et al., 2012). The authors of this study showed that the antibody mAb7a is sensitive to gephyrin phosphorylation at that specific amino acid residue, making it a *bona fide* phospho-Ser270-specific monoclonal antibody. Therefore, the observed drastic reduction of mAb7a immunoreactivity observed upon collybistin knock-down or pharmacological inhibition of CDKs in cultured hippocampal neurons, indicated a reduction in gephyrin phosphorylation at Ser270 not necessarily associated with loss of synaptic gephyrin puncta. Experiments performed by using another gephyrin-specific antibody, not sensitive to its phosphorylation status, indeed demonstrated that the number and size of gephyrin clusters were not significantly affected by these treatments. Based on these results, in a mature cluster, gephyrin is expected to be constitutively phosphorylated at position 270, detectable by the mAb7a antibody, and to undergo selective dephosphorylation upon collybistin down-regulation. In contrast, results obtained from the characterization of GSK-3β dependent phosphorylation of gephyrin support an opposite scenario. Gephyrin assembled into a cluster is expected to be mainly dephosphorylated and to undergo activity-dependent GSK-3β mediated phosphorylation to promote its proteolytic degradation followed by cluster disassembly (Tyagarajan et al., 2011). Several speculations can be put forward to place these conflicting results in a more coherent picture. One possibility is that gephyrin builds different types of clusters, the one detected by mAb7a being characterized by high turnover rates. Alternatively, gephyrin scaffold is heterogenous in respect to gephyrin modifications and that phosphorylation at Ser270, as well as at neighboring positions, may generally act by restricting gephyrin oligomerization potential.

A question raised by these findings is how collybistin exerts its regulatory effect on Cdk5-dependent gephyrin phosphorylation. Collybistin is a key interactor of gephyrin known to participate in its membrane recruitment and synaptic targeting (Papadopoulos and Soykan, 2011). This activity relies on the presence of a Pleckstrin homology domain in collybistin sequence, a domain thought to mediate the attachment of the molecule to the membrane by binding to phosphoinositides (Hyvönen et al., 1995). Most collybistin isoforms expressed in neurons possesses at their N-terminus an SH3 regulatory domain that prevents their membrane-targeting function (Kins et al., 2000; Harvey et al., 2004). At GABAergic synapses only the cell adhesion molecule NL2 (Poulopoulos et al., 2009) and the α2 subunit of $GABA_A$Rs (Saiepour et al., 2010) are capable of relieving such SH3-mediated inhibition, possibly by binding to it, thus promoting a controlled recruitment of gephyrin scaffold. The authors of this study did not investigate the molecular mechanism responsible for collybistin influence on Cdk5 activity. Since Cdk5-dependent phosphorylation of gephyrin is controlled by collybistin expression level, one possible explanation is that Cdk5 catalytic activity is under the control of collybistin because it interacts with it or because gephyrin, while interacting with collybistin, better exposes the side chain of the amino acid residue undergoing post-translational modification.

ERK-DEPENDENT PHOSPHORYLATION OF GEPHYRIN AT Ser268 AFFECTS CLUSTERS SIZE AND DENSITY

Over the past decade, the ERK/MAPK (extracellular signal-regulated protein kinase/mitogen-activated protein kinase) pathway has been implicated in many forms of synaptic plasticity at glutamatergic synapses, including NMDA-dependent and independent forms of LTP. ERK1/2 activity enhances AMPA receptor functional properties by affecting their trafficking, by promoting the structural remodeling of activated spines as well as local protein synthesis (Thomas and Huganir, 2004). At GABAergic synapses ERK1, and to a lesser extent ERK2, were shown to be responsible for gephyrin phosphorylation at a serine residue located in close proximity to the previously recognized target of GSK-3β activity, namely serine 268 (Ser268). This residue attracted attention also because it is not phosphorylated in the C3-gephyrin splice variant, the isoform mainly expressed in non-neuronal cells (Ramming et al., 2000), and this suggests a selective biological significance in neurons.

ERK-mediated phosphorylation at this position was shown to specifically affect the size of post-synaptic gephyrin clusters. Interestingly, ERK and GSK-3β–catalyzed phosphorylations at their corresponding positions became to be functionally interconnected, leading to a coordinated regulation of cluster size

and density paralleled by corresponding changes in amplitude and frequency of GABAergic mIPSCs (Tyagarajan et al., 2013). In other words by inhibiting ERK activity, both cluster density and size were affected, suggesting that ERK exerts a control over GSK-3β activity.l. While the precise dynamics of these events is still unknown it is worth noting that both sites are embedded in a gephyrin domain that contains phosphorylation residues, including putative targets of the prolyl-isomerase Pin1 activity (see below), which render the scenario more complex. Moreover, Ser268 was found acetylated (together with additional nine residues). Even though the functional significance of this type of post-translational modification is unknown, Tyagarajan et al. (2013) hypothesized that acetylation may prevent unwanted phosphorylation by ERK and subsequent down-regulation of GABAergic transmission. Interestingly, ERK activity enhances the strength of glutamateric transmission while decreasing GABAergic transmission, leading to a shift of the E/I balance toward excitation. Therefore, dephosphorylation at Ser268 and/or its acetylation may represent plausible mechanisms to counteract the action of ERK at inhibitory synapses.

Though several issues still remain to be solved, ERK-mediated phosphorylation regulates cluster size *via* calpain activity, as previously demonstrated for GSK-3β–dependent regulation of cluster density. It is interesting to note that application of a broad spectrum phosphatase inhibitor to cultured hippocampal neurons was able to promote the reduction in size of gephyrin clusters, further supporting the functional role of phosphorylation in calpain-dependent gephyrin degradation (Bausen et al., 2010).

Pin1: A NEW PLAYER IN THE ORGANIZATION OF INHIBITORY POST-SYNAPTIC SPECIALIZATIONS

Protein phosphorylation on serine and threonine residues preceding a proline (the so-called proline-directed phosphorylation) has been shown to regulate cell signaling through conformational changes that are not simply due to the phosphorylation event *per se*. Peptidyl-prolyl isomerization of phosphorylated Ser/Thr-Pro sites represents the molecular mechanism utilized by Pro-directed phosphorylation to switch a target substrate between two different functional conformations. The existence of the mechanism relies on the unique stereochemistry of proline residues that within native polypeptides can adopt both *cis* and *trans* conformations. *Cis*-to-*trans* and *trans*-to-*cis* isomerization occur spontaneously but at very low rate: the speed of this event being further reduced upon serine or threonine phosphorylation (Yaffe et al., 1997). These conversions are greatly accelerated by ubiquitous enzymes named peptidyl-prolyl *cis-trans* isomerases (PPIases) or rotamase (Fanghänel and Fischer, 2004). These are divided into 4 families that are unrelated in their primary sequences and three-dimensional structures even though they catalyze the same reaction: cyclophilins (Cyps), FK506-binding proteins (FK506s), parvulins and the PP2A phosphatase activator (PTPA; Jordens et al., 2006). Pin1 and its homologs belong to the parvulin subfamily of PPIase and are the only known enzymes able to isomerise phosphorylated Ser/Thr-Pro sites that become resistant to the catalytic action of conventional prolyl-isomerases (Yaffe et al., 1997). This feature makes the action of Pin1 relevant in the modulation of signaling events, taking into account that Pro-directed kinases and phosphatases are conformation-specific and act only on the *trans* conformation (Weiwad et al., 2000; Zhou et al., 2000).

Pin1 was initially discovered by its ability to interact with the fungal mitotic kinase NIMA (Never In Mitosis A), pointing to an exclusive role for Pin1 in mitosis (Lu et al., 1996). The rapid identification of novel Pin1 substrates has clearly unveiled that this enzyme exerts control over a plethora of cellular processes not only in actively dividing cells but also in fully differentiated cells like post-mitotic neurons. Up to now the best characterized neuronal Pin1 substrates are represented by cytoskeletal proteins such as *tau*, amyloid-β-protein precursor, α-synuclein, and neurofilaments since aberrant interactions with these have implications for the development of neurodegenerative disorders such as Alzheimer disease (Lee et al., 2011), Parkinson disease and amyotrophic lateral sclerosis (Rudrabhatla and Pant, 2010). The involvement of Pin1 in physiological apoptotic events required for the proper development of the nervous system has been also identified (Becker and Bonni, 2006) as well as its contribution for long-lasting forms of synaptic plasticity at excitatory synapses (Westmark et al., 2010).

Gephyrin was identified as a novel target of post-phosphorylation prolyl-isomerization long before its identification as target of Ras/MAPK and PI3K/Akt signaling cascades (Zita et al., 2007). Based on a naïve approach, by inspecting gephyrin amino acid sequence, it was possible to identify 10 putative Pin1 consensus motifs mostly concentrated in the C-domain of gephyrin (**Figure 2**). In particular, while two clusters of three consensus sites were found to be localized within the C-domain, two additional couple of epitopes were located close to the C-terminus of the G-domain and close to the N-terminus of the E-domain, respectively. The C-domain's cluster encompassing the proline-rich region of gephyrin and containing serine 188, 194 and 200, was shown to be responsible for Pin1 recruitment, thus allowing Pin1-driven conformational changes of gephyrin substrate. Functionally, such structural remodeling of gephyrin molecule was shown to affect its binding affinity for the β subunit of the GlyR without affecting its oligomerization properties. In agreement with these findings, hippocampal neurons derived from Pin1 knockout mice demonstrated a loss in the number of GlyR immunoreactive puncta which were mirrored by a concomitant reduction in the amplitude of glycine-evoked currents. These data demonstrated for the first time that post-phosphorylation regulatory mechanisms can affect gephyrin-dependent clustering of inhibitory receptors, rendering it a potential mechanism involved in remodeling the post-synaptic device to sustain synaptic plasticity.

Is Pin1 also involved in GABAergic synaptic signaling? As already mentioned, gephyrin contribution to $GABA_AR$ dynamics requires the coordinated activity of several other associated proteins whose identification and functional characterization has just started to be addressed. At least two key molecules have emerged to play an essential role in regulating gephyrin accumulation at postsynapses, namely NL2 and collybistin (Poulopoulos et al., 2009). These molecules both possess in their sequences

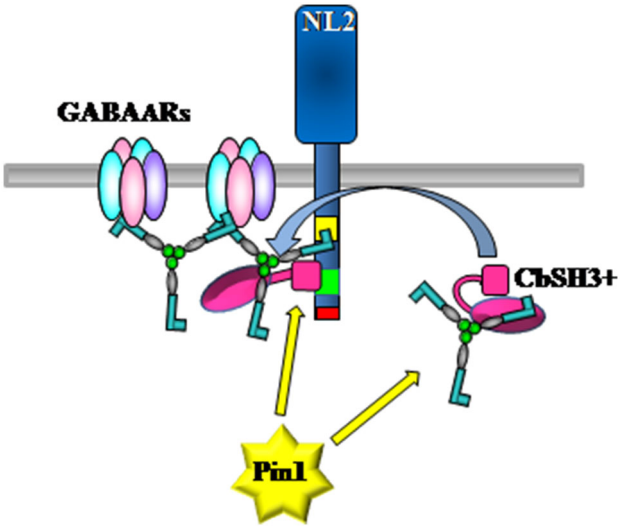

FIGURE 3 | Model of collybistin-driven recruitment of gephyrin by NL2 at GABAergic postsynapses. Pin1 may affect gephyrin/collybistin as well as gephyrin/NL2 interactions leading to an increase or decrease in gephyrin deposition at post-synaptic sites. The cytoplasmic domain of NL2 contains a gephyrin binding domain (yellow), a putative CBD (green) and a C-terminal PDZ binding domain (red).

putative Pin1 consensus motifs, raising the intriguing possibility that post-phosphorylation prolyl-isomerization regulates their reciprocal interaction leading to changes in gephyrin dynamics at synaptic sites (**Figure 3**). Based on this notion, it will be interesting to characterize whether alanine mutagenesis of specific Pin1 consensus sites, in particular the one located within the domains actively engaged in the interaction, would alter (enhancing or weakening) their binding affinity. In addition, it has been demonstrated that, to interact with NL2, gephyrin utilizes a region encompassing the whole C-terminal E-domain linked to a portion of the central region (amino acid 286-736). Two Pin1 consensus sites are present within this gephyrin portion, namely Ser319 and Thr337. As described above, mass spectrometry analysis performed on gephyrin immunoprecipitated from whole rat brain lysates showed that at least Ser319 is phosphorylated *in vivo* (Tyagarajan et al., 2013), making it able to modulate gephyrin/NL2 interaction. In addition, Ser319-Pro is located at the C-terminus of a short amino acid sequence identified as the collybistin binding domain (CBD) on gephyrin (Harvey et al., 2004). Interestingly, the CBD also contains two crucial residues for the interaction with $GABA_A$Rs α1, α2, and α3 subunits, namely Asp327 and Phe330 (Kim et al., 2006; Maric et al., 2011; Tretter et al., 2011). Therefore, a conformational change at this position would influence collybistin recruitment, thus affecting the efficiency of gephyrin synaptic targeting, and perhaps the ability of gephyrin to immobilize $GABA_A$Rs. Pin1 come into play once proline-directed phophorylation has occurred. This molecular switch is therefore positioned downstream the signaling cascades that orchestrate the precise phosphorylation patterns on their corresponding target molecules, thus being able to tune GABAergic transmission.

CONCLUDING REMARKS

The different roles played by the scaffolding molecule gephyrin at GABAergic synapses are still not completely understood. Gephyrin builds a stable scaffold underneath the synaptic plasma membrane to guarantee, over time, the appropriate number of $GABA_A$Rs being juxtaposed to pre-synaptic releasing sites. Despite its overall stability, the gephyrin scaffold must ensure rapid changes in its composition to sustain several forms of synaptic plasticity. One mechanism promoting dynamic changes at inhibitory PSD is represented by post-translational modifications, and in particular by reversible phosphorylation of several key components of the PSDs. The fact that phosphorylation plays a key role in regulating synapse re-arrangement is not new, being extensively characterized at the level of neurotransmitter receptors. The novelty consists in having identified new signaling pathways able to affect synaptic strength by acting on the scaffolding molecule itself *via* alterations of its clustering properties. We are still at the beginning of this new challenge but the data obtained so far disclose a complex scenario. Several serine and threonine residues were found phosphorylated on gephyrin isolated from mouse and rat brains, thus indicating that multiple pathways converge on gephyrin, modifying residues that are very close to each other and possibly functionally interconnected. Interestingly some of the phosphorylated sites were also found acetylated *in vivo*, raising the possibility that acetylation exerts and additional level of control by directly modulating gephyrin protein-protein interaction or by competing with specific phosphorylation targets.

Unveiling the hierarchy of each phosphorylation event, their cross-talks and their respective contribution to the functional organization of GABAergic synapses will require not only the identification of all kinases and phosphatases involved, but also an accurate analysis of their impact on various gephyrin activities, and in particular on $GABA_A$Rs trafficking and synaptic localization.

ACKNOWLEDGMENTS

This work was supported by a grant from Ministero Istruzione Universita' e Ricerca (MIUR, 2011) and from Telethon Foundation (GGP11043) to EC. The authors are grateful to Prof. John Nicholls for carefully reading the manuscript. They wish to thank the colleagues who contributed to some of the original work reported in this review and all members of the laboratory for useful discussions.

REFERENCES

Aranda, S., Alvarez, M., Turró, S., Laguna, A., and de la Luna, S. (2008). Sprouty2-mediated inhibition of fibroblast growth factor signaling is modulated by the protein kinase DYRK1A. *Mol. Cell. Biol.* 28, 5899–5911. doi: 10.1128/mcb.00394-08

Arévalo, J. C., and Wu, S. H. (2006). Neurotrophin signaling: many exciting surprises! *Cell. Mol. Life Sci.* 63, 1523–1537. doi: 10.1007/s00018-006-6010-1

Bausen, M., Weltzien, F., Betz, H., and O'Sullivan, G. A. (2010). Regulation of postsynaptic gephyrin cluster size by protein phosphatase 1. *Mol. Cell. Neurosci.* 44, 201–209. doi: 10.1016/j.mcn.2010.02.007

Becker, E. B., and Bonni, A. (2006). Pin1 mediates neural-specific activation of the mitochondrial apoptotic machinery. *Neuron* 49, 655–662. doi: 10.1016/j.neuron.2006.01.034

Bradley, C. A., Peineau, S., Taghibiglou, C., Nicolas, C. S., Whitcomb, D. J., Bortolotto, Z. A., et al. (2012). A pivotal role of GSK-3 in synaptic plasticity. *Front. Mol. Neurosci.* 5:13. doi: 10.3389/fnmol.2012.00013

Chandramouli, S., Yu, C. Y., Yusoff, P., Lao, D. H., Leong, H. F., Mizuno, K., et al. (2008). Tesk1 interacts with Spry2 to abrogate its inhibition of ERK phosphorylation downstream of receptor tyrosine kinase signaling. *J. Biol. Chem.* 283, 1679–1691. doi: 10.1074/jbc.m705457200

Choquet, D., and Triller, A. (2003). The role of receptor diffusion in the organization of the postsynaptic membrane. *Nat. Rev. Neurosci.* 4, 251–265. doi: 10.1038/nrn1077

Essrich, C., Lorez, M., Benson, J. A., Fritschy, J.-M., and Luscher, B. (1998). Postsynaptic clustering of major GABAA receptor subtypes requires the γ2 subunit and gephyrin. *Nat. Neurosci.* 1, 563–571.

Fanghänel, J., and Fischer, G. (2004). Insights into the catalytic mechanism of peptidyl prolyl cis/trans isomerases. *Front. Biosci.* 9, 3453–3478. doi: 10.2741/1494

Farrant, M., and Nusser, Z. (2005). Variations on an inhibitory theme: phasic and tonic activation of GABAA receptors. *Nat. Rev. Neurosci.* 6, 215–229. doi: 10.1038/nrn1625

Fritschy, J. M., Harvey, R. J., and Schwarz, G. (2008). Gephyrin: where do we stand, where do we go? *Trends Neurosci.* 31, 257–264. doi: 10.1016/j.tins.2008.02.006

Fuhrmann, J. C., Kins, S., Rostaing, P., El Far, O., Kirsch, J., Sheng, M., et al. (2002). Gephyrin interacts with Dynein light chains 1 and 2, components of motor protein complexes. *J. Neurosci.* 22, 5393–53402.

Günther, U., Benson, J., Benke, D., Fritschy, J. M., Reyes, G., Knoflach, F., et al. (1995). Benzodiazepine-insensitive mice generated by targeted disruption of the γ2-subunit gene of γ-aminobutyric acid type A receptors. *Proc. Natl. Acad. Sci. U S A* 92, 7749–7753. doi: 10.1073/pnas.92.17.7749

Hanus, C., Ehrensperger, M. V., and Triller, A. (2006). Activity-dependent movements of postsynaptic scaffolds at inhibitory synapses. *J. Neurosci.* 26, 4586–4595. doi: 10.1523/jneurosci.5123-05.2006

Harvey, K., Duguid, I. C., Alldred, M. J., Beatty, S. E., Ward, H., Keep, N. H., et al. (2004). The GDP-GTP exchange factor collybistin: an essential determinant of neuronal gephyrin clustering. *J. Neurosci.* 24, 5816–5826. doi: 10.1523/jneurosci.1184-04.2004

Hawasli, A. H., Benavides, D. R., Nguyen, C., Kansy, J. W., Hayashi, K., Chambon, P., et al. (2007). Cyclin-dependent kinase 5 governs learning and synaptic plasticity via control of NMDAR degradation. *Nat. Neurosci.* 10, 880–886. doi: 10.1038/nn1914

Herweg, J., and Schwarz, G. (2012). Splice-specific glycine receptor binding, folding and phosphorylation of the scaffolding protein gephyrin. *J. Biol. Chem.* 287, 12645–12656. doi: 10.1074/jbc.m112.341826

Hur, E. M., and Zhou, F. Q. (2010). GSK3 signalling in neural development. *Nat. Rev. Neurosci.* 11, 539–551. doi: 10.1038/nrn2870

Hyvönen, M., Macias, M. J., Nilges, M., Oschkinat, H., Saraste, M., and Wilmanns, M. (1995). Structure of the binding site for inositol phosphates in a PH domain. *EMBO J.* 14, 4676–4685.

Jordens, J., Janssens, V., Longin, S., Stevens, I., Martens, E., Bultynck, G., et al. (2006). The protein phosphatase 2A phosphatase activator is a novel peptidyl-prolyl cis/trans-isomerase. *J. Biol. Chem.* 281, 6349–6357. doi: 10.1074/jbc.m507760200

Kawasaki, B. T., Hoffman, K. B., Yamamoto, R. S., and Bahr, B. A. (1997). Variants of the receptor/channel clustering molecule gephyrin in brain: distinct distribution patterns, developmental profiles and proteolytic cleavage by calpain. *J. Neurosci. Res.* 49, 381–388. doi: 10.1002/(sici)1097-4547(19970801)49:3<381::aid-jnr13>3.0.co;2-2

Kim, E. Y., Schrader, N., Smolinsky, B., Bedet, C., Vannier, C., Schwarz, G., et al. (2006). Deciphering the structural framework of glycine receptor anchoring by gephyrin. *EMBO J.* 25, 1385–1395. doi: 10.1038/sj.emboj.7601029

Kim, H. J., and Bar-Sagi, D. (2004). Modulation of signalling by Sprouty: a developing story. *Nat. Rev. Mol. Cell Biol.* 5, 441–450. doi: 10.1038/nrm1400

Kins, S., Betz, H., and Kirsch, J. (2000). Collybistin, a newly identified brain-specific GEF, induces submembrane clustering of gephyrin. *Nat. Neurosci.* 3, 22–29. doi: 10.1038/71096

Kirsch, J., and Betz, H. (1995). The postsynaptic localization of the glycine receptor-associated protein gephyrin is regulated by the cytoskeleton. *J. Neurosci.* 15, 4148–4156.

Kneussel, M., and Betz, H. (2000). Receptors, gephyrin and gephyrin-associated proteins: novel insights into the assembly of inhibitory postsynaptic membrane specializations. *J. Physiol.* 525(Pt. 1), 1–9. doi: 10.1111/j.1469-7793.2000.t01-4-00001.x

Kowalczyk, S., Winkelmann, A., Smolinsky, B., Förstera, B., Neundorf, I., Schwarz, G., et al. (2013). Direct binding of GABAA receptor β2 and β3 subunits to gephyrin. *Eur. J. Neurosci.* 37, 544–554. doi: 10.1111/ejn.12078

Kuhse, J., Kalbouneh, H., Schlicksupp, A., Mükusch, S., Nawrotzki, R., and Kirsch, J. (2012). Phosphorylation of gephyrin in hippocampal neurons by cyclin-dependent kinase CDK5 at Ser-270 is dependent on collybistin. *J. Biol. Chem.* 287, 30952–30966. doi: 10.1074/jbc.m112.349597

Lai, K. O., and Ip, N. Y. (2009). Recent advances in understanding the roles of Cdk5 in synaptic plasticity. *Biochim. Biophys. Acta* 1792, 741–745. doi: 10.1016/j.bbadis.2009.05.001

Langosch, D., Hoch, W., and Betz, H. (1992). The 93 kDa protein gephyrin and tubulin associated with the inhibitory glycine receptor are phosphorylated by an endogenous protein kinase. *FEBS Lett.* 298, 113–117. doi: 10.1016/0014-5793(92)80034-e

Lee, T. H., Pastorino, L., and Lu, K. P. (2011). Peptidyl-prolyl cis-trans isomerase Pin1 in ageing, cancer and Alzheimer disease. *Expert Rev. Mol. Med.* 13:e21. doi: 10.1017/s1462399411001906

Li, B. S., Sun, M. K., Zhang, L., Takahashi, S., Ma, W., Vinade, L., et al. (2001). Regulation of NMDA receptors by cyclin-dependent kinase-5. *Proc. Natl. Acad. Sci. U S A* 98, 12742–12747. doi: 10.1073/pnas.211428098

Lu, K. P., Hanes, S. D., and Hunter, T. (1996). A human peptidyl-prolyl isomerase essential for regulation of mitosis. *Nature* 380, 544–547. doi: 10.1038/380544a0

Maric, H. M., Mukherjee, J., Tretter, V., Moss, S. J., and Schindelin, H. (2011). Gephyrin-mediated GABA(A) and glycine receptor clustering relies on a common binding site. *J. Biol. Chem.* 286, 42105–42114. doi: 10.1074/jbc.m111.303412

Meier, J., De Chaldée, M., Triller, A., and Vannier, C. (2000). Functional heterogeneity of gephyrins. *Mol. Cell Neurosci.* 16, 566–577. doi: 10.1006/mcne.2000.0899

Morabito, M. A. (2004). Cyclin-dependent kinase 5 phosphorylates the N-terminal domain of the postsynaptic density protein PSD-95 in neurons. *J. Neurosci.* 24, 865–876. doi: 10.1523/jneurosci.4582-03.2004

Mukherjee, J., Kretschmannova, K., Gouzer, G., Maric, H. M., Ramsden, S., Tretter, V., et al. (2011). The residence time of GABA(A)Rs at inhibitory synapses is determined by direct binding of the receptor α1 subunit to gephyrin. *J. Neurosci.* 31, 14677–14687. doi: 10.1523/jneurosci.2001-11.2011

Nelson, C. D., Kim, M. J., Hsin, H., Chen, Y., and Sheng, M. (2013). Phosphorylation of threonine-19 of PSD-95 by GSK-3β is required for PSD-95 mobilization and long-term depression. *J. Neurosci.* 33, 12122–12135. doi: 10.1523/jneurosci.0131-13.2013

Papadopoulos, T., and Soykan, T. (2011). The role of collybistin in gephyrin clustering at inhibitory synapses: facts and open questions. *Front. Cell. Neurosci.* 5:11. doi: 10.3389/fncel.2011.00011

Poo, M. M. (2001). Neurotrophins as synaptic modulators. *Nat. Rev. Neurosci.* 2, 24–32. doi: 10.1038/35049004

Poulopoulos, A., Aramuni, G., Meyer, G., Soykan, T., Hoon, M., Papadopoulos, T., et al. (2009). Neuroligin 2 drives postsynaptic assembly at perisomatic inhibitory synapses through gephyrin and collybistin. *Neuron* 63, 628–642. doi: 10.1016/j.neuron.2009.08.023

Prior, P., Schmitt, B., Grenningloh, G., Pribilla, I., Multhaup, G., Beyreuther, K., et al. (1992). Primary structure and alternative splice variants of gephyrin, a putative glycine receptor-tubulin linker protein. *Neuron* 8, 1161–1170. doi: 10.1016/0896-6273(92)90136-2

Ramming, M., Kins, S., Werner, N., Hermann, A., Betz, H., and Kirsch, J. (2000). Diversity and phylogeny of gephyrin: tissue-specific splice variants, gene structure and sequence similarities to molybdenum cofactor-synthesizing and cytoskeleton-associated proteins. *Proc. Natl. Acad. Sci. U S A* 97, 10266–10271. doi: 10.1073/pnas.97.18.10266

Rechsteiner, M. (1990). PEST sequences are signals for rapid intracellular proteolysis. *Semin. Cell Biol.* 1, 433–440.

Reddy-Alla, S., Schmitt, B., Birkenfeld, J., Eulenburg, V., Dutertre, S., Böhringer, C., et al. (2010). PH-domain-driven targeting of collybistin but not Cdc42 activation is required for synaptic gephyrin clustering. *Eur. J. Neurosci.* 31, 1173–1184. doi: 10.1111/j.1460-9568.2010.07149.x

Rudrabhatla, P., and Pant, H. C. (2010). Phosphorylation-specific peptidyl-prolyl isomerization of neuronal cytoskeletal proteins by Pin1: implications for

therapeutics in neurodegeneration. *J. Alzheimers Dis.* 19, 389–403. doi: 10.3233/JAD-2010-1243

Sabatini, D. M., Barrow, R. K., Blackshaw, S., Burnett, P. E., Lai, M. M., Field, M. E., et al. (1999). Interaction of RAFT1 with gephyrin required for rapamycin-sensitive signaling. *Science* 284, 1161–1164. doi: 10.1126/science.284.5417.1161

Saiepour, L., Fuchs, C., Patrizi, A., Sassoè-Pognetto, M., Harvey, R. J., and Harvey, K. (2010). Complex role of collybistin and gephyrin in $GABA_A$ receptor clustering. *J. Biol. Chem.* 285, 29623–29631. doi: 10.1074/jbc.m110.121368

Sarbassov, D. D., Ali, S. M., and Sabatini, D. M. (2005). Growing roles for the mTOR pathway. *Curr. Opin. Cell Biol.* 17, 596–603. doi: 10.1016/j.ceb.2005.09.009

Schrader, N., Kim, E. Y., Winking, J., Paulukat, J., Schindelin, H., and Schwarz, G. (2004). Biochemical characterization of the high affinity binding between the glycine receptor and gephyrin. *J. Biol. Chem.* 279, 18733–18741. doi: 10.1074/jbc.m311245200

Schwarz, G., Schrader, N., Mendel, R. R., Hecht, H. J., and Schindelin, H. (2001). Crystal structures of human gephyrin and plant Cnx1 G domains: comparative analysis and functional implications. *J. Mol. Biol.* 312, 405–418. doi: 10.1006/jmbi.2001.4952

Sola, M., Bavro, V. N., Timmins, J., Franz, T., Ricard-Blum, S., Schoehn, G., et al. (2004). Structural basis of dynamic glycine receptor clustering by gephyrin. *EMBO J.* 23, 2510–2519. doi: 10.1038/sj.emboj.7600256

Sola, M., Kneussel, M., Heck, I. S., Betz, H., and Weissenhorn, W. (2001). X-ray crystal structure of the trimeric N-terminal domain of gephyrin. *J. Biol. Chem.* 276, 25294–25301. doi: 10.1074/jbc.m101923200

Specht, C. G., Izeddin, I., Rodriguez, P. C., El Beheiry, M., Rostaing, P., Darzacq, X., et al. (2013). Quantitative nanoscopy of inhibitory synapses: counting gephyrin molecules and receptor binding sites. *Neuron* 79, 308–321. doi: 10.1016/j.neuron.2013.05.013

Su, S. C., and Tsai, L. H. (2011). Cyclin-dependent kinases in brain development and disease. *Annu. Rev. Cell Dev. Biol.* 27, 465–491. doi: 10.1146/annurev-cellbio-092910-154023

Südhof, T. C. (2008). Neuroligins and neurexins link synaptic function to cognitive disease. *Nature* 455, 903–911. doi: 10.1038/nature07456

Tanaka, S., Sekino, Y., and Shirao, T. (2000). The effects of neurotrophin3 and brain-derived neurotrophic factor on cerebellar granule cell movement and neurite extension in vitro. *Neuroscience* 97, 727–734. doi: 10.1016/s0306-4522(00)00049-x

Thoenen, H., Barde, Y. A., Davies, A. M., and Johnson, J. E. (1987). Neurotrophic factors and neuronal death. *Ciba Found. Symp.* 126, 82–95.

Thomas, G. M., and Huganir, R. L. (2004). MAPK cascade signalling and synaptic plasticity. *Nat. Rev. Neurosci.* 5, 173–183. doi: 10.1038/nrn1346

Tretter, V., Jacob, T. C., Mukherjee, J., Fritschy, J. M., Pangalos, M. N., and Moss, S. J. (2008). The clustering of GABA(A) receptor subtypes at inhibitory synapses is facilitated via the direct binding of receptor alpha 2 subunits to gephyrin. *J. Neurosci.* 28, 1356–1365. doi: 10.1523/jneurosci.5050-07.2008

Tretter, V., Kerschner, B., Milenkovic, I., Ramsden, S. L., Ramerstorfer, J., Saiepour, L., et al. (2011). Molecular basis of the γ-aminobutyric acid A receptor α3 subunit interaction with the clustering protein gephyrin. *J. Biol. Chem.* 286, 37702–37711. doi: 10.1074/jbc.M111.291336

Tretter, V., Mukherjee, J., Maric, H. M., Schindelin, H., Sieghart, W., and Moss, S. J. (2012). Gephyrin, the enigmatic organizer at GABAergic synapses. *Front. Cell. Neurosci.* 6:23. doi: 10.3389/fncel.2012.00023

Tyagarajan, S. K., Ghosh, H., Yévenes, G. E., Imanishi, S. Y., Zeilhofer, H. U., Gerrits, B., et al. (2013). Extracellular signal-regulated kinase and glycogen synthase kinase 3β regulate gephyrin postsynaptic aggregation and GABAergic synaptic function in a calpain-dependent mechanism. *J. Biol. Chem.* 288, 9634–9647. doi: 10.1074/jbc.m112.442616

Tyagarajan, S. K., Ghosh, H., Yévenes, G. E., Nikonenko, I., Ebeling, C., Schwerdel, C., et al. (2011). Regulation of GABAergic synapse formation and plasticity by GSK3beta-dependent phosphorylation of gephyrin. *Proc. Natl. Acad. Sci. U S A* 108, 379–384. doi: 10.1073/pnas.1011824108

Varoqueaux, F., Jamain, S., and Brose, N. (2004). Neuroligin 2 is exclusively localized to inhibitory synapses. *Eur. J. Cell Biol.* 83, 449–456. doi: 10.1078/0171-9335-00410

Viltono, L., Patrizi, A., Fritschy, J. M., and Sassoè-Pognetto, M. (2008). Synaptogenesis in the cerebellar cortex: differential regulation of gephyrin and GABAA receptors at somatic and dendritic synapses of Purkinje cells. *J. Comp. Neurol.* 508, 579–591. doi: 10.1002/cne.21713

Wang, Y., and Roach, P. J. (1993). Inactivation of rabbit muscle glycogen synthase by glycogen synthase kinase-3. Dominant role of the phosphorylation of Ser-640 (site-3a). *J. Biol. Chem.* 268, 23876–23880.

Weiwad, M., Küllertz, G., Schutkowski, M., and Fischer, G. (2000). Evidence that the substrate backbone conformation is critical to phosphorylation by p42 MAP kinase. *FEBS Lett.* 478, 39–42. doi: 10.1016/s0014-5793(00)01794-4

Westmark, P. R., Westmark, C. J., Wang, S., Levenson, J., O'Riordan, K. J., Burger, C., et al. (2010). Pin1 and PKMzeta sequentially control dendritic protein synthesis. *Sci. Signal.* 3:ra18. doi: 10.1126/scisignal.2000451

Woodgett, J. R., and Cohen, P. (1984). Multisite phosphorylation of glycogen synthase. Molecular basis for the substrate specificity of glycogen synthase kinase-3 and casein kinase-II (glycogen synthase kinase. *Biochim. Biophys. Acta* 788, 339–347.

Wuchter, J., Beuter, S., Treindl, F., Herrmann, T., Zeck, G., Templin, M. F., et al. (2012). A comprehensive small interfering RNA screen identifies signaling pathways required for gephyrin clustering. *J. Neurosci.* 32, 14821–14834. doi: 10.1523/jneurosci.1261-12.2012

Xiang, S., Nichols, J., Rajagopalan, K. V., and Schindelin, H. (2001). The crystal structure of *Escherichia coli* MoeA and its relationship to the multifunctional protein gephyrin. *Structure* 9, 299–310. doi: 10.1016/s0969-2126(01)00588-3

Yaffe, M. B., Schutkowski, M., Shen, M., Zhou, X. Z., Stukenberg, P. T., Rahfeld, J. U., et al. (1997). Sequence-specific and phosphorylation-dependent proline isomerization: a potential mitotic regulatory mechanism. *Science* 278, 1957–1960. doi: 10.1126/science.278.5345.1957

Zhang, S., Edelmann, L., Liu, J., Crandall, J. E., and Morabito, M. A. (2008). Cdk5 regulates the phosphorylation of tyrosine 1472 NR2B and the surface expression of NMDA receptors. *J. Neurosci.* 28, 415–424. doi: 10.1523/jneurosci.1900-07.2008

Zhou, X. Z., Kops, O., Werner, A., Lu, P. J., Shen, M., Stoller, G., et al. (2000). Pin1-dependent prolyl isomerization regulates dephosphorylation of Cdc25C and tau proteins. *Mol. Cell* 6, 873–883. doi: 10.1016/s1097-2765(00)00085-x

Zita, M. M., Marchionni, I., Bottos, E., Righi, M., Del Sal, G., Cherubini, E., et al. (2007). Post-phosphorylation prolyl isomerisation of gephyrin represents a mechanism to modulate glycine receptors function. *EMBO J.* 26, 1761–1771. doi: 10.1038/sj.emboj.7601625

Conflict of Interest Statement: The authors declare that the research was conducted in the absence of any commercial or financial relationships that could be construed as a potential conflict of interest.

Received: 30 January 2014; accepted: 22 March 2014; published online: 09 April 2014.
Citation: Zacchi P, Antonelli R and Cherubini E (2014) Gephyrin phosphorylation in the functional organization and plasticity of GABAergic synapses. Front. Cell. Neurosci. ***8****:103. doi: 10.3389/fncel.2014.00103*
This article was submitted to the journal Frontiers in Cellular Neuroscience.

PAPER GEPHYRIN

Gephyrin Regulates GABAergic and Glutamatergic Synaptic Transmission in Hippocampal Cell Cultures*

Zeynep Kasap Varley,[‡,1] Rocco Pizzarelli,[‡,1] Roberta Antonelli,[‡] Stefka H. Stancheva,[‡] Matthias Kneussel,[§] Enrico Cherubini,[‡] and Paola Zacchi[‡¶,2]

J Biol Chem. 2011 Jun 10; 286(23): 20942–20951.
Published online 2011 Apr 20. doi: 10.1074

THE JOURNAL OF BIOLOGICAL CHEMISTRY VOL. 286, NO. 23, pp. 20942–20951, June 10, 2011

Gephyrin Regulates GABAergic and Glutamatergic Synaptic Transmission in Hippocampal Cell Cultures*[S]

Received for publication, February 24, 2011, and in revised form, April 12, 2011 Published, JBC Papers in Press, April 20, 2011, DOI 10.1074/jbc.M111.234641

Zeynep Kasap Varley[‡1], Rocco Pizzarelli[‡1], Roberta Antonelli[‡], Stefka H. Stancheva[‡], Matthias Kneussel[§], Enrico Cherubini[‡], and Paola Zacchi[‡¶2]

From the [‡]Neurobiology Department and Italian Institute of Technology Unit, International School for Advanced Studies (SISSA) and [¶]Cluster in Biomedicine, Via Bonomea 265, 34136 Trieste, Italy and [§]Center for Molecular Neurobiology, Zentrum für Molekulare Neurobiologie, University of Hamburg Medical School, 20251 Hamburg, Germany

Gephyrin is a scaffold protein essential for stabilizing glycine and $GABA_A$ receptors at inhibitory synapses. Here, recombinant intrabodies against gephyrin (scFv-gephyrin) were used to assess whether this protein exerts a transynaptic action on GABA and glutamate release. Pair recordings from interconnected hippocampal cells in culture revealed a reduced probability of GABA release in scFv-gephyrin-transfected neurons compared with controls. This effect was associated with a significant decrease in VGAT, the vesicular GABA transporter, and in neuroligin 2 (NLG2), a protein that, interacting with neurexins, ensures the cross-talk between the post- and presynaptic sites. Interestingly, hampering gephyrin function also produced a significant reduction in VGLUT, the vesicular glutamate transporter, an effect accompanied by a significant decrease in frequency of miniature excitatory postsynaptic currents. Overexpressing NLG2 in gephyrin-deprived neurons rescued GABAergic but not glutamatergic innervation, suggesting that the observed changes in the latter were not due to a homeostatic compensatory mechanism. Pulldown experiments demonstrated that gephyrin interacts not only with NLG2 but also with NLG1, the isoform enriched at excitatory synapses. These results suggest a key role of gephyrin in regulating transynaptic signaling at both inhibitory and excitatory synapses.

Speed and reliability of synaptic transmission are essential for information coding and require the presence of clustered neurotransmitter receptors at the plasma membrane in precise apposition to presynaptic release sites. The postsynaptic organization comprises a large number of proteins that ensure the correct targeting, clustering, and stabilization of neurotransmitter receptors. Among them, the tubulin-binding protein gephyrin plays a crucial role in the functional organization of inhibitory synapses (1). Through its self-oligomerizing properties, gephyrin can form a hexagonal lattice that traps glycine (2) and $GABA_A$ receptors in the right place at postsynaptic sites (3, 4) by linking them to the cytoskeleton. Disruption of endogenous gephyrin leads to reduced $GABA_A$ receptor clusters (3), an effect that has been shown to be accompanied by a loss of GABAergic innervation (5, 6). This observation suggests the existence of cross-talk between the post- and presynaptic sites. The retrograde control of presynaptic signaling may occur via neuroligins (NLGs),[3] postsynaptic cell adhesion molecules known to transynaptically interact with presynaptic neurexins (7). NLG1 is enriched at glutamatergic synapses (8, 9), whereas NLG2 is preferentially associated with GABAergic connections (10). Overexpression of NLGs has been shown to increase the number of GABAergic and glutamatergic synaptic contacts (11). Interestingly, increasing the expression level of PSD-95, the scaffold molecule that directly binds NLG1, caused an enhancement of the glutamatergic innervation at the expense of the GABAergic one. This effect was accompanied by the recruitment of NLG2 to glutamatergic synapses (11–13). Moreover, the recent demonstration of a direct interaction between NLG2 and gephyrin (14) suggests a role for this protein in regulating transynaptic signaling at inhibitory connections. Altogether, these findings have led to the hypothesis that scaffolding molecules can establish and maintain the proper excitatory (E)/inhibitory (I) balance necessary for the correct functioning of neuronal networks, by modulating neuroligin localization and function at particular synapses (15–17). Understanding the molecular mechanisms involved in the maintenance of a proper E/I balance is a challenge as an alteration of this parameter underlies several devastating forms of neurological diseases including autism spectrum disorders (18). Previous studies on cultured hippocampal neurons have demonstrated that removal of gephyrin with single chain antibody fragments (scFv-gephyrin) (19) produces changes in the gating properties of $GABA_A$ receptors associated with a decrease in GABAergic innervation (6).

In the present study, scFv-gephyrin fragments were used to characterize further the transynaptic contribution of gephyrin to maintaining and stabilizing GABAergic synapses. Double patch experiments from monosynaptically connected cells revealed a reduction in the probability of GABA release to scFv-

* This work was supported by a grant from Ministero Istruzione, Università e Ricerca (MIUR) (to E. C.).

[S] The on-line version of this article (available at http://www.jbc.org) contains supplemental Figs. 1 and 2.

[1] Both authors contributed equally to this work.

[2] To whom correspondence should be addressed: Neurobiology Sector, SISSA, Via Bonomea 265, 34136 Trieste, Italy. Tel.: 39-040-3787773; Fax: 39-040-3787702; E-mail: zacchi@sissa.it.

[3] The abbreviations used are: NLG, neuroligin; D-AP5, D-2-amino-5-phosphonopentanoic acid; DNQX, 6,7-dinitroquinoxaline-2,3-dione; EGFP, enhanced green fluorescent protein; E/I, excitatory/inhibitory; EPSC, excitatory postsynaptic current; IPSC, inhibitory postsynaptic current; PPR, paired-pulse ratio; scFv, single chain antibody fragment; TPMPA, (1,2,5,6-tetrahydropyridin-4-yl)methylphosphinic acid; TTX, tetrodotoxin; VGAT, vesicular GABA transporter; VGLUT, vesicular glutamate transporter.

gephyrin-transfected cells. Moreover, transfection with scFv-gephyrin affected not only GABA but also glutamate release as demonstrated by the reduction in frequency of spontaneous and miniature glutamatergic synaptic events. Immunocytochemical data revealed a significant reduction in the number of NLG2 clusters together with a decrease of VGAT and VGLUT, the vesicular GABA and glutamate transporters, respectively. Finally, biochemical experiments demonstrated that gephyrin can form a complex not only with NLG2 but also with NLG1 in the brain, suggesting a role of this scaffold protein in regulating both excitatory and inhibitory synaptic transmission.

EXPERIMENTAL PROCEDURES

Neuronal and Cell Cultures—All experiments were carried out in accordance with the European Community Council Directive of 24 November 1986 (86/609 EEC) and were approved by the local authority veterinary service. Primary cell cultures were prepared as described previously (20). Briefly, 2–4-day-old (P2–P4) Wistar rats were decapitated after being anesthetized with an intraperitoneal injection of urethane (2 mg/kg). Hippocampi were dissected free, sliced, and digested with trypsin, mechanically triturated, centrifuged twice at 40 × *g*, plated in Petri dishes, and cultured for up to 14 days. Experiments were performed on cells cultured for at least 7 days. For paired recording experiments, neurons were plated at low density (~40,000 cells/ml).

HEK-293 cells were maintained in DMEM supplemented with 10% fetal calf serum, penicillin (100 units/ml), and streptomycin (100 mg/ml) and transiently transfected with various plasmid constructs using the standard calcium phosphate method. Cells were collected 24–48 h after transfection.

Construction of Plasmid Vectors, scFv-Gephyrin—Complementary DNAs encoding full-length FLAG-tagged gephyrin have been described previously (21). The N-terminal truncated gephyrin polypeptide (amino acids 2–188) fused to GFP is described by Maas *et al.* (22). It acts as a dominant negative protein due to its lack of dimerization motif and is able to deplete endogenous gephyrin clusters in neurites within 24 h of expression. The murine HA-tagged NLG1 and HA-tagged NLG2 were constructed as reported elsewhere (23, 24). HA-tagged NLG2Y770A point mutant was kindly provided by Dr. Varoqueaux (14). NLG2-GFP was constructed by using PCR-based mutagenesis. A PvuI restriction site was introduced 10 amino acids downstream of the sequence encoding for the transmembrane domain of NLG2-HA. This restriction site was then used to clone the EGFP coding sequence amplified using oligonucleotides containing PvuI consensus sites.

The last 94 amino acids of the cytoplasmic domains of both NLGs were inserted into pGEX4T1 vector for bacterial expressions as glutathione *S*-transferase (GST)-NLGs 94-amino acid fusion proteins. All PCR-amplified products were fully sequenced to exclude the possibility of second site mutations. The technique for isolating scFv-gephyrin has already been reported (19).

Neuronal Transfection and Immunocytochemistry—Hippocampal neurons in culture were transfected with EGFP alone or co-transfected with EGFP and scFv-gephyrin using the calcium phosphate transfection method. For each Petri dish, 3 μg of DNA was transfected in total. Reliable co-transfection was ensured by routinely transfecting 0.9 μg of EGFP and 2.1 μg of scFv-gephyrin and identified by the increased EGFP signal around the nucleus. For the rescue experiments, scFv-gephyrin and the full-length HA-tagged NLG2 (NLG2-HA), NLG2Y770A (NLG2Y770A-HA), and NLG1 (NLG1-HA) were co-transfected at a ratio of 1:2.

Neurons were transfected at 7 days *in vitro* and used for immunostaining 48 h later. All steps were carried out at room temperature. After fixation with 4% paraformaldehyde in PBS for 10 min, neurons were quenched in 0.1 M glycine in PBS for 5 min and permeabilized with 0.1% Triton X-100 in PBS for 2 min. For the rescue experiments, cells were fixed with pre-cooled 4% paraformaldehyde in PBS for 5 min at 4 °C then 5 min at room temperature. They were then blocked in 0.2% BSA/1% FCS or 10% FCS in PBS for 30 min. After incubation with primary antibodies for 1 h, cells were incubated with Alexa Fluorophore-conjugated secondary antibodies (1:400) for 45 min. In the case of double-immunostaining, cells were incubated with biotinylated secondary antibodies (1:100, 45 min) followed by streptavidin-conjugated fluorophores (1:100, 30 min). The coverslips were washed in PBS, rinsed in water, and mounted with VectaShield (Vector Laboratories).

The antibodies used were as follows: mouse monoclonal anti-VGAT (1:200, Synaptic Systems), mouse monoclonal anti-VGLUT1 (1:200, Synaptic Systems), rabbit polyclonal anti-NGL2 (1:200, Synaptic Systems), biotinylated goat anti-mouse IgG (Vector Laboratories). All secondary antibodies were obtained from Invitrogen.

In Vitro Binding, Immunoprecipitation, and Western Blot Analysis—Transfections were performed with the calcium phosphate method. GST pulldown assays were performed as described previously (21). For NLGs and gephyrin co-immunoprecipitation, HEK 293 cells overexpressing NLG1-HA/NLG2-HA and gephyrin-FLAG were lysed in 50 mM Tris-HCl, pH 7.5, 100 mM NaCl, 0.1% Tween 20, 10% glycerol, 10 mM EDTA, 2 mM $MgCl_2$, and protease inhibitor mixture and immunoprecipitated by the anti-FLAG antibody. Analysis of NLG1/NLG2-gephyrin interactions was performed on postnuclear homogenates from neonatal rat brains using the following lysis buffer: 50 mM-Tris HCl, pH 7.5, 150 mM NaCl, 0.5% CHAPS, 1 mM EDTA, 10% glycerol, and protease inhibitor mixture. After a 2-h incubation with monoclonal anti-gephyrin antibody, an immunoprecipitation experiment was performed according to standard procedures. Primary antibodies were revealed by HRP-conjugated secondary antibodies (Sigma) followed by ECL (Amersham Biosciences). The following primary antibodies were used: mouse monoclonal anti-FLAG M2 (Sigma), mouse monoclonal anti-gephyrin 3B11 (Synaptic Systems), high affinity rat monoclonal anti-HA 3F10 (Roche), rabbit polyclonal anti-NLG2 (Synaptic Systems), and rabbit polyclonal anti-NLG1 (Synaptic Systems).

Confocal Microscopy and Image Analysis—Fluorescence images were acquired on a TCS-SP confocal laser scanning microscope (Leica, Bensheim, Germany) with a 40× 1.4 NA oil immersion objective, additionally magnified 2-fold with the pinhole set at 1 Airy unit. Stacks of *z*-sections with an interval of 0.4 μm were sequentially scanned twice for each emission line

to improve the signal/noise ratio. Cluster analysis was carried out using MetaMorph Imaging System (Universal Imaging, Westchester, PA). First a binary template was created using the EGFP staining to identify transfected neurons, then cluster intensities in regions overlapping with the binary template were analyzed. Images were segmented to select immunofluorescent puncta over background labeling, and clusters were defined as >3 pixels as determined by visual inspection. Integrated Morphometry Analysis function of MetaMorph was used to quantify the number and size of clusters (four or five cells from at least four different experiments). For the rescue experiments, NLG2 staining was used to create the binary template for the NLG2-HA/scFv-gephyrin and NLG2Y770A-HA/scFv-gephyrin co-transfected cells. As excessive NLG2-HA expression masks the rescuing effect and results in an overall increase in synaptic staining (similar to NLG2-HA overexpression alone), cells with a moderate amount of NLG2-HA/NLG2Y770A-HA expression (as identified by the unsaturated NLG2 fluorescence signal) was selected for the analysis of the rescue effect. Representative figures were prepared using ImageJ software.

Electrophysiological Recordings—Spontaneous excitatory and inhibitory postsynaptic currents (EPSCs and IPSCs) were recorded at 9 days *in vitro* from cultured hippocampal neurons (transfected at 7 days *in vitro* with different constructs) at 22–24 °C using a Multiclamp 700A amplifier (Axon Instruments, Foster City, CA). In the case of transfected cells, mIPSCs or mEPSCs were recorded from single transfected cells surrounded by nontransfected ones. Patched cells were identified as putative principal cells on the basis of their passive membrane properties (V_{rest} and R_{input}) which were similar to those described in identified pyramidal neurons in culture at the same days *in vitro* (25). No differences were found in these parameters between control and transfected neurons. Pooled data gave a mean V_{rest} value of -51 ± 1 mV and a mean R_{input} value of 610 ± 43 megohms ($n = 47$). Patch electrodes pulled from borosilicate glass capillaries (Hilgenberg, Malsfeld, Germany) had a resistance of 3–4 megohms when filled with an intracellular solution containing 137 mM CsCl, 1 mM $CaCl_2$, 2 mM $MgCl_2$, 11 mM BAPTA, 2 mM ATP, and 10 mM HEPES (the pH was adjusted to 7.3–7.4 with CsOH). IPSCs were recorded at a holding potential of −70 mV in the presence of 20 μM 6,7-dinitroquinoxaline-2,3-dione (DNQX) and 50 μM D-2-amino-5-phosphonopentanoic acid (D-AP5) to block AMPA and NMDA receptors, respectively. EPSCs were recorded in the presence of 10 μM bicuculline and 50 μM D-AP5 to block $GABA_A$ and NMDA receptors, respectively. Miniature PSCs were recorded in the presence of tetrodotoxin (TTX, 1 μM) to block sodium currents and propagated action potentials and the respective $GABA_A$ or AMPA/NMDA receptor antagonists.

For double patch recordings, pairs of action potentials (at 50-ms interval) were evoked in nontransfected presynaptic neurons (in current clamp mode) by injecting depolarizing current pulses at a frequency of 0.1 Hz. IPSCs were detected from postsynaptic transfected (scFv-gephyrin) and nontransfected (controls) neurons in voltage clamp mode at a holding potential of 0 mV (near the reversal potential for glutamate). In this case, the intracellular solutions contained 135 mM $KMeSO_4$, 10 mM KCl, 10 mM HEPES, 1 mM $MgCl_2$, 2 mM Na_2ATP, and 0.4 mM Na_2GTP (the pH was adjusted to 7.3 with KOH). It is worth noting that the probability of finding interconnected cells was 10–20%. Only ~6% of all neurons in a culture dish are GABAergic, and usually these cells are morphologically distinguishable (26). In all experiments, the cells were perfused with an external solution containing 137 mM NaCl, 5 mM KCl, 2 mM $CaCl_2$, 1 mM $MgCl_2$, 20 mM glucose, and 10 mM HEPES, pH 7.4, with NaOH. Data were sampled at 10 kHz and low pass-filtered at 3 kHz. The stability of the patch was checked by repetitively monitoring the input and series resistances during the experiments. Cells exhibiting 15–20% changes were excluded from the analysis. The series resistance was 10–15 megohms. All drugs (except TTX, which was purchased from Latoxan, Valence, France) were obtained from Tocris (Cookson Ltd., Bristol, UK). All drugs were dissolved in external solution, except DNQX, which was dissolved in dimethyl sulfoxide. The final concentration of dimethyl sulfoxide in the bathing solution was 0.1%. At this concentration, dimethyl sulfoxide alone did not modify the shape or the kinetics of synaptic currents.

Data Analysis—The analysis of spontaneous events was performed with Clampfit 10.1 software (Axon Instruments, Foster City, CA). This program uses a detection algorithm based on a sliding template. The template did not induce any bias in the sampling of events because it was moved along the data trace one point at a time and was optimally scaled to fit the data at each position. The detection criterion was calculated from the template-scaling factor and from how closely the scaled template fitted the data.

For evoked IPSCs, transmission failures were identified visually. Mean IPSC amplitude was obtained by averaging successes and failures. The paired-pulse ratio (PPR), known to be inversely correlated to the initial release probability (27), was calculated as the ratio between the mean amplitudes of IPSC2 over IPSC1. The coefficient of variation (CV^{-2}) was calculated as the square root of the ratio between the standard deviation of IPSC1 and the mean amplitude of IPSC1 (28).

Values are given as mean ± S.E. Unless otherwise stated, significance of differences was assessed by Student's *t* test. The differences were considered significant when $p < 0.05$.

RESULTS

Impairing Gephyrin Function with scFv-Gephyrin Reduces the Probability of GABA Release—As recently reported (6), transfecting cultured hippocampal neurons with scFv-gephyrin reduced the number of gephyrin and synaptic γ2 subunit-containing $GABA_A$ receptor clusters. These effects were associated with a severe impairment of both phasic and tonic $GABA_A$ receptor-mediated inhibition. The mechanisms underlying these effects relied on changes in GABAergic innervation as suggested by the concomitant reduction in the number and size of presynaptic VGAT clusters.

According to the quantal theory, the synaptic efficacy *E*, the mean amplitude of unitary IPSCs, can be defined as $E = mQ$, where *m* is the quantal content or mean number of quanta released per presynaptic action potential and *Q* is the quantal size or amplitude of the unitary IPSC (29). Whereas *Q* depends on both pre- and postsynaptic mechanisms, *m* depends on presynaptic factors, namely the number of release sites *N* and the

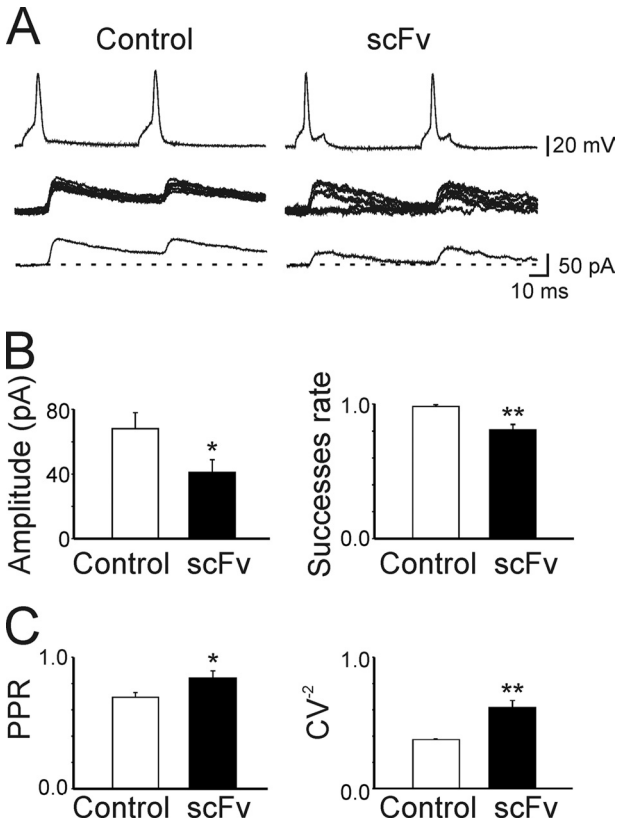

FIGURE 1. **Hampering gephyrin function with scFv-gephyrin reduces the probability of GABA release.** *A*, pair recordings obtained from two interconnected neurons. The postsynaptic cell was transfected with scFv-gephyrin (*right*). As control a neighboring nontransfected cell was used (*left*). *Top traces* are pairs of action potentials evoked in presynaptic cells at a 50-ms interval by depolarizing current steps of variable amplitude every 10 s. *Middle traces* are monosynaptic IPSCs (successes and failures) evoked at 0 mV (E_{GABA} −70 mV) by presynaptic action potentials. *Bottom traces* are averaged responses. *B*, mean amplitude and successes rate obtained in monosynaptically connected cells in control (*white columns*; $n = 7$) and in scFv-transfected neurons (*black columns*). *C*, PPR and CV^{-2} of monosynaptically connected neurons ($n = 6$) recorded from control and scFv-transfected cells. *, $p < 0.05$; **, $p < 0.01$. *Error bars*, S.E.

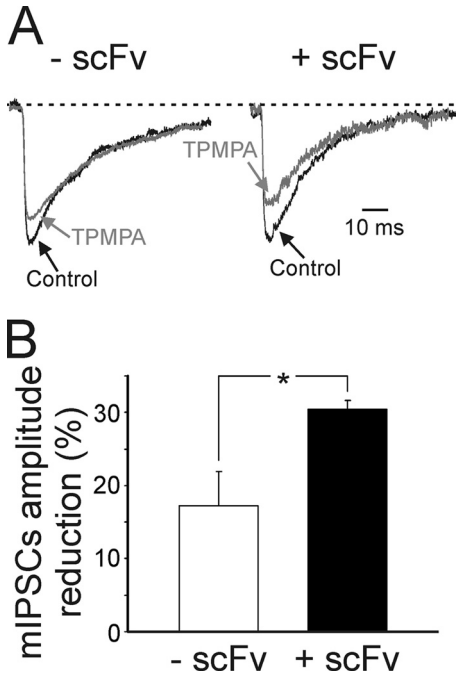

FIGURE 2. **The removal of gephyrin with scFv reduces synaptic GABA transient in the cleft.** *A*, representative traces of mIPSCs recorded at −70 mV (*dashed lines*) from a control (*left*) and from a scFv-gephyrin-transfected cell (*right*) in the absence (*black*) or in the presence of TPMPA 100 μM (gray). In both cases, mIPSC amplitudes are normalized to those obtained in pre-drug conditions. Each *trace* is the average of 20–30 individual traces. *B*, each column representing the mean TPMPA-induced reduction in amplitude of mIPSCs in control (*white*, $n = 7$) and scFv-gephyrin-transfected cells (*black*, $n = 6$; *, $p < 0.05$). Note the significantly larger TPMPA inhibition in transfected cells. *, $p < 0.05$. *Error bars*, S.E.

probability of release (*P*). To see whether a decrease in quantal content could account for the observed effects, simultaneous recordings were obtained from pairs of interconnected neurons (the postsynaptic one expressing or not expressing scFv-gephyrin; see "Experimental Procedures"). As shown in Fig. 1, IPSCs evoked in nontransfected cells by pairs of presynaptic action potentials (50 ms apart, delivered at a frequency of 0.1 Hz, Control) were highly reliable and usually did not exhibit synaptic failures. In contrast, with respect to control, IPSCs from scFv-gephyrin-transfected cells ($n = 6$) exhibited a significant reduction in amplitude (from 68.2 ± 9.7 pA to 41.1 ± 7.8 pA; $p < 0.05$, Mann-Whitney Rank test) and in successes rate (from 0.98 ± 0.01 to 0.80 ± 0.03; $p < 0.01$, Mann-Whitney Rank test; Fig. 1, *A* and *B*). These effects were associated with a significant increase in the PPR (from 0.69 ± 0.03 to 0.84 ± 0.05; $p < 0.05$; Fig. 1*C*), which is considered an index of presynaptic release probability (27, 28). Furthermore, the coefficient of variation (CV^{-2}) was significantly increased (from 0.37 ± 0.007 to 0.61 ± 0.05; $p < 0.01$; Fig. 1*C*), indicating changes in quantal content (28).

To assess further whether gephyrin depletion affects presynaptic GABA release, as an additional approach we used 100 μM TPMPA, a weak competitive $GABA_A$ receptor antagonist that has a very fast dissociation constant and competes with synaptically released GABA for the ligand binding site on $GABA_A$ receptors (30, 31). The reduction of mIPSC amplitude by TPMPA would therefore be influenced by relative changes in synaptic GABA transient in the cleft (31). As shown in Fig. 2, in scFv-gephyrin-transfected cells, the block of mIPSCs by TPMPA was significantly ($p < 0.05$) larger than controls (30.4 ± 1.3% *versus* 17.2 ± 4.7%; $n = 6$ for scFv-gephyrin and 7 for controls; $p < 0.5$; Fig. 2, *A* and *B*), indicating that for scFv-gephyrin-transfected cells, GABA concentration in the cleft was lower than control. Overall, these data strongly suggest that hampering gephyrin function with scFv-gephyrin reduces the release of GABA from presynaptic terminals.

Gephyrin 2–188, a Dominant Negative Form of Gephyrin, Mimics the Effect of scFv-Gephyrin on GABAergic Function—To validate the results obtained with scFv-gephyrin, a truncated gephyrin polypeptide comprising the N-terminal (amino acids 2–188) of gephyrin fused with EGFP, known to act as a dominant negative protein, was used (22). Due to the lack of dimerization motif, this polypeptide interferes with the endogenous gephyrin lattice formation and depletes gephyrin clusters in neurites within 24 h of expression on cultured neurons.

Immunocytochemical experiments on hippocampal neurons transfected with gephyrin 2–188 revealed a significant reduction in the number of VGAT clusters (without an effect on their

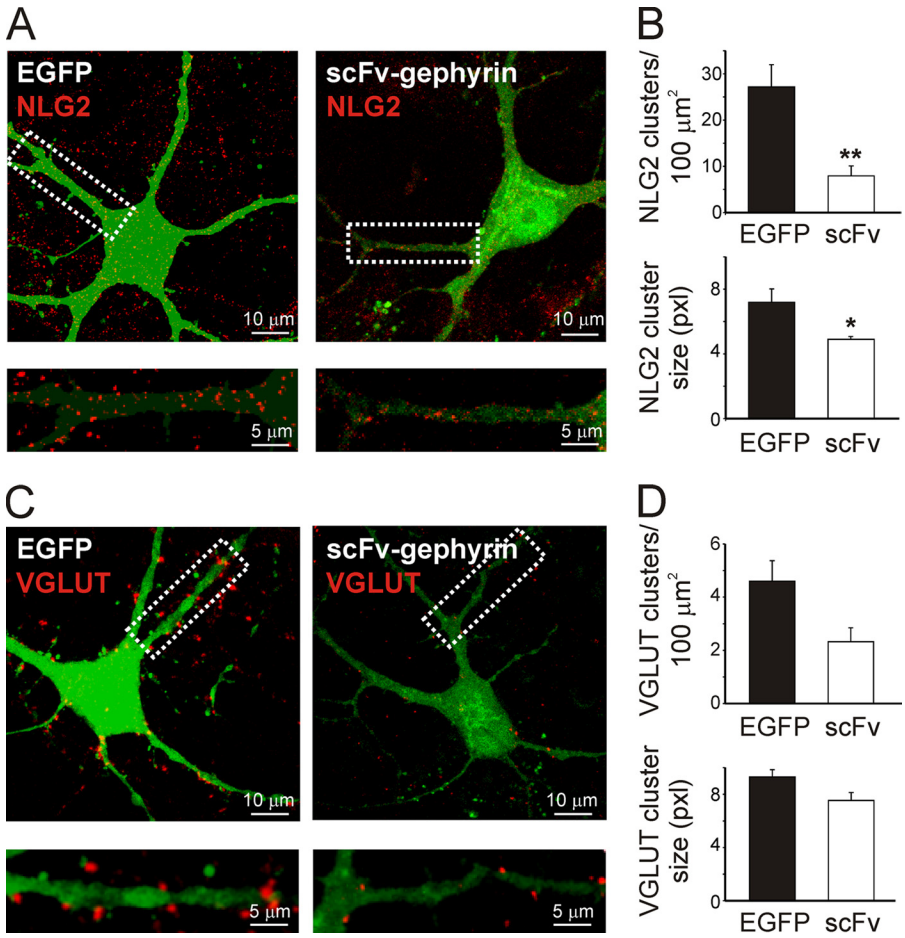

FIGURE 3. **scFv-gephyrin reduces the number and size of NLG2 and VGLUT clusters.** *A*, neurons transfected (*green*) with EGFP (*left*) or EGFP/scFv-gephyrin (*right*) and immunostained for NLG2 (*red*). *Bottom panels* are magnifications of the *white boxes* marked on *top*. *B*, quantification of NLG2 clusters density (*top*) and cluster size (*bottom*). *C* and *D*, as in *A* and *B*, but neurons were immunostained for the presynaptic glutamatergic marker VGLUT (*red*). Note the significant reduction in the density and size of NLG2 and VGLUT clusters. *, $p < 0.05$; **, $p < 0.01$. *Error bars*, S.E.

size), indicating an effect on GABAergic innervation similar to that observed for scFv-gephyrin (supplemental Fig. 1, *A* and *B*). As with scFv-gephyrin, this effect was accompanied by a significant reduction in amplitude and frequency of spontaneous and miniature IPSCs (in cells transfected with gephyrin 2–188 the reduction in amplitude of sIPSCs and mIPSCs was 54 ± 9% and 79 ± 9% of controls, respectively; the reduction in frequency of sIPSCs and mIPSCs was 32 ± 7% and 37 ± 1% of controls, respectively; supplemental Fig. 1, *C–E*). These data further support the hypothesis that gephyrin not only regulates postsynaptic organization of synaptic $GABA_A$ receptors but also GABAergic innervation.

Gephyrin Removal Reduces the Density and Size of Neuroligin 2 Clusters—How can gephyrin interfere with GABA release? One possibility is that this protein interacts with cell adhesion molecules such as neuroligins which, by binding neurexins, ensure the cross-talk between the pre- and postsynaptic sites (7). Of particular interest is NLG2, because this protein is known to play a pivotal role in the organization of GABAergic synapses (14). To verify whether disrupting gephyrin affects NLG2 distribution, hippocampal neurons transfected with scFv-gephyrin were immunostained for NLG2.

As shown in Fig. 3, *A* and *B*, scFv-gephyrin-transfected neurons exhibited a significant reduction in the density of NLG2-positive clusters compared with EGFP-transfected controls (7.9 ± 2.1 clusters/100 μm^2 for scFv-gephyrin *versus* 27.2 ± 4.8 clusters/100 μm^2 for EGFP; $p < 0.01$; $n = 9$). In addition, the average size of these clusters was smaller for scFv-gephyrin- than for EGFP-transfected neurons (4.9 ± 0.2 μm^2 for scFv-gephyrin *versus* 7.2 ± 0.8 μm^2 for EGFP; $p < 0.05$; $n = 9$). NLG2 did not relocalize to glutamatergic synapses because the synaptic fraction co-localized with VGLUT was barely detectable (4.1 ± 0.01% in control and 5.3 ± 0.02% in scFv-gephyrin-transfected cells, respectively; these values were not significantly different; $p > 0.05$; data not shown).

Impairing Gephyrin Function with scFv-Gephyrin Reduces Glutamatergic Innervation—The interaction of NLGs with scaffolding proteins is crucial for ensuring the correct excitatory/inhibitory balance, critical for the proper functioning of neuronal networks. Therefore, the following experiments were performed to assess whether disrupting gephyrin function with scFv-gephyrin can affect not only GABAergic but also glutamatergic transmission.

To this aim, cultured hippocampal neurons transfected with scFv-gephyrin were immunostained for VGLUT, a widely used marker for presynaptic glutamatergic terminals (32). Compared with controls (EGFP-transfected cells) in scFv-gephyrin-transfected cells VGLUT-immunopositive clusters were signif-

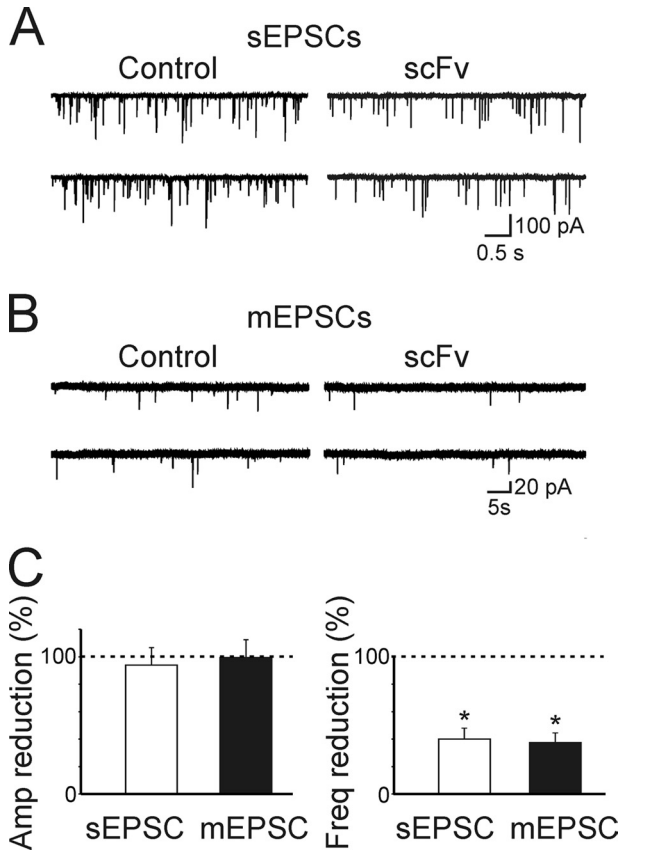

FIGURE 4. **scFv-gephyrin reduces the frequency but not the amplitude of sEPSCs and mEPSCs.** *A*, samples of spontaneous EPSCs recorded from controls and scFv-gephyrin-transfected neurons at a holding potential of −70 mV in the presence of 10 μM bicuculline and 50 μM D-AP5. *B*, samples of miniature EPSCs recorded from controls and scFv-gephyrin-transfected neurons at a holding potential of −70 mV in the presence of 1 μM TTX. *C*, each *column* reprsents the reduction in amplitude (*left*) and in frequency (*right*) of sIPSC (*white*) and mIPSCs (*black*) obtained from scFv-gephyrin-transfected neurons ($n = 12$) and expressed as percentage of controls ($n = 12$; *dashed lines*). *, $p < 0.05$. *Error bars*, S.E.

icantly reduced in density and size (Fig. 3, *C* and *D*). In particular, the density of VGLUT clusters was reduced from 4.6 ± 0.8 clusters/100 μm^2 in EGFP to 2.3 ± 0.5 clusters/100 μm^2 in scFv-gephryin ($p < 0.05$; $n = 12$). The size of these clusters was reduced from 9.3 ± 0.5 μm^2 to 7.5 ± 0.6 μm^2 ($p < 0.05$). Furthermore, whole cell voltage clamp recordings performed in the presence of bicuculline (10 μM) and D-AP5 (50 μM), to block $GABA_A$ and NMDA receptors, respectively, revealed a significant reduction in frequency (but not in amplitude) of spontaneous EPSCs (the frequency reached 40 ± 8%; $p < 0.05$; $n = 12$; the amplitude 95 ± 13%; $p > 0.05$; $n = 12$) recorded from scFv-gephyrin-transfected neurons compared with controls (Fig. 4, *A* and *C*). Similarly, in scFv-gephyrin-transfected cells, the frequency of miniature EPSCs recorded in the presence of TTX was significantly reduced with respect to controls (to 37 ± 7%; $p < 0.05$; from 0.78 ± 0.14 Hz to 0.32 ± 0.05 Hz; $n = 12$) whereas the amplitude was unchanged (to 100 ± 13%; $p > 0.05$; from 34 ± 6 pA to 34 ± 5 pA; $n = 7$; Fig. 4, *B* and *C*). Altogether, these results strongly support the involvement of gephyrin in regulating not only GABAergic but also glutamatergic synaptic transmission.

The Loss of GABAergic but Not Glutamatergic Innervation in Gephyrin-deprived Neurons Can Be Rescued by Overexpressing NLG2—To assess further the possibility that the reduced GABAergic innervation in scFv-gephyrin-transfected cells is mediated by NLG2 which may convey information in a retrograde way from post- to presynaptic sites, NLG2 was co-expressed with scFv-gephyrin. In immunocytochemical experiments, co-expression of NLG2 with scFv-gephyrin induced a significant increase in the density of VGAT-positive clusters compared with cells transfected with scFv-gephyrin alone (180 ± 8%; from 10.6 ± 0.7 clusters/100 μm^2 to 19.1 ± 0.9 clusters/100 μm^2; $p < 0.01$; $n = 11$ and 8 for scFv and scFv/NLG2, respectively), restoring VGAT cluster density to control levels (Fig. 5, *A* and *B*). In line with previous studies (9), overexpression of NLG2 alone led to a 2-fold increase in the density of VGAT clusters compared with EGFP-transfected controls (data not shown).

Parallel electrophysiological experiments from cultured neurons revealed no changes in amplitude and frequency of spontaneous mIPSCs between cells co-transfected with scFv-gephyrin/NLG2 and controls (neighboring nontransfected cells). On average, the frequency of mIPSCs was 0.211 ± 0.040 Hz and 0.213 ± 0.044 Hz ($p = 0.97$) whereas the amplitude was −55 ± 4 pA and −53 ± 6 pA ($p = 0.7$) in control ($n = 7$) and in co-transfected neurons ($n = 8$), respectively (Fig. 5*B*).

To see whether the observed rescue was gephyrin-dependent, similar experiments were performed using the NLG2 mutant (NLG2Y770A-HA) which lacks gephyrin binding (14). In this case, the number of VGAT-positive clusters/100 μm^2 was 19.8 ± 1.7 ($n = 9$), a value not significantly different from that obtained with NLG2 ($p > 0.5$; supplemental Fig. 2*A*).

In electrophysiological recordings, no changes in amplitude or frequency of mIPSCs were detected between scFv-gephyrin/NLG2Y770A-transfected cells and controls. The frequency of mIPSCs was 0.22 ± 0.07 Hz and 0.16 ± 0.06 Hz in control ($n = 7$) and in scFv-gephyrin/NLG2Y770A-transfected cells ($n = 6$), respectively ($p > 0.05$; supplemental Fig. 2, *B* and *C*). The amplitude of mIPSCs was 42 ± 5 pA and 32 ± 5 pA in the absence or in the presence of scFv-gephyrin/NLG2Y770A, respectively (supplemental Fig. 2, *B* and *C*).

Altogether, these experiments indicate that overexpression of NLG2 is able to rescue the loss of GABAergic innervation induced by scFv-gephyrin. However, our data with NLG2Y770A suggest that this effect only partially relies on the direct recruitment of gephyrin by NLG2 at inhibitory synapses (see "Discussion").

It is possible that the observed reduction in glutamatergic innervation following gephyrin depletion with scFv-gephyrin represents a homeostatic compensatory mechanism to prevent hyperexcitability and to maintain the right E/I balance within the neuronal network (33). If this is the case, rescuing GABAergic innervation should lead to a concomitant change in glutamatergic transmission. However, this was not the case because overexpressing NLG2 in gephyrin-depleted neurons failed to restore VGLUT immunoreactive puncta (0.5 ± 0.1 and 0.6 ± 0.1 clusters/100 μm^2 for scFv and scFv/NLG2, respectively; $p > 0.5$; Fig. 5*C*) as well as the frequency of mEPSCs to control levels. The frequency of mEPSCs was 0.64 ± 0.16 Hz and 0.26 ±

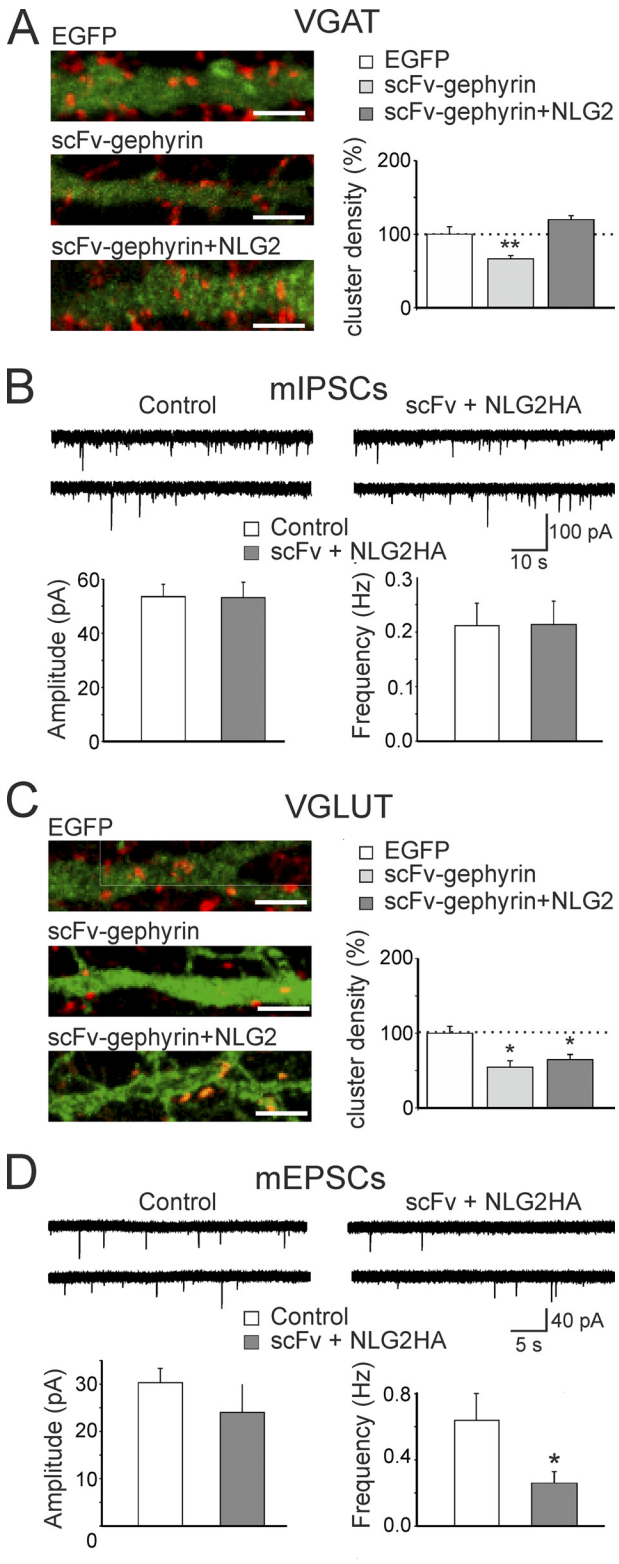

FIGURE 5. **Co-expression of NLG2 with scFv-gephyrin restores the loss of GABAergic but not glutamatergic innervation.** *A*, *left*, representative images of neurons transfected with EGFP (*top*), scFv-gephyrin (*middle*) or co-transfected with scFv-gephyrin and NLG2-HA (*bottom*). Dendrites were visualized by EGFP signal or NLG2 staining (*green*). Neurons were immunostained for VGAT (*red*). *Scale bars*, 5 μm. *Right*, quantification of VGAT cluster densities relative to the mean value obtained from EGFP-transfected neurons (*dashed line*). **, $p < 0.01$. *C* and *D*, as in *A* and *B* but for neurons immunostained for VGLUT (*red*). *Scale bars*, 5 μm. *B*, samples of spontaneous mIPSCs recorded from cells co-transfected with scFv-gephyrin plus NLG2-HA and from neighboring nontransfected cells (*Control*) at a holding potential of −70 mV in the presence of 1 μM TTX, 20 μM DNQX, and 50 μM D-AP5. The *columns* below the *traces* represent the mean amplitude (*left*) and frequency (*right*) of mIPSC from control (*white*; $n = 7$) and from scFv-gephyrin-transfected cells (*gray*; $n = 8$). *C*, as in *A* but for cells immunostained for VGLUT. *D*, as in *B* but for mEPSCs. These were recorded from cells co-transfected with scFv-gephyrin plus NLG2-HA ($n = 9$) and from neighboring nontransfected cells (*Control*, $n = 8$) in the presence of 1 μM TTX and 10 μM bicuculline. *Error bars*, S.E.

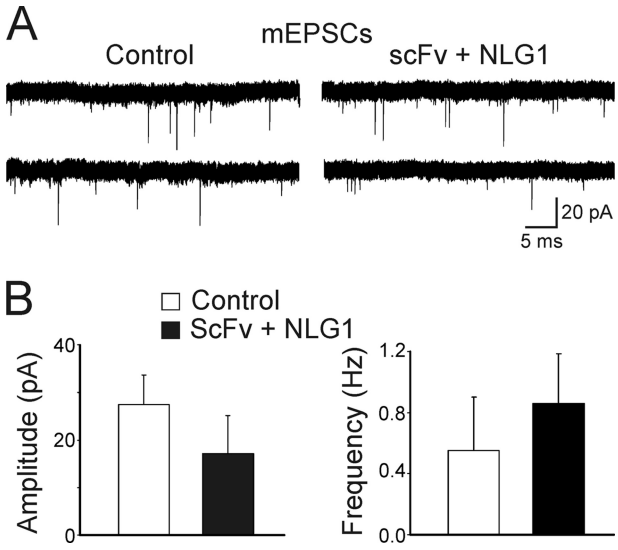

FIGURE 6. **Co-expression of NLG1 with scFv-gephyrin restores glutamatergic innervation.** *A*, samples of spontaneous mIPSCs recorded from cells co-transfected with scFv-gephyrin plus NLG1 and from neighboring non-transfected cells (*Control*) at a holding potential of −70 mV in the presence of 1 μM TTX and 10 μM bicuculline are shown. *B*, each column represents the mean amplitude (*left*) and frequency (*right*) of mIPSC from control (*white*, $n = 7$) and from scFv-gephyrin/NLG1-transfected cells (*black*, $n = 5$).

0.07 Hz in the absence or presence of NLG2 overexpression; $p < 0.05$; the amplitude of mEPSCs was 29 ± 3 pA and 25 ± 7 pA in the absence ($n = 8$) or in the presence ($n = 9$) of NLG2 overexpression ($p > 0.05$; Fig. 5*D*).

However, the co-expression of NLG1 with scFv-gephyrin was able to rescue the frequency of mEPSCs to control levels. The frequency of mEPSCs was 0.55 ± 0.35 Hz and 0.86 ± 0.33 Hz in control ($n = 7$) and in scFv-gephyrin/NLG1-transfected cells ($n = 5$), respectively ($p > 0.05$; Fig. 6). No changes in mEPSC amplitude were detected between control and scFv-gephyrin/NLG1-transfected cells (27 ± 6 pA in the absence and 17 ± 8 pA in the presence of NLG1 overexpression; $p > 0.05$; Fig. 6). Overall, these data indicate that the observed NLG1-induced rescue of glutamatergic function in gephyrin-deprived neurons is at least partially dependent on gephyrin activity.

Gephyrin Interacts Directly with NLG1—It has been recently reported that at inhibitory synaptic contacts gephyrin binds NLG2 directly (14). The amino acid sequence identified as gephyrin-binding motif on NLG2 is highly conserved in all NLGs, and indeed gephyrin binds to all four NLGs in yeast two-hybrid assays (14). To test whether gephyrin can form a complex with NLG1 in mammalian cells, lysates of HEK-293 cells transfected with gephyrin-FLAG were subjected to a pull-down assay with beads loaded with GST-NLG1 cytoplasmic domain ($NLG1_{CD}$), GST-$NLG2_{CD}$, or with GST alone as a negative control. In agreement with previous observations (14), $NLG2_{CD}$ was able to precipitate a consistent amount of gephy-

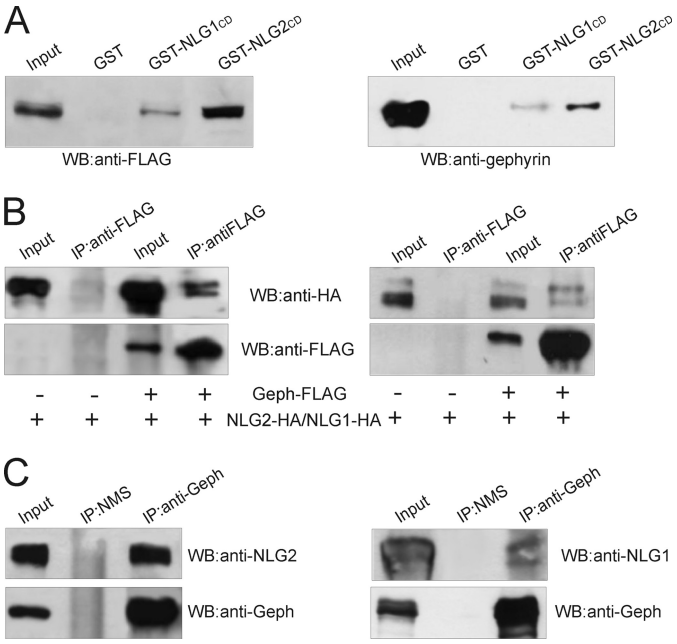

FIGURE 7. **Gephyrin interacts with NLG2 and NLG1.** *A*, GST-NLG1/2$_{CD}$ pull-down assay using lysates of HEK-293 cells transfected with gephyrin-FLAG (*left*) and rat brain lysates (*right*). *B*, lysates of HEK-293 cells transfected with either NLG2-HA (*left*) or NLG1-HA (*right*) in the presence of gephyrin-FLAG or with the vector alone (as a negative control) immunoprecipitated with monoclonal anti-FLAG antibodies. Immunoprecipitates were analyzed by Western blotting using anti-HA and anti-FLAG monoclonal antibodies. *C*, co-immunoprecipitation experiments on rat brain lysates using a monoclonal anti-gephyrin antibody and normal mouse serum (*NMS*) as negative control. Immunoprecipitates were analyzed by Western blotting using a monoclonal anti-gephyrin antibody and a polyclonal antibody against NLG2 and NLG1.

rin-FLAG (Fig. 7*A*, *left*). Interestingly, a small but significant fraction of gephyrin-FLAG was also found in complex with GST-NLG1$_{CD}$ (Fig. 7). Similar pulldown experiments were then performed to assay the ability of endogenous gephyrin present on neonatal rat brain homogenates to interact with NLG1 and NLG2. Also in this case gephyrin was not only associated with GST-NLG2$_{CD}$ fusion protein but also with GST-NLG1$_{CD}$ (Fig. 7*A*, *right*). Here, the immunoblot analysis was performed using a monoclonal antibody raised against the C-terminal domain of gephyrin.

We then performed immunoprecipitation experiments to investigate the presence of NLG1-HA/gephyrin-FLAG complexes *in vitro*. HEK-293 cells were co-transfected with plasmids encoding for NLG1/2-HA and gephyrin-FLAG, or NLG1/2-HA alone, and cell lysates were immunoprecipitated with the anti-FLAG monoclonal antibody. The bound protein complexes were analyzed by Western blotting using anti-HA and anti-FLAG for NLG1 and gephyrin detection, respectively. As shown in Fig. 7*B* (*right*), NLG1-HA was immunoprecipitated only from cells co-expressing gephyrin-FLAG. The same experimental conditions were also applied to detect the expected presence of NLG2-HA/gephyrin-FLAG complexes in mammalian cells. Indeed, we found that a lower amount of gephyrin-FLAG was able to precipitate a higher amount of NLG2-HA compared with NLG1-HA, thus supporting previous *in vitro* observations. Finally, endogenous NLG1 and NLG2 were found in native complexes with gephyrin upon co-immunoprecipitation from mouse brain homogenates (Fig. 7*C*). These data suggest that gephyrin, by interacting directly with NLG2 and to a lesser extent with NLG1, may affect not only GABAergic but also glutamatergic synaptic transmission.

DISCUSSION

The tubulin-binding protein gephyrin is a core protein of inhibitory postsynaptic densities that interacts with the cytoskeleton to stabilize inhibitory receptors in precise apposition to presynaptic active zones (1). In a previous study, we have demonstrated that disrupting endogenous gephyrin with selective scFv-gephyrin altered the gating properties of GABA$_A$ receptors, an effect that was found to be associated with modifications of GABAergic innervation (6). In the present study we hypothesized that hampering gephyrin function affects not only the number of release sites (as suggested by the reduction in VGAT clusters) but also the probability of GABA release. In support of this view, in double patch experiments from interconnected neurons, we found that, with respect to controls, scFv-gephyrin-expressing cells exhibited a significant decrease in the amplitude of individual synaptic currents accompanied by a clear increase in the number of transmitter failures and a reduction in the PPR. Changes in transmitter failures and in PPR are consistent with a decrease in release probability (27, 28). This would lead to a reduction in GABA concentration in the synaptic cleft as suggested by the TPMPA experiments.

The role of gephyrin in ensuring a correct communication between pre- and postsynaptic elements of synapses was further validated by the experiments in which a truncated form of gephyrin (gephyrin 2–188; 22) was used. This gephyrin mutant lacks the dimerization motif, but it can still interact with endogenous gephyrin molecules, producing dominant negative effects on postsynaptic gephyrin clusters. Similar to scFv-gephyrin, overexpression of gephyrin 2–188 caused a reduction in GABAergic innervation and a decrease in frequency of spontaneous and miniature IPSCs, further confirming a key role of gephyrin in maintaining the stability of GABAergic connections within the neuronal network. The ability of gephyrin to influence presynaptic innervation was already suggested by Yu *et al.*, even though no mechanistic interpretation was provided (5).

The presynaptic action of gephyrin on GABA release implies the coordinated activity of other signaling molecules that interact directly or indirectly with gephyrin to ensure the corrected cross-talk between the post- and presynaptic elements of the synapse. Possible candidates are NLGs, specialized cell adhesion molecules that functionally couple the postsynaptic densities with the transmitter release machinery by forming transsynaptic complexes with their presynaptic binding partners, neurexins (7). In particular, NLG2 is preferentially concentrated at inhibitory synapses (10) and binds gephyrin directly through a conserved cytoplasmic domain (14). Consistent with this finding, hampering gephyrin function with scFv-gephyrin promoted a significant decrease in the total number and size of NLG2 clusters upon scFv-induced gephyrin removal. It is interesting to note that in a recent study (34), knocking down gephyrin with siRNA led to a shift of endogenous NLG2 from inhibitory to excitatory synapses, in the absence of any change in the density of NLG2 clusters. In the present experiments instead

we have observed a clear reduction in the density of NLG2 clusters without a detectable relocalization of this protein to glutamatergic synapses. Because scFv-mediated removal of gephyrin is associated with a significant reduction of synaptic γ2-containing $GABA_A$ receptors (6) and evidence has been provided for the reciprocal stabilization of NLG2 by $GABA_A$ receptors (35), the reduction of NLG2 staining could be a consequence of the loss of gephyrin-dependent $GABA_A$ receptor clustering. We cannot exclude the possibility that scFv-gephyrin may affect the function of additional gephyrin-bound factors important for the efficient localization of NLG2 to and from GABAergic terminals. Conventional kinesin (KIF5) and the dynein motor complex have been shown to be involved in microtubule-dependent transport of gephyrin, thus contributing to postsynaptic remodeling (22, 36). Because microtubule motors transport and remodel a variety of transmembrane and submembrane postsynaptic proteins (37, 38), similar mechanisms may account for NLG2 transport.

The role of NLG-neurexin complex as a coordinator between postsynaptic and presynaptic sites has been investigated at excitatory CA3-CA1 synapses in the hippocampus. This study has revealed a retrograde modulation of neurotransmitter release by PSD-95-NLG complex (39). The authors found that overexpression of the glutamatergic scaffold protein PSD-95 enhanced release probability via a mechanism involving the NLG-neurexin complex.

Along the same line, at GABAergic synapses, evidence has been provided that knocking down NLG2 produces a reduction in quantal content associated with a decrease in quantal size of unitary responses (40). In agreement with our electrophysiological data, these findings suggest a crucial role of gephyrin-NLG2 interaction on GABA release.

In our experiments, the reduction in the probability of GABA release after scFv-gephyrin transfection seems to involve a mechanism that only partially relies on the direct NLG2-gephyrin interaction. Hence, the NLG2 point mutant, NLG2Y770A, unable to bind gephyrin was as effective as the wild-type protein in rescuing GABAergic transmission in scFv-gephyrin-deprived neurons. Two possible hypotheses, which are not mutually exclusive, can be put forward to explain our results.

First, although the NLG2Y770A mutant is impaired in gephyrin binding activity it still maintains the ability to induce the activation of collybistin (14), a gephyrin partner known to promote its synaptic targeting *in vivo* (14). Interestingly, in collybistin knock-out mice, a reduction in frequency of mIPSCs similar to that detected in the present experiments was observed (41), thus suggesting a possible involvement of collybistin in transynaptic signaling.

Second, NLGs form homomultimers through the extracellular acetylcholinesterase-homologous domain (42). Therefore, it is possible that overexpressing NLG2Y770A in hippocampal neurons containing endogenous NLG2 allows the formation of multimers. As a consequence this mutant recruited at inhibitory synapses would act in concert with endogenous NLG2 to rescue GABAergic transmission.

Unexpectedly, hampering gephyrin function with scFv-gephyrin produced a significant reduction not only of GABAergic but also of glutamatergic innervation as assessed by the significant decrease in density of VGLUT-positive puncta associated with a significant reduction in frequency, but not in amplitude, of spontaneous and miniature glutamatergic events. This effect was not due to a homeostatic plasticity mechanism because overexpressing NLG2 in gephyrin-depleted neurons failed to reestablish glutamatergic innervation. However, a rescue was obtained by co-expressing NLG1 with scFv-gephyrin. Because the overexpression of NLG1 alone has been shown to enhance glutamatergic innervation by severalfold (9) the fact that this does not occur in gephyrin-deprived neurons suggests that the scaffold protein contributes to modulate NLG1-dependent transynaptic signaling. In support of this observation, co-immunoprecipitation experiments revealed the existence of native complexes not only between gephyrin and NLG2 but also with NLG1, which is localized primarily at excitatory synapses (8), thus confirming and extending previous data obtained with the yeast two-hybrid system (14). Moreover, in favor of the possible involvement of gephyrin in regulating transynaptic signaling at excitatory synapses is the observation that, at least in immature hippocampal neurons *in vitro* (as those used in the present study), this protein has been found localized opposite to glutamatergic release sites (43, 44). The presence of gephyrin at both GABAergic and glutamatergic synapses may be relevant for neuronal development. Altogether, these results show that gephyrin interacts, at least in immature neurons, with both NLG2 and NLG1 to regulate both excitatory and inhibitory inputs converging on the same neuron thus controlling the E/I balance at the network level.

Acknowledgments—We are grateful to P. Scheiffele (Biozentrum, Basel, Switzerland) for providing NLG1-HA and NLG2-HA constructs and F. Varoqueaux (Max Planck, Göttingen) for the NLG2Y770A-HA. We thank B. Pastore for excellent technical assistance on hippocampal neuronal cultures.

REFERENCES

1. Fritschy, J. M., Harvey, R. J., and Schwarz, G. (2008) *Trends Neurosci.* **31,** 257–264
2. Sola, M., Bavro, V. N., Timmins, J., Franz, T., Ricard-Blum, S., Schoehn, G., Ruigrok, R. W., Paarmann, I., Saiyed, T., O'Sullivan, G. A., Schmitt, B., Betz, H., and Weissenhorn, W. (2004) *EMBO J.* **23,** 2510–2519
3. Kneussel, M., Brandstätter, J. H., Laube, B., Stahl, S., Müller, U., and Betz, H. (1999) *J. Neurosci.* **19,** 9289–9297
4. Tretter, V., Jacob, T. C., Mukherjee, J., Fritschy, J. M., Pangalos, M. N., and Moss, S. J. (2008) *J. Neurosci.* **28,** 1356–1365
5. Yu, W., Jiang, M., Miralles, C. P., Li, R. W., Chen, G., and de Blas, A. L. (2007) *Mol. Cell. Neurosci.* **36,** 484–500
6. Marchionni, I., Kasap, Z., Mozrzymas, J. W., Sieghart, W., Cherubini, E., and Zacchi, P. (2009) *Neuroscience* **164,** 552–562
7. Südhof, T. C. (2008) *Nature* **455,** 903–911
8. Song, J. Y., Ichtchenko, K., Südhof, T. C., and Brose, N. (1999) *Proc. Natl. Acad. Sci. U.S.A.* **96,** 1100–1105
9. Chih, B., Engelman, H., and Scheiffele, P. (2005) *Science* **307,** 1324–1328
10. Varoqueaux, F., Jamain, S., and Brose, N. (2004) *Eur J. Cell Biol.* **83,** 449–456
11. Levinson, J. N., Chéry, N., Huang, K., Wong, T. P., Gerrow, K., Kang, R., Prange, O., Wang, Y. T., and El-Husseini, A. (2005) *J. Biol. Chem.* **280,** 17312–17319
12. Gerrow, K., Romorini, S., Nabi, S. M., Colicos, M. A., Sala, C., and El-Husseini, A. (2006) *Neuron* **49,** 547–562
13. Prange, O., Wong, T. P., Gerrow, K., Wang, Y. T., and El-Husseini, A.

(2004) *Proc. Natl. Acad. Sci. U.S.A.* **101,** 13915–13920
14. Poulopoulos, A., Aramuni, G., Meyer, G., Soykan, T., Hoon, M., Papadopoulos, T., Zhang, M., Paarmann, I., Fuchs, C., Harvey, K., Jedlicka, P., Schwarzacher, S. W., Betz, H., Harvey, R. J., Brose, N., Zhang, W., and Varoqueaux, F. (2009) *Neuron* **63,** 628–642
15. Craig, A. M., and Kang, Y. (2007) *Curr. Opin. Neurobiol.* **17,** 43–52
16. Dalva, M. B., McClelland, A. C., and Kayser, M. S. (2007) *Nat. Rev. Neurosci.* **8,** 206–220
17. Gerrow, K., and El-Husseini, A. (2006) *Front. Biosci.* **11,** 2400–2419
18. Rubenstein, J. L., and Merzenich, M. M. (2003) *Genes Brain Behav.* **2,** 255–267
19. Zacchi, P., Dreosti, E., Visintin, M., Moretto-Zita, M., Marchionni, I., Cannistraci, I., Kasap, Z., Betz, H., Cattaneo, A., and Cherubini, E. (2008) *J. Mol. Neurosci.* **34,** 141–148
20. Andjus, P. R., Stevic-Marinkovic, Z., and Cherubini, E. (1997) *J. Physiol.* **504,** 103–112
21. Zita, M. M., Marchionni, I., Bottos, E., Righi, M., Del Sal, G., Cherubini, E., and Zacchi, P. (2007) *EMBO J.* **26,** 1761–1771
22. Maas, C., Tagnaouti, N., Loebrich, S., Behrend, B., Lappe-Siefke, C., and Kneussel, M. (2006) *J. Cell Biol.* **172,** 441–451
23. Scheiffele, P., Fan, J., Choih, J., Fetter, R., and Serafini, T. (2000) *Cell* **101,** 657–669
24. Chih, B., Gollan, L., and Scheiffele, P. (2006) *Neuron* **51,** 171–178
25. Yang, J., Thio, L. L., Clifford, D. B., and Zorumski, C. F. (1993) *Brain Res. Dev. Brain Res.* **71,** 19–26
26. Benson, D. L., Watkins, F. H., Steward, O., and Banker, G. (1994) *J. Neurocytol.* **23,** 279–295
27. Dobrunz, L. E., and Stevens, C. F. (1997) *Neuron* **18,** 995–1008
28. Korn, H., and Faber, D. S. (1991) *Trends Neurosci.* **14,** 439–445
29. Katz, B. (1969) *The Release of Neural Transmitter Substances*, Liverpool University Press, Liverpool, UK
30. Jones, M. V., Jonas, P., Sahara, Y., and Westbrook, G. L. (2001) *Biophys. J.* **81,** 2660–2670
31. Barberis, A., Petrini, E. M., and Cherubini, E. (2004) *Eur. J. Neurosci.* **20,** 1803–1810
32. Yu, W., and De Blas, A. L. (2008) *J. Neurochem.* **104,** 830–845
33. Turrigiano, G. G., and Nelson, S. B. (2004) *Nat. Rev. Neurosci.* **5,** 97–107
34. Levinson, J. N., Li, R., Kang, R., Moukhles, H., El-Husseini, A., and Bamji, S. X. (2010) *Neuroscience* **165,** 782–793
35. Dong, N., Qi, J., and Chen, G. (2007) *Mol. Cell. Neurosci.* **35,** 14–23
36. Maas, C., Belgardt, D., Lee, H. K., Heisler, F. F., Lappe-Siefke, C., Magiera, M. M., van Dijk, J., Hausrat, T. J., Janke, C., and Kneussel, M. (2009) *Proc. Natl. Acad. Sci. U.S.A.* **106,** 8731–8736
37. Hirokawa, N., and Takemura, R. (2005) *Nat. Rev. Neurosci.* **6,** 201–214
38. Kneussel, M. (2005) *EMBO Rep.* **6,** 22–27
39. Futai, K., Kim, M. J., Hashikawa, T., Scheiffele, P., Sheng, M., and Hayashi, Y. (2007) *Nat. Neurosci.* **10,** 186–195
40. Gibson, J. R., Huber, K. M., and Südhof, T. C. (2009) *J Neurosci* **29,** 13883–13897
41. Papadopoulos, T., Korte, M., Eulenburg, V., Kubota, H., Retiounskaia, M., Harvey, R. J., Harvey, K., O'Sullivan, G. A., Laube, B., Hülsmann, S., Geiger, J. R., and Betz, H. (2007) *EMBO J.* **26,** 3888–3899
42. Comoletti, D., Grishaev, A., Whitten, A. E., Tsigelny, I., Taylor, P., and Trewhella, J. (2007) *Structure* **15,** 693–705
43. Studler, B., Sidler, C., and Fritschy, J. M. (2005) *J. Comp. Neurol.* **484,** 344–355
44. Anderson, T. R., Shah, P. A., and Benson, D. L. (2004) *Neuropharmacology* **47,** 694–705

ADDITIONS AND CORRECTIONS

This paper is available online at www.jbc.org

THE JOURNAL OF BIOLOGICAL CHEMISTRY VOL. 286, NO. 35, p. 31062, September 2, 2011

VOLUME 286 (2011) PAGES 20942–20951
DOI 10.1074/jbc.A111.234641

Gephyrin regulates GABAergic and glutamatergic synaptic transmission in hippocampal cell cultures.

Zeynep Kasap Varley, Rocco Pizzarelli, Roberta Antonelli, Stefka H. Stancheva, Matthias Kneussel, Enrico Cherubini, and Paola Zacchi

PAGE 20949:

Lines 16 and 17 under "Discussion" should read "by a clear increase in the number of transmitter failures and in the PPR . . . "

VOLUME 286 (2011) PAGES 24553–24560
DOI 10.1074/jbc.A110.202341

mTORC2 protein-mediated protein kinase B (Akt) serine 473 phosphorylation is not required for Akt1 activity in human platelets.

Samantha F. Moore, Roger W. Hunter, and Ingeborg Hers

mTORC2 is a protein complex and not a protein. Akt and not protein kinase B is used throughout the article. Because of this, the title of the article should read "mTORC2 Protein Complex-mediated Akt (Protein Kinase B) Serine 473 Phosphorylation Is Not Required for Akt1 Activity in Human Platelets."

Neurobiology:

Gephyrin Regulates GABAergic and Glutamatergic Synaptic Transmission in Hippocampal Cell Cultures

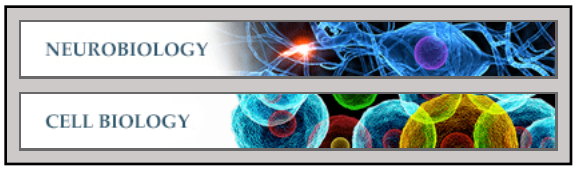

Zeynep Kasap Varley, Rocco Pizzarelli, Roberta Antonelli, Stefka H. Stancheva, Matthias Kneussel, Enrico Cherubini and Paola Zacchi

J. Biol. Chem. 2011, 286:20942-20951.
doi: 10.1074/jbc.M111.234641 originally published online April 20, 2011